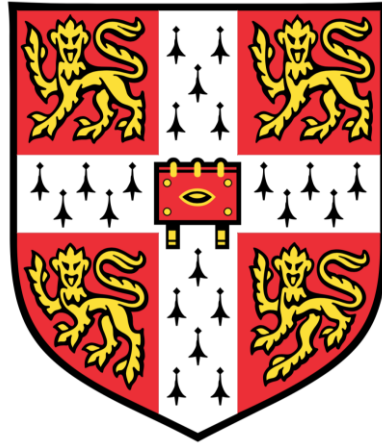


# Environmental change impacts on the shell characteristics of rhychonelliform brachiopods



Emma Cross  
Clare College  
University of Cambridge

This dissertation is submitted for the degree of  
*Doctor of Philosophy*

Department of Earth Sciences and  
the British Antarctic Survey

2016

To my Family and Friends

## Acknowledgements

I would like to give a very big thank you to my supervisors Prof. Lloyd Peck and Dr Elizabeth Harper for their continual support and guidance throughout my PhD. I am very grateful for the opportunity to explore this fascinating area of scientific research and for all the exciting and thorough discussions. Without their encouragement and constant feedback, this PhD would have been less achievable. Special thanks as well for all the great memories from our New Zealand fieldwork which I will always cherish.

Many thanks to Dr Simon Morley for his friendly advice and to Dr Melody Clark for organising the finances of this PhD. I am very grateful to the Natural Environment Research Council (NERC) for funding this PhD studentship under the NERC grant NE/I019565/1. Thank you to the scientific dive team at the British Antarctic Survey Rothera Research Station for collecting the *Liothyrella uva* specimens and also to Dr Coleen Suckling, Dr Simon Morley and Rebecca Smith for their help in the set-up and maintenance of the polar experimental system. I am grateful to our collaborator Dr Miles Lamare for his assistance in the organisation and collection of the New Zealand brachiopods for the temperate experiment. Thanks also to Shaun Cunningham, Esther Stuck and the field and laboratory staff at the Portobello laboratory for their help in the set-up and maintenance of the temperate experimental system. I would also like to thank Rob Clarke, Dr Iris Buisman and Dr Giulio Lampronti for their assistance in sample preparation and training on the Scanning Electron Microscopes and Electron Microprobe. I am very grateful to Te Papa Museum, the National Institute of Water and Atmospheric Research (NIWA), Canterbury Museum, University of Otago's Geology Department, Auckland Museum and University of Auckland for the donations of the historic specimens. I would also like to thank Prof. Maggie Cusack and Dr David Aldridge for examining and discussing results and outcomes of this thesis.

Thanks also to my friends in the department particularly Jo, Jen, Jake, Sarah P, Tom and India, at the British Antarctic Survey particularly Elise, Cat, Emma S, Sarah C, Leyre, Teja, Vicky, Tommy, Ceilia and Ryan and at Clare College especially Laura, Jo, Moos, Chrysa, Becky, Freddie, Callum and Jolle as without all their encouragement and friendship this PhD would have been far less enjoyable. Many thanks to all my rotating housemates Emma H, Lizzie, Bec, Ju, Emily and Sarah H for listening to my daily updates on PhD life and for buying/donating me food. Living with you all has greatly contributed to my enjoyable time in Cambridge. Thanks also to Amy for the uplifting cards throughout and flowers in the final week. I would like to especially thank my best friends Jenni and Mandy for being my biggest cheerleaders and always being there. This PhD would have been a lot harder without the constant support and advice from the two people that know me the best.

And lastly, I would like to give a special thank you to my parents for everything that they do for me. I am particularly grateful for the regular care packages in the post from my Mum and for the uplifting and motivational daily messages from my Dad! I will forever be indebted to you both for your continual support, love and always believing in me.

## **Declaration**

I hereby declare that except where specific reference is made to the work of others, the contents of this dissertation are original and have not been submitted in whole or in part for consideration for any other degree or qualification in this, or any other University. This dissertation is the result of my own work and includes nothing which is the outcome of work done in collaboration, except where specifically indicated in the text. This dissertation is less than 225 pages of text, appendices, illustrations and bibliography.

Emma Cross  
August 2016

## Abstract

Since the Industrial Revolution, anthropogenically-increased CO<sub>2</sub> has altered oceanic surface seawaters through warming and acidification. Previous ocean acidification research has mainly focussed on short-term laboratory manipulations of conditions. Incorporating different approaches investigating both the impacts of past and future environmental change provides a more complete understanding of organisms' responses. Rhynchonelliform brachiopods inhabit all of the world's oceans, have been important marine taxa for 550 million years and are potentially one of the most vulnerable phyla to ocean acidification because >90% of their dry mass resides in their skeleton. Little is known, however, about the effects of lowered pH and warming on these taxa. A polar (*Liothyrella uva*) and a temperate (*Calloria inconspicua*) brachiopod were cultured under predicted end-century environmental conditions in separate CO<sub>2</sub> perturbation experiments for 7 months and 3 months, respectively. Multiple shell characteristics were analysed to determine the effects of future ocean acidification and warming on shell production and maintenance. Impacts of past environmental change were also evaluated on shell characteristics of *C. inconspicua* using museum specimens collected from the same sampling site in New Zealand every decade since 1900 to the present day. In the experiments on live specimens, lowered pH did not affect shell growth rates, ability to repair shells, punctal densities, calcite fibre size or elemental composition in either species. Shell dissolution with decreasing pH will impose a threat to both species, with more extensive dissolution occurring in *L. uva* because of the lower temperatures in its habitat. This was correlated with a decrease in the thickness of the primary layer that was counteracted by an increase in secondary layer thickness and total shell thickness in *L. uva*. The less extensive dissolution in *C. inconspicua* was reflected in the unaffected inner shell layers thicknesses and total shell thickness with decreasing pH. Shell growth rate was only affected by temperature in *L. uva*, with a 2°C rise increasing growth. Similarly, calcification index, total shell thickness, primary and secondary layer thickness, punctal density and elemental composition of *C. inconspicua* have not changed over the last century. Shell density in *C. inconspicua*, however, increased from 1900 to 2014 as this species appeared to lay down more shell by constructing thinner punctae. The majority of shell characteristics have remained unchanged over the last 110 years and are likely to continue to be unaffected by environmental change over the next 84 years. This indicates that shell production and maintenance are robust in a polar and a temperate brachiopod to recent past and predicted end-century acidified and warming conditions. Long-term laboratory experiments and historical specimens in this study have produced insights into how these species can acclimate and their possible ability to adapt to future change.

# Contents

Acknowledgements .....	i
Declaration .....	ii
Abstract .....	iii
Contents .....	iv
List of figures .....	vii
List of tables .....	x
<b>1. Introduction .....</b>	<b>1</b>
<b>1.1 Ocean acidification .....</b>	<b>1</b>
<b>1.2 Ocean acidification research methods .....</b>	<b>3</b>
1.2.1 Laboratory experiments .....	3
1.2.2 Field experiments .....	5
1.2.3 Historic data from museum collections .....	6
<b>1.3 Brachiopods and ocean acidification .....</b>	<b>7</b>
<b>1.4 Phylum Brachiopoda .....</b>	<b>8</b>
<b>1.5 Study areas and species .....</b>	<b>13</b>
1.5.1 The Southern Ocean .....	13
1.5.1.1 The polar brachiopod - <i>Liothyrella uva</i> .....	14
1.5.2 New Zealand .....	15
1.5.2.1 The temperate brachiopod - <i>Calloria inconspicua</i> .....	15
<b>1.6 Aims and objectives .....</b>	<b>17</b>
<b>2. Do predicted end-century acidified conditions impact shell growth or repair in <i>Liothyrella uva</i>, <i>Calloria inconspicua</i>, <i>Liothyrella neozelanica</i> and <i>Notosaria nigricans</i>? .....</b>	<b>18</b>
<b>2.1 Introduction .....</b>	<b>18</b>
<b>2.2 Materials and Materials .....</b>	<b>19</b>
2.2.1 Sampling collection .....	19
2.2.2 Experimental design .....	22
2.2.2.1 Polar experiment .....	22
2.2.2.2 Temperate experiment .....	24
2.2.3 Growth rates .....	26
2.2.4 Shell repair frequencies .....	28
2.2.5 Statistical analyses .....	28

<b>2.3</b>	<b>Results</b> .....	<b>28</b>
2.3.1	Saturation states.....	28
2.3.2	Mortality.....	29
2.3.3	Shell repair frequencies.....	31
2.3.4	Growth rates.....	35
<b>2.4</b>	<b>Discussion</b> .....	<b>40</b>
<b>3.</b>	<b>Do polar and temperate brachiopods produce the same shell structurally and elementally under forecasted end-century acidified conditions?</b> .....	<b>45</b>
<b>3.1</b>	<b>Introduction</b> .....	<b>45</b>
<b>3.2</b>	<b>Materials and Materials</b> .....	<b>49</b>
3.2.1	Experimental design.....	49
3.2.2	Sample preparation.....	49
3.2.3	Punctal density.....	53
3.2.4	Calcite fibre size.....	53
3.2.5	Elemental composition.....	54
3.2.6	Statistical analyses.....	55
<b>3.3</b>	<b>Results</b> .....	<b>57</b>
3.3.1	Punctal densities.....	57
3.3.2	Calcite fibre dimensions.....	59
3.3.3	Elemental composition.....	61
<b>3.4</b>	<b>Discussion</b> .....	<b>67</b>
3.4.1	Punctal densities.....	67
3.4.2	Calcite fibre size.....	69
3.4.3	Elemental composition.....	69
3.4.4	Conclusions.....	72
<b>4.</b>	<b>Do polar and temperate brachiopods maintain their shell integrity under predicted end-century acidified conditions?</b> .....	<b>73</b>
<b>4.1</b>	<b>Introduction</b> .....	<b>73</b>
<b>4.2</b>	<b>Materials and Materials</b> .....	<b>74</b>
4.2.1	Experimental design.....	74
4.2.2	Sample preparation.....	74
4.2.3	Shell condition index.....	77
4.2.4	Shell thickness.....	79
4.2.5	Statistical analyses.....	79
<b>4.3</b>	<b>Results</b> .....	<b>80</b>
4.3.1	Shell condition index.....	80
4.3.2	Shell thickness.....	87
4.3.2.1	Primary layer thickness.....	87
4.3.2.2	Secondary layer thickness.....	88

4.3.2.3	Total shell thickness.....	90
4.4	<b>Discussion</b> .....	<b>92</b>
<b>5.</b>	<b>Acclimation of <i>Calloria inconspicua</i> to environmental change over the last 110 years</b> .....	<b>99</b>
<b>5.1</b>	<b>Introduction</b> .....	<b>99</b>
<b>5.2</b>	<b>Materials and Materials</b> .....	<b>101</b>
5.2.1	Sample collection.....	101
5.2.2	Morphometrics.....	101
5.2.3	Calcification index.....	106
5.2.4	Shell density.....	107
5.2.5	Punctae.....	107
5.2.5.1	Punctal densities.....	107
5.2.5.2	Punctal width.....	108
5.2.6	Elemental composition.....	109
5.2.7	Shell condition index.....	110
5.2.8	Shell thickness.....	110
5.2.9	Statistical analyses.....	111
<b>5.3</b>	<b>Results</b> .....	<b>112</b>
5.3.1	Morphometrics.....	112
5.3.2	Calcification index.....	115
5.3.3	Shell density.....	115
5.3.4	Punctae.....	116
5.3.4.1	Punctal densities.....	116
5.3.4.2	Punctal width.....	116
5.3.5	Elemental composition.....	118
5.3.6	Shell condition index.....	121
5.3.7	Shell thickness.....	125
<b>5.4</b>	<b>Discussion</b> .....	<b>125</b>
<b>6.</b>	<b>General discussion</b> .....	<b>129</b>
<b>6.1</b>	<b>Summary</b> .....	<b>129</b>
<b>6.2</b>	<b>Future research</b> .....	<b>132</b>
<b>6.3</b>	<b>Conclusions</b> .....	<b>135</b>
<b>7.</b>	<b>References</b> .....	<b>137</b>
<b>8.</b>	<b>Appendices</b> .....	<b>165</b>

## List of Figures

1.1 – Latitudinal variations in $[\text{CO}_3^{2-}]$ .....	3
1.2 – Brachiopod organs.....	9
1.3 – Brachiopod shell layers.....	11
1.4 – Periostracum vesicles.....	12
1.5 – Brachiopod shell production.....	13
1.6 – <i>Liothyrella uva</i> .....	15
1.7 – <i>Calloria inconspicua</i> .....	16
2.1 – Trolval Island, Adelaide Island, Antarctica.....	20
2.2 – Portobello Bay, Otago Harbour, New Zealand.....	21
2.3 – Tricky Cove, Doubtful Sound, New Zealand.....	22
2.4 – Polar experiment microcosm.....	23
2.5 – Temperate experiment perturbation system.....	25
2.6 – Length measurements.....	27
2.7 – <i>L. uva</i> larvae and juveniles.....	30
2.8 – <i>L. uva</i> shell repair.....	32
2.9 – <i>C. inconspicua</i> shell repair.....	33
2.10 – <i>Liothyrella neozelanica</i> shell repair.....	34
2.11 – <i>Notosaria nigricans</i> shell repair.....	35
2.12 – <i>L. uva</i> growth rates in the higher temperature treatments.....	37
2.13 – <i>L. uva</i> growth rates in the temperature control.....	38
2.14 – <i>C. inconspicua</i> growth rates.....	39
3.1 – SEM micrograph of brachiopod shell layers.....	46
3.2 – Puncta.....	47
3.3 – Position of brachial valve cross sections.....	50
3.4 – Punctal density calculations in the experimental specimens.....	53
3.5 – Calcite fibre size measurements in the experimental specimens.....	54
3.6 – Elemental composition analysis methods in the experimental specimens.....	55
3.7 – <i>L. uva</i> average punctal densities.....	58
3.8 – <i>C. inconspicua</i> average punctal densities.....	58

3.9 – Average calcite fibre sizes for both species .....	59
3.10 – <i>L. uva</i> microstructure .....	60
3.11 – <i>C. inconspicua</i> microstructure .....	60
3.12 – <i>L. uva</i> average element concentrations .....	65
3.13 – <i>C. inconspicua</i> average element concentrations .....	66
4.1 – Shell condition index methods for experimental specimens .....	77
4.2 – Shell thickness measurements for experimental specimens .....	79
4.3 – <i>L. uva</i> SEM micrographs of shell surfaces .....	82
4.4 – <i>L. uva</i> average shell condition index .....	83
4.5 – <i>C. inconspicua</i> SEM micrographs of shell surfaces .....	85
4.6 – <i>C. inconspicua</i> average shell condition index .....	86
4.7 – <i>L. uva</i> average primary layer thickness .....	87
4.8 – <i>C. inconspicua</i> average primary layer thickness .....	88
4.9 – <i>L. uva</i> average secondary layer thickness .....	89
4.10 – <i>C. inconspicua</i> average secondary layer thickness .....	90
4.11 – <i>L. uva</i> average total shell thickness .....	91
4.12 – <i>C. inconspicua</i> average total shell thickness .....	92
5.1 – Paterson Inlet, Stewart Island, New Zealand .....	100
5.2 – Temperature and CO <sub>2</sub> concentration over the last 120 years .....	100
5.3 – Morphometric measurements .....	101
5.4 – Calcification index calculations .....	107
5.5 – Punctal density calculations of the historic specimens .....	108
5.6 – Punctal width measurements of the historic specimens .....	109
5.7 – Elemental composition analysis methods of the historic specimens .....	110
5.8 – Shell condition index methods of the historic specimens .....	110
5.9 – Shell thickness measurements of the historic specimens .....	111
5.10 – Morphometrics over the last 110 years .....	113
5.11 – Calcification index over the last 110 years .....	115
5.12 – Shell density over the last 110 years .....	115
5.13 – Average punctal density over the last 110 years .....	116
5.14 – Average punctal widths over the last 110 years .....	117
5.15 – Average elemental composition over the last 110 years .....	120
5.16 – Average shell condition index over the last 110 years .....	121

5.17a – SEM micrographs of shell surfaces 1900-1960 .....	122
5.17b – SEM micrographs of shell surfaces 1967-2014 .....	123
5.18 – Average inner shell layers and total shell thickness over the last 110 years .....	125

*Appendices Figures*

A1 – <i>L. uva</i> individual punctal densities .....	166
A2 – <i>C. inconspicua</i> individual punctal densities .....	167
A3 – <i>L. uva</i> individual vertical profiles of Na, Mg, Sr and P .....	171
A4 – <i>L. uva</i> individual vertical profiles of Ca .....	172
A5 – <i>C. inconspicua</i> individual vertical profiles of Na, Mg, Sr and P .....	173
A6 – <i>C. inconspicua</i> individual vertical profiles of Ca .....	174
A7 – <i>L. uva</i> individual spot point method elemental concentrations of Ca .....	175
A8 – <i>L. uva</i> individual spot point method elemental concentrations of Mg .....	176
A9 – <i>L. uva</i> individual spot point method elemental concentrations of Na .....	177
A10 – <i>L. uva</i> individual spot point method elemental concentrations of Sr .....	178
A11 – <i>L. uva</i> individual spot point method elemental concentrations of P .....	179
A12 – <i>C. inconspicua</i> individual spot point method elemental concentrations of Ca .....	180
A13 – <i>C. inconspicua</i> individual spot point method elemental concentrations of Mg .....	181
A14 – <i>C. inconspicua</i> individual spot point method elemental concentrations of Na .....	182
A15 – <i>C. inconspicua</i> individual spot point method elemental concentrations of Sr .....	183
A16 – <i>C. inconspicua</i> individual spot point method elemental concentrations of P .....	184
B1 – <i>L. uva</i> individual shell condition index .....	185
B2 – <i>C. inconspicua</i> individual shell condition index .....	186
B3 – <i>L. uva</i> individual inner layers and total shell thickness .....	187
B4 – <i>C. inconspicua</i> individual inner layers and total shell thickness .....	188
C1 – Individual Ca concentrations over the last 110 years .....	190
C2 – Individual Mg concentrations over the last 110 years .....	191
C3 – Individual Na concentrations over the last 110 years .....	192
C4 – Individual Sr concentrations over the last 110 years .....	193
C5 – Individual P concentrations over the last 110 years .....	194
C6 – Average shell condition index for each year over the last 110 years .....	195
C7 – Individual inner shell layers and total shell thickness over the last 110 years .....	196

## List of Tables

2.1 – Polar experiment seawater parameters .....	24
2.2 – Temperate experiment seawater parameters .....	26
2.3 – Mortality .....	30
2.4 – <i>L. uva</i> shell repair frequencies .....	31
2.5 – <i>C. inconspicua</i> shell repair frequencies .....	33
2.6 – <i>L. neozelanica</i> shell repair frequencies .....	34
2.7 – <i>N. nigricans</i> shell repair frequencies .....	35
3.1 – <i>L. uva</i> morphometrics of individuals used in Chapter 3 .....	51
3.2 – <i>C. inconspicua</i> morphometrics of individuals used in Chapter 3 .....	52
3.3 – Electron Microprobe detection limits for experimental specimens .....	61
3.4 – <i>L. uva</i> elemental composition data summary .....	62
3.5 – <i>C. inconspicua</i> elemental composition data summary .....	63
3.6 – Elemental composition statistical analysis results comparing the two species .....	64
3.7 – <i>L. uva</i> elemental composition statistical analysis from spot point method .....	64
3.8 – <i>C. inconspicua</i> elemental composition statistical analysis from spot point method .....	67
4.1 – <i>L. uva</i> morphometrics of individuals used in Chapter 4 .....	75
4.2 – <i>C. inconspicua</i> morphometrics of individuals used in Chapter 4 .....	76
4.3 – Descriptions of each shell type in shell condition index .....	78
5.1 – Historic specimens morphometrics of individuals used in Chapter 5 .....	112
5.2 – Morphometrics overall regression analysis results .....	112
5.3 – Morphometrics regression equations for each year over the last 110 years .....	114
5.4 – Electron Microprobe detection limits for the historic specimens .....	118
5.5 – Elemental composition data summary over the last 110 years .....	119
5.6 – Shell condition index statistical analysis results over the last 110 years .....	124
<i>Appendices Tables</i>	
A1 – <i>L. uva</i> elemental composition statistical results comparing the methods .....	168
A2 – <i>C. inconspicua</i> elemental composition statistical results comparing the methods .....	169
A3 – <i>L. uva</i> elemental composition statistical results from the vertical profiles .....	170

A4 – <i>C. inconspicua</i> elemental composition statistical results from the vertical profiles.....	170
C1 – Collection and storage details of the historic specimens .....	189



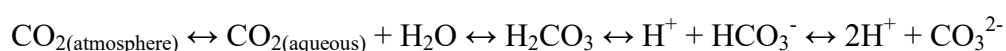
# Chapter One

## Introduction

### 1.1 Ocean Acidification

Since the industrial revolution, atmospheric carbon dioxide has increased 100 times faster ( $\sim 0.5\% \text{ year}^{-1}$  compared to  $\sim 0.005\% \text{ year}^{-1}$  in the past 650,000 years) than the Earth has ever previously experienced (Doney & Schimel, 2007; Doney et al., 2009). The oceans have absorbed 25-30% of the total carbon dioxide released through burning fossil fuels and other human activities (Siegenthaler & Sarmiento, 1993; Sabine et al., 2004; Siegenthaler et al., 2005; Forster et al., 2007; Doney et al., 2009; Le Quéré et al., 2013). While this has mitigated global warming, it has caused the oceans to become more acidic (Caldeira & Wickett, 2003, 2005; Feely et al., 2004; Orr et al., 2005; Gattuso et al., 2014). This has resulted in the average surface ocean pH decrease of 0.1 pH units ( $\sim 30\%$  increase in hydrogen ion concentration) over the last 250 years to pH 8.1 (Brewer, 1997; Caldeira & Wickett, 2003; Orr, 2011). This rate of change is expected to increase significantly causing pH to decrease further by 0.3 pH units by 2050 and 0.5 pH units by 2100 (Caldeira & Wickett, 2005; Orr et al., 2005; Ciais et al., 2013; IPCC, 2013).

Increased anthropogenic carbon dioxide has also caused a change in our surface ocean seawater carbonate chemistry. The ocean carbonate system is governed by a series of chemical reactions:



Once atmospheric  $\text{CO}_2$  is dissolved in seawater it reacts with water to form carbonic acid ( $\text{H}_2\text{CO}_3$ ) which can then disassociate by losing hydrogen ions to form bicarbonate ( $\text{HCO}_3^-$ ) and carbonate ( $\text{CO}_3^{2-}$ ) ions (Doney et al., 2009; Fabry et al., 2009). All these reactions are reversible and near equilibrium. Increasing atmospheric  $\text{CO}_2$  increases aqueous  $\text{CO}_2$ ,

bicarbonate and hydrogen ion concentrations which lowers seawater pH because  $\text{pH} = -\log_{10}[\text{H}^+]$ . Carbonate ion concentration decreases, however, due to the increasing  $\text{H}^+$  concentrations (Guinotte & Fabry, 2008).

Ocean acidification may have profound effects on marine biota directly through the impact of lowered pH on extracellular, intracellular and intercellular transport mechanisms that control the physiology and metabolism of marine organisms (Kroeker et al., 2013). The most susceptible animal group to ocean acidification is considered to be marine calcifying organisms due to the predicted reduction in the availability of carbonate ions making it more difficult and/or require marine calcifiers to use more energy to make their calcium carbonate structural components such as skeletons and shells (Doney et al., 2009; Cummings et al., 2011; Watson et al., 2012; Kroeker et al., 2013). Rates of calcium carbonate ( $\text{CaCO}_3$ ) formation and dissolution vary with saturation state ( $\Omega$ ) which is defined as the ion product of calcium and carbonate ion concentrations (Guinotte & Fabry, 2008; Doney et al., 2009; Fabry et al., 2009):

$$\Omega = [\text{Ca}^{2+}][\text{CO}_3^{2-}] / K'_{\text{sp}}$$

The apparent solubility product  $K'_{\text{sp}}$  depends on temperature, salinity, pressure and the mineral phase (Feely et al., 2004). Therefore, the extent that marine calcifiers are affected by ocean acidification depends largely on which  $\text{CaCO}_3$  polymorph is used to construct their skeleton/shell. Aragonite is the most soluble form followed by high magnesium calcite then calcite and lastly low magnesium calcite (Andersson et al., 2008; Gattuso & Hansson, 2011). Generally, shell formation occurs in supersaturated conditions ( $\Omega > 1$ ) and dissolution occurs in undersaturated waters ( $\Omega < 1$ ) (Doney et al., 2009; Fabry et al., 2009). The depth of the calcite and aragonite saturation horizons determine the limit at which precipitation of biogenic calcium carbonate by marine calcifiers is favoured (above the saturation horizon) and when dissolution will occur (below the saturation horizon) in the absence of protective mechanisms (Figure 1.1; Guinotte & Fabry, 2008). The forecasted changes in seawater pH and ocean carbonate chemistry could have significant consequences for individual marine organisms, communities, ecosystems and food webs (Doney et al., 2009; Kroeker et al., 2013). However, many biological questions remain unanswered including the timing, scale and magnitude of effects.

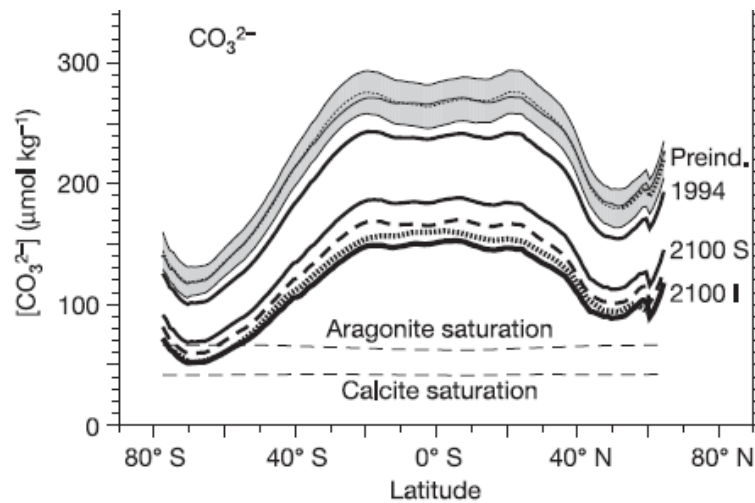


**Figure 1.1 – Increases in atmospheric CO<sub>2</sub> cause decreases in [CO<sub>3</sub><sup>2-</sup>] at all latitudes. Data shown are global zonal averages for preindustrial ('Preind.') ocean, from 1994, and for two IPCC scenarios for 2100 (worst case IS92a = 'I' and best case S650 = 'S'; adapted from Orr et al., 2005).**

## 1.2 Ocean acidification research methods

A number of methods have been used in ocean acidification research. Studies have, however, largely been based on laboratory experiments to assess the effect of future pH conditions on marine species. Field experiments, such as mesocosms, CO<sub>2</sub> vent sites and more recently free-ocean CO<sub>2</sub> enrichment (FOCE) systems, have also been incorporated in attempts to understand the impacts of future environmental conditions on organisms and ecosystems. Investigating how animals have already responded to past environmental change, through analysing historic specimens, is another useful tool employed by researchers in this field. All these approaches have benefits and limitations with no single ideal method. A combination of approaches provides data and information that allow a mechanistic understanding of the impacts of ocean acidification and the necessary power to predict responses to future change (Dupont & Pörtner, 2013; Andersson et al., 2015).

### 1.2.1 Laboratory experiments

Early ocean acidification studies investigating organism responses mainly involved placing individuals in lowered pH seawater by acid addition (Marubini & Atkinson, 1999; Riebesell et al., 2000; Zondervan et al., 2001). This method decreases the pH, but the dissolved inorganic carbon (DIC) concentration remains constant. These early studies generated very high mortality rates and drastically decreased physiological processes (Gattuso & Hansson, 2011). Laboratory studies then moved to more realistic experiments by bubbling CO<sub>2</sub> gas into

seawater to lower pH and elevate DIC concentration. These CO<sub>2</sub> perturbation experiments were originally short term, lasting only a few days to weeks and with pH levels well below the predicted levels for 2100. These early perturbation studies suggested negative effects on growth, calcification and survival (e.g. Ringwood & Keppeler, 2002; Kurihana et al., 2004; Michaelidis et al., 2005; Berge et al., 2006). Most laboratory based experiments are still short to medium term (days to 1-2 months). There has, however, been a recent increase in long-term studies (many months to over a year) (e.g. Hazan et al., 2014; Suckling et al., 2014; Cross et al., 2015, 2016; Queirós et al., 2015). Long-term experiments are crucial to evaluate a species' ability to acclimate and possibly adapt over multiple generations to ocean acidification. Laboratory experiments have produced mixed responses of marine species to lowered pH with positive, negative and neutral effects on a range of physiological processes (Doney et al., 2009; Ries et al., 2009; Hofmann et al., 2010; Byrne, 2011; McCulloch et al., 2012; Parker et al., 2013). The general consensus is that differences are due to species-specific responses related to different calcification mechanisms (Gattuso & Hansson, 2011).

Laboratory experiments have the advantage of manipulating seawater to mimic future predicted environmental conditions and measure the response of marine organisms to specific parameters or the interaction of multiple stressors (Andersson et al., 2015). They also are often cost-effective, offer high levels of replication and are excellent at identifying individual species responses to ocean acidification. Limitations of this most commonly employed approach include difficulties generating reliable long-term predictions of responses due to their relatively short durations, although, longer term experiments can produce data on the acclimation and/or adaptation potential in organisms with short generation times (Collins et al., 2014; Andersson et al., 2015). Secondly, the change in pH in such experiments is abrupt with wild caught individuals exposed either immediately to low pH conditions or over a period of days to weeks which wild populations would not experience. Most laboratory experiments have also not incorporated the role of intraspecific variation in responses, although differences among populations due to plasticity or local adaptation are likely a major long-term response in many species (Hofmann et al., 2010). Few studies also include effects on ecological interactions, e.g. predation and competition (see review by Kroeker et al., 2014), and community level impacts (Peck et al., 2015; Ghedini & Connell, 2016). Multistressor laboratory studies are increasing with these studies focusing on temperature, food availability and hypoxia which can modify organism responses to lowered pH (e.g. Rosa & Siebel, 2008; Rodolfo-Metalpa et al., 2011; Thomsen et al., 2013). However, other factors

such as wave exposure are largely neglected in laboratory studies. Nevertheless, long-term laboratory experiments allow the testing of single or multiple environmental variables in highly controlled settings which can reveal the sensitivities and potential acclimation abilities of marine species to lowered pH.

### **1.2.2 Field experiments**

*In situ* mesocosms were developed to increase the degree of realism and allow the study of species and population/community responses in a more natural context (Nagelkerken & Munday, 2015). Limitations include the difficulty of maintaining acidified conditions *in situ* for sufficient periods, the acclimation and adaptation potential of organisms is not assessed due to their relatively short duration times, they are costly and logistically challenging (Nagelkerken & Munday, 2015). To date, they have only been used with smaller organisms such as plankton (Riebesell et al., 2013).

Comparison of areas with different carbonate chemistry conditions such as near CO<sub>2</sub> vents (Hall-Spencer et al., 2008; Martin et al., 2008; Fabricus et al., 2011; Uthicke et al., 2016) or along spatial gradients (Thresher et al., 2011) provide insights into longer term impacts of acidification on benthic species, communities and ecosystems (Hall-Spencer et al., 2008; Martin et al., 2008; Wootton et al., 2008; Fabricus et al., 2011; Uthicke et al., 2016). CO<sub>2</sub> vents eject volcanic fluids which alter the local ocean chemistry on large spatial and temporal scales (Hall-Spencer et al., 2008). They are common in Mediterranean rocky shores (Hall-Spencer et al., 2008), White Island New Zealand (Nagelkerken & Munday, 2015) and in coral reefs in the Mariana Islands and Papua New Guinea (Fabricus et al., 2011; Enochs et al., 2015; Uthicke et al., 2016), and are considered natural laboratories for ocean acidification research. Along with the ability to investigate long-term direct effects, this approach considers potential secondary ecological consequences of ocean acidification such as habitat modification and altered food supply (Nagelkerken & Connell, 2015; Nagelkerken & Munday, 2015). Limitations of spatial comparisons include no control of treatment conditions where organisms near vent sites are locally exposed to short-term extreme pH levels as well as vents releasing potentially harmful gases. The movement of animals in and out of experimental sites also makes results difficult to interpret (Gattuso et al., 2014; Andersson et al., 2015). Furthermore, replication is limited, and it is difficult to determine the separate effects of multiple drivers, and the potential for the seawater chemistry not to be

representative of other oceanic regions (Andersson et al., 2015). Lastly, there is little knowledge of the history of exposure to acidified conditions, which produces both spatial and temporal uncertainty.

The newest methods in ocean acidification research are the free-ocean CO<sub>2</sub> enrichment (FOCE) systems which are designed to assess the impact of lowered pH on biological communities *in situ* over weeks to months (Kline et al., 2012; Barry et al., 2014; Gattuso et al., 2014; Kirkwood et al., 2015). They are partially open systems that aim to provide natural conditions, apart from pH, to prevail in the manipulated areas despite the partial confinement. They allow control of pH while retaining a flow-through of ambient seawater using a CO<sub>2</sub> mixing system (Barry et al., 2014; Kirkwood et al., 2015). Sensors monitor the ambient and enclosure pH where a control loop regulates the addition of gases or liquids to each enclosure. These systems have the advantage that CO<sub>2</sub> enrichment is controlled accurately by maintaining pH as an offset of ambient pH, thus including natural daily and seasonal pH changes. They also include interspecific relationships, food webs and keep communities in their natural environment over relatively long timescales (Kline et al., 2012; Gattuso et al., 2014). The movement of CO<sub>2</sub> perturbation experiments into field settings is still relatively novel, with only five FOCE systems currently deployed in different habitats across latitudes (Gattuso et al., 2014). The logistics of these systems are extremely challenging with replication being a particular limitation due to cost and feasibility. Future FOCE developments aim to include other stressors e.g. oxygen and temperature (Gattuso et al., 2014; Kirkwood et al., 2015).

### **1.2.3 Historic data from museum collections**

While both laboratory and field experiments provide useful insights into how marine organisms could respond to future environmental change, museum specimens demonstrate how organisms have already responded to changing abiotic and biotic conditions (Hoeksema et al., 2011; Lister, 2011). Historical specimens collected since the Industrial Revolution can also be used as a reference for future responses by providing unique data on rates and magnitude of change we might expect in wild populations. They also provide long-term data that could allow the assessment of possible adaptations that have already occurred in marine calcifiers. The use of museum collections in addition to field and laboratory experiments,

provides greater understanding of species responses to environmental change. Despite all these benefits, this approach is rarely used in ocean acidification research.

### 1.3 Brachiopods and ocean acidification

Brachiopods have existed for over 550 million years, surviving mass extinctions and rapid shifts in environmental conditions indicating the resilience of this phylum (Rudwick, 1970; Richardson, 1981a; Rhodes & Thompson, 1992). Rhynchonelliform brachiopods inhabit all the world's oceans from the intertidal to hadal depths (James et al., 1992; Peck, 2001a) and are one of the most calcium carbonate dependent groups of marine animals because their calcareous skeleton and other support structures make up > 90% of their dry mass (Peck, 1993, 2008). They are also locally important organisms in shallow water communities by providing a habitat for a diverse range of epifauna including encrusting sponges and algae (Barnes & Peck, 1996) as well as being a main consumer of sedimenting biomass. A large scale loss of brachiopods would therefore not only affect local communities, but could also have wider consequences such as eutrophication which potentially could lead to changes in benthic ecosystems (Peck, 2008). Despite this, there are limited studies that have addressed the potential climate change impacts on extant brachiopods (Peck, 2008; McClintock et al., 2009; Peck et al., 2009; Watson et al., 2012; Clark et al., 2016). Peck (2008) highlighted the biological traits of brachiopods that suggest they potentially might not cope with climate change. These include a low energy lifestyle and slow rates in life history characteristics inferring poor abilities to raise metabolic rates to cope with elevated temperature or other stressors. Peck (2008) also suggested that brachiopods are less likely to adapt than other marine taxa due to slow growth rates, deferred maturity and low feeding rates with their restricted ability to migrate to new more favourable sites increasing their vulnerability. Peck et al. (2009) and Clark et al. (2016) investigated the temperature tolerance in Antarctic marine invertebrates including *Liothyrella uva*, which is one of the target taxa in this thesis. Peck et al. (2009) discovered that smaller individuals survived to higher temperatures than larger individuals within a species and sessile species were less resilient to warming than more active species. Clark et al. (2016) reported that *L. uva* has intermediate thermal tolerance in comparison to five other Antarctic marine invertebrates with an upper lethal temperature limit of 18.1°C at a warming rate of 1°C h<sup>-1</sup>. McClintock et al. (2009) and Watson et al. (2012) both investigated ocean acidification impacts on *L. uva*. Watson et al. (2012) measured shell thickness in a number of marine invertebrates from polar and temperate latitudes and reported no latitudinal trend in shell thickness among brachiopod species *L. uva* (polar species from

Adelaide Island, Antarctica) and *Liothyrella neozelanica* (temperate species from Doubtful Sound, New Zealand). That study did, however, report that skeleton mass decreased at polar, low temperatures. McClintock et al. (2009) used laboratory experiments similar to those in this study to investigate acidification impacts on the shell of *L. uva*. They found significant shell dissolution after only 14 days in pH 7.4 conditions, however, only dried empty valves were used so the biological response and ability of *L. uva* to compensate any acidification impacts on their shells remains unknown.

#### **1.4 Phylum Brachiopoda**

Brachiopods are ciliary suspension-feeding marine invertebrates enclosed by two calcareous valves (James et al., 1992; Williams, 1997). The phylum Brachiopoda was restructured into three subphyla in 1996 from their previous two classes (articulate and inarticulate) following advances in the understanding of anatomy, shell morphology, ontogeny and phylogeny (Williams et al., 1996). The three subphyla are now Linguliformea, Craniiformea and Rhynchonelliformea (Williams et al., 1996; Emig, 2009). Linguliformea have organophosphatic shells and the pedicle develops from the ventral mantle (MacFarlan et al., 2009). Craniiformea have calcium carbonate shells and no pedicle. Instead, in this subphylum shells are directly cemented to the substratum (MacFarlan et al., 2009). Rhynchonelliformea also have calcium carbonate shells and the pedicle develops from a larval segment during ontogeny (MacFarlan et al., 2009).

Brachiopod valves are typically bilaterally symmetrical with the valves differing in size, shape and ornamentation between species. The pedicle (ventral) valve is usually larger than the brachial (dorsal) valve (James et al., 1992; Williams, 1997). These shells enclose the interior organs (Figure 1.2), with the coelomate body being divided dorsoventrally. The main portion of the coelom lies posteriorly with a pair of mantle lobes extending anteriorly (James et al., 1992). This posterior coelomic cavity, which contains all the major organs, is separated from the mantle cavity by the anterior body wall. The mantle cavity encloses the feeding organ, the lophophore (Figure 1.2). Brachiopods also have nervous, digestive, open circulatory, reproductive and muscular systems and pairs of metanephridia which function as excretory organs and gonoducts (Rudwick, 1970; Richardson, 1986; James et al., 1992). Another brachiopod characteristic is the pedicle (Figure 1.2) which they use to attach to the substratum or to anchor themselves within sediment. It may be a relatively rigid structure that

acts as a pivot around which the shell moves as a result of the contraction and relaxation of attached muscle to favourably orient themselves in the direction of water flow (James et al., 1992).

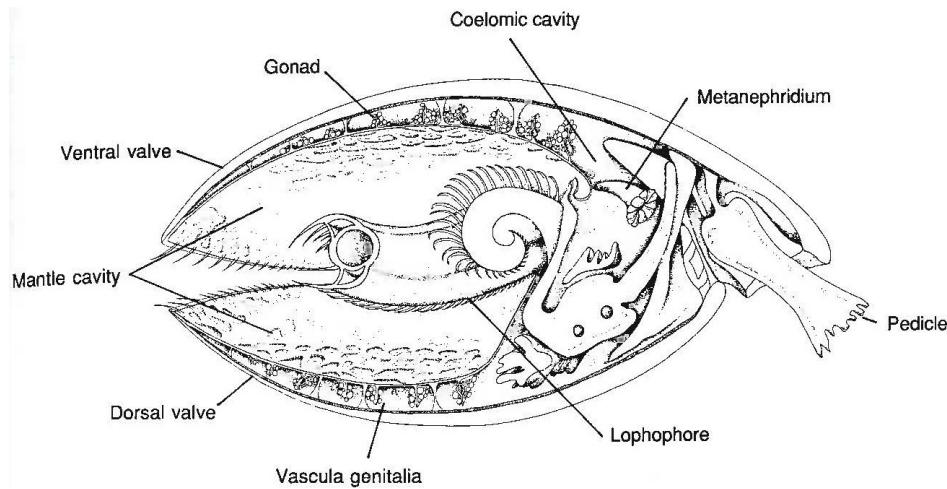


**Figure 1.2 – Diagrammatic representation of the principal brachiopod organs as typified by *Terebratulina retusa* (from James et al., 1992).**

Brachiopods may be unique among metazoans in their continuity and diversity in the geological record (Williams, 1997) and are well represented among the earliest Cambrian fossil assemblages (Rudwick, 1970; Richardson, 1981a; James et al., 1991). They were dominant marine invertebrates in both diversity and abundance throughout the Paleozoic and Mesozoic eras (Curry et al., 1989; Rhodes & Thompson, 1992; Lee, 2008). Their decline was primarily caused by the majority of brachiopod species becoming extinct during the Permo-Triassic mass extinction event approximately 245 million years ago (Thayer, 1986; Pennington & Stricker, 2001). Only 400 species from 100 genera remain today from the 5000 genera identified from fossil records (Lee, 2008; Zezina, 2008; Emig, 2009). The Permo-Triassic extinction also caused global plankton compositions to change, which affected many brachiopod species that had evolved specialised feeding habits (Zezina, 2008). It has been suggested that this resulted in bivalves outcompeting brachiopods due to their broad feeding capabilities and occupying the many ecological niches that were once occupied by brachiopods (Zezina, 2008). Bivalves have since radiated throughout the world's oceans and brachiopods have been generally confined to areas where competition between the two phyla is low (Rhodes & Thompson, 1992, 1993). It has, however, also been argued that there was no direct competition and these differences are niche separation as they each coped differently with post-Paleozoic times (Gould & Calloway, 1980). Bivalves tend to dominate high-energy, food-rich, near-shore habitats whereas brachiopods generally occur in low-energy, food-poor habitats such as caves, overhangs, dark fiord walls, polar regions and abyssal waters

(Rudwick, 1970; Rhodes & Thompson, 1992; Lee, 2008). Brachiopods have been able to occupy areas of low bivalve competition due to their low metabolic rates and low energy demands (Richardson, 1986; Grange & Singleton, 1988; Rhodes & Thompson, 1992).

The majority of research on brachiopods is confined to palaeontology and geology due to their high abundance and diversity throughout the fossil record and because they have little or no commercial value (Richardson, 1986; Pennington & Stricker, 2001). Brachiopod shells have been extensively used to study isotopic signatures of past environments due to their thermodynamically stable low magnesium calcite being less susceptible to diagenetic alteration than the less stable aragonitic shells of many molluscs (e.g. Lowenstam, 1961; Grossman et al., 1996; Veizer et al., 1999; Brand et al., 2003; Schmahl et al., 2004; Perez-Huerta et al., 2008; Brand et al., 2013). Research on living brachiopods has increased markedly over the last 40 years focussing on the distribution, ecology and their general biology, as they are considered model organisms for understanding adaptations needed to survive in relatively harsh conditions (Peck et al., 1986a,b, 1987a,b; James et al., 1992; Lee, 2008). Due to the typically inaccessible habitats of most brachiopods, research on extant species has been mainly conducted in areas with high numbers of relatively accessible individuals, e.g. Antarctica and New Zealand (Peck et al., 1986a,b, 1987a,b, 1997, 2001, 2005; Peck, 1989, 1992, 1993, 2001a,b; Peck & Holmes, 1989a,b; Peck & Brey, 1996; Hiller et al., 2008; Harper et al., 2009, 2011; Peck & Harper, 2010; Lee et al., 2010; Cohen et al., 2011).

The standard brachiopod shell consists of an outer organic layer, the periostracum, underlain by two or three biomineralised inner layers, the primary, secondary and tertiary layers (Figure 1.3; Williams, 1997). The periostracum and primary layer are always present, with the secondary layer almost always present apart from in thecideidines where it is absent and the tertiary layer is limited to a minority of extant species (Williams, 1997). The function of the periostracum is to separate the site of calcification from external seawater, to provide a template for the shell to form and to protect the underlying shell layers (Harper, 1997). The terebratulide periostracum consists of a basal layer which underlies a superstructure of vesicles, the pitted layer (Figure 1.4; Williams & McKay, 1978). The distribution of these vesicles varies between species with radially aligned casts in *L. uva* and constant pits in *Calloria inconspicua*. The vesicles in the terebratelloid periostracum vary from spherical

bodies (up to 2  $\mu\text{m}$  in diameter) to flattened disks (up to 250 nm thick) which are commonly stacked against one another (Williams, 1997). The function of these vesicles is unknown (Williams, 1997). The primary layer of calcitic brachiopods is usually finely granular or acicular (Williams, 1968a, 1973, 1997; MacKinnon & Williams, 1974). The secondary layer constitutes the majority of the shell which can comprise three structurally different fabrics including calcitic fibres, tabular lamination or cross-bladed lamination (Williams, 1997). A fibrous fabric is the most common feature of calcitic brachiopods, which comprises single fibres in protein membrane sheaths interlocking with each other to form a shell layer of stacked fibres.

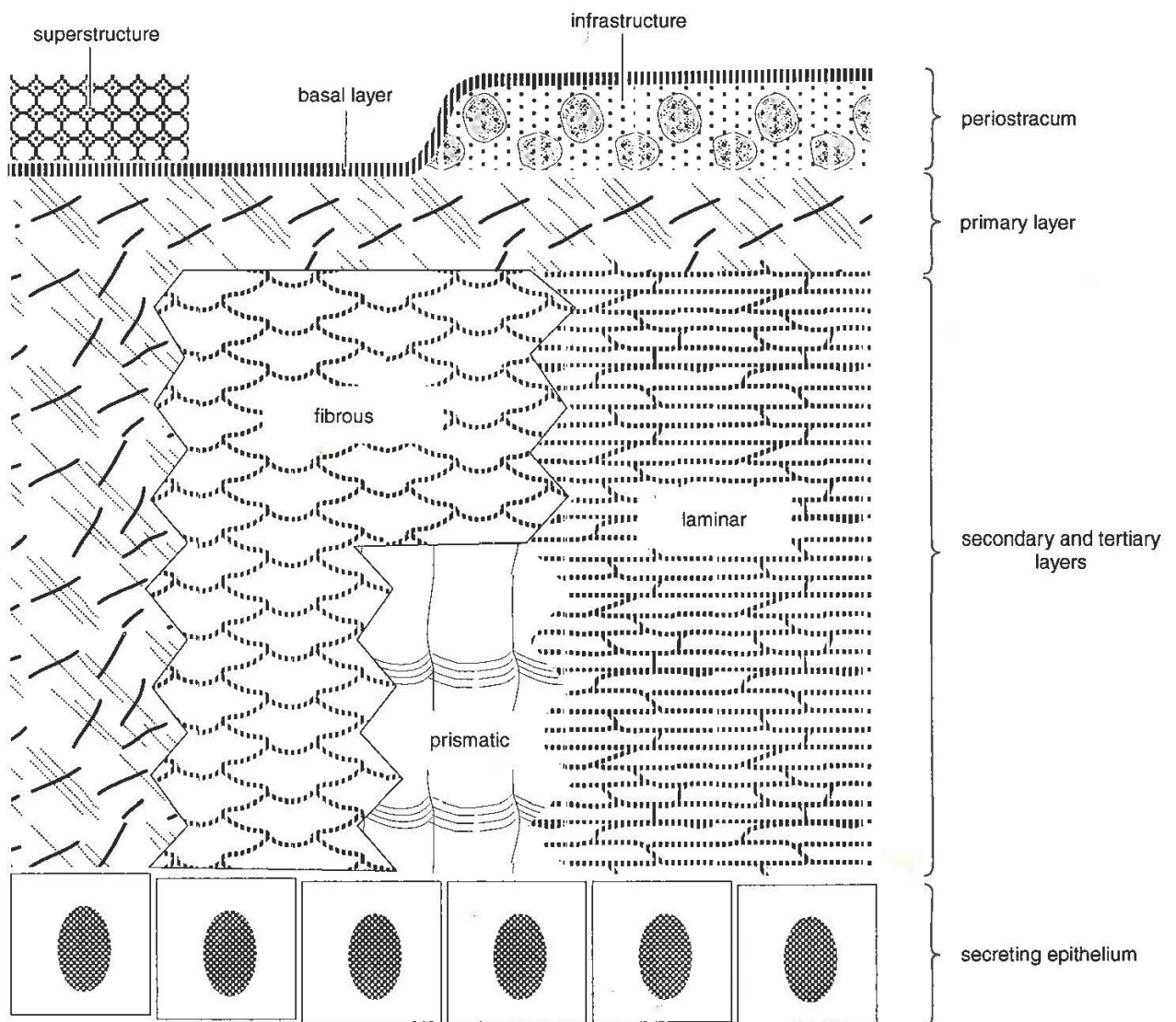


**Figure 1.3 – Schematic representation of the main components of calcitic-shelled brachiopods (from Williams, 1997).**

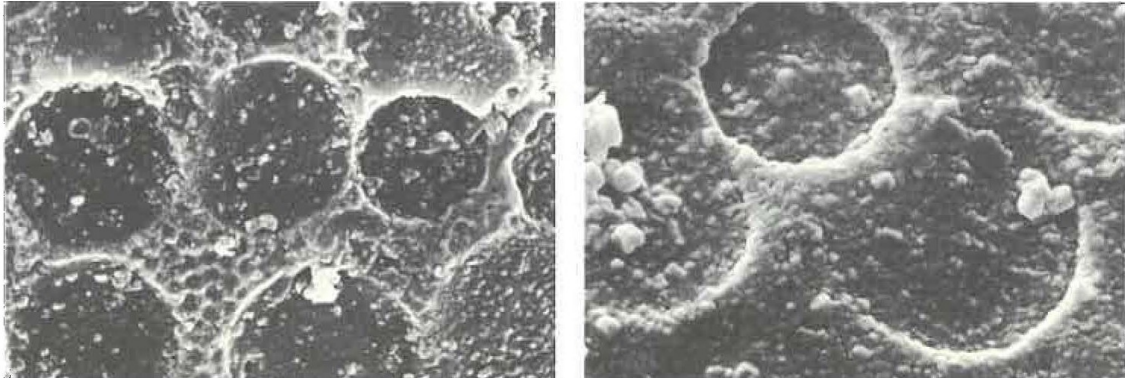


**Figure 1.4 – Scanning electron micrographs (x4000 magnification) of the vesicles in the pitted layer in the outermost part of the periostracum in the terebratulid brachiopod *Magellania australis* (from Williams, 1997).**

Biom mineralisation processes differ between the three brachiopod subphyla resulting in dissimilar microstructures. Rhynchonelliforms grow their shell from the protogulum to the anterior margin, which is called mixoperipheral growth (Williams et al., 1997; Perez-Huerta & Cusack, 2008). Shell growth is a biochemical process controlled by the outer epithelial cells of the mantle lining of the shell (Williams, 1956, 1968a,b; Williams & Wright, 1970). Each cell performs a range of secretory operations with each calcite fibre emerging from a single mantle epithelial cell (Figure 1.5). These secretory cells originate in a groove separating the inner and outer lobes of the mantle edge. The outer lobe is a mantle fold which acts like a conveyor belt moving these newly proliferated cells posteriorly along the shell generative zone by the addition of new cells behind them (James et al., 1992). The youngest cells secrete the proteinaceous periostracum (Williams, 1966). When these cells reach the mantle tip they start secreting calcite crystallites between the periostracum and the underlying cell walls which form the start of the calcareous primary layer (Williams, 1966). This layer is continuously made across intercellular boundaries and forms a rigid constant layer without imprints of cell outlines (Williams, 1956). Primary layer thickness depends on the number of rows of epithelial cells involved in its secretion which is fairly constant within a species. Adding new cells at the tip of the mantle lobe moves the cells along the conveyor to form the innermost rows underlying the primary layer (Williams, 1966). Here these cells exude protein through the anterior intercellular boundaries as well as secrete calcite crystallites laid down within the protein boundaries. Secondary layer calcite is segregated into fibres by the continuous deposition of protein along the intercellular boundaries where each fibre is contained by a protein sheath (Williams, 1956, 1966). Further calcite fibre growth is controlled by the outer surface of the cell and secondary layer thickness is highly variable (Williams, 1956). Energetic costs of shell formation in 15 prosobranch gastropods were

estimated to be < 0.07-0.3% than that of protein synthesis (Palmer, 1983). These costs have not been investigated in brachiopods, however, the energetic cost of shell production could be higher due to the larger ratio of shell to animal tissue. Future predicted increases in acidity and warming could make this crucial process more expensive. The impact of an increased cost is unclear, but it could have long-term detrimental effects to this highly calcium carbonate dependent phyla.

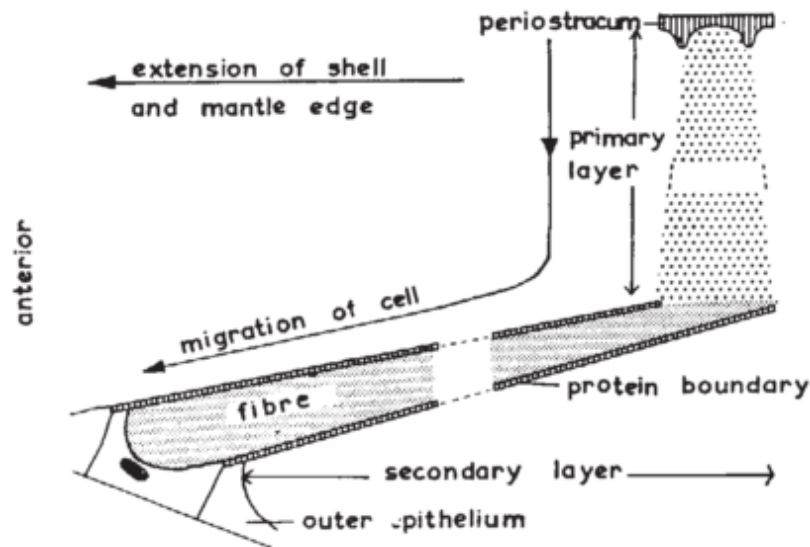


**Figure 1.5 – Schematic of the longitudinal section of a shell indicating the relationship between an outer epithelial cell and the three layers of rhynchonelliform brachiopods (from Williams, 1966).**

## 1.5 Study areas and species

### 1.5.1 The Southern Ocean

The fastest rates of change in carbonate chemistry are expected in the Southern Ocean (Figure 1.1; Caldeira & Wickett, 2005; McNeil & Matear, 2008). Carbon dioxide is more soluble in cold water (Revelle & Fairbridge, 1957) resulting in naturally low carbonate ion saturation levels compared to temperate and tropical regions. Acid-base coefficients are also more sensitive in cold temperatures making this high latitude region a forerunner of biological ocean acidification impacts for other oceans (Fabry et al., 2009). Furthermore, the absence of shell-crushing predators, such as brachyuran crabs, lobsters and heavily jawed fish (Aronson et al., 2007) and the difficulty of extracting  $\text{Ca}^{2+}$  from seawater at low temperature (Harper, 2000; Aronson et al., 2007) has resulted in Antarctic species generally having thin, weakly calcified shells (Vermeij, 1978; Watson et al., 2012). This, added to the low physiological rates of Antarctic marine species (Peck et al., 2007), especially low metabolic rates (Peck & Conway, 2000), slow growth rates (Arntz et al., 1994; Peck, 2016), delayed reproduction

(Pearse et al., 1991; Meidlinger et al., 1998; Tyler et al., 2003) and high longevity (Pearse et al., 1991), indicates that these organisms are likely to be amongst the most vulnerable worldwide to acidifying oceans. There are several studies on the potential impacts of this aspect of climate change on the larval stages of Antarctic calcifying organisms (see review by Byrne (2011)), but studies on adults are limited (McClintock et al., 2009; Cummings et al., 2011; Watson et al., 2012), and the longest of these lasted 4 months (Cummings et al., 2011).

#### **1.5.1.1 The polar brachiopod - *Liothyrella uva***

*L. uva* (Broderip, 1833) is a large (up to 55 mm), epifaunal, sessile terebratulide brachiopod with a circumpolar distribution (Figure 1.6; Peck et al., 2001). It is found down to 300 m and is highly abundant in habitats protected from anchor ice and ice scour with reported densities up to 3000 individuals m<sup>-2</sup> (Foster, 1974; Brey et al., 1995; Peck et al., 2001). *L. uva* is typically found attached singly or in clumps to vertical and overhanging rocks around the South Orkney Islands, the Antarctic Peninsula and Peter I Island (Foster, 1974).

Previous research on *L. uva* describes body size and morphology (Peck et al., 1987a, Peck & Holmes, 1989a; Peck, 1992), seasonal changes in tissue-mass (Peck & Holmes, 1989b), respiration and metabolism (Peck et al., 1986b, 1987a,b; Peck, 1989, 1996), larval development (Peck & Robinson, 1994), reproduction (Meidlinger et al., 1998), feeding (Peck & Holmes, 1989b; Peck et al., 2005) and growth rates (Peck & Brey, 1996; Peck et al., 1997). Shell growth in *L. uva* has been reported to be slower than temperate rhynchonelliform species with the Antarctic brachiopod living for over 55 years (Peck & Brey, 1996; Peck et al., 1997). Faster growth rates were also recorded in winter to maximise the efficiency of annual resource utilisation (Peck et al., 1997). *L. uva* shell microstructure consists of a nanocrystalline primary layer and a fibrous secondary layer (Parkinson et al., 2005; Goetz et al., 2009) and the shell texture more defined than the temperate rhynchonelliform *Kakanuiella chathamensis* (Goetz et al., 2009). There was no difference in shell texture between *L. uva* and the closely related temperate *L. neozelanica* although *L. uva* shells were reported as harder than *L. neozelanica* (Goetz et al., 2009). Studies have also shown the Antarctic brachiopod has limited tolerance to raised temperature with a long-term upper thermal limit reported as 4.5°C (Peck, 2005; Peck et al., 2001, 2014). Given that polar marine calcifiers are considered the most vulnerable species to acidifying oceans due to difficulties extracting Ca<sup>2+</sup>

from low temperature seawater, *L. uva* is an ideal species to study future change impacts on this highly calcium carbonate dependent taxon.

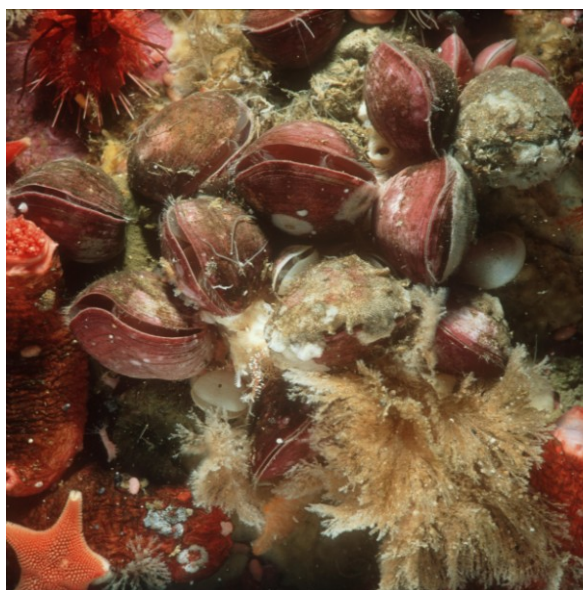


**Figure 1.6 – *L. uva* (Broderip 1833) on a vertical rock wall at Adelaide Island, Antarctica (Photograph from Pete Bucktrout, British Antarctic Survey).**

## **1.5.2 New Zealand**

Carbon dioxide concentration has increased by 90-100 ppm over the last 120 years in New Zealand (<http://www.climatechange.govt.nz/science/>). Brachiopods are found worldwide, but often with patchy distributions. In New Zealand, many species live at relatively accessible shallow depths (< 30 metres) at several different locations, including drowned valleys, harbours, the Hauraki Gulf, Stewart Island and in the fiords such as Doubtful Sound (Rudwick, 1962; Doherty, 1979; Grange et al., 1981; Richardson, 1981b; Peck, 2001a; Lee et al., 2010). Brachiopod biodiversity is also high in New Zealand with 22 genera and 50 species living in this biogeographic region, which represent 13% of the extant brachiopod fauna (Dawson, 1991; Lee, 1991; MacFarlan et al., 2009; Lee et al., 2010). These factors make New Zealand an ideal temperate study site for this type of research and for comparisons with Antarctic *L. uva*.

### **1.5.2.1 The temperate brachiopod - *Calloria inconspicua***

*C. inconspicua* (Sowerby, 1846) is a small (up to 28 mm; Stewart 1981), epifaunal, sessile terebratellid brachiopod endemic to New Zealand (Figure 1.7; Doherty, 1979). It has a widespread distribution throughout New Zealand and is highly abundant in intertidal and shallow subtidal habitats, with reported densities of over 1000 individuals m<sup>-2</sup> (Doherty,

1979). *C. inconspicua* is usually found individually or in conspecific clumps attached to hard substrata such as rock, other brachiopods, bivalves, bryozoans, gastropods and corals (Lee, 1991).

*Calloria inconspicua* was first classified as *Waltonia inconspicua* by Davidson (1850). This name was abandoned by Davidson in 1861 who realised that the genus *Waltonia* was based on a juvenile, imperfect specimen of a ribbed brachiopod belonging to the genus, *Terebratula* (Sowerby, 1846). *C. inconspicua* was referred to as *T. inconspicua* until Cooper & Lee (1993) eliminated the confusion of these names and proposed the new name of *Calloria inconspicua*. This complex history of the nomenclature of *C. inconspicua* was attributed in part to the limited knowledge of brachiopod loop development in the mid-nineteenth century (Cooper & Lee, 1993). Previous research on *C. inconspicua* has focussed on demography (Doherty, 1979), shell morphology (Aldridge, 1981), mortality (Doherty, 1979), longevity (Rickwood, 1977; Doherty, 1979), respiration (Shumway, 1982), larval development (Chuang et al., 1996; Lüter, 1998), reproduction (Rickwood, 1977; Doherty, 1979; Lüter, 1998; Lee et al., 2010), predation (Harper et al., 2011) and growth rates (Percival, 1944; Rickwood, 1977; Doherty, 1979). An early study reported slow growth in this species which is unevenly distributed throughout life; fastest during the first four years (up to 10 mm length) and decreasing after reproduction commences (Rickwood, 1977). Shell microstructure of *C. inconspicua* is similar to the Antarctic brachiopod with an outer proteinaceous periostracum and inner calcareous primary and secondary layers (Williams, 1968a,b). Unlike *L. uva*, *C. inconspicua* has a broad temperature tolerance of 8-18°C (Lee, 1991). *C. inconspicua* is in the same order as *L. uva*, therefore, the impacts of predicted end-century conditions on this species provides a good comparison to the polar brachiopod.



**Figure 1.7 – *C. inconspicua* (Sowerby 1846) collected from a shallow subtidal site on Stewart Island, New Zealand (Photograph by Dr Elizabeth Harper, University of Cambridge).**

## 1.6 Aims and objectives

The shell is essential to the existence of rhynchonelliform brachiopods, providing protection from predators, preventing encounters with harmful substances and the loss of body fluids (Harper et al., 2012). Any environmental insult negatively impacting the production, maintenance and/or integrity of the shell could thus prove fatal. Ocean acidification research is now moving towards more long-term studies, which is crucial to better understand responses to climate change and abilities to acclimate and adapt to changing environmental conditions. Given this, and the limited knowledge on how one of the most calcium carbonate dependent groups of organisms will be impacted by future environmental change, the overall aim of this thesis is to determine how the shell characteristics of a polar and a temperate brachiopod will be impacted by ocean acidification and warming.

Aim 1: Investigate how shell characteristics of rhynchonelliform brachiopods will be affected by an increase in seawater acidity and temperature predicted to occur over the next 84 years.

Objectives: Evaluate the impact of long-term exposure to lowered pH and increased temperature conditions predicted for 2050 and 2100 on the ability of a polar brachiopod *L. uva* (7 months) and a temperate brachiopod *C. inconspicua* (3 months) to continue shell deposition (Chapter 2); produce the same shell in terms of structure and elemental composition (Chapter 3); and to maintain shell integrity (Chapter 4). This was determined through measuring shell growth rates and the ability to repair shell (Chapter 2), calculating punctal densities, calcite fibre dimensions and elemental compositions (Chapter 3) and assessing shell condition and shell thickness (Chapter 4).

Aim 2: Determine how shell characteristics of rhynchonelliform brachiopods have been impacted by environmental change over the last 110 years.

Objectives: Establish the effect of changing environmental conditions on the shell properties of museum collections of a temperate brachiopod *C. inconspicua* from a single sampling site (Paterson Inlet, Stewart Island, New Zealand) every decade from 1900 to 2014 (Chapter 5). Shell characteristics measured were morphometrics, calcification index, shell density, punctal density, punctal width, elemental composition, shell condition index and shell thickness (Chapter 5).



## Chapter Two

### **Do predicted end-century acidified and warming conditions impact shell growth or repair in *Liothyrella uva*\*, *Calloria inconspicua*\*\*\*, *Liothyrella neozelanica* and *Notosaria nigricans*?**

\*Cross, E. L., Peck, L. S. and Harper, E. M., 2015. Ocean acidification does not impact shell growth or repair of the Antarctic brachiopod *Liothyrella uva* (Broderip, 1833). *Journal of Experimental Marine Biology and Ecology*, 462: 29-35.

\*\*Cross, E. L., Peck, L. S. Lamare, M. D. and Harper, E. M., 2016. No ocean acidification effects on shell growth and repair in the New Zealand brachiopod *Calloria inconspicua* (Sowerby, 1846). *ICES Journal of Marine Science*, 73: 920-926.

#### **2.1 Introduction**

Shells are essential to the existence of shell-bearing organisms as they provide protection from predators and desiccation in intertidal species, prevent any encounters with harmful substances and prevent the loss of body fluids (Harper et al., 2012). Rhynchonelliform brachiopods are potentially one of the most calcium carbonate dependent groups of marine animals as a result of their large shell in comparison to the small proportion of animal tissue (Peck, 1993, 2008), therefore, shell production is a critical process for their survival. Growth is also an indicator of an animal's well-being in a particular environment as it represents the combination of responses of physiological, cellular and biochemical processes within the organism (Riisgård & Randløv, 1981). Another essential process to the existence of the vast majority of marine shelled organisms is shell repair. Brachiopods become damaged in their natural environment due to impacts from a variety of causes including trauma from saltating clasts and predator attack (Harper et al., 2009). Such damage requires quick shell repair for survival (Harper et al., 2012). Shell repair from external trauma can be very common in some populations previously recorded to range up to repair frequencies of 0.355 (number of

damaged individuals/total number of individuals) in *C. inconspicua* (Harper & Peck, 2016). Any environmental insult negatively impacting the production, maintenance and/or repair of their shell could thus prove fatal (Vermeij, 1983).

Many ocean acidification studies have investigated calcification with the general consensus that the response of marine organisms is species-specific (Ries et al., 2009). However, these studies have all been conducted on marine calcifiers such as corals (e.g. Gattuso et al., 1998; Form & Riebesell, 2012; Hennige et al., 2014) and molluscs (e.g. Nienhuis et al., 2010; Thomsen et al., 2010; Hiebenthal et al., 2012). There is limited research on the impact of acidified conditions on brachiopods (Peck, 2008; McClintock et al., 2009; Watson et al., 2012). Other than this chapter (see Cross et al., 2015, 2016), no other study, to my knowledge, has involved ocean acidification effects on brachiopod shell growth rates and repair.

Given the importance of understanding the limits to maintaining shell production and repair, in addition to the restricted research on ocean acidification effects on brachiopods, the aims of this chapter were to establish how shell growth and the ability to repair shell in *L. uva*, *C. inconspicua*, *L. neozelanica* and *N. nigricans* were affected by forecasted future environmental conditions. Growth rates and the frequency of shell repair following damage were measured in pH controlled conditions and predicted mid and end-century pH levels in these species and also in increased temperature conditions in *L. uva*.

## **2.2 Materials and Methods**

### **2.2.1 Sampling collection**

Specimens of *L. uva* (Broderip, 1833) were hand collected by SCUBA divers from Trolval Island, Ryder Bay, Antarctica (67° 35.44' S, 68° 12.44' W) at 15-25 m depth in May 2012 (Figure 2.1). Animals were kept in their conspecific clumps with only the pedicle of the central brachiopod attached to the cliff face being cut ensuring that the majority of specimens were not damaged during collection. Environmental conditions in Ryder Bay at 15-25 m depth consist of seawater temperatures that range from -1.8 to +1.0°C, however, temperatures rarely exceed +0.5°C and salinity is 33.0-34.0 (Clarke et al., 2008) and the pH range is 8.04-8.10 (McNeil and Matear, 2008). Brachiopods were kept underwater during the short

transportation from the sampling site to the marine laboratory in Rothera and in recirculating aquaria ( $0.0 \pm 0.5^{\circ}\text{C}$ ) whilst being transported back to the UK. Specimens remained in an ambient recirculating seawater system in the UK in similar conditions for a further two weeks to habituate to aquarium conditions before the experiment began.

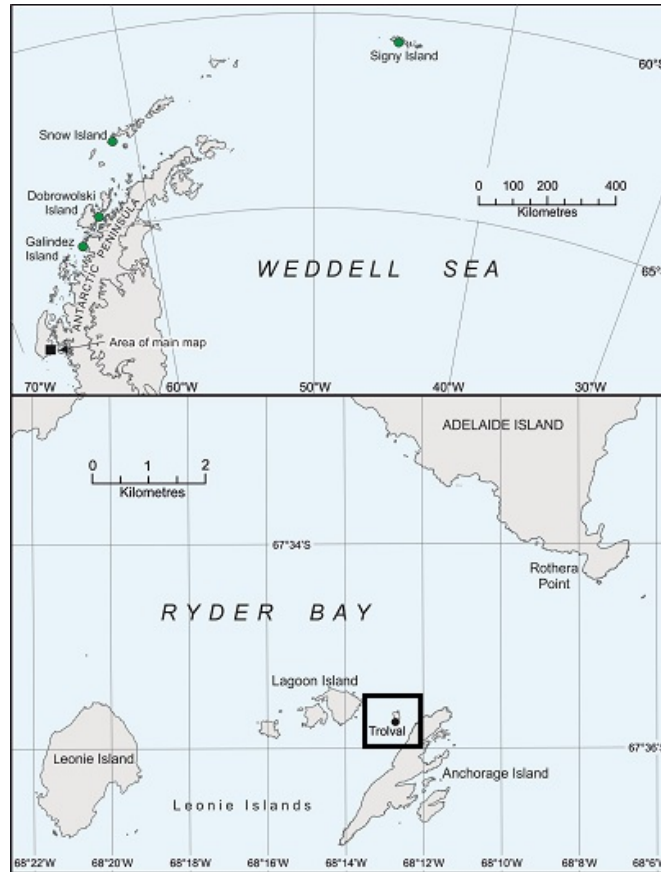


**Figure 2.1 - Location of sample collection site for *L. uva* (Trolval Island, Ryder Bay, Adelaide Island, Antarctica,  $67^{\circ} 35.44' \text{ S}$ ,  $68^{\circ} 12.44' \text{ W}$ ).**

Specimens of *C. inconspicua* were hand collected at low tide from under rocks in Portobello Bay, Otago Harbour, New Zealand ( $45^{\circ} 82.000' \text{ S}$ ,  $170^{\circ} 70.00' \text{ E}$ ) in January 2013 (Figure 2.2). Samples were kept in their conspecific clumps and, in order to minimise disturbance, were only collected if they were attached to removable substratum to ensure that no pedicles were cut. Environmental conditions in Otago Harbour are surface seawater temperatures of  $6.4\text{-}16.0^{\circ}\text{C}$  (Roper & Jillett, 1981; Greig et al., 1988), pH range of 8.10-8.21 (K. Currie, pers. comm.) and salinity is 32.5-34.8 (Roper & Jillett, 1981). Brachiopods were kept in seawater during the short transportation from the sampling site to Portobello Marine Laboratory, Otago Peninsula. Specimens were then immediately placed in the experimental system.

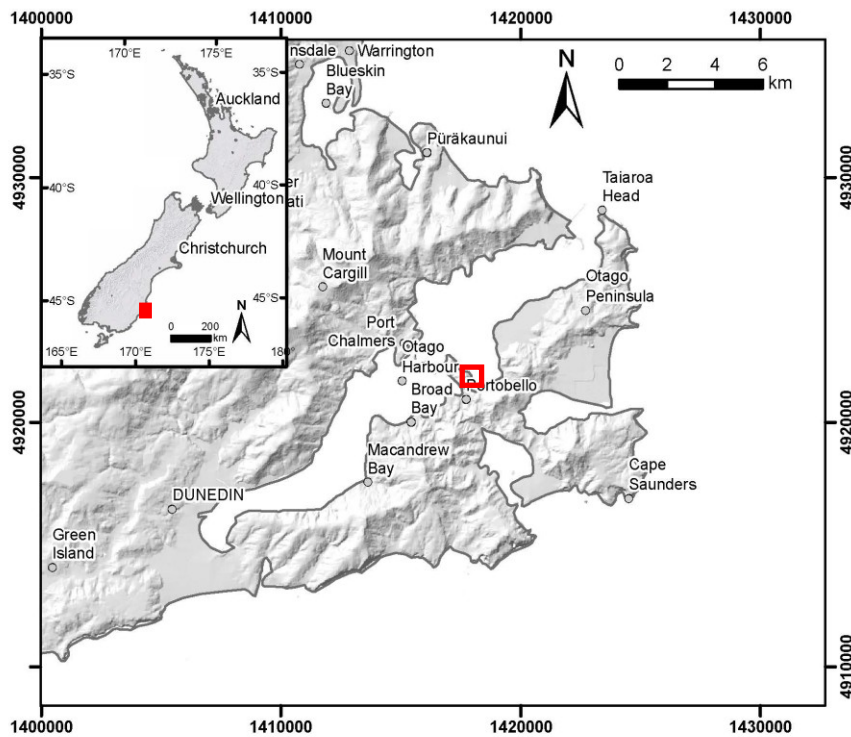


**Figure 2.2 - Location of sample collection site for *C. inconspicua* (Portobello Bay, Otago Harbour, New Zealand, 45° 52.00'S, 170° 00.00'E).**

Specimens of *L. neozelanica* and *N. nigricans* were collected by SCUBA divers at 18-20 m at Tricky Cove, Doubtful Sound, Fiordland, New Zealand (45° 20.478'S, 167° 02.381'E) in January 2013 (Figure 2.3). To minimise disturbance, only the pedicle of the individual attached to the wall was cut ensuring all specimens remained in their conspecific clumps. Environmental conditions in Doubtful Sound are seawater temperatures of 7.5-15°C (Peake et al., 2001), average pH of pH 8.1 ± 0.01 SE (Clark et al., 2009) and salinity of 32.0-35.0 below the surface low salinity layer (Peake et al., 2001). Specimens were placed in lidded buckets with fresh seawater for transport back to Portobello Marine Laboratory, Otago Peninsula with the seawater being replaced in the buckets after an hour of transport to try to minimise temperature and oxygen stress on the brachiopods.

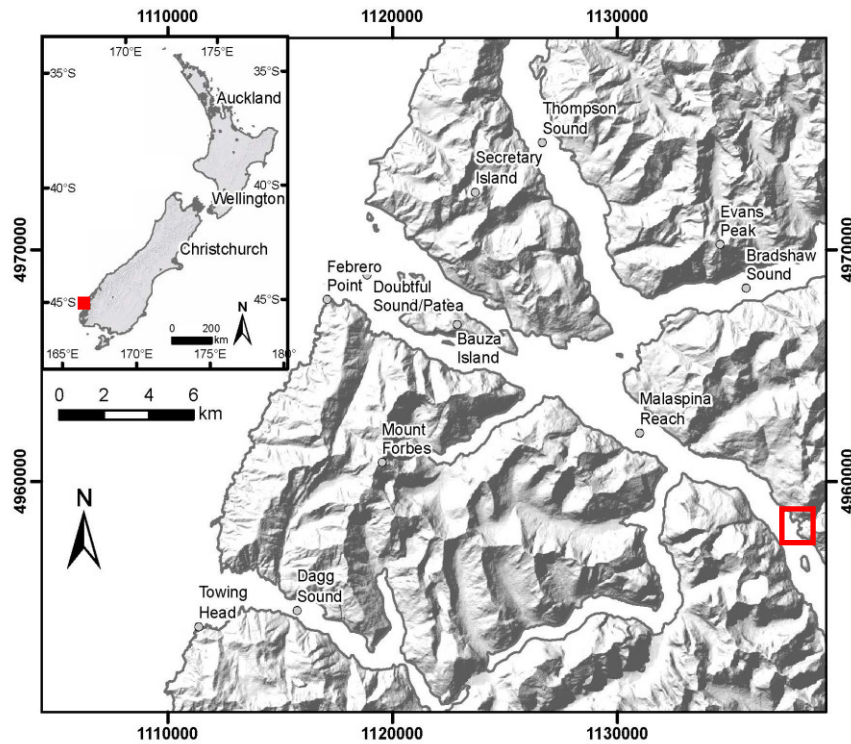
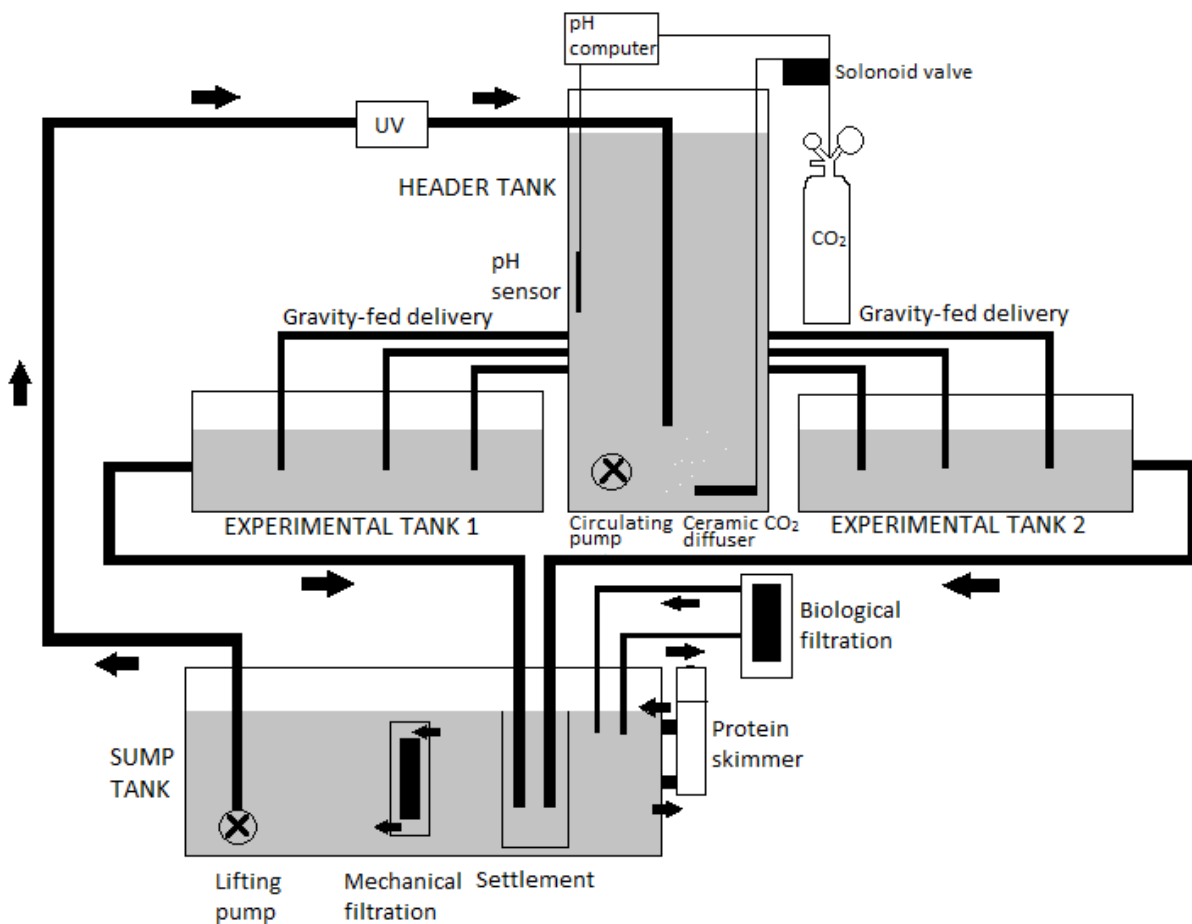


Figure 2.3 - Location of sample collection site for *L. neozelanica* and *N. nigricans* (Tricky Cove, Doubtful Sound, Fiordland, New Zealand (45° 20.478'S, 167° 02.381'E).

## 2.2.2 Experimental design

### 2.2.2.1 Polar experiment

A temperature-controlled recirculating CO<sub>2</sub> microcosm at the British Antarctic Survey (BAS), UK was adapted from Suckling et al. (2014) and used for the experiment involving the Antarctic brachiopod, *L. uva* (Figure 2.4). Four separate closed-circuit systems were used as different treatments where two functioned as lowered pH treatments (pH 7.75 and pH 7.54) based on the IPCC 'business-as-usual' scenario of the predicted reduction of 0.3-0.5 pH units from the present day average of pH 8.05 in oceanic surface waters by 2100 (Table 2.1) (IPCC, 2013). The third was a pH control as the seawater remained at ambient pH (pH 8.05). As a concurrent 2°C increase in temperature is expected to occur alongside this forecasted decrease in pH by the end of the century (Mitchell et al., 1998), these three systems were maintained at 2°C throughout the experiment. The fourth remaining system was a temperature control which was held at the present day average summer surface seawater temperature for Ryder Bay, 0°C (Clarke et al., 2008). The average pH of this treatment was pH 7.98 which was slightly lower than, but close to, the pH of the pH control treatment probably as a result of the increased solubility of CO<sub>2</sub> and carbonates (CO<sub>3</sub><sup>2-</sup>) in seawater at the lower temperatures.



**Figure 2.4 – Schematic of the Antarctic CO<sub>2</sub> microcosm with an 80 L header tank, two 20 L experimental tanks and a 120 L sump tank (adapted from Suckling, 2012). Arrows indicate direction of water flow.**

The pH of the acidified treatments was controlled by intermittently bubbling CO<sub>2</sub> gas through a ceramic diffuser to maintain the pH at the predetermined levels via a solenoid valve connected to an Aqua Medic pH controlled computer and glass electrode (with plastic shaft) system. The pH control treatment had a similar set up but without the pH control system. An Aqua Medic Ocean Runner power head 2000 circulated the seawater in the mixing tank to ensure a constant pH. Seawater was then gravity fed from each mixing tank at a rate of  $0.65 \pm 0.03 \text{ L min}^{-1}$  into the experimental tanks. Seawater temperature was manipulated by the use of temperature-controlled laboratories. Air temperature was maintained at  $-2.5^{\circ}\text{C}$  in the laboratory with the pH control and both lowered pH treatments but the lifting pumps (Aqua Medic Ocean Runner 3500) and the mixing power heads (Aqua Medic Ocean Runner 2000) in each treatment's mixing tank caused the seawater temperature to be raised to the desired  $\sim 2^{\circ}\text{C}$ , with little variability (Table 2.1). The temperature control treatment was situated in the main BAS aquarium where the air temperature was set at  $-1.5^{\circ}\text{C}$  and the absence of lifting and circulating pumps caused the seawater temperature to be maintained at  $\sim 0^{\circ}\text{C}$ .

**Table 2.1 - Mean ( $\pm$  SD) seawater parameters in all four treatments during the 7 month experiment following the format recommended by Barry et al. (2010). Values for  $p\text{CO}_2$ ,  $\Omega$  calcite and  $\Omega$  aragonite were calculated from CO2SYS (Lewis et al., 1998) with refitted constants (Mehrbach et al., 1973; Dickson & Millero, 1987).**

Seawater Parameter	Temperature control	pH Control	pH 7.75	pH 7.54
$\text{pH}_{\text{NIST}}$	$7.98 \pm 0.02$	$8.05 \pm 0.03$	$7.75 \pm 0.03$	$7.54 \pm 0.03$
$p\text{CO}_2$ ( $\mu\text{atm}$ )	$417 \pm 15$	$365 \pm 67$	$725 \pm 133$	$1221 \pm 179$
$\Omega$ Calcite	$1.20 \pm 0.10$	$1.49 \pm 0.15$	$0.78 \pm 0.11$	$0.50 \pm 0.10$
$\Omega$ Aragonite	$0.75 \pm 0.06$	$0.94 \pm 0.10$	$0.49 \pm 0.07$	$0.32 \pm 0.06$
Temperature ( $^{\circ}\text{C}$ )	$-0.3 \pm 0.1$	$1.7 \pm 0.3$	$1.9 \pm 0.4$	$2.2 \pm 0.4$
Salinity	$35 \pm 1$	$35 \pm 1$	$35 \pm 1$	$35 \pm 1$

Seawater temperatures ( $^{\circ}\text{C}$ , Digital Testo 106) and  $\text{pH}_{\text{NIST}}$  (Aquamedic pH controlled computer and electrode system) were monitored and recorded daily.  $\text{pH}_{\text{NIST}}$  was also more accurately measured ( $\pm 0.01$  pH units) once a week with a temperature compensated HANNA bench top meter pH/ORP 115 v pH21-01). Salinity (Tropical Marine Centre V2 Handheld refractometer),  $\text{TCO}_2$  ( $\text{mmol L}^{-1}$ ; Ciba Corning  $\text{TCO}_2$  Analyzer 965, Olympic Analytical, UK) and nutrient content (silicate and phosphate; according to methods in Nickell et al. (2003)) of each treatment were also measured weekly. Twice a week, the Aqua Medic pH probes were calibrated with NIST certified pH buffers. Other carbonate system parameters, including the partial pressure of  $\text{CO}_2$  ( $p\text{CO}_2$ ) and the saturation values for calcite ( $\Omega_{\text{C}}$ ) and aragonite ( $\Omega_{\text{A}}$ ), were modelled from applying  $\text{TCO}_2$  and  $\text{pH}_{\text{NIST}}$  data to the program CO2SYS (Lewis et al., 1998) with refitted constants (Mehrbach et al., 1973; Dickson & Millero, 1987). Brachiopods in each treatment were fed weekly with microalgal concentrate of approximately  $331 \times 10^4$  cells  $\text{L}^{-1}$  which is within the natural range of phytoplankton cell abundance along the west Antarctic Peninsula ( $62\text{--}1150 \times 10^4$  cells  $\text{L}^{-1}$ ; Garibotti et al., 2003, 2005). Water quality was maintained and alkalinity and other ions replenished through water changes twice a week and weekly siphoning of the aquaria to remove any debris.

#### 2.2.2.2 Temperate experiment

The temperate experiment was conducted in a flow-through  $\text{CO}_2$  perturbation system which involved *C. inconspicua*, *L. neozelanica* and *N. nigricans*. Seawater pumped from Otago Harbour passed through sand filters ( $50 \mu\text{m}$ ) and a finer cartridge filter ( $5\text{--}10 \mu\text{m}$ ) before entering the system (Figure 2.5). Three treatments were used; a control at the average local

current  $pH_{NIST}$  (8.1), the predicted oceanic pH for 2050 (pH 7.8) and the predicted pH for 2100 (pH 7.6) according to the IPCC ‘business-as-usual’ scenario of the forecasted reduction of 0.3-0.5 pH units (IPCC, 2013) with three replicate 10 L tanks for each treatment. The pH of the acidified treatments was lowered in header tanks by intermittently bubbling  $CO_2$  gas through a ceramic diffuser to maintain the pH at predetermined levels via a solenoid valve connected to a TUNZE 7070/2 pH controlled computer and electrode system. The experimental pH control system had an identical set up except that it lacked  $CO_2$  injection. A circulating pump in each mixing header tank ensured a constant pH. This set up previously provided stable pH conditions over > 200 days (Cunningham et al., 2016). Seawater was gravity fed from each header tank at a rate of  $1.05 \pm 0.05 \text{ L min}^{-1}$  into the experimental tanks.

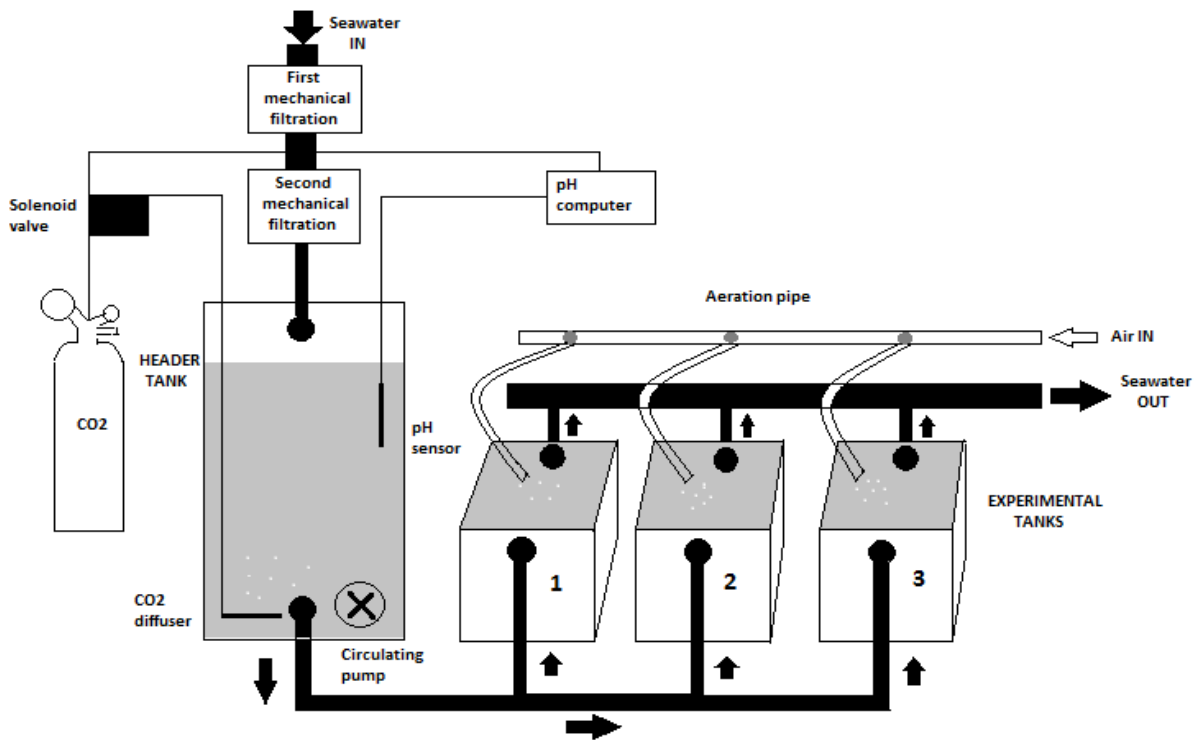


**Figure 2.5 – Schematic of the flow-through New Zealand  $CO_2$  perturbation system with an 80 L header tank and three 10 L experimental tanks. Arrows indicate the direction of water flow.**

Seawater temperature was not manipulated and was ambient for Otago Harbour. It was measured up to three times a day ( $^{\circ}C$ , Digital Testo 106) with only small differences ( $< 0.5^{\circ}C$ ) between treatments (Table 2.2) and no variation between replicate tanks in each treatment. Flow rate was also checked three times per day as was the computer controlled pH.  $pH_{NIST}$  was measured in each treatment tank accurately ( $\pm 0.01$  pH units) twice weekly with a EUTECH instruments pH 5-10 pH/mV/ $^{\circ}C$  meter and calibrated with pH buffers of pH 4.0, 7.0 and 9.2 (Pro-analys, Biolab, New Zealand). Salinity was measured once a week using a YSI data logger. A water sample from each treatment was fixed with saturated mercuric

chloride (HgCl<sub>2</sub>) at the beginning, middle and end of the experiment. DIC (dissolved inorganic carbon) and total alkalinity were later determined from these samples by a Single Operator Multi-parameter Metabolic Analyser (SOMMA) and closed-cell potentiometric titration, respectively (Dickson et al., 2007). Other carbonate system parameters, including the partial pressure of CO<sub>2</sub> (*p*CO<sub>2</sub>) and the saturation values for calcite ( $\Omega_C$ ) and aragonite ( $\Omega_A$ ) were calculated using CO<sub>2</sub>calc (Robbins et al., 2010). Seawater properties were determined using CO<sub>2</sub> equilibrium constants from Mehrbach et al. (1973) refitted by Dickson & Millero (1987) as recommended by (Wanninkhof et al., 1999). Brachiopods were fed three times a week with microalgal concentrate of approximately 397 x 10<sup>4</sup> cells mL<sup>-1</sup> of *Tetraselmis* spp., which is within the natural range of phytoplankton cell abundance in Otago Harbour. Faeces and other debris were removed twice weekly by siphon.

**Table 2.2 - Mean ( $\pm$  SD) seawater parameters in all three treatments during the 12 week experiment following the format recommended by Barry et al. (2010). Values for *p*CO<sub>2</sub>,  $\Omega$  calcite and  $\Omega$  aragonite were calculated using CO<sub>2</sub>calc (Robbins et al. 2010) with refitted constants (Mehrbach et al. 1973; Dickson & Millero 1987) as recommended by Wanninkhof et al. (1999).**

Seawater parameter	pH control	pH 7.8	pH 7.6
pH <sub>NIST</sub>	8.16 $\pm$ 0.03	7.79 $\pm$ 0.06	7.62 $\pm$ 0.05
DIC ( $\mu$ mol kg <sup>-1</sup> )	2082.8 $\pm$ 22.0	2211.4 $\pm$ 8.3	2252.4 $\pm$ 25.3
Alkalinity ( $\mu$ mol kg <sup>-1</sup> )	2278.5 $\pm$ 18.8	2269.7 $\pm$ 9.2	2271.9 $\pm$ 6.5
<i>p</i> CO <sub>2</sub> ( $\mu$ atm)	464.8 $\pm$ 82.8	1130.2 $\pm$ 11.8	1535.6 $\pm$ 234.8
$\Omega$ Calcite	3.5 $\pm$ 0.5	1.6 $\pm$ 0.0	1.3 $\pm$ 0.2
$\Omega$ Aragonite	2.2 $\pm$ 0.3	1.0 $\pm$ 0.0	0.8 $\pm$ 0.1
Temperature (°C)	16.5 $\pm$ 1.7	16.9 $\pm$ 1.7	16.6 $\pm$ 1.7
Salinity	33.9 $\pm$ 0.2	33.9 $\pm$ 0.2	33.9 $\pm$ 0.2

### 2.2.3 Growth rates

One hundred and eleven *L. uva* specimens across a wide size range (2.6-40.9 mm length (maximum shell dimension)) comprising clumps with a varying number of individuals in each conspecific clump (30 clumps with 2-15 individuals and 20 single specimens) were used in the polar experiment. Prior to the beginning of the experiment, shell lengths of each individual in each clump were measured to the nearest 0.1 mm using Vernier calipers. Clumps were placed into one of the four treatments ensuring there was a similar size range of specimens, numbers of conspecific clumps and single individuals in each treatment. The

experiment began in mid June 2012 and lasted for 7 months. At the mid-way and end of the experiment, the length of each specimen was measured again, recorded and the shell edge photographed. Growth rates ( $\mu\text{m day}^{-1}$ ) were then calculated from the increase in length.

One hundred and twenty three *C. inconspicua* specimens between 0.7-14.5 mm length (Figure 2.6), one hundred and forty eight *L. neozelanica* specimens between 1.7-44.9 mm length and one hundred and eight *N. nigricans* individuals between 1.4-18.5 mm length were used in the temperate experiment. At the start of the experiment, shell lengths of each individual  $> 3$  mm in length were measured to the nearest 0.1 mm using Vernier calipers. For individuals  $< 3$  mm, shell lengths were measured on a graticule eyepiece in a field microscope. The conspecific clumps of each species were then divided evenly across all tanks ensuring a similar size range of specimens in each treatment. The experiment began in January 2013 and lasted for 12 weeks. After 6 weeks and at the end of the experiment, individual lengths were measured and the shell edge photographed. Growth rates were again calculated from the increase in length.

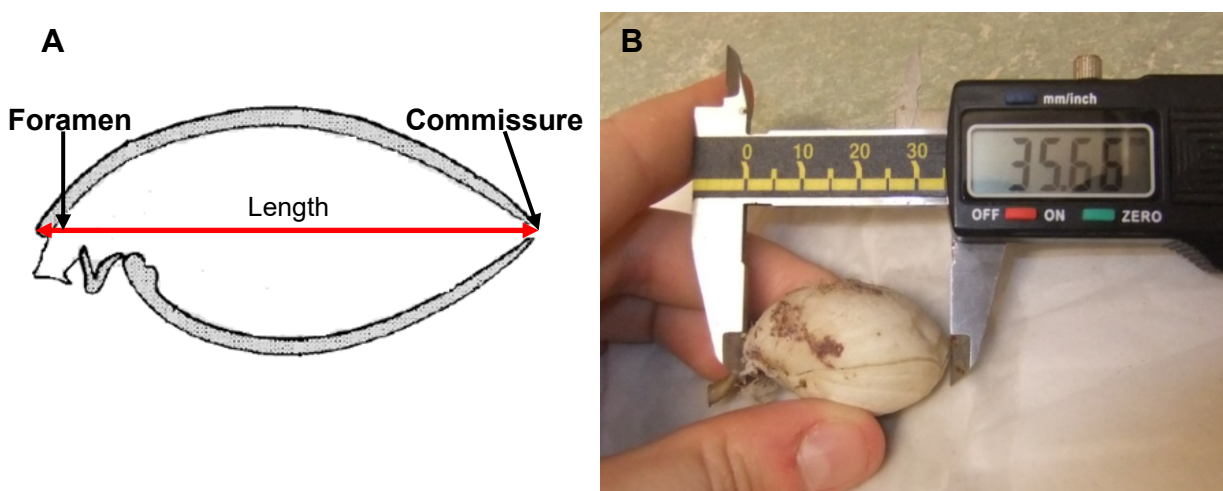


**Figure 2.6 – (A) Schematic of the length measurement defined as the measurement between the foramen and the commissure. (B) Vernier callipers were used to measure the morphometrics of each species.**

#### **2.2.4 Shell repair frequencies**

Forty two *L. uva* specimens (8-12 individuals in each treatment) of 5.0-37.0 mm length were selected at random and damaged by creating a 1-2 mm deep notch at the valve edge using a metal file. Care was taken to create notches of similar size and severity and not to break shells or cause other damage. This style of injury replicated damage seen in natural populations of

rhynchonelliform brachiopods and interpreted as indicative of either predator attacks or abiotic stresses (Harper et al., 2009). After 3.5 and 7 months of the experiment, lengths were measured for each specimen and the damaged region of the shell edge photographed.

The largest 10 or 11 *C. inconspicua* individuals (> 14 mm length), 15 *L. neozelanica* individuals (> 40 mm length) and 10 *N. nigricans* individuals (> 16 mm length) in each treatment were also damaged using a metal file creating a 1-2 mm deep notch at the valve edge. Again, notches of similar size and extent were made and care was taken not to break shells or cause other damage. After 6 and 12 weeks, the damaged section of each shell edge was photographed.

### **2.2.5 Statistical analyses**

All data were analysed using Minitab (Statistical Software™ Version 15). Growth rate data in each treatment for both *L. uva* and *C. inconspicua* were all significantly different from normal (Anderson-Darling Test;  $p < 0.008$ ). These data were still not normally distributed after square root, logarithmic or double logarithmic transformations because of the presence of zeros in the dataset. Non-parametric Kruskal-Wallis tests were thus used to determine whether treatment affected growth rates in *L. uva* and *C. inconspicua* and whether damage affected growth rate in each treatment in *L. uva*. When significant differences were found in the different data sets, further Kruskal-Wallis Multiple Comparison tests were used to identify which treatments were different from each other. Chi-squared tests were used to determine if treatment affected the percentage of individuals that had completed shell repair and the percentage of undamaged individuals that did not grow throughout the experiment in *L. uva*, *C. inconspicua*, *L. neozelanica* and *N. nigricans*. Chi-squared tests were also performed to reveal if treatment affected the percentage of *L. uva* individuals that had produced shell after fully repairing their notch.

## **2.3 Results**

### **2.3.1 Saturation states**

Throughout the polar 7 month experiment, the saturation states of aragonite and calcite were close to, but just below the range usually reported for polar shallow coastal seawater (Table 2.1; Barry et al. (2010)). In both controls, aragonite was slightly undersaturated ( $\Omega < 1$ )

whereas calcite was supersaturated ( $\Omega > 1$ ). Saturation states with respect to aragonite and calcite in every other treatment were undersaturated (Table 2.1). The order of treatments with decreasing saturation state with respect to calcite was pH control > temperature control > pH 7.75 > pH 7.54.

In the temperate experiment, all seawater parameters in the control were within the ranges reported for shallow surface seawater (Table 2.2; Barry et al. (2010)) although seawater temperature was unusually high for Otago Harbour in January-April 2013 (M. Lamare, pers. obs.) and slightly above the reported range of 6.4-16.0°C (Roper & Jillett, 1981; Greig et al., 1988). Saturation states with respect to calcite and aragonite in both acidified treatments were just below the reported shallow surface seawater values ( $\Omega < 1.9$  and  $\Omega < 1.2$ , respectively), however, calcite was supersaturated ( $\Omega > 1$ ) in both treatments and aragonite was supersaturated in pH 7.8 but undersaturated ( $\Omega < 1$ ) in the pH 7.6 treatment.

### **2.3.2 Mortality**

Despite the potentially challenging conditions in both experiments, mortality in *L. uva* across all treatments was low at 3.9% (total N = 155) with no differences between treatments (temperature control = 4% (n=3), pH control = 8% (n=2), pH 7.75 = 0% (n=0) and pH 7.54 = 4% (n=1)) and no mortality occurred in *C. inconspicua* in any treatment. Also, both these species showed none of the previously reported signs of stress (slow snapping responses, remaining closed for extended periods, wide gape when open; Peck (2001b)) and responded rapidly to physical stimulation when disturbed, throughout each experiment. A few females of *L. uva* in each treatment also managed to successfully complete brooding and release larvae with large numbers (up to 100) settling on shells of older brachiopods and continuing development to juveniles (Figure 2.7). Survival of these newly settled juveniles between 3 and 7 months was also high (> 90%).

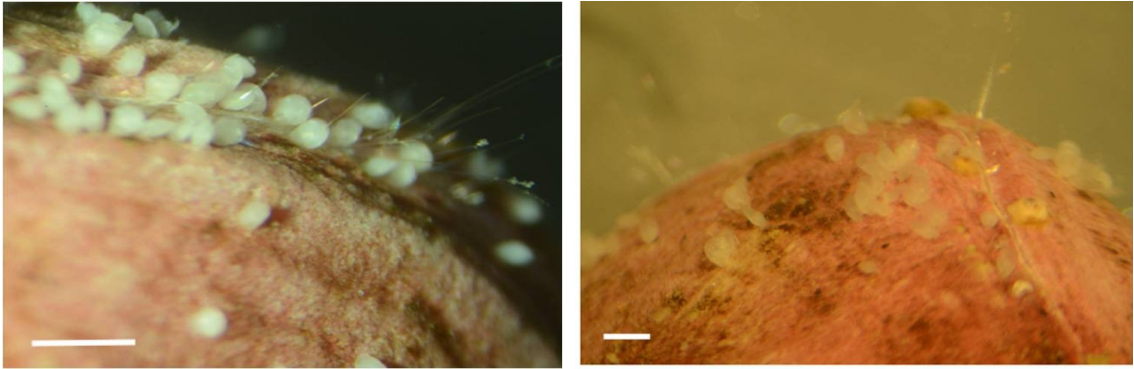


**Figure 2.7 – *L. uva* – Examples of larvae released during the experiment, settled on adult brachiopod shells and continuing development to juveniles after 3 months (A) and 7 months (B). Scale bar = 100  $\mu$ m.**

Mortality across all treatments in both *L. neozelanica* and *N. nigricans* was higher than *L. uva* and *C. inconspicua* at 8.8% (N = 193) and 18.8% (N = 138), respectively. Treatment did not affect mortality in *L. neozelanica* ( $\chi^2 = 2.889$ ,  $p = 0.236$ ), but acidified conditions affected mortality in *N. nigricans* ( $\chi^2 = 10.758$ ,  $p = 0.005$ ), with lower mortality in the most acidified treatment (Table 2.3). *L. neozelanica* and *N. nigricans* both showed all the reported signs of stress throughout the experiment (Peck, 2001b).

**Table 2.3 – Mortality in each species in every treatment at the end of each experiment. N denotes the total number of individuals in treatment.**

Experiment	Species	Treatment	Percentage of mortality
Polar	<i>L. uva</i>	Temperature control	4% (N=80)
		pH control	8% (N=25)
		pH 7.75	0% (N=24)
		pH 7.54	4% (N=26)
Temperate	<i>C. inconspicua</i>	pH control	0% (N=50)
		pH 7.8	0% (N=52)
		pH 7.6	0% (N=48)
	<i>L. neozelanica</i>	pH control	10% (N=62)
		pH 7.8	12% (N=69)
		pH 7.6	5% (N=62)
	<i>N. nigricans</i>	pH control	28% (N=47)
		pH 7.8	23% (N=40)
		pH 7.6	8% (N=51)

### 2.3.3 Shell repair frequencies

In the Antarctic *L. uva*, all damaged individuals had started shell repair after 3 months with > 50% of individuals fully repairing their notch across all treatments (Table 2.4). Following the completion of shell repair, > 33% of specimens had also produced new shell at the anterior margin (Figure 2.8). After 7 months, > 83% of individuals had completed shell repair in every treatment (Table 2.4) with no significant difference between treatments ( $\chi^2 = 0.839$ ,  $p = 0.840$ ). Punctae, shell perforations, which are part of the shell structure in most rhynchonelliform brachiopods, apart from the rhynchonellids, were present in all the repaired notches and the new shell growth (Figure 2.8I, J, K, L). A high proportion (> 64%) of specimens had also produced new shell at the growth margin in three of the four treatments, including in both acidified treatments. However, only a moderate proportion (38%) of specimens produced growth at the shell margin in the pH control treatment. Treatment affected the proportion of individuals that had continued shell production after the completion of repair ( $\chi^2 = 9.670$ ,  $p = 0.022$ ), however, a further Chi-squared test on the same dataset but excluding the pH control indicated there was no significant difference ( $\chi^2 = 0.815$ ,  $p = 0.665$ ). All individuals that had completed shell repair and then made new shell growth after 3 months continued to produce new shell after 7 months (Figure 2.8).

**Table 2.4 – *L. uva* – Shell repair frequencies and the proportion of specimens that had produced further shell growth after completion of shell repair after 3 and 7 months in the stated conditions. n denotes the number of individuals that had completed shell repair or produced further shell growth after completion of shell repair.**

Treatment	Number of individuals damaged at start of experiment	Length range of damaged individuals (mm)	Percentage of individuals that had completed repair		Percentage of individuals that had produced further shell growth after completion of repair	
			After 3 months	After 7 months	After 3 months	After 7 months
Temperature control	12	9.2-37.0 (mean = 22.3)	75% (n=9)	83% (n=10)	78% (n=7)	70% (n=7)
pH control	8	5.0-24.5 (mean = 15.5)	75% (n=6)	100% (n=8)	33% (n=2)	38% (n=3)
pH 7.75	10	11.0-27.7 (mean = 15.7)	50% (n=5)	90% (n=9)	60% (n=3)	78% (n=7)
pH 7.54	12	5.0-22.9 (mean = 12.6)	58% (n=7)	92% (n=11)	71% (n=5)	64% (n=7)

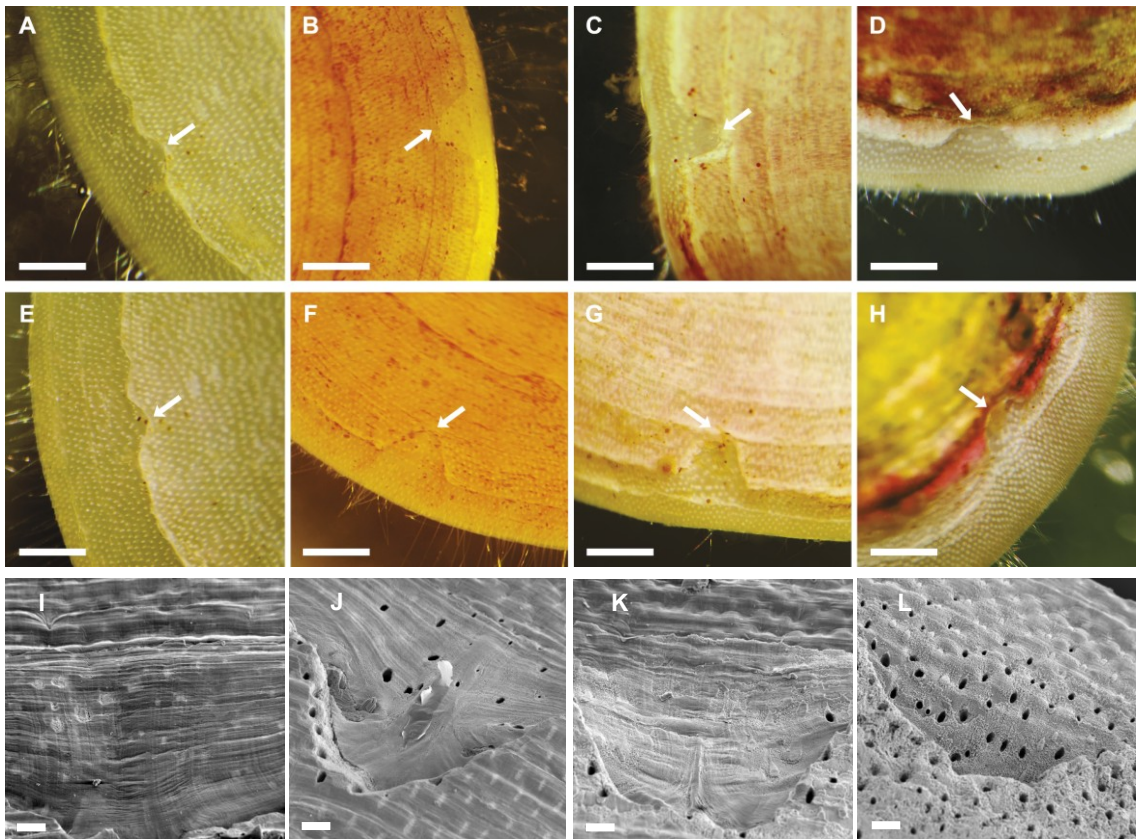


**Figure 2.8 – *L. uva* – Optical microscope images of shell repair and further shell growth in damaged individuals after 3 months (top row) and 7 months (middle row) and SEM micrographs of shell repair after 7 months (bottom row) in pH control (A, E, I), temperature control (B, F, J), pH 7.75 (C, G, K) and pH 7.54 (D, H, L). The same individual is shown for each treatment where the arrow indicates the notch created at the start of the experiment. Scale bar = 100  $\mu$ m.**

All damaged *C. inconspicua* had started to repair their notch after 6 weeks and > 36% of specimens had completed shell repair across all treatments (Table 2.5). Treatment had no effect on shell repair frequencies ( $\chi^2 = 1.714$ ,  $p = 0.424$ ). After 12 weeks, > 80% of individuals had fully repaired their notch in every treatment (Table 2.4; Figure 2.9) with only 3 individuals (1 specimen in pH 7.8 and 2 specimens in the pH 7.6 treatment) not completing shell repair. Treatment did not affect overall shell repair frequencies ( $\chi^2 = 1.173$ ,  $p = 0.556$ ) or the morphology of the shell repair (Figure 2.9D, E, F). Even though the majority of the damaged individuals managed to fully repair their shell, none of the large (> 14 mm length), notched individuals continued to produce new shell once the repair was complete.

**Table 2.5 – *C. inconspicua* – Shell repair frequencies after 6 weeks and 12 weeks in the stated conditions. n denotes the number of individuals that had completed shell repair.**

Treatment	Number of individuals damaged at the start of the experiment	Length range of damaged individuals (mm)	Percentage of individuals that had completed repair	
			After 6 weeks	After 12 weeks
pH control	11	14.2-17.8 (mean = 15.6)	36% (n=4)	100% (n=11)
pH 7.8	10	14.1-17.6 (mean = 15.8)	40% (n=4)	90% (n=9)
pH 7.6	10	14.1-17.5 (mean = 15.3)	50% (n=5)	80% (n=8)

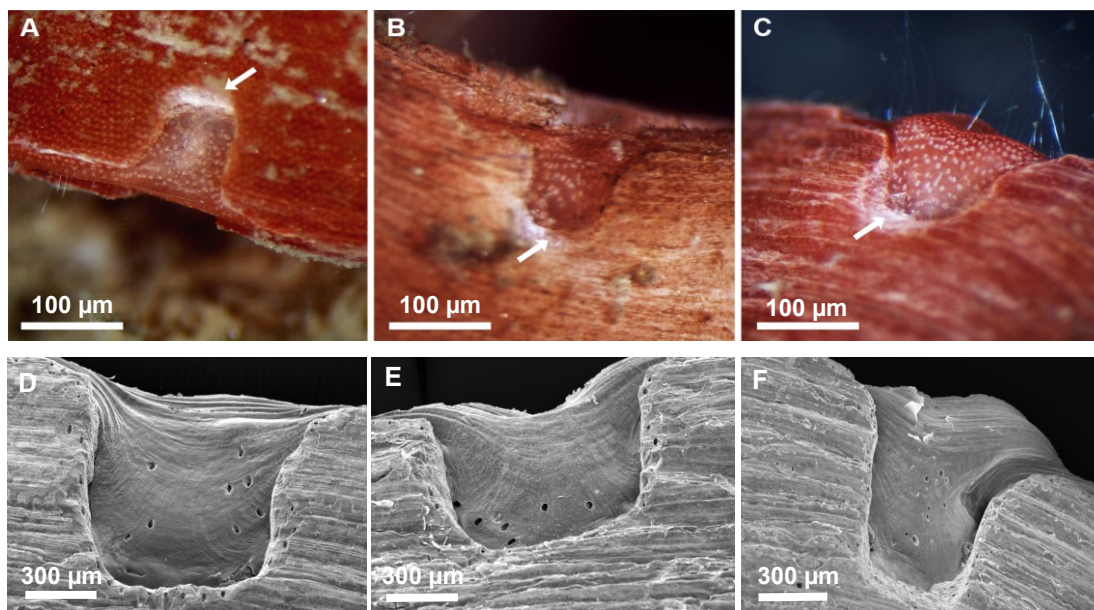


**Figure 2.9 – *C. inconspicua* – Examples of completed shell repair in damaged individuals after 12 weeks in the pH control (A, D), pH 7.8 (B, E), and pH 7.6 (C, F) treatment. The arrow indicates the notch created at the start of the experiment. Scale bars indicated.**

In *L. neozelanica*, > 80% of individuals in each treatment had started to repair their notch after 4 weeks, but no specimen had completed shell repair in any treatment (Table 2.6; Figure 2.10). After 10 weeks, only 40-47% of individuals in each treatment had completed shell repair and there was no effect of treatment on the ability to repair shell ( $\chi^2 = 0.458$ ,  $p = 0.795$ ). Of the individuals that did complete shell repair, none continued to produce new shell once the repair was complete.

**Table 2.6 – *L. neozelanica* – Shell repair frequencies after 4 weeks and 10 weeks in the stated conditions.**

Treatment	Number of individuals damaged at start of experiment	Length range of damaged individuals (mm)	Percentage of individuals that had completed repair	
			After 4 weeks	After 10 weeks
pH control	15	42.9-55.9 (mean = 46.8)	0%	47% (n=7)
pH 7.8	13	45.4-51.9 (mean = 47.9)	0%	46% (n=6)
pH 7.6	15	41.1-50.8 (mean = 46.4)	0%	40% (n=6)

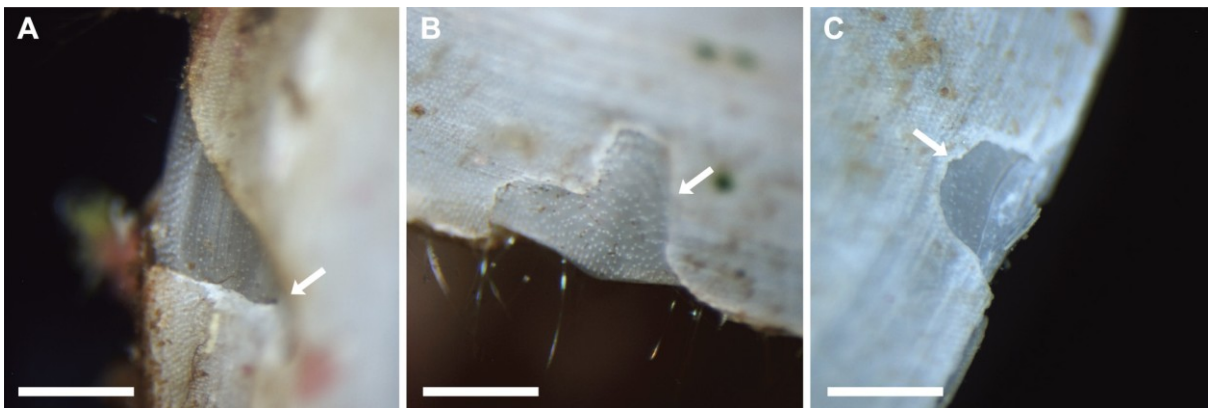


**Figure 2.10 – *L. neozelanica* – Examples of completed shell repair in damaged individuals after 10 weeks in the pH control (A), pH 7.8 (B) and pH 7.6 treatment (C). The arrow indicates the notch created at the start of the experiment. Scale bar = 100  $\mu$ m.**

In *N. nigricans*, > 80% of specimens in each treatment had started shell repair after 3 weeks, but no individuals had completed shell repair in any treatment (Table 2.7; Figure 2.11). After 9 weeks, only 50% of individuals in each treatment had fully completed repairing their shell across all treatments, with no effect of treatment on the ability to repair shell. Again, of the individuals that did complete shell repair, none continued to produce new shell once shell repair was complete. It is noteworthy that shell repair proceeded differently in *N. nigricans* than the three terebratulid species investigated in this chapter. Images of incomplete shell repair after 3 weeks (Figure 2.11A, B, C) demonstrate that the shell is repaired from the side of the notch first then both sides join to fully repair the notch. This is in contrast to repairs in the terebratulids which lay down new shell to repair the damage from the base of the notch to the shell margin (Figures 2.8-2.10).

**Table 2.7 – *N. nigricans* – Shell repair frequencies after 3 weeks and 9 weeks in the stated conditions.**

Treatment	Number of individuals damaged at start of experiment	Length range of damaged individuals (mm)	Percentage of individuals that had completed repair	
			After 4 weeks	After 10 weeks
pH control	10	17.3-21.3 (mean = 18.8)	0%	50% (n=5)
pH 7.8	10	16.6-21.7 (mean = 18.1)	0%	50% (n=5)
pH 7.6	10	18.0-20.5 (mean = 18.9)	0%	50% (n=5)

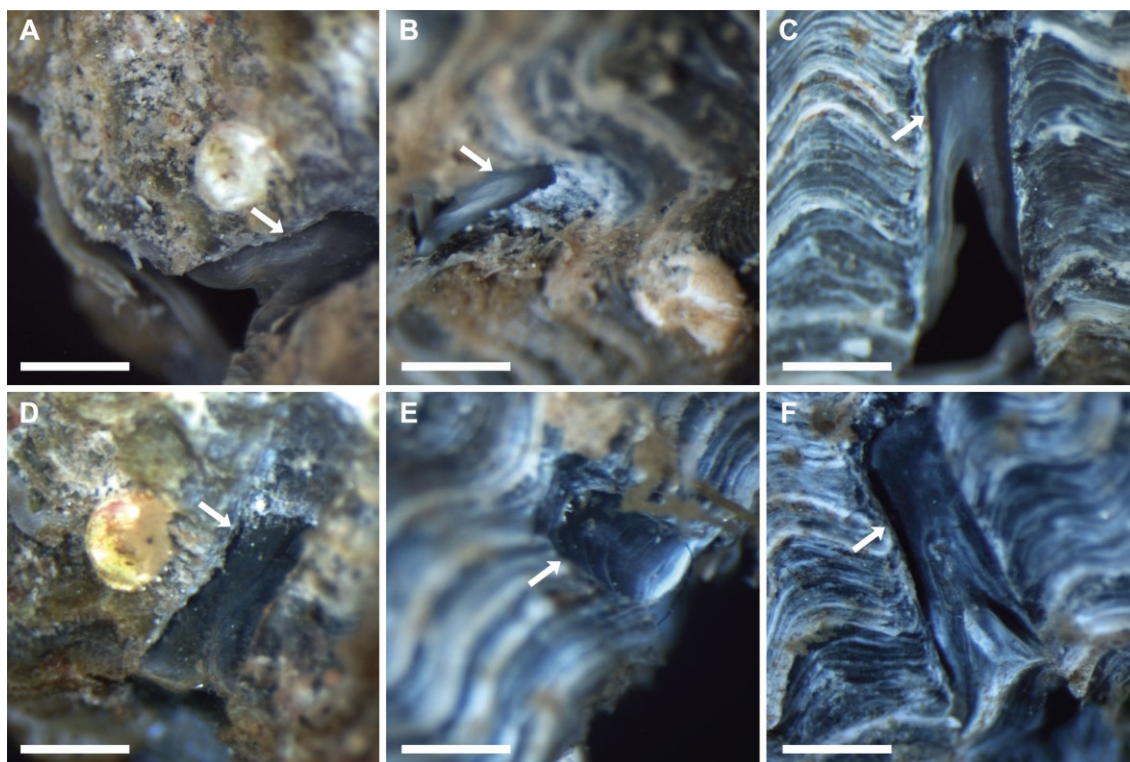


**Figure 2.11 – *N. nigricans* – Examples of completed shell repair in damaged individuals after 3 weeks (top row) and 9 weeks (bottom row) in the pH control (A, D), pH 7.8 (B, E), and pH 7.6 treatment (C, F). The arrow indicates notch created at the start of the experiment. Scale bar = 100  $\mu\text{m}$ .**

### 2.3.4 Growth rates

In *L. uva*, the majority of the undamaged individuals, but not all, grew (Figure 2.12 and 2.13). In those that did grow, growth rates ranged from 2.4-33.7  $\mu\text{m day}^{-1}$  in all three treatments at the higher temperature (pH control, pH 7.75 and pH 7.54; Figure 2.12). However, growth rates in the lower temperature trial (temperature control treatment) were lower ranging from 1.2-13.2  $\mu\text{m day}^{-1}$  (Figure 2.13). The only clear ontogenetic trend in every treatment was that

individuals with initial lengths of  $> 32.0$  mm produced no growth. Growth rates of undamaged individuals in both the acidified treatments were not significantly different from the pH control (Kruskal-Wallis,  $H = 3.96$ ,  $p = 0.138$ ). A further Kruskal-Wallis test including the temperature control, showed a significant effect of treatment on the growth rate ( $H = 13.06$ ,  $p = 0.005$ ). A Kruskal-Wallis Multiple Comparisons test indicated that higher temperature increased the growth rate over the temperature control in two treatments (pH control:  $Z = 2.20$ ,  $p = 0.028$ ; pH 7.75:  $Z = 3.21$ ,  $p = 0.001$ ), but growth rate in the lowest pH treatment (pH 7.54) was not significantly different from the temperature control ( $Z = 0.93$ ,  $p = 0.352$ ). Damaged *L. uva* individuals that produced new growth at the shell margin, grew  $1.2$ - $23.1$   $\mu\text{m day}^{-1}$  across all treatments with no ontogenetic trend (Figure 2.12 and 2.13), and there was no effect of treatment on growth rate of damaged individuals (Kruskal-Wallis,  $H = 1.24$ ,  $p = 0.743$ ). Growth rates were not significantly different in damaged and undamaged individuals in any treatment (Temperature control –  $H = 0.24$ ,  $p = 0.623$ ; pH control –  $H = 2.82$ ,  $p = 0.093$ ; pH 7.75 –  $H = 3.96$ ,  $p = 0.046$ ; pH 7.54 –  $H = 0.06$ ,  $p = 0.807$ ). Treatment also had no detectable effect on the proportion of damaged or undamaged individuals that did not grow in the experiment ( $\chi^2 = 2.590$ ,  $p = 0.459$ ).

The majority of *C. inconspicua* individuals grew with growth rates ranging to  $> 15$   $\mu\text{m day}^{-1}$  in the pH control and the pH 7.6 treatment and up to  $10.70$   $\mu\text{m day}^{-1}$  in the pH 7.8 treatment (Figure 2.14). The only detectable ontogenetic trend was a slight decrease in growth rates for individuals  $> 10$  mm in length. Growth rates of undamaged individuals  $> 3$  mm in both acidified conditions were not significantly different from the pH control (Kruskal-Wallis,  $H = 4.04$ ,  $p = 0.133$ ). Whereas growth rates did differ among treatments in undamaged individuals  $< 3$  mm ( $H = 6.23$ ,  $p = 0.044$ ) and also when all undamaged individuals across the total size range were pooled ( $H = 7.90$ ,  $p = 0.019$ ). A further Kruskal-Wallis Multiple Comparison test on undamaged individuals  $< 3$  mm indicated that growth rates were higher in the most acidified treatment (pH 7.6) ( $Z = 2.488$ ,  $p = 0.013$ ) compared to the moderately acidified treatment (pH 7.8) but not in comparison to the pH control ( $Z = 0.826$ ,  $p = 0.409$ ). Growth rates of undamaged individuals  $< 3$  mm in the moderately acidified treatment were not significantly different to the pH control ( $Z = 0.746$ ,  $p = 0.456$ ). A further Kruskal-Wallis Multiple Comparison test on all undamaged individuals indicated that in the most acidified treatment growth rates were higher than in the pH control ( $Z = 2.762$ ,  $p = 0.006$ ) but not in comparison to the moderately acidified treatment ( $Z = 1.918$ ,  $p = 0.055$ ). Growth rates of all undamaged individuals in the moderately acidified treatment were also not significantly

different to the pH control ( $Z = 0.980$ ,  $p = 0.327$ ). There was also no treatment effect on the proportion of undamaged individuals that did not grow throughout the experiment ( $\chi^2 = 1.500$ ,  $p = 0.472$ ).

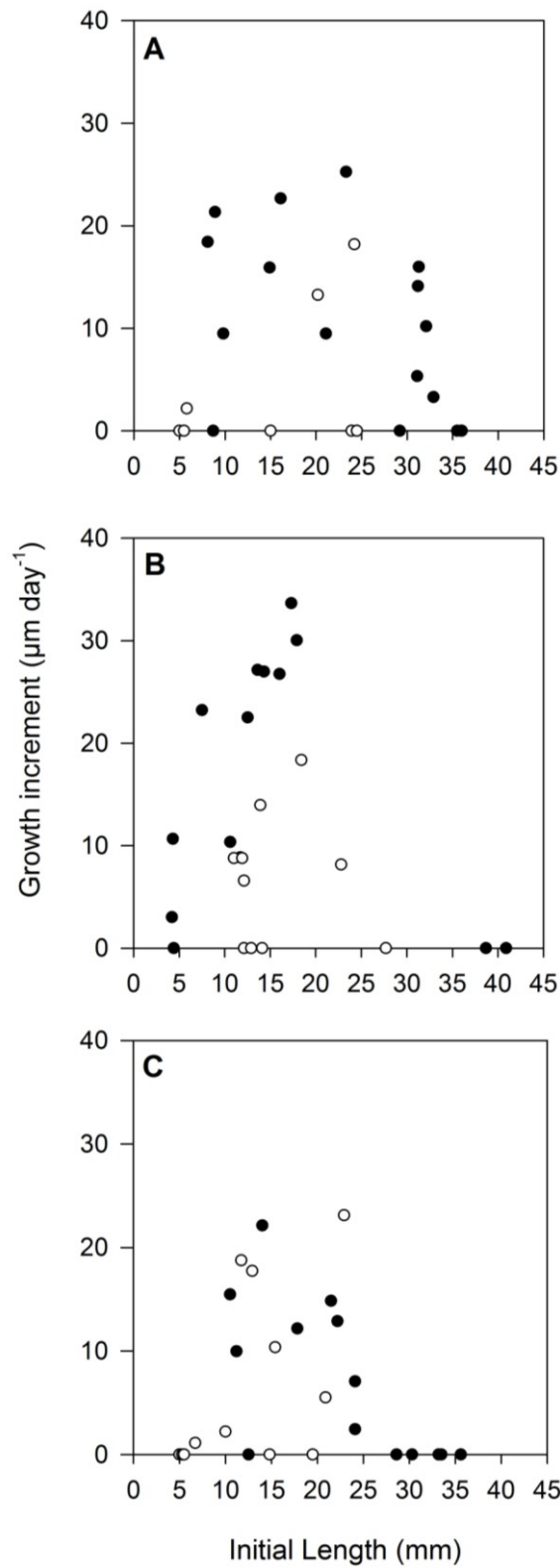


**Figure 2.12 – *L. uva* – Growth rates of specimens that were left undamaged (●) and were damaged at the start of the experiment (○) after 7 months in the treatments kept at the higher temperature; (A) pH control (pH  $8.05 \pm 0.03$ ,  $T = 1.7 \text{ }^\circ\text{C} \pm 0.3$ ), (B) pH 7.75 (pH  $7.75 \pm 0.03$ ,  $T = 1.9 \text{ }^\circ\text{C} \pm 0.4$ ) and (C) pH 7.54 (pH  $7.54 \pm 0.03$ ,  $T = 2.2 \text{ }^\circ\text{C} \pm 0.4$ ).**

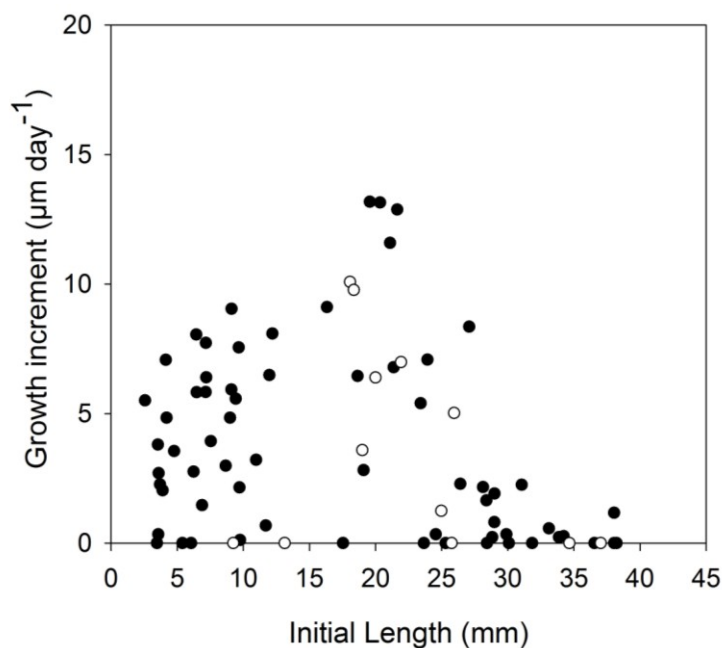


**Figure 2.13 – *L. uva* – Growth rates of specimens that were left undamaged (●) and were damaged at the start of the experiment (○) after 7 months in the low temperature control (pH  $7.98 \pm 0.02$ , T =  $-0.3 \text{ °C} \pm 0.1$ ).**

The majority of the undamaged *L. neozelanica* and *N. nigricans* specimens did not grow with very low growth rates in both species across all treatments. Only 15.3% of *L. neozelanica* and 6.8% of *N. nigricans* grew  $> 5 \text{ } \mu\text{m day}^{-1}$  during the 10 week and 9 week experiments, respectively. These low growth rates in addition to the higher mortality, reduced shell repair frequencies and prolonged signs of stress indicate that all individuals of both species were stressed throughout the experiment. Therefore, subsequent analysis on their shell characteristics is not considered representative of their response to acidified conditions. Thus these species have been removed from further analysis.

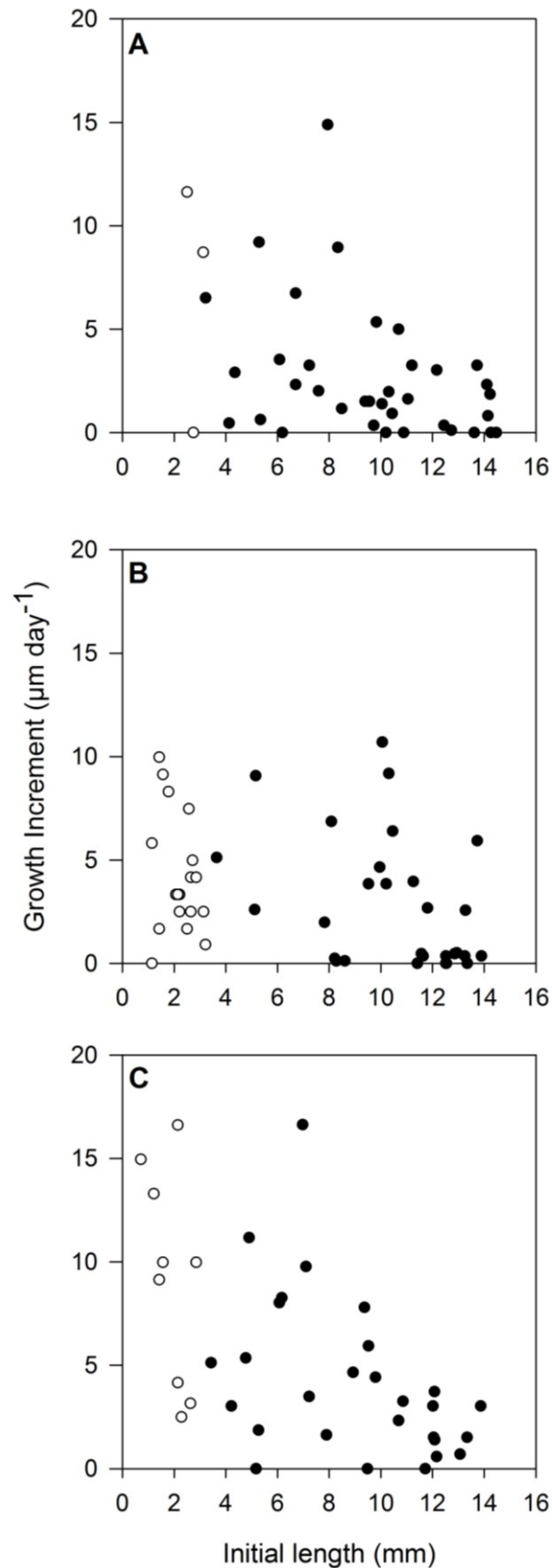


**Figure 2.14 – *C. inconspicua* – Growth rates of individuals < 3 mm (○) and > 3 mm (●) that were left undamaged at the start of the experiment after 12 weeks in (A) the pH control ( $\text{pH } 8.16 \pm 0.03$ ), (B) pH 7.8 ( $\text{pH } 7.79 \pm 0.06$ ), and (C) pH 7.6 ( $\text{pH } 7.62 \pm 0.05$ ) treatments. Different symbols have been used for individuals above and below 3 mm for the two different methods used.**

## 2.4 Discussion

All individuals of both *L. neozelanica* and *N. nigricans* were clearly stressed throughout their 9-10 week experiments. However, it is unlikely that this stress was caused by acidified conditions as every treatment had high mortality, low shell repair frequencies and low growth rates as well as prolonged signs of stress. Instead, it is likely that the stress came from transportation from the field collection site to the experimental laboratory and the holding conditions in the Portobello aquarium. Both these species were collected from Doubtful Sound on the southwest coast of New Zealand, which is a 5 hour drive from where the experiment was conducted in the Portobello Marine Laboratory, Otago Peninsula on the southeast coast of New Zealand. During transport, measures were taken to minimise stress such as replacing 50% of the seawater in the transport containers during the journey to replenish oxygen levels. On arrival at the Portobello Laboratory, specimens were placed in ambient aquarium conditions for 2-3 weeks to acclimate to the Otago Harbour environmental conditions. Seawater temperatures in the aquarium system were higher than expected at the beginning of the experiment because Otago Harbour was experiencing higher than usual summer temperatures (M. Lamare, pers. obs.). Therefore, it is likely that all individuals in every treatment were experiencing oxidative and temperature stress, which they did not recover from during the experiment. As a result, both species have been removed from further analysis.

The polar brachiopod *L. uva* and the temperate brachiopod *C. inconspicua* are clearly able to tolerate predicted 2050 and 2100 pH levels as specimens showed no signs of prolonged stress and mortality was low in *L. uva* at 3.9% and no mortalities occurred in *C. inconspicua*. A similar mortality rate of *L. uva* was recorded in a study of growth rates of this species in their natural habitat (2% yr<sup>-1</sup>; Peck et al. (1997)). Mortality rate in a similar ocean acidification study with the mollusc *Arctica islandica* was also low at 3.3% (Hiebenthal et al., 2012).

The ability of damaged *L. uva* to repair their shells was not affected by acidified conditions or temperature and > 90% of all injured specimens had completed shell repair and > 63% had continued shell deposition after completion of repair after 7 months. Acidified conditions also did not impact the ability of damaged *C. inconspicua* to repair their shell as > 80% of injured specimens in all treatments completed shell repair after 12 weeks. Shell repair and growth in the pH manipulated conditions was therefore not different to the controls in both the polar and

temperate brachiopod. This suggests that *L. uva* and *C. inconspicua* will be able to repair shell damage and continue to produce shell in the natural environment in the next 84 years. The Antarctic experiment was conducted over 7 months whereas the temperate experiment lasted 12 weeks, suggesting repair mechanisms may be faster in temperate brachiopods than Antarctic species as has been reported for growth (Peck et al., 1997; Baird et al., 2013). Growth and development in Antarctic marine invertebrates has recently been shown to be markedly slower than expected, or predicted from normal temperature effects on biological systems (Peck, 2016). Shell repair in the gastropod *Subninella undulata* was also unaffected by ocean acidification, however, the gastropod *Austrocochlea porcata* had a decreased shell repair rate suggesting a species-specific response of marine calcifiers in the ability to repair shell (Coleman et al., 2014). Shell repair rates in living brachiopods have previously only been investigated in purposely damaged specimens of the temperate brachiopod, *Terebratulina retusa*, in ambient seawater where shell repair began after four weeks and caeca developed after eight weeks (Alexander et al., 1992). This species had the ability to repair drill holes, slits and bevelled anterior shell regions but not the most severe damage of amputations of the anterior third of one valve (Alexander et al., 1992). All notches in both *L. uva* and *C. inconspicua* were made in the anterior margin where new shell is laid down, and so relatively easily repaired. The chemical environments differed between the treatments in each experiment, but this did not affect repair rate in either species, possibly reflecting an increase in the rate of shell regeneration in the altered pH conditions as seen in some other species (e.g. Wood et al., 2008). The majority of damaged *L. uva* also continued shell production after the completion of repair further demonstrating the tolerance of this species. No *C. inconspicua* laid down new shell after repairing their notch, even though the majority of the damaged individuals managed to repair their shell fully. This is probably a result of the wider size range (5.0-37.0 mm length) of *L. uva* used in comparison to only using large *C. inconspicua* (> 14 mm) in the temperate experiment. This size coincides with the reported 14-16 mm size of sexual maturity in *C. inconspicua* (Doherty, 1979; Lee & Wilson, 1979) indicating that growth rates were already low in these individuals due to a transfer of resources from somatic growth to reproduction. Therefore, once the critical process of repair was complete, these individuals were much less likely to grow than specimens of all ages included in the Antarctic experiment. Growth in undamaged reproductively mature individuals was low in both species (Figure 2.12 and Figure 2.13), furthering supporting this explanation. Shell repair in *N. nigricans* occurs from the sides of the notch as opposed to from the base of the notch in the other three species investigated in this chapter. This could be a result of phylogenetic differences between different orders of brachiopods as *N. nigricans* is a

rhynchonellid whereas *L. uva*, *L. neozelanica* and *C. inconspicua* are all in the order terebratulid. However, more research on multiple species from each order of brachiopods is needed to confirm this possible pattern.

Growth rates in both undamaged and damaged *L. uva* were not different among any of the treatments indicating that *L. uva* has the phenotypic plasticity to make shell in predicted end-century pH conditions without any genetic adaptation that may occur in the next 84 years. This species should, therefore, be able to continue shell production in the predicted future ocean acidification conditions even after the disturbance of completing repair to shell damage. Shell production in *C. inconspicua* should also be unaffected by changing pH levels in the natural environment up to the year 2100, as growth rates in undamaged individuals were either not affected (> 3 mm in length) or positively affected (< 3 mm in length) by acidified conditions. Other studies of shell growth in altered pH conditions, which have all been conducted on molluscs, have demonstrated mixed responses. Early studies showed reduced growth in two congeneric bivalves, *Mytilus galloprovincialis* (Michaelidis et al., 2005) and *M. edulis* (Berge et al., 2006), after medium-term exposure of 90 and 44 days, respectively. However, strongly acidified conditions as low as pH 7.3 (Michaelidis et al., 2005) and pH 6.7 (Berge et al., 2006) were used and no growth occurred in the latter. The negative effect in *M. edulis* started between pH 7.4 and pH 7.1 (Berge et al., 2006), a level which is below the range of pH used in the current work, but also well below the predicted end-century acidified oceans (IPCC, 2013). More recently, studies have predominantly used predicted mid and end-century pH levels (> pH 7.5). However, short or medium-term exposure (49-84 days, or less) is still generally the norm and this might not allow for phenotypic plasticity through acclimation to become effective, and does not incorporate other response mechanisms such as any trans-generational effects. Decreased growth rates in some molluscs (*Urosalpinx cinerea*, *Littorina littorea*, *Nucella lamellosa*) are still seen in more environmentally relevant experiments (Nienhuis et al., 2010; Ries et al., 2009). In contrast, lowered pH conditions have had no impact on growth rates in some molluscs (*Arctica islandica* and *Mytilus edulis*) (Hiebenthal et al., 2012; Ries et al., 2009; Thomsen et al., 2010) and *Crepidula fornicata* has even demonstrated a positive response to intermediate  $p\text{CO}_2$  levels (605 and 903 ppm) (Ries et al., 2009). An extensive study on 18 benthic marine calcifiers concluded that the effect of ocean acidification on the calcification process is species-specific (Ries et al., 2009). The ability of *L. uva* and *C. inconspicua* to continue shell production in low pH indicates that these species can generate suitable conditions at the site of calcification (Ries, 2011; Gazeau

et al., 2013; Wittmann & Pörtner, 2013). It is believed that marine calcifiers elevate pH in calcifying compartments to facilitate calcium carbonate precipitation, however, the mechanisms are largely unknown, especially in the less-studied taxa such as brachiopods. Potential methods are via either proton channelling (McConnaughey & Falk, 1991),  $\text{Ca}^{2+}$ -activated proton-translocating ATPase (McConnaughey & Falk, 1991; McConnaughey & Whelan, 1997; Cohen & McConnaughey, 2003), transcellular symporter and co-transporter proton-solute shuttling (McConnaughey & Whelan, 1997) or cellular extrusion of hydroxyl ions into the calcifying medium (Ries et al., 2009; Ries, 2011). Further research is needed to determine which mechanism is used in brachiopods, however, it is apparent that *L. uva* and *C. inconspicua* have a robust control of the calcification process similar to molluscs.

Increasing temperature to predicted end-century conditions alongside ocean acidification positively affected growth rates in *L. uva*. This suggests shell deposition could be faster in 50-100 years as a consequence of elevated temperatures despite the predicted fall in ocean pH. The long-term upper temperature tolerance limit of the Antarctic brachiopod is 4.5°C (Peck, 1989) and higher shell growth rates have been shown with increasing temperatures in other species (Almada-Vilela et al., 1982; Stor et al., 1982; Lewis & Cerrato, 1997). The data here show warming to 2°C does not have any negative impacts on shell growth rates. A warming to this level over the next 84 years is unlikely to negatively impact shell production in *L. uva*. Several ocean acidification studies have combined low pH with other environmental variables, especially temperature (Reynaud et al., 2003; Findlay et al., 2008; Martin & Gattuso, 2009; Rodolfo-Metalpa et al., 2011; Hiebenthal et al., 2012; Courtney et al., 2013; Wolfe et al., 2013; Hardy & Byrne, 2014; Hyun et al., 2014). Organism responses involving the interaction of temperature have both increased and decreased ocean acidification effects (Ericson et al., 2012; Ko et al., 2014), which has been found in closely related molluscs, *Mytilus edulis* and *M. galloprovincialis* (Rodolfo-Metalpa et al., 2011; Hiebenthal et al., 2012). Rodolfo-Metalpa et al. (2011) found a negative synergistic effect of low pH ( $\text{pH}_T$  7.4) and elevated temperature (25°C) on the gross calcification rate of *M. galloprovincialis* whereas Hiebenthal et al. (2012) reported acidified conditions ( $p\text{CO}_2$   $1093.3 \pm 123.6$   $\mu\text{atm}$  and  $1654.5 \pm 82.7$   $\mu\text{atm}$ ) did not impact shell growth of closely related *M. edulis* but elevated temperature did. Growth in *M. edulis* increased up to 20°C but then decreased at 25°C indicating that 25°C is above this species temperature threshold limit (Pörtner, 2008; Hiebenthal et al., 2012). Growth rates in the temperature control treatment here, which was used to compare the predicted scenarios to current Antarctic conditions, were in the same

range (0-15  $\mu\text{m day}^{-1}$ ) as individuals of the same size (2.5-40.9 mm) in a study of *L. uva* growth rates in the wild (Peck et al., 1997). Other variables included in multiple stressor ocean acidification studies are food availability and hypoxia which often have a greater effect on marine species than lowered pH (Rosa & Seibel, 2008; Thomsen et al., 2013), although some studies demonstrate an interactive effect (Reymond et al., 2013; Gobler et al., 2014). Thomsen et al. (2013) found that an abundant food supply outweighed ocean acidification effects on calcification and growth in *M. edulis*. Oxygen availability, along with temperature but not  $p\text{CO}_2$ , were also the dominating factors determining metabolic rate in the squid *Dosidicus gigas* (Rosa & Seibel, 2008).

Even though brachiopods have possibly the largest proportion of skeleton to tissue mass of any group (Peck, 1993), data in this chapter show that both polar (*L. uva*) and temperate (*C. inconspicua*) brachiopods can survive, repair shell damage and deposit new shell after 7 months and 12 weeks exposure, respectively, to forecasted 2050 and 2100 pH conditions. *L. uva* has the additional challenge of inhabiting the Southern Ocean which has the globally lowest carbonate ion saturation levels, further indicating the tolerance of this species. Studies reporting resilience of marine species to ocean acidification are increasing, especially with the wider use of longer term experiments which allow for acclimation and adaptation (Hazan et al., 2014; Suckling et al., 2014; Queirós et al., 2015; Cross et al., 2015, 2016). There may, however, be a cost to this apparent resilience under future climate change scenarios. The ophiuroid brittlestar, *Amphiura filiformis*, increased its metabolism and calcification to compensate for increased seawater acidity, which came as a substantial cost as muscle wastage was reported to coincide with this increase (Wood et al., 2008). Therefore, further research is essential to determine whether these brachiopods will be able to continue to produce the same shell and maintain their shell integrity as well as maintaining all other critical biological functions for even longer term survival than that studied here under changing environmental conditions.



## Chapter Three

# Do polar and temperate brachiopods produce the same shell structurally and elementally under forecasted end-century acidified conditions?

### 3.1 Introduction

Robust external skeletons are crucial to the survival of shell-bearing organisms due to the protection the shell provides from abiotic and biotic stresses. The shell microstructure of both *L. uva* and *C. inconspicua* consists of an outer periostracum, a nanocrystalline inner primary layer and an inner fibrous secondary layer (Williams, 1968a,b; Williams, 1997; Goetz et al., 2009). The primary layer consists of nano- to micro-sized calcite crystallites, and is the only shell layer where growth lines persist. The secondary layer below is constructed of thin, long monocryalline calcite fibres, organised in a stacked array just below the primary layer, with a section below this of disorientation with the calcite fibres occurring in different directions (Figure 3.1; Williams, 1968a; Goetz et al., 2009). Increased disorientation occurs in *L. uva* compared to other brachiopods from less extreme habitats, such as *Terebratalia transversa* (Griesshaber et al., 2007) and *Notosaria nigricans* (Griesshaber et al., 2008), which often display large stacks or layers of parallel fibres (Goetz et al., 2009). To date, no studies of brachiopod shell microstructure have investigated any effects of environmental fluctuations, therefore, the ability of these highly calcium carbonate dependent organisms to produce the same shell structurally under predicted end-century acidified and warming conditions remains unknown.

Most living brachiopods, except the rhynchonellides, are characterised by conspicuous microscopic perforations called punctae that extend from the inner to outer surfaces of the shell (Figure 3.2). Punctae link the outer mantle epithelium and connective tissue with the periostracum, by papillose mantle extensions called caeca (Williams, 1968c; MacKinnon & Williams, 1974; Williams, 1997; Perez-Huertes et al., 2008). Each caecum inside each puncta is separated from the periostracum by a brush-like structure comprising fine, hollow, tubular extensions of a proteinaceous membrane (Owen & Williams, 1969; Rudwick, 1970; Williams,

1997; Pérez-Huerta et al., 2009). Membrane secretions, lipids, proteins and polysaccharides are present within each puncta (Williams, 1997). Punctae persist through both the primary and secondary layers of the shell, becoming narrower proximally due to the thickening of the secondary layer (Williams, 1997). Punctae also deflect the calcite fibres in the secondary layer (Figure 3.1). Punctal morphology is species-specific (Pérez-Huerta et al., 2009) with punctae in *C. inconspicua* and *L. neozelanica*, a close relative of *L. uva*, described as simple cylindrical structures that curve in the posterior end of the shell (MacKinnon & Williams, 1974; Pérez-Huerta et al., 2009). The distribution of punctae is essentially regular with the arrangement in terebratulides defined as being arranged at intervals of about 45  $\mu\text{m}$  in a dominantly hexagonal, close packing pattern (Cowen, 1966; Owen & Williams, 1969; Williams, 1973; Williams, 1997). Densities of punctae vary between species, and this character has been extensively used in species identification (Foster, 1974).

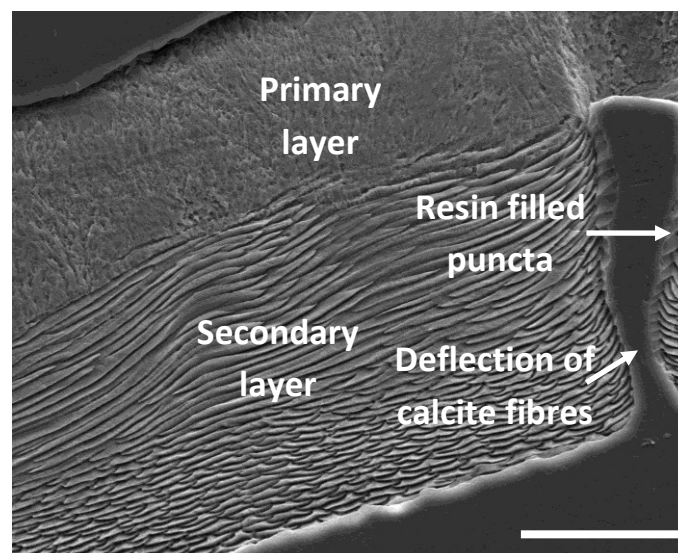


**Figure 3.1 - Scanning electron micrograph of a cross section of *L. uva* illustrating the rhynchonelliform brachiopod shell layers and the deflection of calcite fibres in the secondary layer caused by punctae. Scale bar = 50  $\mu\text{m}$ .**

Punctae are one of the most characteristic features of the shell structure of rhynchonelliform brachiopods and even though a significant proportion (70-80% in 5-7 mm length individuals and 30-45% in 25 mm length individuals (Peck et al., 1987a)) of the soft tissue of the animal is situated within them, their role is still undetermined. Suggested functions are sensory (Sollas, 1886), storage (Owen & Williams, 1969; Curry & Ansell, 1986; Curry, 1983a; Pan & Watabe, 1988; Curry et al., 1989) and in respiration (Thayer, 1986; Shumway, 1982). The early idea that punctae are sensory devices was dismissed as many punctate species are heavily encrusted with other organisms and punctae do not have direct contact with the exterior due to the periostracum overlaying the whole shell surface. Furthermore, punctae

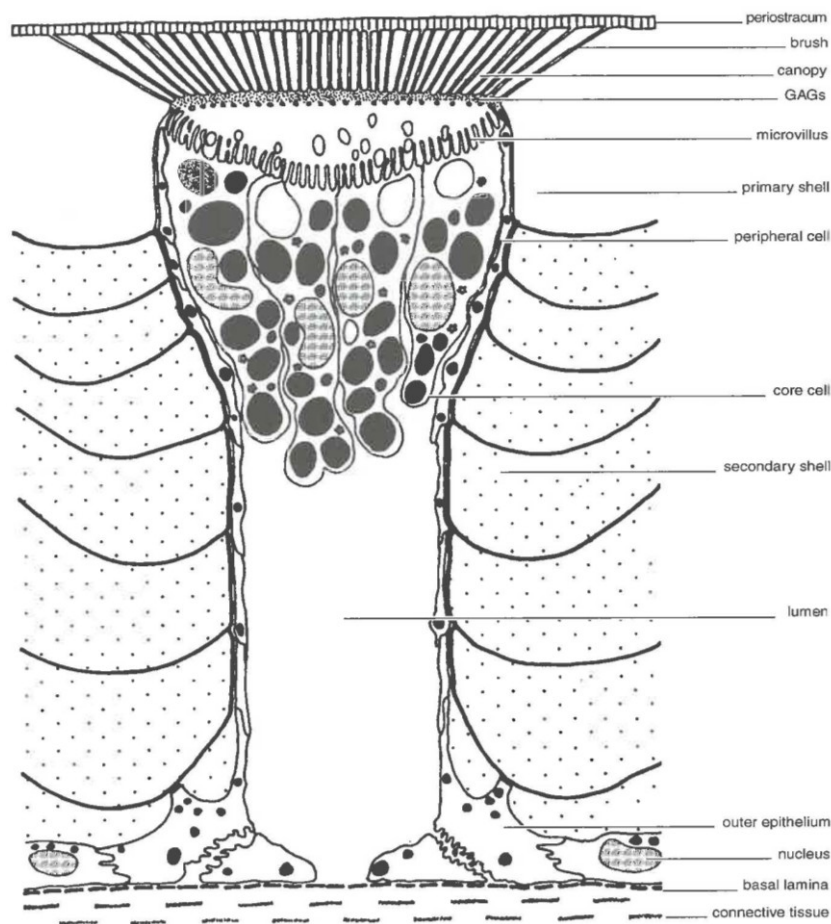


**Figure 3.2 - Diagram of cross section of terebratulide puncta and caecum showing the relation to shell and mantle (Williams, 1997).**

lack any obvious receptors, pigment spots or nerve endings (Rudwick, 1970) so are unlikely to be sensory devices. Caeca mainly consists of core cells, situated just below the brush-like structure, which contain glyco- and mucoproteins with some protein, glycogen and a small amount of lipid (Owen & Williams, 1969), supporting the idea that punctae serve as storage compartments. Although, this idea is questionable as the only function as punctal morphology varies markedly amongst terebratulide brachiopods (Pérez-Huerta et al., 2009), yet recent rhynchonelliform brachiopods have similar metabolic and physiological requirements (Peck, 2008). Punctae could also aid in respiration. Originally they were thought to act as avenues for diffusion to the inner mantle tissues potentially enabling their wide distribution in various environments with differing oxygen availabilities (Shumway, 1982; Thayer, 1986). However, the periostracum and/or encrusting organisms overlaying punctae would also limit this oxygen diffusion. Peck et al. (1986a,b) reported decreased oxygen tension resulting in the animal switching to anaerobic metabolism in experiments monitoring the oxygen tension within the mantle cavity of closed brachiopods. This demonstrated that diffusion through caeca does not provide a significant amount of oxygen to the mantle tissues. Peck et al.

(1986a) concluded that caeca absorb enough oxygen to meet the respiratory demands of the caecal tissue itself, which could represent a significant proportion of the total respiratory requirement of the animal. This could explain the variation in punctal morphology between brachiopods living in environments with different oxygen availability as different surface areas of punctae would be required to provide enough oxygen to the caeca (Pérez-Huerta et al., 2009). Even though the function of punctae remains in dispute, punctae house extensions of the soft tissue of the animal which accounts for a large portion of the tissue mass of punctate brachiopods. Therefore, any modification to the density or size of punctae could have an effect on their defence against increasing ocean acidity and seawater temperatures.

Rhynchonelliform brachiopods contain low Mg-calcite where some of the calcium ions have been replaced by magnesium ions in the calcite lattice (Chave, 1952; Brand et al., 2003; Andersson et al., 2008). Substitution of calcium ions with much smaller magnesium ions in a random fashion causes variations in the mineralogical structure such as a disorder of carbonate anion and cation positions in comparison with pure calcite (Reeder, 1983; Tribble et al. 1995). This results in Mg-calcite being less thermodynamically stable than pure calcite. However, low Mg-calcite is considered to be less susceptible to diagenetic alteration than other calcium carbonate polymorphs (Brand et al., 2003), which coupled with the extensive geological record of brachiopods has enabled this phylum to be extensively used as proxies to reconstruct ancient ocean conditions (Lowenstam, 1961; Veizer et al., 1986; Bates & Brand, 1991; Brand et al., 2003). These studies assume that brachiopod shell calcite is precipitated in near elemental equilibrium with ambient seawater. The same principle and laboratory methods can be used to determine how future predicted environmental conditions will affect shell elemental composition by measuring shell precipitated under such conditions. To date, ocean acidification and warming studies investigating elemental compositions of marine calcifiers have focussed on other taxa such as corals (Cohen et al., 2009; Bray et al., 2014) and bivalves (Hahn et al., 2012, 2014). It is important to determine if end-century environmental conditions will affect shell geochemistry of skeletal/shell-bearing organisms, including brachiopods, as any variations to their current elemental composition could affect their shell integrity.

*L. uva* and *C. inconspicua* will be able to continue shell production and repair shell damage under future environmental conditions up to 2100 (Chapter 2; Cross et al., 2015, 2016),

however, it is unknown whether these species will be able to produce the same shell both structurally and elementally. Any variation to shell structure or elemental composition could negatively affect shell integrity and prove potentially fatal. Therefore, the aims of this chapter were to determine whether rhynchonelliform brachiopods will be able to produce shell of similar punctal density, calcite fibre size and shell elemental composition under predicted end-century acidified conditions in both *L. uva* and *C. inconspicua* and also in increased temperature conditions for *L. uva*.

## **3.2 Materials and Methods**

### **3.2.1 Experimental design**

Experimental design details for both CO<sub>2</sub> perturbation experiments of *L. uva* and *C. inconspicua* are presented in section 2.2.2.

### **3.2.2 Sample preparation**

After the completion of the CO<sub>2</sub> perturbation experiments, all individuals were carefully killed by removing them from the substratum, separating the valves to drain seawater from the internal cavity and then being placed in 70% ethanol. All specimens were stored individually in sample tubes and labelled with species name, treatment and individual number. For each species, five undamaged specimens with the highest experimental growth increments were selected from each treatment for further shell analysis. Morphometric data for each specimen are detailed in Tables 3.1 and 3.2. Due to laboratory equipment time constraints, only three specimens from each treatment were analysed for elemental composition. Specimens were carefully cleaned of epibiota including bryozoans, sponges, polychaete tubes and other brachiopods using a scalpel. Extra care was taken to avoid damaging the shell surface. If epibiota could not easily be removed then that area was avoided in later shell analysis. The valves of each specimen were separated, the soft tissues removed and the empty valves were further cleaned in an ultrasonic bath for 3 minutes. All samples were then air dried for 24 hours before the pedicle valves were used in analyses that investigated the shell surfaces and the brachial valves were used for methods using shell cross sections.

Dry pedicle valves were carefully placed with the outer shell surface facing upwards on aluminium stubs. The pedicle valves were then gold coated (EMITECH K550 sputter coater)

for 1 minute at three different valve orientations (rotated 120° after each 1 minute coating) to ensure the whole specimen was coated and prepared for Scanning Electron Microscopy (SEM; JEOL 820 for *L. uva* specimens and FEI QEMSCAN 650F for *C. inconspicua*).

Brachial valves were placed with the outer shell surface facing downwards in 35 mm by 35 mm plastic moulds with roughly a 5 mm layer of set Metprep Kleer-set Type FF resin to ensure the shell was not touching the base of the mould. Resin was poured into the moulds ensuring the entire valve was submerged and left for 24 hours in a fume cupboard for the resin to harden. The resin blocks were removed from their moulds and labelled using an etching pen on both sides of the resin block. A 1 mm thick Diamant Boart diamond rock cutting saw was used to cut the valves longitudinally from the hinge to the commissure along the growth axis (Figure 3.3). One half of the valve was used in further shell analysis and the other half was stored as a spare. A lapping wheel with 180 sized grit was used to remove the larger scratches from the cutting saw on each cross section which was then placed in an ultrasonic bath for 2 minutes to remove excess grit. Each resin block was then polished by hand using an increasingly fine sequence of Kemet met papers of grit size P400, P800, P2500 and P4000 then placed in an ultrasonic bath for 3 minutes to remove excess grit and reduce contamination. Further polishing followed with MetPrep diamond solutions at 6 µm, 3 µm and 1 µm to ensure a smooth shell surface, with individuals being placed in an ultrasonic bath after each stage. To provide a thin conductive coat over the cross sections, the resin blocks were carbon coated for 20 seconds using an Edwards Auto 306 carbon coater ready for analysis in a Cameca SX100 Electron Microprobe and SEM.

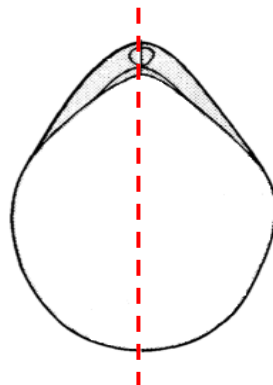


**Figure 3.3 – Schematic to illustrate the longitudinal cut of the brachial valves from the hinge to the commissure.**

**Table 3.1 - *L. uva* – Morphometrics of individuals selected for further shell analysis of punctal density, calcite fibre size and elemental composition. Initial length is given to indicate size of the individual. Grey cells indicate the use of this specimen in the respective shell analysis.**

Treatment	Individual ID	Initial Length (mm)	Overall Growth (mm)	Shell characteristics		
				Pedicle valves	Brachial valves	
				Punctal density	Calcite fibre size	Elemental composition
Temperature Control	Temperature control - N7	19.6	1.1			
	Temperature control - N20	20.3	1.2			
	Temperature control - N28	7.2	0.7			
	Temperature control - N49	12.2	0.7			
	Temperature control - N52	9.1	0.8			
pH control	pH control - N4	8.9	1.6			
	pH control - N5	8.1	1.4			
	pH control - N6	9.8	0.8			
	pH control - N7	16.1	1.7			
	pH control - N9	14.9	1.3			
	pH control - N10	23.3	2.0			
pH 7.75	pH 7.75 - N1	7.5	1.9			
	pH 7.75 - N2	10.6	0.9			
	pH 7.75 - N5	13.6	2.3			
	pH 7.75 - N8	17.3	2.7			
	pH 7.75 - N9	17.9	2.5			
pH 7.54	pH 7.54 - N1	10.5	1.3			
	pH 7.54 - N4	14.0	1.8			
	pH 7.54 - N5	17.8	1.0			
	pH 7.54 - N6	21.5	1.2			
	pH 7.54 - N8	22.2	1.0			

**Table 3.2 - *C. inconspicua* – Morphometrics of individuals selected for analysis of punctal density, calcite fibre size and elemental composition. Initial length is given to indicate the size of the individual. Grey cells indicate the use of this specimen in the respective shell analysis.**

Treatment	Individual ID	Initial Length (mm)	Overall Growth (mm)	Shell characteristics		
				Pedicle valves	Brachial valves	
				Punctal density	Calcite fibre size	Elemental composition
pH control	pH control - N1	6.7	0.6			
	pH control - N13	8.0	1.3			
	pH control - N14	5.3	0.8			
	pH control - N29	8.3	0.8			
	pH control - N49	9.8	0.5			
pH 7.8	pH 7.8 - N3	10.1	0.9			
	pH 7.8 - N5	10.5	0.6			
	pH 7.8 - N8	10.3	0.8			
	pH 7.8 - N14	5.2	0.8			
	pH 7.8 - N25	8.1	0.6			
pH 7.6	pH 7.6 - N11	7.0	1.4			
	pH 7.6 - N19	4.9	1.0			
	pH 7.6 - N31	6.2	0.7			
	pH 7.6 - N40	6.1	0.7			
	pH 7.6 - N46	7.1	0.8			

### 3.2.3 Punctal densities

Scanning Electron Microscopes (JEOL 820 for *L. uva* specimens and FEI QEMSCAN 650F for *C. inconspicua*) at the Department of Earth Sciences, University of Cambridge, UK were used to image the pedicle valves of 19 undamaged specimens (4-5 in each treatment) of *L. uva* and 15 undamaged individuals (5 in each treatment) of *C. inconspicua* to calculate punctal densities. Both JEOL 820 and FEI QEMSCAN 650F were operated using an accelerating voltage of 20 kV. Micrographs of 1 mm by 1 mm were collected at 10 different areas on each specimen; 5 areas in the growth laid down in their natural environment and 5 areas in the growth laid down in the experiment (Figure 3.4a). Punctal density ( $\text{mm}^{-2}$ ) was calculated by counting the number of punctae in each  $1 \text{ mm}^2$  micrograph (Figure 3.4b). To minimise human error, each micrograph was counted three times on different days with the mean punctal density and standard error (typically  $\pm 2$ ) used in later statistical analyses.

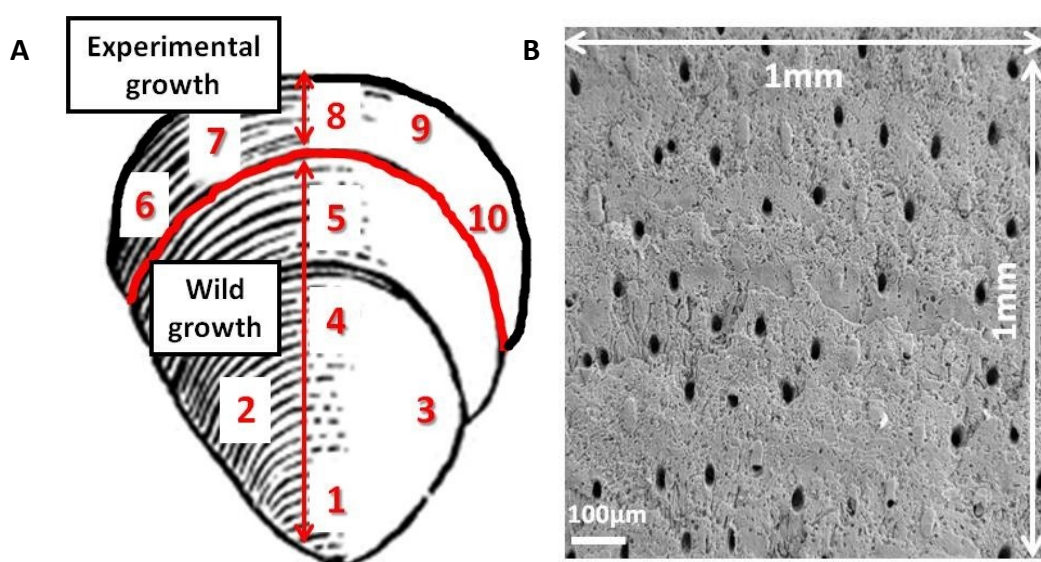


**Figure 3.4 – Calculating punctal densities: (A) schematic of a pedicle valve indicating the 5 areas of shell laid down in the wild and the 5 areas laid down in the experiment where SEM micrographs were collected for analysis and (B) an example of a  $1 \text{ mm}^2$  SEM micrograph of the outer shell surface of *L. uva* collected to count punctal densities.**

### 3.2.4 Calcite fibre size

Polished brachial valve cross sections were etched (1% HCl for 20 seconds) and then carbon coated for analysis of the calcite fibres. A FEI QEMSCAN 650F SEM at the Department of Earth Sciences, University of Cambridge, UK was operated with a 20 kV accelerating voltage to collect SEM micrographs of shell laid down in the wild and of shell formed in the experiment from cross sections of the brachial valves of *L. uva* and *C. inconspicua*. Three different areas in both the wild growth and experimental growth were imaged from two

individuals from the pH control and compared to two specimens from the most acidified treatment for each species (Figure 3.5). SEM micrographs were taken of the total thickness of the cross section and also of higher magnification areas of each shell layer. ImageJ was used to measure the thickness and length of 10 randomly selected calcite fibres from each 0.2 mm x 0.07 mm micrograph in *L. uva* and 0.3 mm x 0.15 mm micrograph in *C. inconspicua*. Care was taken only to measure whole fibres and each micrograph was counted three times on different days, to minimise human error, with the mean thickness or length and standard error used in statistical analyses.

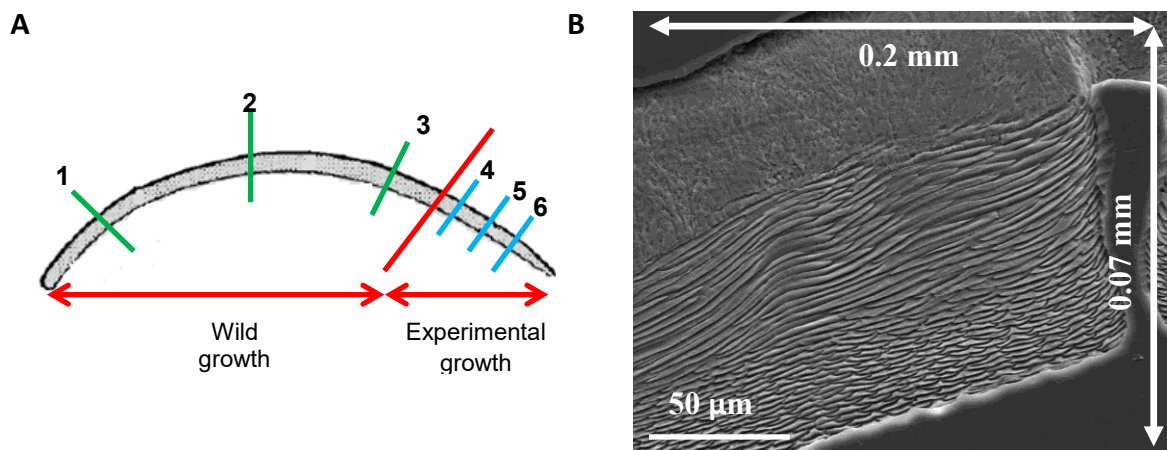


**Figure 3.5 – Measuring calcite fibre dimensions: (A) Schematic of the cross section view of a valve indicating where the SEM micrographs were taken in the wild growth (green box) and experimental growth (blue box) and (B) an example of an SEM micrograph of the cross section of *L. uva* collected to measure calcite fibre dimensions.**

### 3.2.5 Elemental composition

A Cameca SX100 electron microprobe at the Department of Earth Sciences, University of Cambridge, UK was used to measure the elemental composition of brachial valves cross sections of three undamaged specimens of both *L. uva* and *C. inconspicua* in each treatment (12 and 9 individuals in total, respectively). The probe was operated at 15 keV acceleration voltage, a 20 nA beam current and a 5 µm spot size. Barium (Ba), calcium (Ca), iron (Fe), magnesium (Mg), manganese (Mn), phosphorus (P), silicon (Si), sodium (Na) and strontium (Sr) were measured. Apatite (P), benitoite (Ba), celest (Sr), diopside (Ca & Si), fayalite (Fe), jadeite (Na), manganese (Mn) and olivine (St John's) (Mg) were used as standards. Matrix correction was performed following Pouchou and Pichoir (1984) (the PAP procedure). Standard analysis reproducibility was < 1% for each element analysed. PAP corrected data were stoichiometrically calculated as carbonate (Reed, 1993).

Elemental composition of the shell was determined at randomly selected individual points starting at the top of the secondary layer and moving diagonally through the thickness of secondary layer to the bottom of this shell layer in a horizontal direction in both wild shell growth and in the experimental growth (Figure 3.6B). This spot point method covered all of the shell growth laid down in the experiment and an equivalent area of shell laid down in the wild (Figure 3.6A). To ensure elemental composition did not change vertically through the thickness of secondary layer, one vertical profile from each growth type was also measured and compared to data from the spot point method. The vertical profiles involved analysing points from the outer surface of the shell every 10  $\mu\text{m}$  to the inner surface (Figure 3.6D). Punctae and other shell perforations were avoided in both methods by visual selection of areas for analysis.

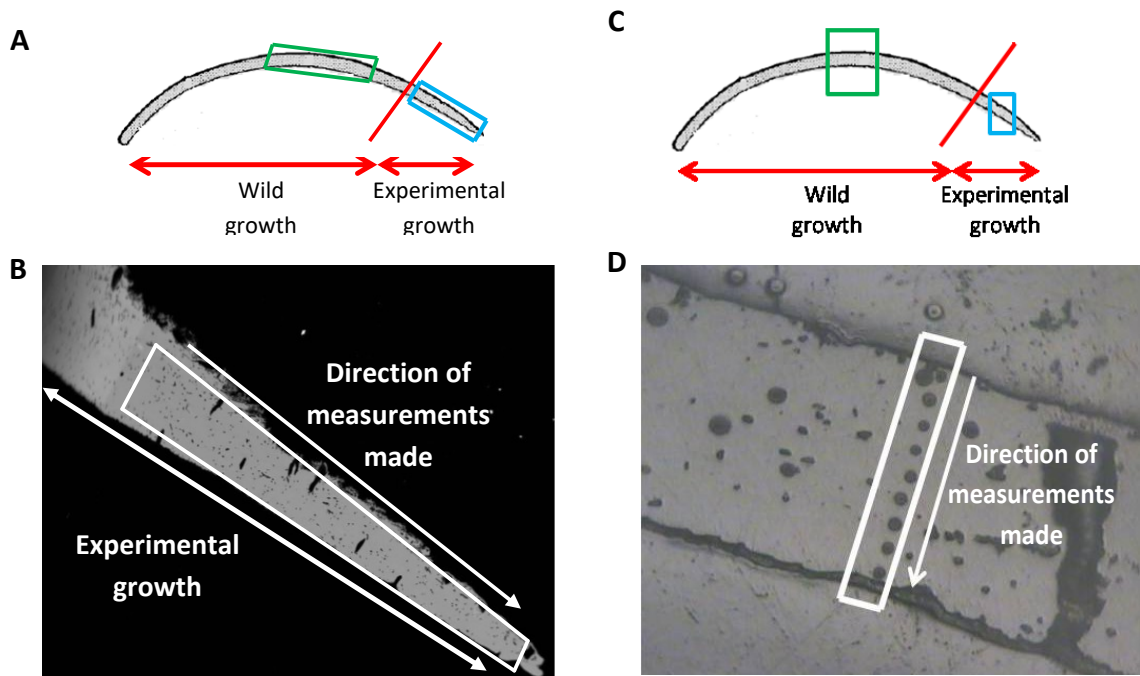


**Figure 3.6 – Elemental composition analysis methods: (A, B) spot point method and (C, D) vertical profile method. (A) schematic illustrating the areas in wild and experimental growth where individual points were measured, (B) SEM micrograph example of *L. uva* indicating the diagonal direction of individual points being collected in the horizontal direction, (C) schematic illustrating where the vertical profiles were taken in the wild and experimental growth and (D) SEM micrograph of *L. uva* indicating the points analysed in a vertical profile.**

### 3.2.6 Statistical Analyses

All data were analysed using Minitab (Statistical Software™ Version 17). Punctal density data for both *L. uva* and *C. inconspicua* were normally distributed (Anderson-Darling test;  $p > 0.05$ ), apart from when comparing the two species, even after square root, logarithmic, double logarithmic and arcsin transformations. Therefore, a non-parametric Kruskal-Wallis test was

used on this latter data set. Parametric one-way ANOVA tests were used to determine if there were any differences in punctal density in the growth laid down in the wild to ensure punctal density was similar amongst individuals used in each experiment. Parametric two-way ANOVA's were then used to determine if treatment and/or growth period (wild vs experimental growth) affected punctal density in each species. One-way ANOVA tests were also used to determine if shell position influenced punctal density in each species to assess if different shell regions varied in this characteristic. Calcite fibre thickness and length data in each species were all normally distributed (Anderson-Darling test;  $p > 0.05$ ), therefore, two-way ANOVA's were conducted on these characteristics to determine if treatment and/or wild vs experimental growth affected calcite fibre size. Thickness data comparing the two species was also normally distributed, however, length data was only normal after log transformation. One-way ANOVA's were, therefore, used to compare both calcite fibre thickness and length between *L. uva* and *C. inconspicua*. Elemental composition data for *L. uva* and *C. inconspicua* were also mainly normally distributed (Anderson-Darling test;  $p > 0.05$ ) apart from P data from the spot point method in *L. uva* which were non-normal even after square root, logarithmic, arcsin, double square root and double arcsine transformations. Mg concentration data from the spot point method in *L. uva* and *C. inconspicua* were normally distributed after square-root and log transformations, respectively. Data comparing Mg, Na and Sr concentrations between the two species were also non-normally distributed after all of the above transformations. Data comparing the P concentrations between the two species were normal after log transformation. Two-way ANOVA's were used to assess if treatment and/or growth period (wild vs experimental growth) affected each element in both the spot point method and the vertical profiles. For the non-normally distributed P data in *L. uva*, a two-way ANOVA was still performed but after ranking the data as there is no equivalent non-parametric test that includes the factor interactions. One-way ANOVA's were used to compare the two methods to assess any differences horizontally or vertically in the secondary layer and to compare the Ca and log transformed P concentrations between species. For the non-normally distributed Mg, Na and Sr concentration data to compare between the species, Kruskal-Wallis tests were used. Data from the primary layer in the vertical profiles were excluded from this analysis. Post-hoc Tukey tests were performed when significant differences were found to determine which treatments, growth period and/interaction factors were causing the differences.

### 3.3 Results

#### 3.3.1 Punctal densities

Punctal density in *L. uva* ranged from 69-96 mm<sup>-2</sup> (Appendix Figure A1) and the mean was 82.1 ± 0.4 mm<sup>-2</sup>. *C. inconspicua* had significantly higher punctal densities with values in the range of 141-168 mm<sup>-2</sup> (Appendix Figure A2) and a mean of 156.3 ± 0.4 mm<sup>-2</sup> (Kruskal-Wallis: H = 143.41, p < 0.001). There was no significant difference in punctal densities in shell deposited in their natural environment between treatments in *L. uva* (Figure 3.7 and Appendix Figure A1; One-way ANOVA: F<sub>3,80</sub> = 0.66, p = 0.582) or in *C. inconspicua* (Figure 3.8 and Appendix Figure A2; One-way ANOVA: F<sub>2,63</sub> = 1.80, p = 0.173). All individuals of each species, therefore, had similar punctal densities before the experiments began. Acidified conditions or increased temperature did not affect punctal density in *L. uva* (Figure 3.7 and Appendix Figure A1; Two-way ANOVA – Treatment: F<sub>3,168</sub> = 0.94, p = 0.422; Wild vs Experimental growth: F<sub>1,168</sub> = 0.17, p = 0.676; Interaction: F<sub>3,168</sub> = 0.93, p = 0.425). Similarly, lowered pH did not affect punctal densities in *C. inconspicua* (Figure 3.8 and Appendix Figure A2; Two-way ANOVA – Treatment: F<sub>2,134</sub> = 2.32, p = 0.102; Wild vs Experimental growth: F<sub>1,134</sub> = 1.68, p = 0.198; Interaction: F<sub>2,134</sub> = 1.82, p = 0.166). There is also no indication of a difference in punctal density between different areas of the shell in either *L. uva* (Appendix Figure A1; One-way ANOVA: F<sub>9,166</sub> = 0.62, p = 0.779) or *C. inconspicua* (Appendix Figure A2; One-way ANOVA: F<sub>9,130</sub> = 1.04, p = 0.414).

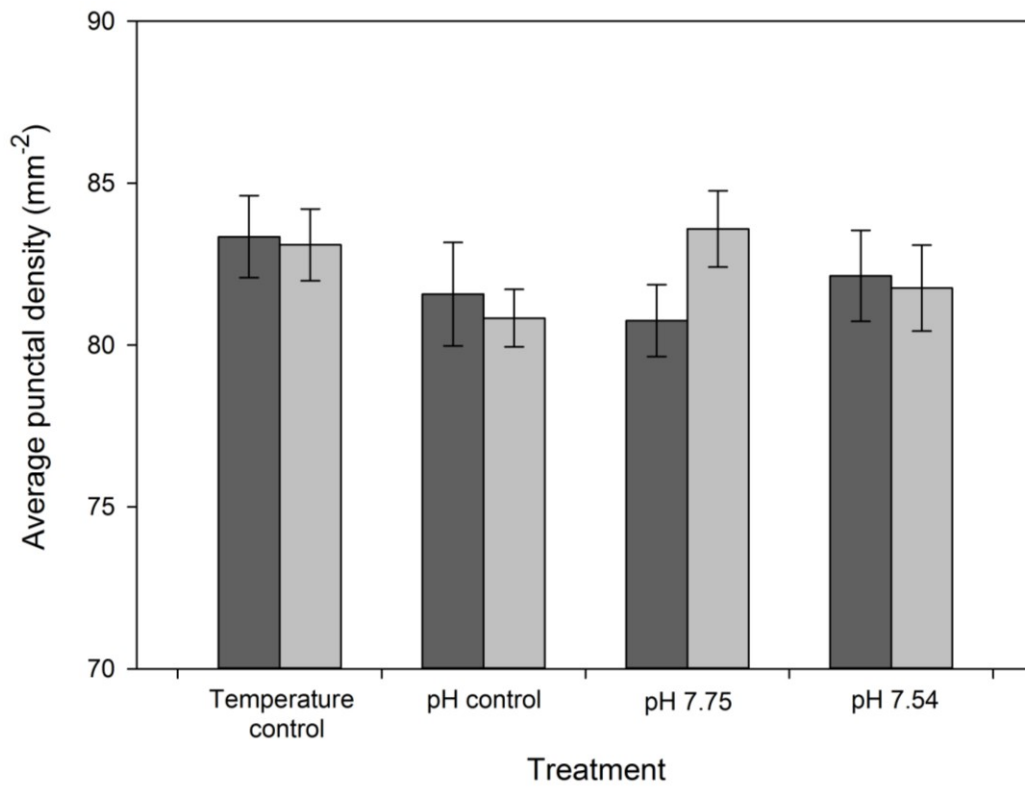


**Figure 3.7 – *L. uva* – Average punctal density for shell growth laid down in the wild (dark bars) and growth laid down in the experiment (light bars) for each treatment. Values plotted are mean  $\pm$  SE.**

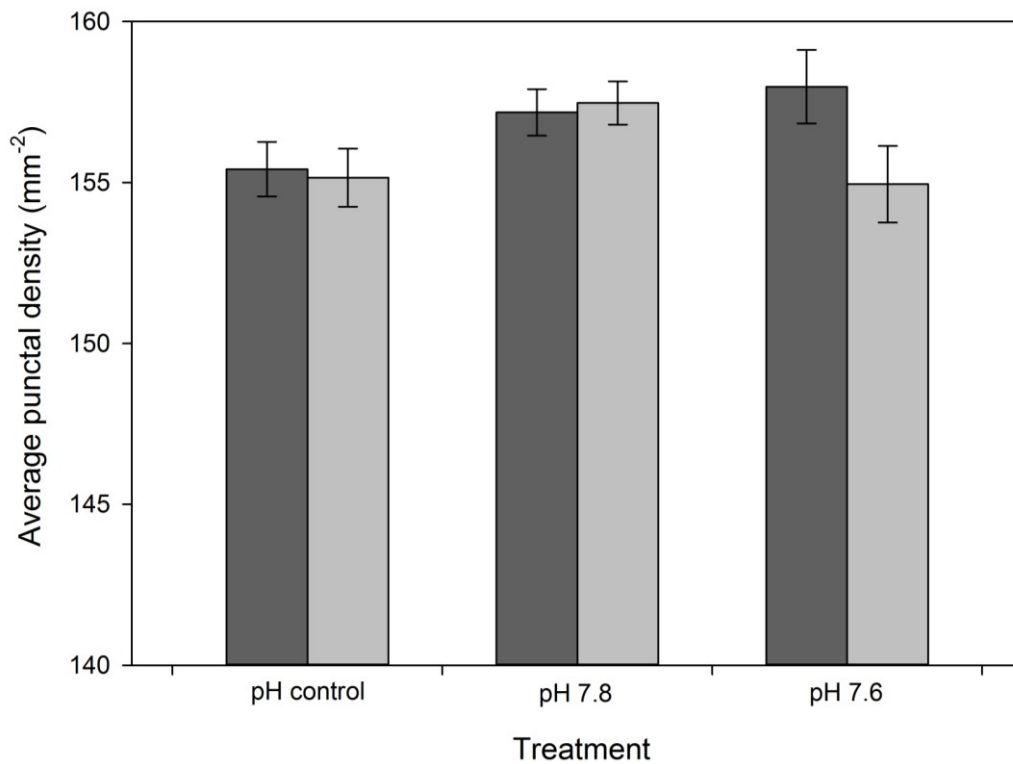


**Figure 3.8 – *C. inconspicua* – Average punctal density for shell growth laid down in the wild (dark bars) and growth laid down in the experiment (light bars) for each treatment. Values plotted are mean  $\pm$  SE.**

### 3.3.2 Calcite fibre dimensions

Secondary layer calcite fibres in *L. uva* ranged from 3.04-4.61  $\mu\text{m}$  thickness x 140.6-185.4  $\mu\text{m}$  length in the pH control and 3.00-4.96  $\mu\text{m}$  x 140.1-191.9  $\mu\text{m}$  in the pH 7.54 treatment. *C. inconspicua* had significantly smaller secondary layer calcite fibres with a thickness of 2.14-4.07  $\mu\text{m}$  and length of 126.0-173.5  $\mu\text{m}$  in the pH control and 2.26-4.10  $\mu\text{m}$  thickness x 133.5-179.6  $\mu\text{m}$  length in pH 7.6 (Thickness – One-way ANOVA:  $F_{1,239} = 119.55$ ,  $p < 0.001$ ; Length – One-way ANOVA:  $F_{1,239} = 42.13$ ,  $p < 0.001$ ). Lowered pH had no effect on thickness (Figure 3.9; Two-way ANOVA – Treatment:  $F_{1,116} = 0.01$ ,  $p = 0.916$ ; Wild vs Experimental growth:  $F_{1,116} = 0.02$ ,  $p = 0.881$ ; Interaction:  $F_{1,116} = 1.24$ ,  $p = 0.267$ ) or length (Figure 3.9; Two-way ANOVA – Treatment:  $F_{1,116} = 0.05$ ,  $p = 0.821$ ; Wild vs Experimental growth:  $F_{1,116} = 0.35$ ,  $p = 0.556$ ; Interaction:  $F_{1,116} = 0.03$ ,  $p = 0.856$ ) of the calcite fibres in *L. uva*. Similarly, acidified conditions had no impact on the fibre thickness (Figure 3.9; Two-way ANOVA – Treatment:  $F_{1,116} = 0.13$ ,  $p = 0.722$ ; Wild vs Experimental growth:  $F_{1,116} = 0.03$ ,  $p = 0.866$ ; Interaction:  $F_{1,116} = 0.06$ ,  $p = 0.805$ ) or length (Figure 3.9; Two-way ANOVA – Treatment:  $F_{1,116} = 0.12$ ,  $p = 0.726$ ; Wild vs Experimental growth:  $F_{1,116} = 0.85$ ,  $p = 0.359$ ; Interaction:  $F_{1,116} = 0.00$ ,  $p = 0.959$ ) of calcite fibres in *C. inconspicua*. Therefore, calcite fibres laid down in acidified conditions were the same size as those produced under ambient pH levels in both species on the scale investigated here (Figure 3.10 and 3.11).

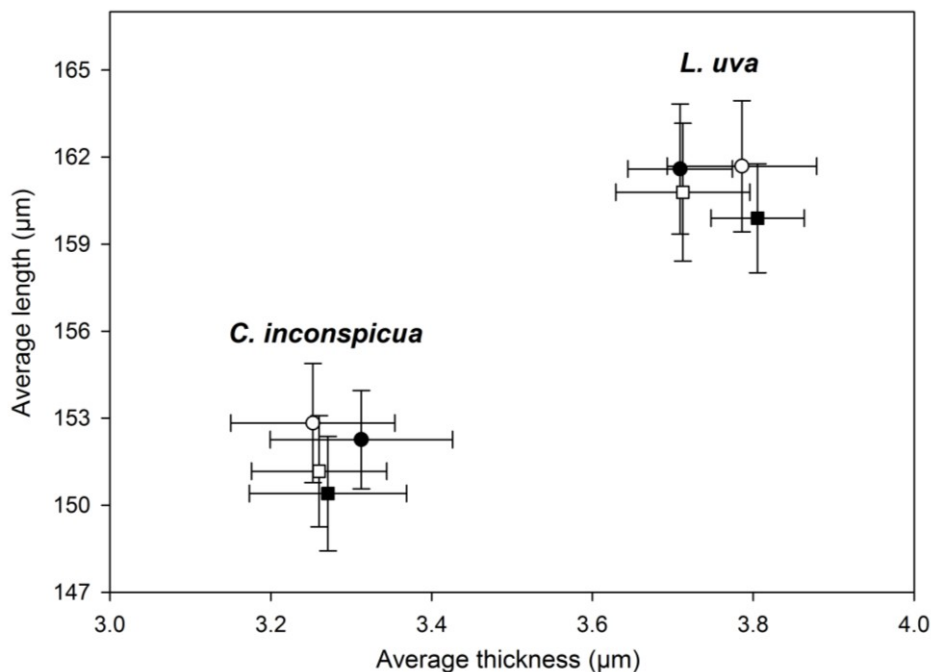


**Figure 3.9** –Average calcite fibre dimensions of both species in shell laid down in the wild (black circles) and in the experiment (black squares) in the pH control and in shell precipitated in the wild (white circles) and in the experiment (white squares) in the most acidified treatment. Values plotted are mean  $\pm$  SE.

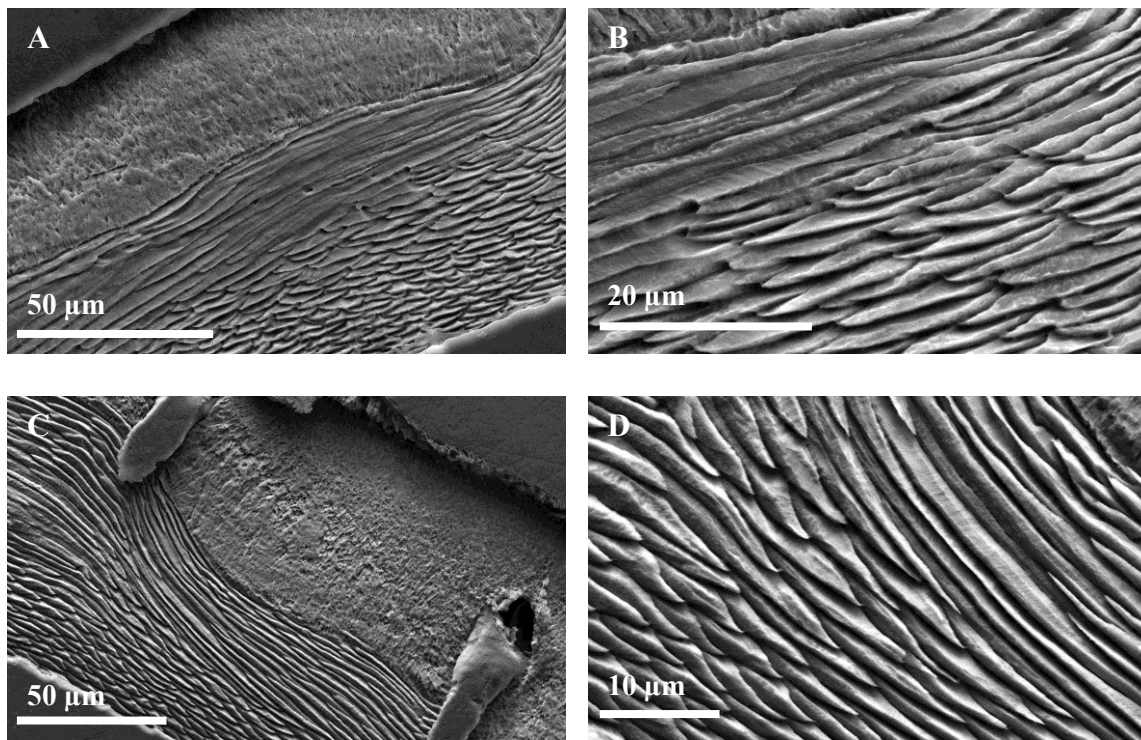


Figure 3.10 – Microstructure of *L. uva* – SEM micrographs indicating calcite fibres in the secondary layer in the experimental growth of an individual from the pH control (A, B) and from an individual from the pH 7.54 treatment (C, D). Scale bars are indicated on each micrograph.

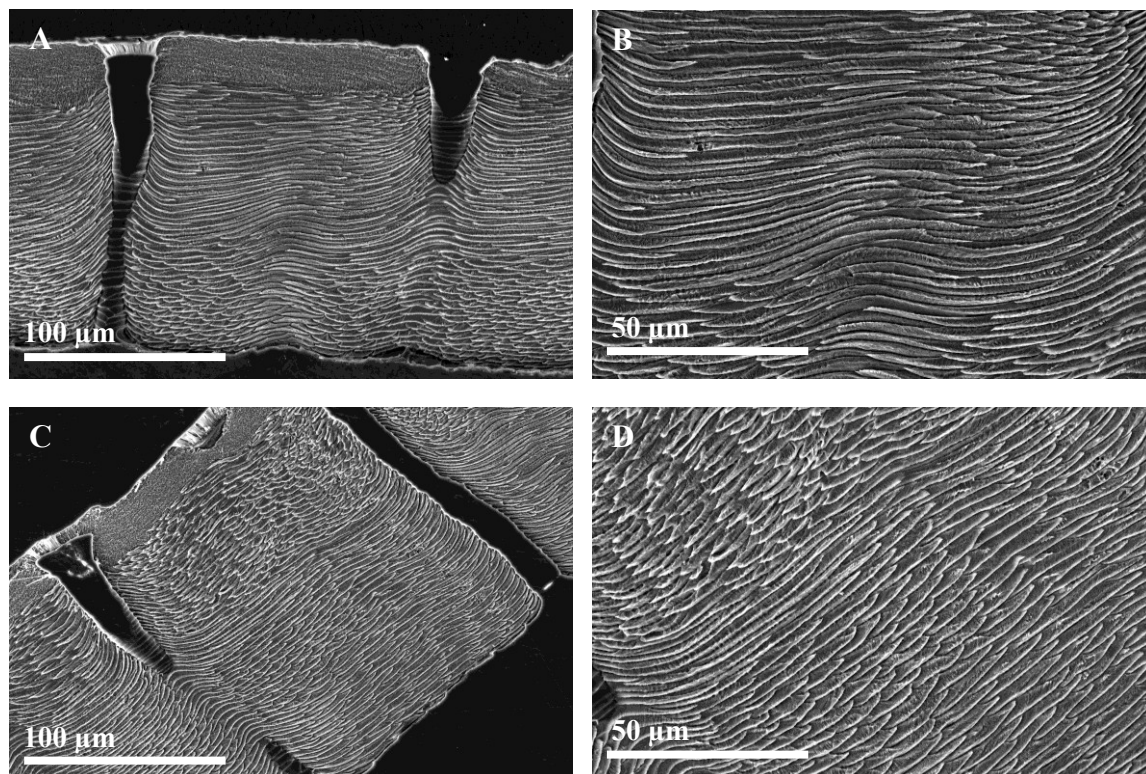


Figure 3.11 – Microstructure of *C. inconspicua* – SEM micrographs indicating calcite fibres in the secondary layer in the experimental growth of an individual from the pH control (A, B) and from an individual from the pH 7.6 treatment (C, D). Scale bars are indicated on each micrograph.

### 3.3.3 Elemental composition

All the major elements (Ca, Mg, Na, Sr and P) were above the Electron Microprobe detection limits whereas all the minor elements (Si, Fe, Mn and Ba) were consistently below detection limits in both *L. uva* and *C. inconspicua* (Table 3.3). The minor elements were thus excluded from further analysis.

**Table 3.3 – Detection limits for all major and minor elements measured.**

Major elements			Minor Elements		
Element	Mean (wt %)	SE	Element	Mean (wt %)	SE
Ca	0.14	< 0.01	Si	0.02	< 0.01
Mg	0.01	< 0.01	Fe	0.05	< 0.01
Na	0.04	< 0.01	Mn	0.07	< 0.01
Sr	0.05	< 0.01	Ba	0.21	< 0.01
P	0.01	< 0.01			

Overall, Ca concentration in *L. uva* ranged from 38.38-40.01 wt %, Mg from 0.02-0.57 wt %, Na from 0.24-0.40 wt %, Sr from 0.10-0.24 wt % and P from 0.01-0.05 wt % (Table 3.4). Ca concentration in *C. inconspicua* was higher than *L. uva* ranging from 38.31-40.34 wt % (Table 3.5) whereas all other major elements had lower concentrations in *C. inconspicua* than *L. uva* (Table 3.6). Mg concentration in *C. inconspicua* ranged from 0.04-0.20 wt %, Na from 0.15-0.30 wt%, Sr from 0.06-0.20 wt % and P from 0.01-0.05 wt % (Table 3.5). There was no significant difference in any element between the spot point method and the vertical profiles in both *L. uva* (Appendix Table A1) and *C. inconspicua* (Appendix Table A2). Elemental composition, therefore, did not vary horizontally or vertically throughout the secondary layer within the accuracy attainable here and further analysis focussed on the spot point method. Data from the vertical profiles in *L. uva* can be found in Appendix Table A3 and Appendix Figures A3 and A4 and in *C. inconspicua* in Appendix Table A4 and Appendix Figures A5 and A6. Concentrations of all major elements were not affected by acidified conditions or temperature in *L. uva* (Table 3.7, Appendix Table A3, Figure 3.12 and Appendix Figures A7-A11) or by acidified conditions in *C. inconspicua* (Table 3.8, Appendix Table A4, Figure 3.13 and Appendix Figures A12-A16). However, Ca concentrations in the experimental growth of *L. uva* (Figure 3.12) and Mg and Na concentrations in the experimental growth in *C. inconspicua* (Figure 3.13) in all treatments were significantly higher than growth laid down in the wild. These trends were not reflected in the vertical profiles (Appendix Figure A4 and A5), apart from Mg concentration in *C. inconspicua* (Appendix Figure A5), therefore, more data are needed to confirm any possible patterns.

**Table 3.4- *L. uva* – minimum, maximum and mean weight % and standard error of each element from each growth period from each treatment.**

Treatment	Element	Wild growth				Experimental growth			
		Minimum (wt %)	Maximum (wt %)	Mean (wt %)	S.E.	Minimum (wt %)	Maximum (wt %)	Mean (wt %)	S.E.
Temperature control	Ca	38.42	40.01	39.10	0.05	38.52	39.88	39.21	0.05
	Mg	0.08	0.57	0.24	0.01	0.07	0.49	0.29	0.01
	Na	0.25	0.40	0.31	< 0.01	0.24	0.38	0.32	< 0.01
	Sr	0.12	0.23	0.16	< 0.01	0.14	0.23	0.18	< 0.01
	P	0.02	0.04	0.03	< 0.01	0.02	0.05	0.03	< 0.01
pH control	Ca	38.41	39.85	39.12	0.05	38.51	39.86	39.25	0.05
	Mg	0.02	0.55	0.23	0.02	0.03	0.56	0.26	0.02
	Na	0.25	0.38	0.31	< 0.01	0.24	0.39	0.31	0.01
	Sr	0.08	0.24	0.16	0.01	0.11	0.24	0.17	< 0.01
	P	0.02	0.05	0.02	< 0.01	0.01	0.04	0.02	< 0.01
pH 7.75	Ca	38.38	39.85	39.09	0.04	38.56	39.87	39.20	0.03
	Mg	0.06	0.53	0.22	0.01	0.07	0.54	0.25	0.01
	Na	0.24	0.40	0.32	< 0.01	0.25	0.39	0.32	< 0.01
	Sr	0.12	0.24	0.17	< 0.01	0.12	0.24	0.16	< 0.01
	P	0.02	0.04	0.03	< 0.01	0.02	0.04	0.02	< 0.01
pH 7.54	Ca	38.51	39.91	39.02	0.05	38.51	39.98	39.18	0.05
	Mg	0.07	0.44	0.27	0.02	0.03	0.48	0.25	0.02
	Na	0.26	0.38	0.32	< 0.01	0.26	0.38	0.31	< 0.01
	Sr	0.11	0.22	0.17	< 0.01	0.11	0.22	0.16	< 0.01
	P	0.02	0.04	0.03	< 0.01	0.01	0.05	0.02	< 0.01

**Table 3.5 – *C. inconspicua* - minimum, maximum and mean weight % and standard error of each element from each growth period from each treatment.**

Treatment	Element	Wild growth				Experimental growth			
		Minimum (wt %)	Maximum (wt %)	Mean (wt %)	S.E.	Minimum (wt %)	Maximum (wt %)	Mean (wt %)	S.E.
pH control	Ca	38.44	40.34	39.25	0.04	38.44	40.08	39.18	0.06
	Mg	0.04	0.19	0.10	< 0.01	0.07	0.16	0.13	< 0.01
	Na	0.15	0.30	0.22	< 0.01	0.15	0.25	0.22	< 0.01
	Sr	0.06	0.16	0.12	< 0.01	0.07	0.20	0.12	< 0.01
	P	0.01	0.05	0.02	< 0.01	0.01	0.05	0.03	< 0.01
pH 7.8	Ca	38.47	40.03	39.24	0.04	38.43	40.19	39.28	0.07
	Mg	0.05	0.20	0.11	< 0.01	0.04	0.19	0.13	0.01
	Na	0.15	0.29	0.21	< 0.01	0.16	0.30	0.22	< 0.01
	Sr	0.07	0.16	0.11	< 0.01	0.07	0.17	0.11	< 0.01
	P	0.01	0.05	0.02	< 0.01	0.01	0.04	0.03	< 0.01
pH 7.6	Ca	38.49	40.25	39.22	0.04	38.31	40.23	39.16	0.05
	Mg	0.04	0.18	0.10	< 0.01	0.05	0.20	0.12	< 0.01
	Na	0.15	0.29	0.20	< 0.01	0.15	0.29	0.22	< 0.01
	Sr	0.06	0.15	0.11	< 0.01	0.07	0.15	0.11	< 0.01
	P	0.01	0.04	0.02	< 0.01	0.01	0.04	0.02	< 0.01

**Table 3.6 –Statistical analysis results comparing elemental composition data between the two species. One-way ANOVA and post-hoc Tukey tests were used on normally distributed data and Kruskal-Wallis tests on non-normally distributed data to determine differences. Significant differences are highlighted in bold.**

Element	Mean wt % of <i>L. uva</i>	Mean wt % of <i>C. inconspicua</i>	Statistical analysis results	Post-hoc analysis results
Ca	39.10	39.22	<b>One-way ANOVA:</b> $F_{1,802} = 18.15,$ $p < 0.001$	<i>C. inconspicua</i> has a higher concentration than <i>L. uva</i>
Mg	0.26	0.11	<b>Kruskal-Wallis:</b> $H = 421.54,$ $p < 0.001$	<i>L. uva</i> has a higher concentration than <i>C. inconspicua</i>
Na	0.32	0.21	<b>Kruskal-Wallis:</b> $H = 559.38,$ $p < 0.001$	<i>L. uva</i> has a higher concentration than <i>C. inconspicua</i>
Sr	0.17	0.11	<b>Kruskal-Wallis:</b> $H = 499.44,$ $p < 0.001$	<i>L. uva</i> has a higher concentration than <i>C. inconspicua</i>
P	0.03	0.02	<b>One-way ANOVA:</b> $F_{1,631} = 5.81,$ $p = 0.016$	<i>L. uva</i> has a higher concentration than <i>C. inconspicua</i>

**Table 3.7 – *L. uva* - Statistical analysis results of elemental composition data from the spot point method. Two-way ANOVA and post-hoc Tukey tests determined significant effects of treatment, growth period and interaction of the two factors. Significant differences are highlighted in bold.**

Element	Spot point method			Post-hoc Tukey results
	Two-way ANOVA results (Response: weight %, Factors: treatment, wild vs experimental growth)			
	Treatment	Wild vs Experimental growth	Interaction	
Ca	$F_{3,476} = 0.91,$ $p = 0.438$	<b><math>F_{1,476} = 14.80,</math></b> <b><math>p &lt; 0.001</math></b>	$F_{3,476} = 0.13,$ $p = 0.966$	Experimental growth has a higher concentration than wild growth.
Mg	$F_{3,465} = 2.30,$ $p = 0.076$	$F_{1,465} = 2.74,$ $p = 0.099$	$F_{3,465} = 2.46,$ $p = 0.062$	N/A
Na	$F_{3,473} = 4.67,$ $p = 0.047$	$F_{1,473} = 1.16,$ $p = 0.283$	$F_{3,473} = 2.76,$ $p = 0.046$	N/A
Sr	$F_{3,476} = 1.60,$ $p = 0.188$	$F_{1,476} = 0.15,$ $p = 0.703$	$F_{3,476} = 2.59,$ $p = 0.052$	N/A
P	$F_{3,345} = 1.71,$ $p = 0.165$	$F_{1,345} = 2.68,$ $p = 0.102$	$F_{3,345} = 0.61,$ $p = 0.608$	N/A

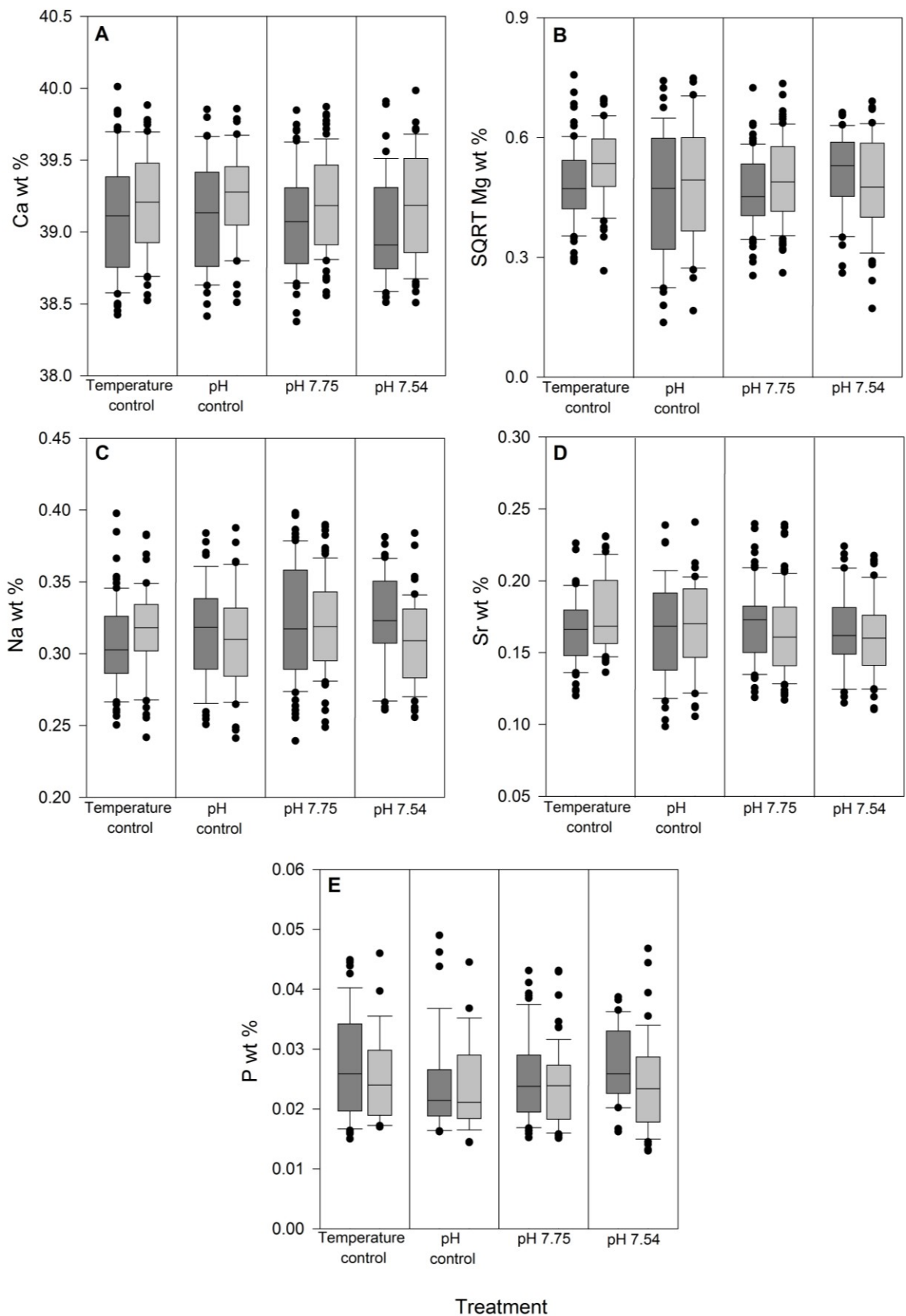


**Figure 3.12 – *L. uva* – Ca (A), square root of Mg (B), Na (C), Sr (D) and P (E) concentrations in wild growth (dark box plots) and experimental growth (light box plots) in each of the four treatments.**

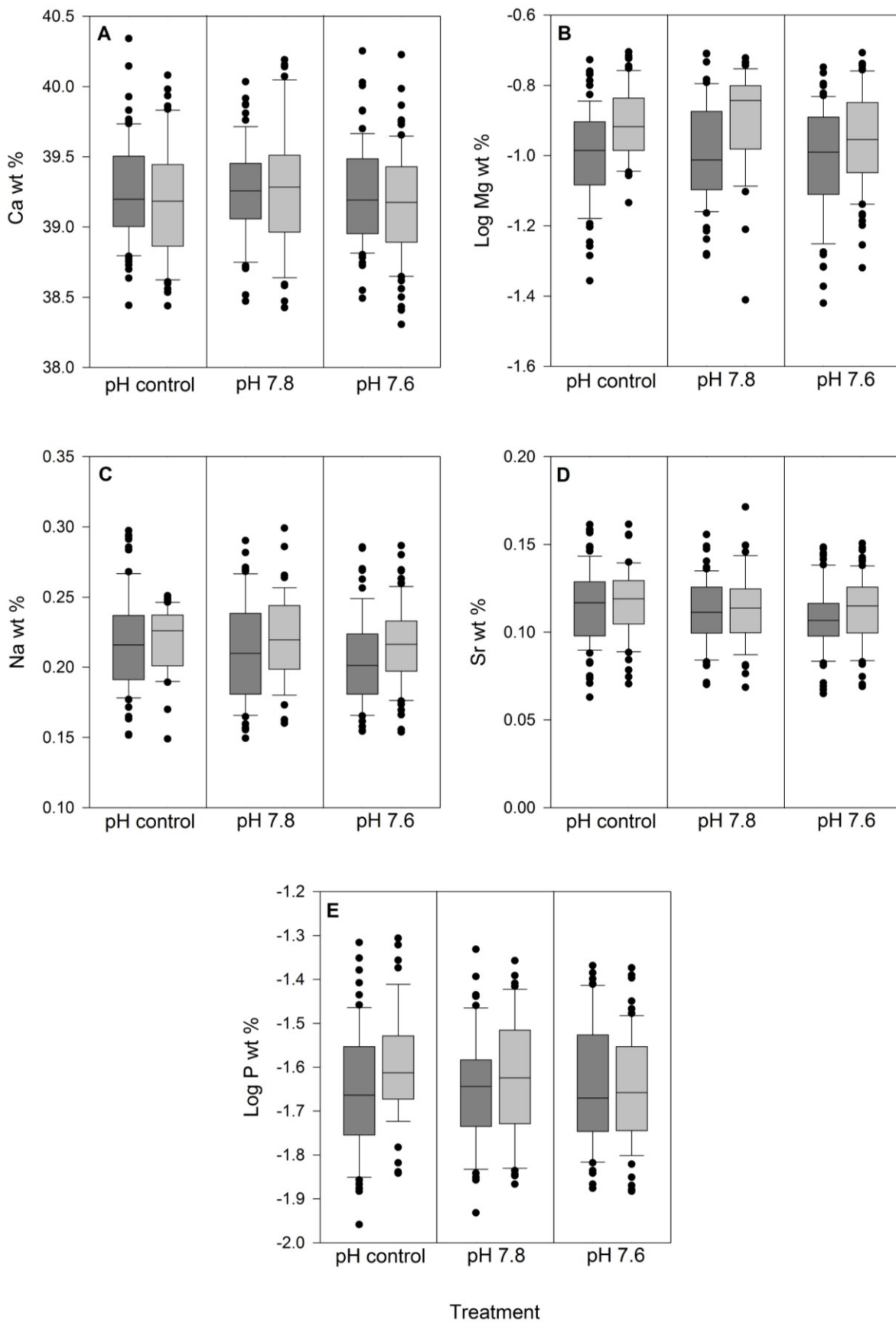


**Figure 3.13 – *C. inconspicua*– Ca (A), square root of Mg (B), Na (C), Sr (D) and P (E) concentrations in wild growth (dark box plots) and experimental growth (light box plots) in each of the four treatments.**

**Table 3.8 – *C. inconspicua* - Statistical analysis results of elemental composition data from the spot point method. Two-way ANOVA and post-hoc Tukey tests determined significant effects of treatment, growth period and interaction of these two factors. Significant differences are highlighted in bold.**

Element	Spot point method			
	Two-way ANOVA results (Response: weight %, Factors: treatment, wild vs experimental growth)			Post-hoc Tukey results
	Treatment	Wild vs Experimental growth	Interaction	
Ca	$F_{2,381} = 1.15$ , $p = 0.317$	$F_{1,381} = 0.65$ , $p = 0.421$	$F_{2,381} = 0.73$ , $p = 0.484$	N/A
Mg	$F_{2,379} = 2.23$ , $p = 0.109$	<b><math>F_{1,379} = 30.44</math></b> , <b><math>p &lt; 0.001</math></b>	$F_{2,379} = 0.70$ , $p = 0.498$	Experimental growth has a higher concentration than wild growth.
Na	$F_{2,369} = 2.38$ , $p = 0.094$	<b><math>F_{1,369} = 5.09</math></b> , <b><math>p = 0.025</math></b>	$F_{2,369} = 0.97$ , $p = 0.380$	Experimental growth has a higher concentration than wild growth.
Sr	$F_{2,380} = 2.85$ , $p = 0.059$	$F_{1,380} = 1.81$ , $p = 0.179$	$F_{2,380} = 0.46$ , $p = 0.634$	N/A
P	$F_{2,329} = 0.67$ , $p = 0.510$	$F_{1,329} = 1.37$ , $p = 0.256$	$F_{2,329} = 1.37$ , $p = 0.256$	N/A

### 3.4 Discussion

Both *L. uva* and *C. inconspicua* have a robust ability to produce shell with the same punctal density, calcite fibre size and elemental composition under forecasted pH conditions in both species and also in *L. uva* in warming expected by 2100. This, in addition to the unaffected shell growth rates and ability to repair shell (Chapter 2; Cross et al., 2015, 2016), further illustrates the resilience of shell production in a polar and a temperate brachiopod under future environmental change.

#### 3.4.1 Punctal density

Punctal density in *L. uva* was not affected by acidified conditions or increased temperature and in *C. inconspicua* was not affected by lowered pH. Wild populations of both species should, therefore, be able to produce shell with similar punctal density over the next 84 years. This shell characteristic has not been included in the few previous ocean acidification studies on brachiopods (McClintock et al., 2009; Watson et al., 2012; Cross et al., 2015, 2016) and cannot be compared to equivalent research on other marine calcifiers as punctae only occur in brachiopods. Lowered pH did not impact punctal density in two species from different

habitats suggesting that it is unlikely that acidified conditions affect this characteristic. Temperature has been suggested to control punctal density due to variations between closely related species in different geographical areas with varying seawater temperatures (Foster, 1974). The general trend was increasing punctal density with increasing seawater temperature. Punctal densities of six *Liothyrella* species, including *L. uva*, and eleven terebratellid species, including *C. inconspicua*, from several locations of varying winter seawater temperature were positively correlated with temperature (correlation coefficient for *Liothyrella* species: 0.687,  $p < 0.01$ ; correlation coefficient for terebratellid species: 0.457,  $p < 0.05$ ; Foster, 1974). This correlation between punctal density and seawater temperature could be related to temperature effects on shell growth rates. Polar marine invertebrates grow slow due to the difficulty of depositing  $\text{CaCO}_3$  at low temperature (Graus, 1974; Vermeij, 1978; Clarke, 1990, 1993) and their low metabolic rates (Peck & Conway, 2000; Peck et al., 1997). Slow growth could alter the spacing of punctae and, therefore, punctal density. This could explain the significantly higher densities in the temperate *C. inconspicua* than in polar *L. uva*. Even though a temperature effect on punctal density was previously identified based on variability between habitats, data here suggests that predicted end-century warming will not impact this shell characteristic within a species.

On evolutionary scales, food availability is a potential driver of punctal density (Peck & Holmes, 1989a). Punctae house significant portions (70-80% in 5-7 mm length individuals and 30-45% in 25 mm individuals (Peck et al., 1987a)) of the animal's soft tissue to reduce space constraints within the mantle cavity. Higher punctal densities may, therefore, persist in species inhabiting environments with abundant food supplies. Punctal density has been reported to vary within an individual with a wide range of densities (56-108  $\text{mm}^{-2}$ ) recorded within one valve of the terebratellid *Magellania joubini* (Williams & Rowell, 1965). Punctal densities in *L. uva* and *C. inconspicua* here did not vary between different shell areas. This could be attributed to the careful consideration of each micrograph before measuring, ensuring punctae were clear enough to count accurately as some areas had extensive wear on the shell surface or the periostracum was so intact that the punctae underneath were difficult to see.

### 3.4.2 Calcite fibre size

Calcite fibre size in both *L. uva* and *C. inconspicua* did not differ between the pH controls and the most acidified treatments. This demonstrates that these species can make shell with the same calcite fibre sizes under predicted end-century conditions in terms of the scale used in this study. This is in contrast to increased calcite lath thickness recorded in the oyster *Crassostrea virginica* under low pH conditions (Beniash et al., 2010). The authors speculated that in lowered pH cell division rates in mantle tissue decrease, as a result of their measured reduced somatic growth rates. The slower mantle growth allows increased time for the deposition of a single calcite folium. Fitzner et al. (2014a) showed shell production in *Mytilus edulis* was maintained in 1000  $\mu\text{atm } p\text{CO}_2$ . Shell integrity was, however, compromised as disorientated calcite crystals occurred instead of the uniform structural orientation produced under ambient  $p\text{CO}_2$  conditions. Therefore, shell production under predicted end-century pH conditions comes at a cost to shell integrity, which could impact shell strength and reduce protection from predators and changing environments. Shell texture was not assessed in this study, but lowered pH did not impact calcite fibre size suggesting brachiopods could have a stronger control on biomineralisation processes than mussels.

The calcite fibre sizes in *L. uva* were similar to those previously reported for *L. uva* (150-200  $\mu\text{m} \times 5 \mu\text{m}$ ) by Goetz et al. (2009), but they were significantly larger than the fibres in *C. inconspicua*. Shells in colder waters tend to have a coarser shell mosaic as determined by crystal fibre sizes in the inner secondary layer. An early study by Wilbur (1960) showed that low temperatures slowed growth and produced larger crystals in molluscs, which is the same trend in the rhynchonelliform brachiopods in this chapter. Similar numbers of crystal fibres have been reported between each puncta in brachiopods of widely varying punctal density (Foster, 1974). This suggests that punctae are formed after a certain number of crystals are deposited. Species with larger calcite fibres should, therefore, have more space between punctae and a lower punctal density. The larger calcite fibres in *L. uva* complement the lower punctal density in the polar brachiopod compared to the temperate species in this chapter.

### 3.4.3 Elemental composition

None of the major elements concentrations (Ca, Mg, Na, Sr and P) were impacted by lowered pH in *L. uva* or *C. inconspicua*. Therefore, both species can produce shell with the same elemental composition in predicted pH conditions for the next 84 years. Ocean acidification

research on other marine calcifiers has demonstrated varying effects on elemental composition, with greater impacts reported in Mg, Na and Sr. Na and Mg concentrations both decreased in *Mytilus galloprovincialis* shell laid down in low pH environments near CO<sub>2</sub> vents compared to individuals in control conditions (Hahn et al., 2012). Reduced Na concentrations were attributed to the lack of nacreous layer production in low pH conditions as Na concentrations are higher in nacre than the calcite layer. Mg is only present in the calcite layer of *M. galloprovincialis*, therefore, shell microstructure does not explain the decrease in Mg concentration in shell precipitated in low pH conditions and the reasons for this decrease remain unknown. These results must be interpreted with caution though as only one individual was used in the shell geochemistry analysis by Hahn et al. (2012). Sr concentrations were higher in the sea urchin *Paracentrotus lividus* but not in *Arbacia lixula* in response to low pH environments whereas Ca, Mg, Na and various other elements in both species did not vary significantly with pH (Bray et al., 2014). Higher Sr concentrations in lowered pH have also been reported in the urchin *Strongylocentrotus purpuratus* (LaVigne et al., 2013). Both these studies suggest increased Sr incorporation, albeit with no parallel decrease in Mg concentration, could indicate an increased mineral precipitation rate at the calcification site (LaVigne et al., 2013; Bray et al., 2014). This could be due to the positive relationship of Sr incorporation and precipitation rate in sea urchins (Kinsman & Holland, 1969; Carpenter & Lohman, 1992). The absence of this trend in Sr concentration in *A. lixula* indicates that impacts of lowered pH on elemental composition are species-specific (Ries et al., 2009; Bray et al., 2014). Diet has a stronger effect on Mg/Ca ratios in juveniles of the sea urchin *P. lividus* than lowered pH (Asnaghi et al., 2014). This study found that urchins fed with the calcifying macroalgae *Corallina* had a higher Mg/Ca ratio in elevated pCO<sub>2</sub>, whereas urchins fed with non-calcifying macroalgae did not show any differences in this ratio with increased pCO<sub>2</sub>. This highlights the importance of multifactor ocean acidification studies to provide more environmentally relevant data on variations in elemental compositions in marine calcifiers.

Increased temperature did not affect concentrations of any major element in *L. uva* indicating this polar species can produce shell with the same elemental composition in warmed end-century predicted conditions. This contrasts with other elemental composition studies on brachiopods as concentrations of major elements, including Na and Sr but particularly Mg, generally increase with elevated temperature (Bickmore et al., 1994; Mii & Grossman, 1994; Grossman et al., 1996). An inverse correlation between Mg and <sup>18</sup>O concentrations was also

recorded in the Carboniferous brachiopod *Neospirifer dunbari* shell which was consistent with a temperature effect (Grossman et al., 1996). Concentrations of Ca in *L. uva* and Mg and Na in *C. inconspicua* were higher in experimental growth in all treatments compared to wild growth. These trends were present in the pH control as well as both acidified treatments, and are thus not an effect of low pH. The higher Mg and Na concentrations in experimental growth of *C. inconspicua* could result from the high, but similar, temperatures in all three treatments due to unusually high seawater temperatures in Otago Harbour during the 12 week temperate experiment (Chapter 2; Cross et al., 2016). Temperature cannot explain the higher Ca concentrations in *L. uva* experimental growth as this trend was present in the higher temperature treatments as well as the temperature control. Seawater used in the closed-circuit polar experiment was sourced from the Norfolk coast, therefore, this pattern could be due to potentially different Ca concentrations of the North Sea and the Southern Ocean.

Other factors that might affect brachiopod shell elemental composition are taxonomy, shell growth rate and microstructure (Lowenstam, 1961; Buening & Carlson, 1992). A taxonomic effect on Sr and Mg was suggested to superimpose on the temperature effect (Lowenstam, 1961). Faster shell growth rates in *L. uva* at higher temperature (Chapter 2; Cross et al., 2015) and elemental composition not differing between treatments, indicate that shell growth rates do not affect concentrations of any major element in *L. uva*. Ca concentration was higher in *C. inconspicua* than *L. uva* and Mg, Na, Sr and P concentrations were higher in *L. uva* than *C. inconspicua*. This supports the suggestion that taxonomy might be a major factor dictating elemental composition. Taxonomic differences could be explained by different precipitation rates of different shell types and some elements are affected by precipitation rate. For example, Na concentration is higher in fibrous *Eridmatus* shell than in prismatic *Neospirifer* shell (Grossman et al., 1996), which could be explained by fibrous shell being precipitated faster than prismatic shell (Busenberg & Plummer, 1985). *L. uva* has higher Na, Sr and P concentrations than *C. inconspicua*, which could be explained by the faster growth rate of larger *L. uva*.

All trace elements (Si, Fe, Mn and Ba) were below the Electron Microprobe detection limits. Any effects of predicted end-century pH and warming conditions on concentrations of these elements in rhynchonelliform brachiopods thus remain unknown. Low pH increased Mn concentrations in both *P. lividus* (541% increase) and *A. lixula* (243% increase) and lowered

Zn concentrations in *P. lividus* (66% decrease; Bray et al., 2014). Reasons for these differences are unclear, however, the decrease in Zn was suggested to be due to reproductive status differences between sites as this element is essential for reproduction and present in high concentrations in female urchin gonads. Mn incorporation in crystal lattices often leads to abnormal skeletal growth (Richter et al., 2003), which suggests these urchin species might have further problems in future acidified conditions.

#### 3.4.4 Conclusions

Despite rhynchonelliform brachiopods being one of the most highly calcium carbonate dependent organisms, both *L. uva* and *C. inconspicua* can repair shell damage and deposit new shell (Chapter 2; Cross et al., 2015, 2016) in predicted environmental conditions for 2100. The tolerance of this polar and temperate species has further been demonstrated in this chapter through their ability to produce the same shell structurally, in terms of punctal density, calcite fibre size and elemental composition. However, data on more shell characteristics, such as texture, hardness and organic content, are needed to fully understand the resilience of the shell production process to predicted future conditions. Biomineralisation in marine calcifiers is facilitated by actively elevating pH and thus the saturation states in the calcifying compartments above that of ambient seawater (Al-Horani et al., 2003; Cohen et al., 2009; Ries et al., 2009). This reduction in  $H^+$  concentration converts  $HCO_3^-$  to  $CO_3^{2-}$  which elevates  $CO_3^{2-}$  concentration within the calcifying compartments. Marine calcifiers that can elevate their calcifying fluid pH above ambient levels are generally less negatively affected by low pH than species that only maintain pH at lower levels (Ries et al., 2009). pH in the calcifying compartment in brachiopods is unknown. It is likely, however, that this phylum can increase this pH and consequently has a strong control on biomineralisation.

# Chapter Four

## **Do polar and temperate brachiopods maintain their shell integrity under predicted end-century acidified conditions?**

### **4.1 Introduction**

The shell is crucial for protection in shell-bearing organisms (Vermeij, 1977), therefore, any negative impacts to shell integrity could compromise its protective function and potentially prove fatal. Shell integrity can be affected by erosion from natural scour or attack from shell-boring organisms and dissolution. Abrasion of the shell surface occurs through the movement of individuals against each other, with other calcified biota or substrata. Rhynchonelliform brachiopods typically settle on hard substrata or on older conspecific individuals in some species forming large clusters of animals in close proximity (James et al., 1992). In these clusters any movement is likely to cause shell erosion. Rhynchonelliform brachiopod shells are also susceptible to infestation of shell-boring organisms, which penetrate the periostracum and erode the inner shell layers (Curry, 1983b). Dissolution is a physicochemical process largely driven by the solubility of the biomineral, the chemical characteristics of the surrounding seawater and also by potential effects of the metabolic by products released by the adhering biofilm (Nienhuis et al., 2010). Environmental conditions predicted for 2100 will shift seawater carbonate chemistry to the point where  $\text{CaCO}_3$  dissolution is favoured, which potentially could further decrease the shell integrity of rhynchonelliform brachiopods already subject to being compromised by physical abrasion and shell-boring organisms.

Shell dissolution at the external surface cannot be regulated by the organism. Marine calcifiers could, however, counteract this potentially fatal effect of ocean acidification through compensatory mechanisms. Phenotypic plasticity of shell morphology has been reported in shelled organisms in response to the presence of predators (Brönmark et al., 2011) as well as changing environmental conditions (Peyer et al., 2010; Fitzner et al., 2015a). These responses include shell thickening and production of a more rotund shell as seen in molluscs (Vermeij,

1982; Freeman & Byers, 2006; Fisher et al., 2009; Peyer et al., 2010; Brönmark et al., 2011; Fitzner et al., 2015a). Production of a thicker periostracum could also withstand more wear and deter dissolution. These indicate possible compensatory mechanisms to enhance protection from abiotic and biotic stresses, including predation and altered conditions, which could also be present in rhynchonelliform brachiopods.

Calcification and dissolution are two of the primary processes investigated in ocean acidification research due to their direct importance to the survival of marine calcifiers (reviewed by Kroeker et al., 2013). While there have been varied impacts on calcification, which are generally considered to be species-specific (Ries et al., 2009; Kroeker et al., 2013), dissolution and subsequent compensation appears to be more challenging and potentially more of a threat to calcifying organisms (Nienhuis et al., 2010; Roleda et al., 2010). Shell growth rates of the rhynchonelliforms *L. uva* and *C. inconspicua* are not impacted by predicted acidified conditions (Chapter 2; Cross et al., 2015, 2016), but dissolution increased in the Antarctic brachiopod in pH 7.4 conditions after only 14 days (McClintock et al., 2009). Only empty dried valves were used by McClintock et al. (2009), so the compensatory ability of brachiopods to shell dissolution remained unknown. The aims of this chapter, therefore, were to investigate dissolution effects and potential compensatory mechanisms of rhynchonelliform brachiopods under acidified and warming conditions. Specifically, the extent of dissolution and thickness of whole valves and individual shell layers were assessed under predicted end-century pH levels in *L. uva* and *C. inconspicua* and also under increased temperature in *L. uva*.

## **4.2 Materials and methods**

### **4.2.1 Experimental design**

Experimental design details for both CO<sub>2</sub> perturbation experiments conducted on *L. uva* and *C. inconspicua* are presented in section 2.2.2.

### **4.2.2 Sample preparation**

Sample preparation details are presented in section 3.2.2. For each species, five undamaged specimens with the largest experimental growth increments were selected from each treatment for further shell analysis. Morphometric data for each specimen are given in Tables 4.1 and 4.2.

**Table 4.1 – *L. uva* - Morphometrics of the individuals selected for further shell analysis of shell condition index and thickness. Initial length is given to indicate size of the individual. Grey cells indicate the use of this specimen in the respective shell analysis.**

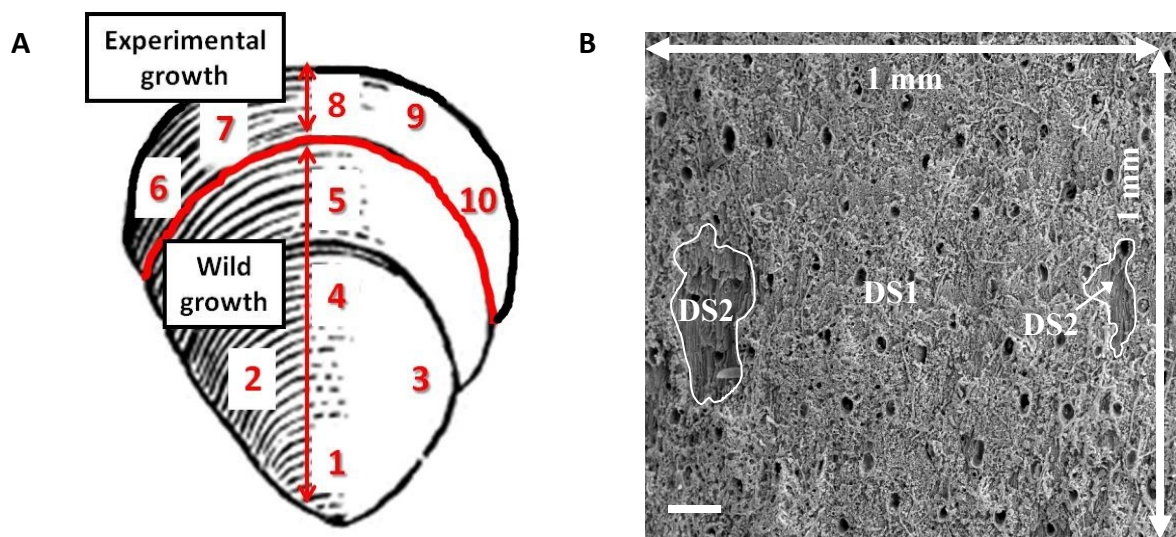
Treatment	Individual ID	Initial length (mm)	Overall growth (mm)	Shell characteristics	
				Pedicle valves	Brachial valves
				Shell condition index	Shell thickness
Temperature Control	Temperature control - N7	19.6	1.1		
	Temperature control - N20	20.3	1.2		
	Temperature control - N28	7.2	0.7		
	Temperature control - N49	12.2	0.7		
	Temperature control - N52	9.1	0.8		
pH control	pH control - N4	8.9	1.6		
	pH control - N5	8.1	1.4		
	pH control - N6	9.8	0.8		
	pH control - N7	16.1	1.7		
	pH control - N9	14.9	1.3		
	pH control - N10	23.3	2.0		
pH 7.75	pH 7.75 - N1	7.5	1.9		
	pH 7.75 - N2	10.6	0.9		
	pH 7.75 - N5	13.6	2.3		
	pH 7.75 - N8	17.3	2.7		
	pH 7.75 - N9	17.9	2.5		
pH 7.54	pH 7.54 - N1	10.5	1.3		
	pH 7.54 - N4	14.0	1.8		
	pH 7.54 - N5	17.8	1.0		
	pH 7.54 - N6	21.5	1.2		
	pH 7.54 - N8	22.2	1.0		
	pH 7.54 - N9	24.1	0.6		

**Table 4.2 – *C. inconspicua* - Morphometrics of the individuals selected for further shell analysis of shell condition index and shell thickness. Initial length is given to indicate the size of the individual. Grey cells indicate the use of this specimen in the respective shell analysis.**

Treatment	Individual ID	Initial length (mm)	Overall growth (mm)	Shell characteristics	
				Pedicle valves	Brachial valves
				Shell condition index	Shell thickness
pH control	pH control - N1	6.7	0.6		
	pH control - N13	8.0	1.3		
	pH control - N14	5.3	0.8		
	pH control - N29	8.3	0.8		
	pH control - N49	9.8	0.5		
pH 7.8	pH 7.8 - N3	10.1	0.9		
	pH 7.8 - N5	10.5	0.6		
	pH 7.8 - N8	10.3	0.8		
	pH 7.8 - N14	5.2	0.8		
	pH 7.8 - N25	8.1	0.6		
pH 7.6	pH 7.6 - N11	7.0	1.4		
	pH 7.6 - N19	4.9	1.0		
	pH 7.6 - N31	6.2	0.7		
	pH 7.6 - N40	6.1	0.7		
	pH 7.6 - N46	7.1	0.8		

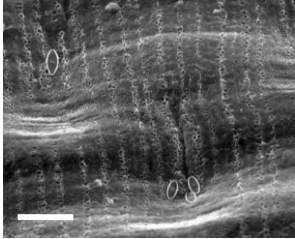
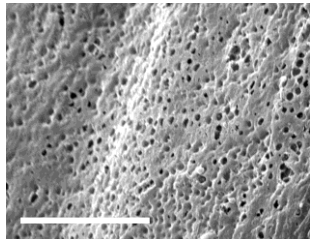
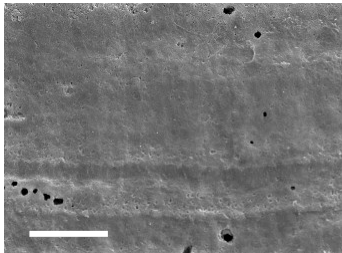
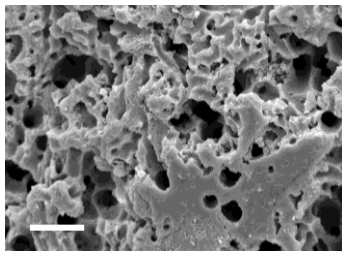
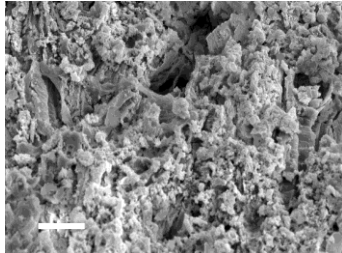
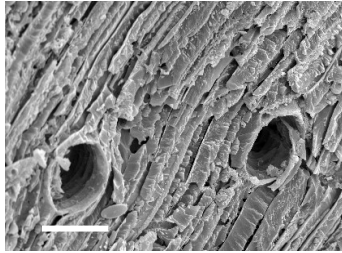
### 4.2.3 Shell condition index

Scanning Electron Microscopes (JEOL 820 for *L. uva* and FEI QEMSCAN 650F for *C. inconspicua*; both operated using an accelerating voltage of 20 kV) in the Department of Earth Sciences at the University of Cambridge, UK were used to image pedicle valves of both *L. uva* and *C. inconspicua* from each treatment to determine shell condition. Five types of shell condition were present including intact periostracum with pitted layer (stage 0), intact periostracum without pitted layer (wear stage 1), wear but no dissolution (wear stage 2), dissolution in the primary layer (dissolution stage 1) and extensive dissolution exposing the secondary layer (dissolution stage 2). Full descriptions and examples of each type of shell condition for both species are presented in Table 4.3. Micrographs (1 mm x 1 mm) were collected at 5 areas in shell laid down in the natural environment and 5 areas from growth in the experiments (Figure 4.1A). Percentage areas of each type of shell condition from each SEM micrograph were measured in ImageJ (Figure 4.1B). To minimise operator error, assessments of each type of shell condition were made three times on each micrograph on different days with the average areas used in statistical analysis.



**Figure 4.1 – Shell condition index: (A) schematic of a pedicle valve indicating the 5 areas in the growth laid down in the wild and the 5 areas in experimental growth where SEM micrographs were collected for analysis and (B) a typical 1 mm by 1 mm SEM micrograph of the outer shell surface collected to determine shell condition index. DS1 = dissolution stage 1, DS2 = dissolution stage 2. Scale bar = 100  $\mu$ m**

**Table 4.3 – Shell condition index - Descriptions of each type of shell condition with SEM examples. Examples given apply to both species unless stated otherwise. Scale bar = 20 µm.**

Shell condition index	Description	SEM examples
<p><b>Stage 0:</b> Intact periostracum with pitting layer</p>	<p>Smooth, intact periostracum with no signs of wear or dissolution with a complete covering of the pitted layer on the surface.</p>	<p><i>L. uva:</i>  <i>C. inconspicua:</i> </p>
<p><b>Wear Stage 1:</b> Intact periostracum without pitting layer</p>	<p>Smooth intact periostracum without any extensive signs of wear, however, the pitted layer is absent probably due to less invasive wear.</p>	
<p><b>Wear Stage 2:</b> Wear but no dissolution</p>	<p>Abrasion of the periostracum causes rough, blunt and sharp surfaces or cylindrical, hollow meandering paths from shell-boring organisms. Despite exposing the inner shell layers, no dissolution occurs.</p>	
<p><b>Dissolution Stage 1:</b> Dissolution in the primary layer</p>	<p>Corrosion of the primary layer with flaky, dissolved calcite crystals and the formation of large dissolution pits within this shell layer. The secondary layer is never exposed in this stage.</p>	
<p><b>Dissolution Stage 2:</b> Dissolution exposing the secondary layer</p>	<p>Extensive dissolution causing the complete removal of the primary layer and exposing the underlying secondary layer.</p>	

#### 4.2.4 Shell thickness

Polished cross sections of brachial valves were etched with 1% HCl for 30 seconds before acetate peel replicas of the etched surfaces were prepared of each specimen. Acetate peels were prepared according to Richardson et al. (1979). Briefly, acetone was poured onto the resin block and small strips of replicating material (Agar Scientific cellulose acetate) were placed on the etched surface allowing the acetate to become almost pliable after 30 seconds in acetone. After 15 minutes, the acetone had evaporated and the peel was removed and mounted between a microscope slide and a cover slip. Thickness measurements ( $\pm 0.1$  mm) of the primary layer, secondary layer and total shell were then made from 3 areas of wild growth and 3 areas of experimental growth (Figure 4.2) on a Swift monocular petrological microscope with fitted micrometer.

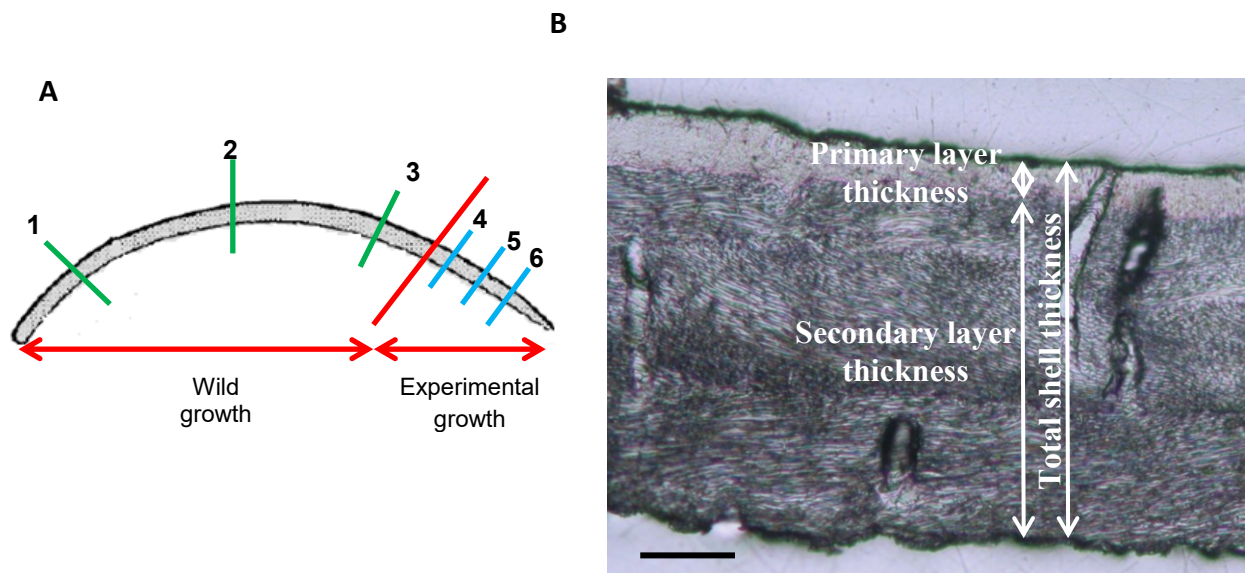


**Figure 4.2 – Thickness measurements: (A) Schematic illustrating the areas in the shell laid down in the wild (green lines) and the shell laid down in the experiment (blue lines) where thickness measurements were made and (B) optical image indicating the primary and secondary layers. Scale bar = 100  $\mu$ m.**

#### 4.2.5 Statistical analysis

All data were analysed using Minitab (Statistical Software<sup>TM</sup> Version 17). To attempt to meet the assumptions of parametric statistics, percentage area data for the shell condition index of both *L. uva* and *C. inconspicua* were arcsin transformed to remove imposed limits, however, the arcsin values were not normally distributed because there were zeros in the dataset (Anderson-Darling test;  $p < 0.05$ ). Therefore, non-parametric Kruskal-Wallis tests were used to determine whether treatment and area number affected the median percentage area of each type of shell condition in the wild growth and experimental growth separately. Each growth

period was analysed separately to determine whether treatment and area number affected thickness of shell that had already been potentially subjected to substantial wear (wild growth) and newly produced shell with less time subjected to wear (experimental growth). When significant differences were found, a further Kruskal-Wallis Multiple Comparisons test was conducted to identify which treatments were statistically different from each other. Thickness data for both *L. uva* and *C. inconspicua* were normally distributed (Anderson-Darling test;  $p > 0.05$ ). Two-way ANOVA's were conducted on primary layer, secondary layer and total shell thickness measurements in wild growth and in experimental growth separately to determine if treatment and/or shell position, where measurements were made, affected thickness. Each growth period was analysed separately to determine whether treatment and shell position affected shell maintenance (thickness of shell laid down in the wild) and shell production (thickness of shell laid down in the experiment). Post-hoc Tukey tests were performed when significant differences were found to determine which treatments, shell position and/or interaction factors were responsible.

### 4.3 Results

#### 4.3.1 Shell condition index

In *L. uva* wild growth, intact periostracum with pitted layer (stage 0) was only observed in the two controls (Figure 4.3A, B and Figure 4.4), and only one individual exhibited this shell condition in the temperature control (Appendix Figure B1A) and it was only present in areas 4 and 5 (averages of 19.8% and 22.1%, respectively) in the pH control (Figure 4.4 and Appendix Figure B1C). Intact periostracum without pitted layer (wear stage 1) was present in *L. uva* wild growth in all treatments, but only one individual exhibited this shell condition in the most acidified treatment (Appendix Figure B1G). Treatment significantly affected the area of intact periostracum without pitted layer (Kruskal-Wallis:  $H = 60.98$ ,  $p < 0.001$ ). The lower percentage areas of this type of wear occurred in the acidified treatments (Kruskal-Wallis Multiple Comparison test: pH control vs pH 7.75:  $Z = 4.187$ ,  $p < 0.001$ , pH control vs pH 7.54:  $Z = 6.918$ ,  $p < 0.001$ ), with a larger percentage area in the pH 7.75 treatment compared to pH 7.54 ( $Z = 2.971$ ,  $p = 0.003$ ). Temperature, however, did not have an effect (Figure 4.4; Temperature control vs pH control:  $Z = 0.735$ ,  $p = 0.462$ ). Temperature appeared to impact the percentage area of wear but not dissolution (wear stage 2) in *L. uva* wild growth as significantly lower percentage areas were present in the three higher temperature (2°C) treatments (Kruskal-Wallis Multiple Comparison test, pH control:  $Z = 3.543$ ,  $p < 0.001$ , pH

7.75:  $Z = 2.873$ ,  $p < 0.001$ , pH 7.54:  $Z = 2.767$ ,  $p = 0.006$ ). Percentage areas of dissolution in the primary layer (dissolution stage 1) were significantly higher in both acidified treatments compared to both controls (Figure 4.4; Kruskal-Wallis Comparison test, temperature control vs pH 7.75:  $Z = 6.367$ ,  $p < 0.001$ , temperature control vs pH 7.54:  $Z = 6.557$ ,  $p < 0.001$ , pH control vs pH 7.75:  $Z = 5.203$ ,  $p < 0.001$ , pH control vs pH 7.54:  $Z = 5.459$ ,  $p < 0.001$ ) with no significant difference between pH 7.75 and pH 7.54 ( $Z = 0.553$ ,  $p = 0.580$ ). Dissolution exposing the secondary layer (dissolution stage 2) was absent in both controls. It accounted for only 0.4-1.8% area of wild growth in the pH 7.75 treatment (Figure 4.3A, C, E, G and Figure 4.4). The most acidified treatment, however, had significantly higher percentage areas of this dissolution stage compared to the other treatments (Kruskal-Wallis Multiple Comparison test, temperature control:  $Z = 5.857$ ,  $p < 0.001$ , pH control:  $Z = 5.611$ ,  $p < 0.001$ , pH 7.75:  $Z = 3.949$ ,  $p < 0.001$ ).

*L. uva* experimental growth was mainly characterised by intact periostracum with pitted layer (stage 0) as  $> 58.9\%$  of all individuals exhibited intact shell (Figure 4.3B, D, F, H and area numbers 6-10 in Figure 4.4). Percentage area of stage 0 was significantly lower in the most acidified treatment compared to the other treatments (Temperature control:  $Z = 3.899$ ,  $p < 0.001$ ; pH control:  $Z = 6.302$ ,  $p < 0.001$ ; pH 7.75:  $Z = 4.730$ ,  $p < 0.001$ ). Intact periostracum without pitted layer (wear stage 1) was only found in one individual in both the pH control and pH 7.75 treatments (Appendix Figure B1B, D). Temperature appeared to impact the percentage area of wear but not dissolution (wear stage 2) in *L. uva* experimental growth as significantly lower percentage areas were present in the three higher temperature ( $2^{\circ}\text{C}$ ) treatments (Kruskal-Wallis Multiple Comparison test, pH control:  $Z = 5.877$ ,  $p < 0.001$ , pH 7.75:  $Z = 3.805$ ,  $p < 0.001$ , pH 7.54:  $Z = 5.476$ ,  $p < 0.001$ ). The percentage area of dissolution in the primary layer (dissolution stage 1) increased with increasing acidity (Figure 4.3; Kruskal-Wallis Multiple Comparison test, pH control vs pH 7.75:  $Z = 2.405$ ,  $p = 0.016$ , pH control vs pH 7.54:  $Z = 7.101$ ,  $p < 0.001$ , pH 7.75 vs pH 7.54:  $Z = 4.834$ ,  $p < 0.001$ ), but temperature did not have an effect (Figure 4.4; Kruskal-Wallis Multiple Comparison test, Temperature control vs pH control:  $Z = 0.216$ ,  $p = 0.829$ ). Dissolution exposing the secondary layer (dissolution stage 2) was absent in *L. uva* experimental growth in all treatments (Figure 4.3B, D, F, H and Figure 4.4).

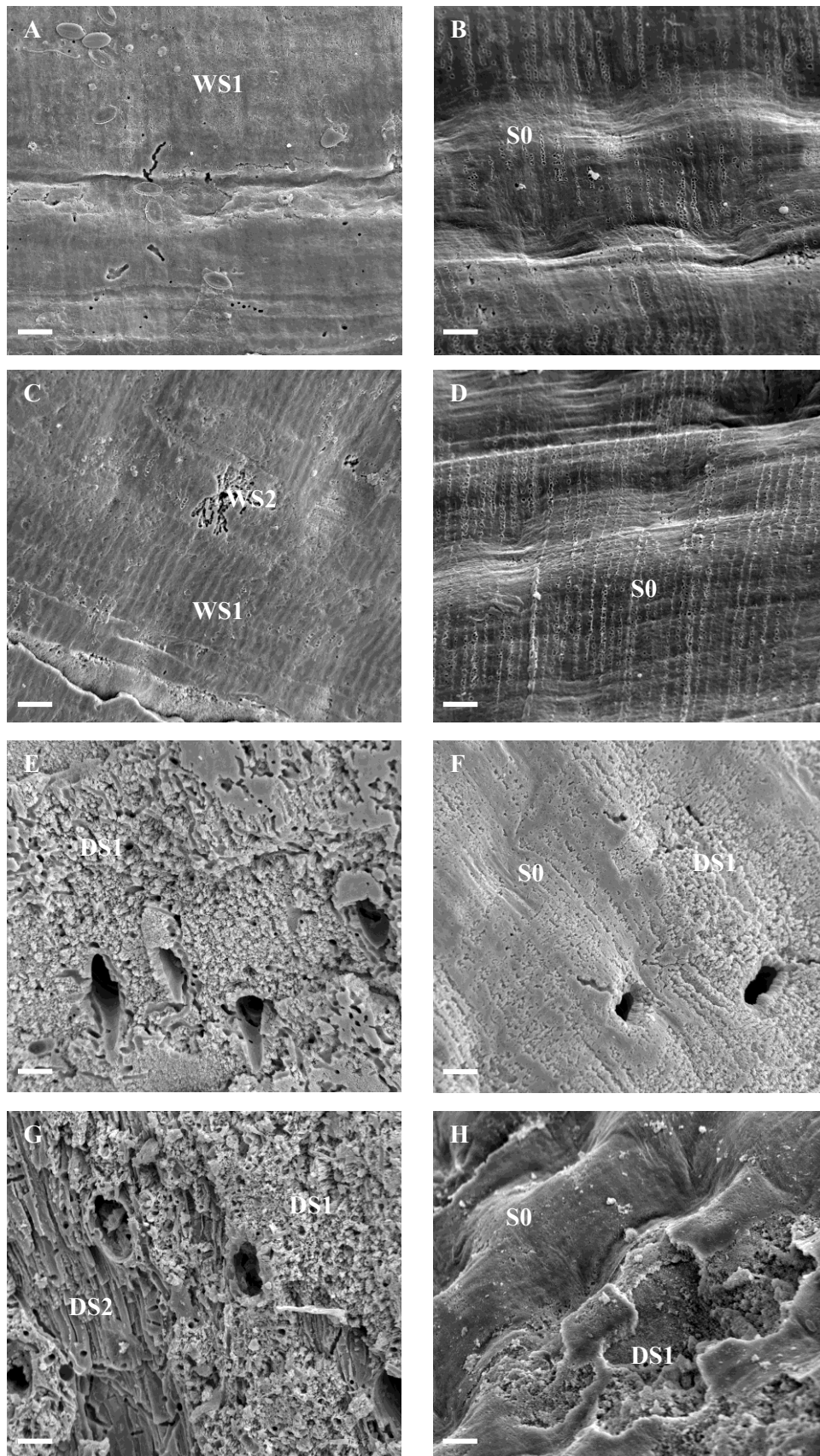


**Figure 4.3 – *L. uva* – Examples of SEM micrographs of shell surfaces of shell laid down in the wild (A, C, E, G) and in the experiment (B, D, F, H) in temperature control (A, B), pH control (C, D), pH 7.75 (E, F) and pH 7.54 treatment (G, H). S0 = stage 0, WS1 = wear stage 1, WS2 = wear stage 2, DS1 = dissolution stage 1 and DS2 = dissolution stage 2. Scale bar = 20  $\mu\text{m}$ .**

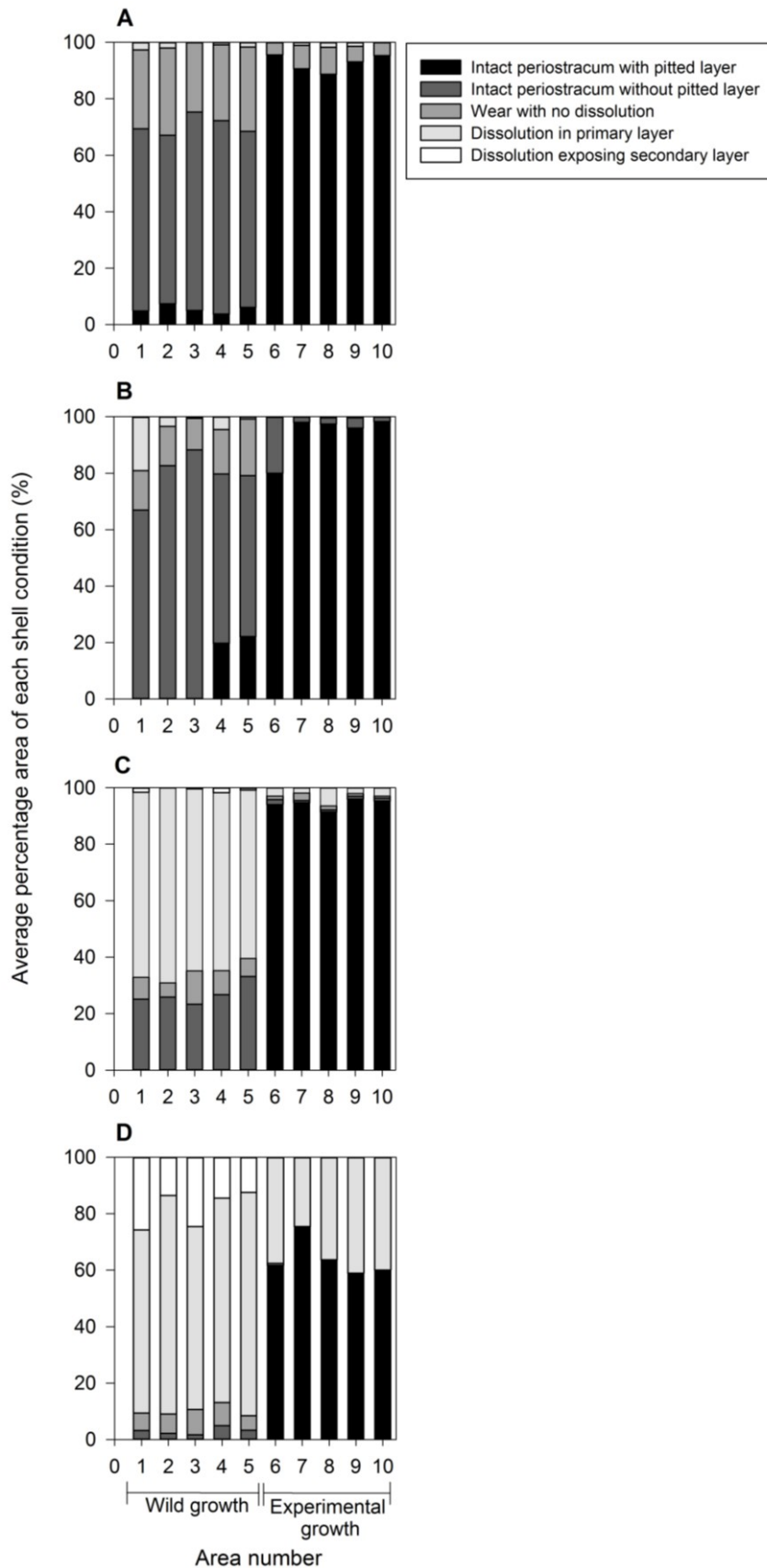


**Figure 4.4 – *L. uva* – Average percentage area of the different types of shell conditions in wild growth (area numbers 1-5) and experimental growth (area numbers 6-10) in temperature control (A), pH control (B), pH 7.75 (C) and pH 7.54 treatment (D). Lighter grey tones indicate an increase in wear and/or shell dissolution (see legend).**

In contrast to *L. uva*, *C. inconspicua* wild growth in all treatments was mainly characterised by intact periostracum with pitted layer (stage 0; > 43% across all treatments; Figure 4.5 and Figure 4.6). There was, however, a treatment effect on this shell condition (Kruskal-Wallis,  $H = 44.49$ ,  $p < 0.001$ ). The most acidified treatment had a significantly lower percentage area of stage 0 than the pH 7.8 treatment and the pH control (Kruskal-Wallis Multiple Comparisons test, pH 7.8:  $Z = 4.562$ ,  $p < 0.001$ ; pH control:  $Z = 6.495$ ,  $p < 0.001$ ) with no differences between pH 7.8 and the pH control ( $Z = 1.934$ ,  $p = 0.053$ ). The percentage area of intact periostracum without pitted layer (wear stage 1) was also affected by treatment (Kruskal-Wallis,  $H = 7.89$ ,  $p = 0.020$ ). There were significantly lower percentage areas of intact periostracum without pitted layer in the pH 7.6 treatment than both the other treatments (Kruskal-Wallis Multiple Comparisons test, pH 7.8:  $Z = 2.564$ ,  $p = 0.010$ ; pH control:  $Z = 2.274$ ,  $p = 0.023$ ) with no differences between pH 7.8 and the pH control ( $Z = 0.290$ ,  $p = 0.772$ ). The percentage area of dissolution in the primary layer (dissolution stage 1) increased with increasing acidity (Figure 4.5 and Figure 4.6; Kruskal-Wallis Multiple Comparison test, pH control vs pH 7.8:  $Z = 4.032$ ,  $p < 0.001$ , pH control vs pH 7.6:  $Z = 7.316$ ,  $p < 0.001$ , pH 7.8 vs pH 7.6:  $Z = 3.284$ ,  $p < 0.001$ ). Treatment did not affect the proportion of wear without dissolution (wear stage 2) in the wild growth (Kruskal-Wallis,  $H = 0.02$ ,  $p = 0.988$ ) and dissolution exposing the secondary layer (dissolution stage 2) did not occur in any treatment (Figure 4.6; Appendix Figure B2).

Similar to *L. uva*, *C. inconspicua* experimental growth in all treatments mainly consisted of intact periostracum with pitted layer (stage 0) with > 71.4% of all experimental areas classified as this shell condition (Figure 4.5 and 4.6). There was a significant effect of treatment on the percentage cover of stage 0 (Kruskal-Wallis,  $H = 20.96$ ,  $p < 0.001$ ). Significantly lower percentage areas occurred in the most acidified treatment compared to the pH control (Kruskal-Wallis Multiple Comparisons test,  $Z = 2.810$ ,  $p = 0.005$ ) and the pH 7.8 treatment ( $Z = 4.535$ ,  $p < 0.001$ ). There was, however, no significant difference between pH 7.8 and the pH control ( $Z = 1.725$ ,  $p = 0.085$ ). Treatment affected the percentage area of experimental growth exhibiting wear but no dissolution (wear stage 2; Kruskal-Wallis,  $H = 10.67$ ,  $p = 0.005$ ). Percentage cover of this wear was higher in the pH control than in both acidified treatments (Kruskal-Wallis Multiple Comparison test, pH 7.8:  $Z = 2.377$ ,  $p = 0.018$ ; pH 7.6:  $Z = 3.130$ ,  $p = 0.002$ ). Primary layer dissolution (dissolution stage 1) in experimental growth was only present in the most acidified treatment (Figure 4.6). Intact periostracum without pitted layer (wear stage 1) and dissolution exposing the secondary layer (dissolution

stage 2) was absent in the experimental growth in all treatments (Figure 4.6; Appendix Figure B2).

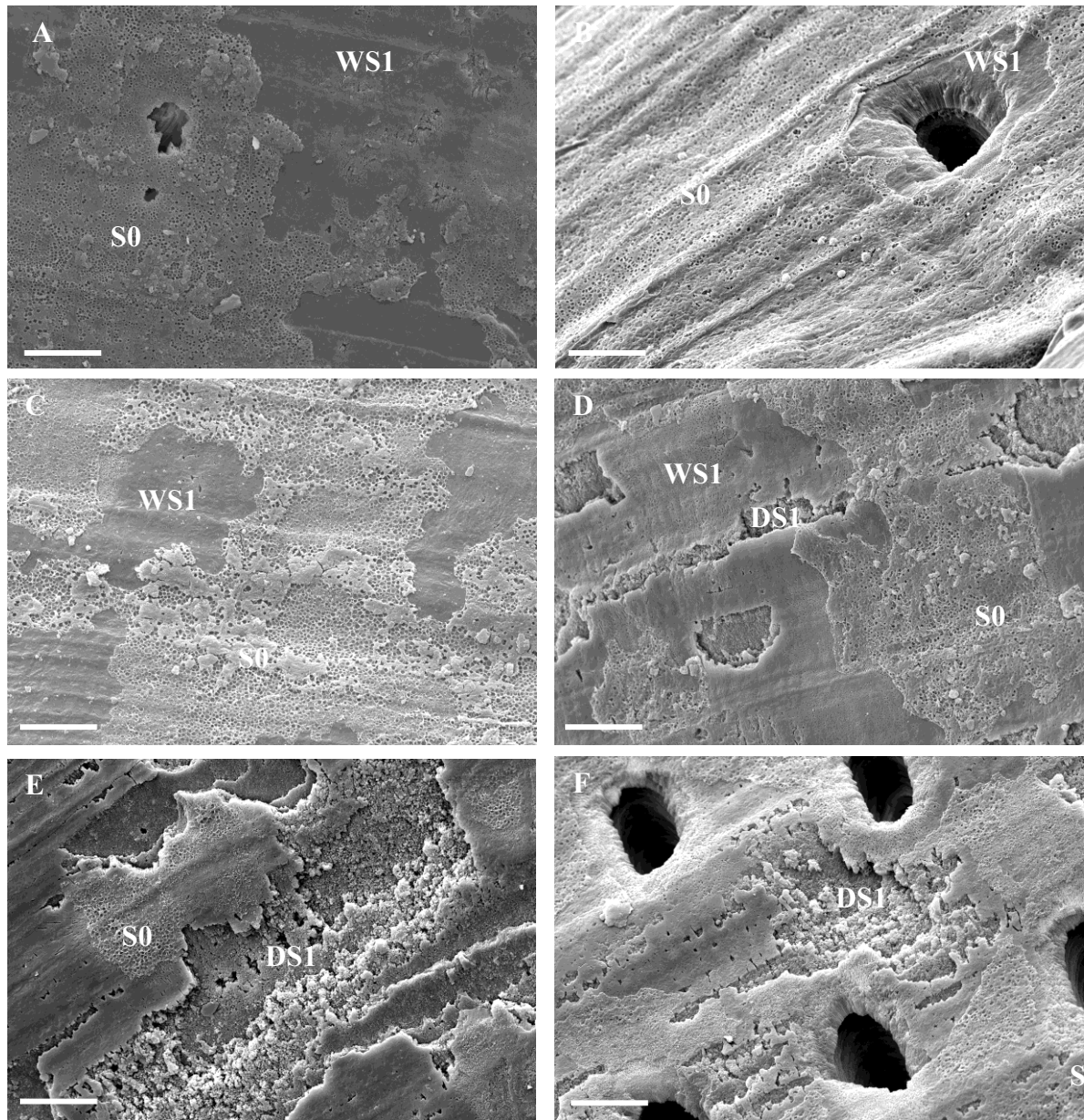


**Figure 4.5 – *C. inconspicua* – SEM micrographs of shell surfaces of shell laid down in the wild (A, C, E) and in the experiment (B, D, F) in pH control (A, B), pH 7.8 (C, D) and pH 7.6 (E, F). S0 = stage 0, WS1 = wear stage 1, WS2 = wear stage 2 and DS1 = dissolution stage 1. DS2 (dissolution stage 2) was absent in all treatment in this species. Scale bar = 20  $\mu$ m.**

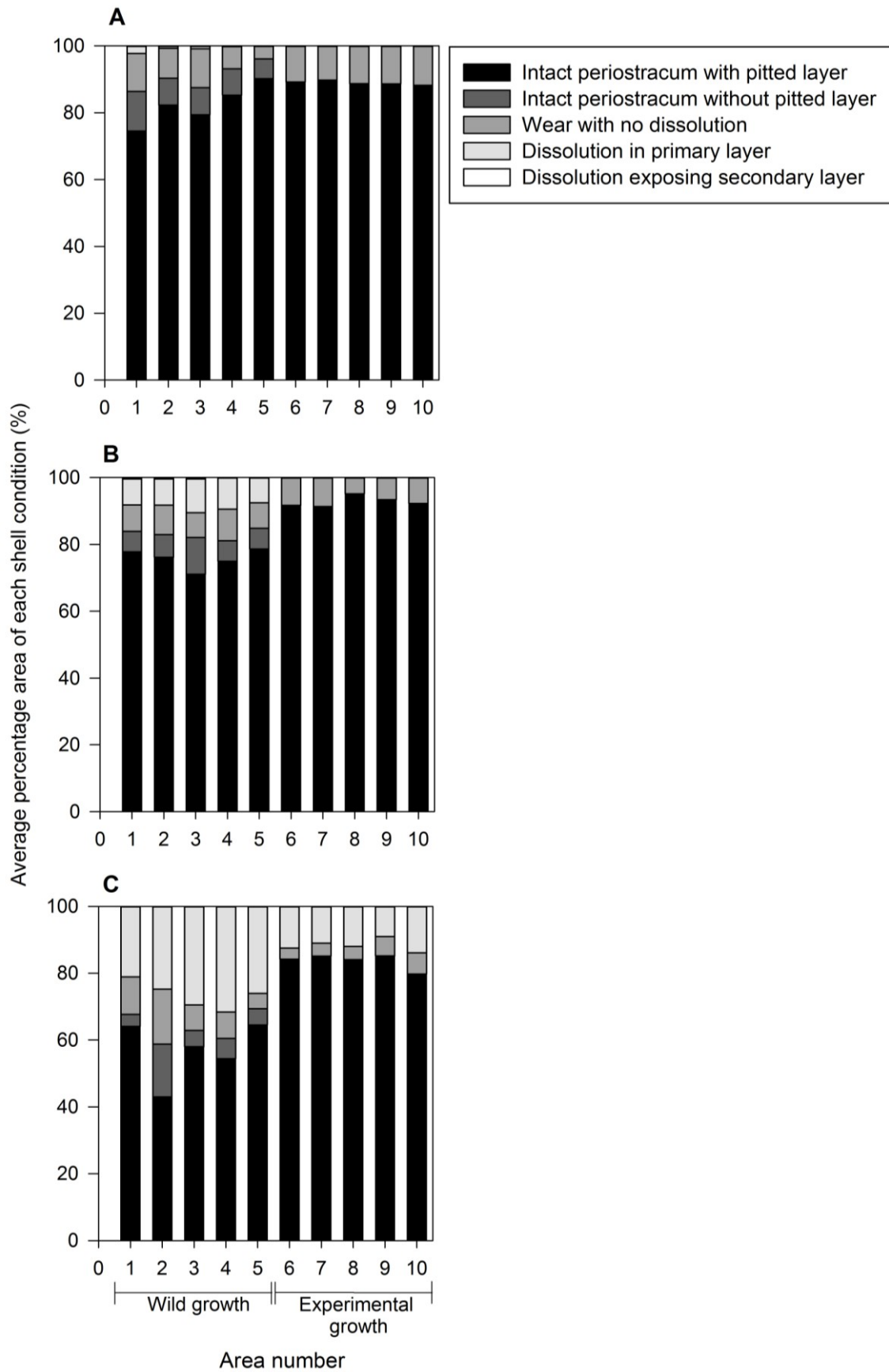


**Figure 4.6 – *C. inconspicua* – Average percentage area of the different shell conditions in wild growth (area numbers 1-5) and experimental growth (area numbers 6-10) in pH control (A), pH 7.8 (B) and pH 7.6 (C). Lighter grey tones indicate an increase in wear and/or shell dissolution (see legend).**

### 4.3.2 Shell thickness

#### 4.3.2.1 Primary layer thickness

Primary layer thickness in *L. uva* ranged from 0-96.7  $\mu\text{m}$  (black bars in Appendix Figure B3). In *L. uva* wild growth, lowered pH caused the primary layer to become progressively thinner. There was no difference between the two controls but the primary layer was thinner in pH 7.75 and was thinnest in pH 7.54 (Figure 4.7A; Two-way ANOVA - Treatment:  $F_{3,45} = 68.20$ ,  $p < 0.001$ ). The primary layer also got progressively thinner towards the umbo (black bars in Appendix Figure B3A, C, E, G; Two way ANOVA - Shell position:  $F_{2,45} = 22.41$ ,  $p < 0.001$ ). All three positions in pH 7.54 were thinner than all other treatments. Umbo regions (position 1) in both controls and pH 7.75 were thinner than the middle of the shell (position 2) and nearer the experimental growth (position 3). Each position in pH 7.75 was thinner than the equivalent position in both controls (black bars in Appendix Figure B3A, C, E, G; Two-way ANOVA - Interaction:  $F_{6,45} = 3.69$ ,  $p = 0.005$ ). In *L. uva* experimental growth, primary layer thickness was not affected by treatment, shell position or the interaction of the two factors (Figure 4.7B and black bars in Appendix Figure B3B, D, F, H; Two-way ANOVA - Treatment:  $F_{3,45} = 1.35$ ,  $p = 0.271$ ; Shell position:  $F_{2,45} = 0.17$ ,  $p = 0.840$ ; Interaction:  $F_{6,45} = 1.15$ ,  $p = 0.360$ ). Temperature did not affect primary layer thickness in *L. uva* wild or experimental growth.

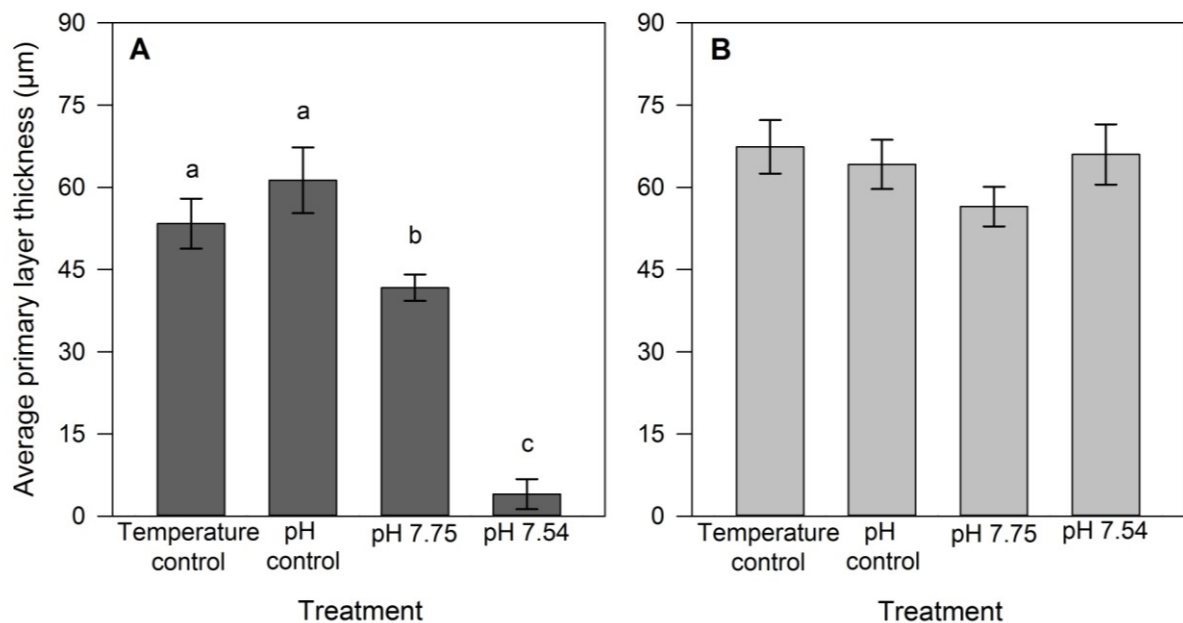


**Figure 4.7 – *L. uva* – Average primary layer thickness in wild growth (A) and experimental growth (B) in all four treatments. Values plotted are mean  $\pm$  SE. Different letters above columns indicate significant differences ( $p < 0.05$ ).**

*C. inconspicua* primary layer thickness ranged from 14.3-40.9  $\mu\text{m}$  (black bars in Appendix Figure B4). In *C. inconspicua* wild growth, primary layer thickness was not affected by treatment or the interaction of treatment and shell position (Figure 4.8A; Two-way ANOVA - Treatment:  $F_{2,36} = 1.85$ ,  $p = 0.172$ ; Interaction:  $F_{4,36} = 1.69$ ,  $p = 0.175$ ). Primary layer near the umbo (position 1), however, was thinner than the middle of the shell (position 2) and nearer the experimental growth (position 3; black bars in Appendix Figure B4A, C, E; Two way ANOVA - Shell position:  $F_{2,36} = 5.46$ ,  $p = 0.008$ ) in all treatments. In *C. inconspicua* experimental growth, primary layer thickness was not affected by treatment, position or the interaction of the two factors (Figure 4.8B and black bars in Appendix Figure B4B, D, F; Two-way ANOVA - Treatment:  $F_{2,36} = 1.25$ ,  $p = 0.297$ ; Shell position:  $F_{2,36} = 1.97$ ,  $p = 0.154$ ; Interaction:  $F_{4,36} = 1.43$ ,  $p = 0.245$ ).

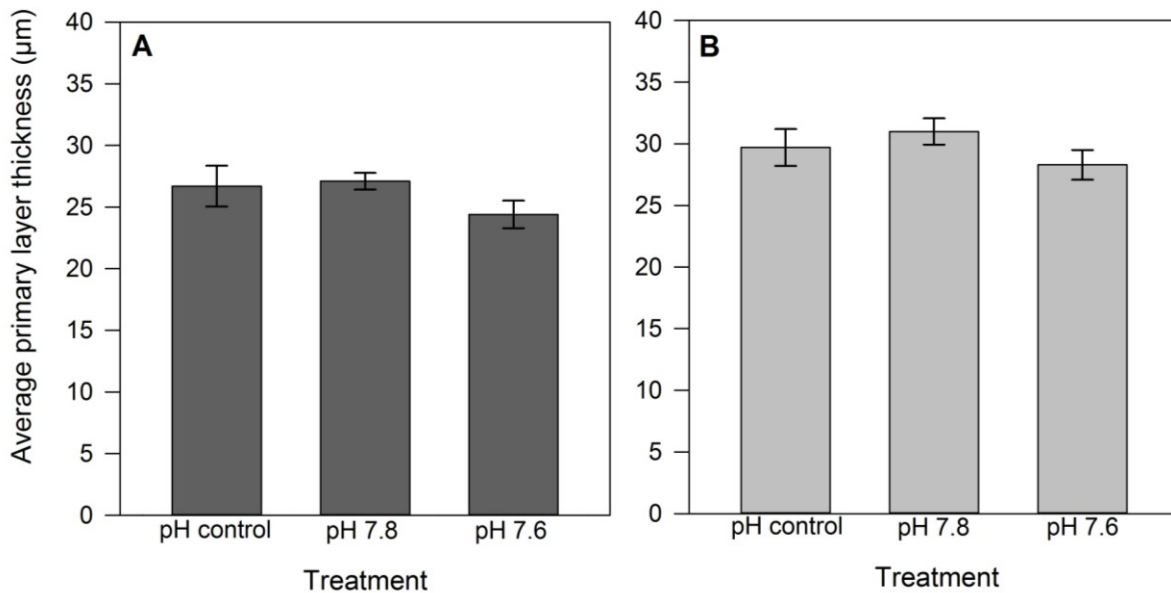


**Figure 4.8 – *C. inconspicua* – Average primary layer thickness in wild growth (A) and experimental growth (B) in all three treatments. Values plotted are mean  $\pm$  SE.**

#### 4.3.2.2 Secondary layer thickness

Secondary layer thickness in *L. uva* ranged from 84.3-339.8  $\mu\text{m}$  (grey bars in Appendix Figure B3). In *L. uva* wild growth, secondary layer thickness was affected by acidified conditions with the most acidified treatment causing a significant increase in thickness but there was no difference between pH 7.75 and the controls (Figure 4.9A; Two-way ANOVA - Treatment:  $F_{3,45} = 15.27$ ,  $p < 0.001$ ). Shell position and the interaction of treatment and shell position did not affect the thickness of this shell layer (grey bars in Appendix Figure B3A, C, E, G; Two-way ANOVA - Shell position:  $F_{2,45} = 0.09$ ,  $p = 0.915$ ; Interaction:  $F_{6,45} = 0.10$ ,  $p = 0.996$ ). In *L. uva* experimental growth, treatment and the interaction of treatment and shell position did not impact secondary layer thickness (Figure 4.9B; Two-way ANOVA -

Treatment:  $F_{3,45} = 2.61$ ,  $p = 0.063$ ; Interaction:  $F_{6,45} = 1.79$ ,  $p = 0.123$ ). However, this shell layer did get progressively thinner with the direction of growth (from position 4 to position 6; grey bars in Appendix Figure B3B, D, F, H; Two-way ANOVA - Shell position:  $F_{2,45} = 26.92$ ,  $p < 0.001$ ). Temperature did not affect secondary layer thickness in *L. uva* wild or experimental growth.

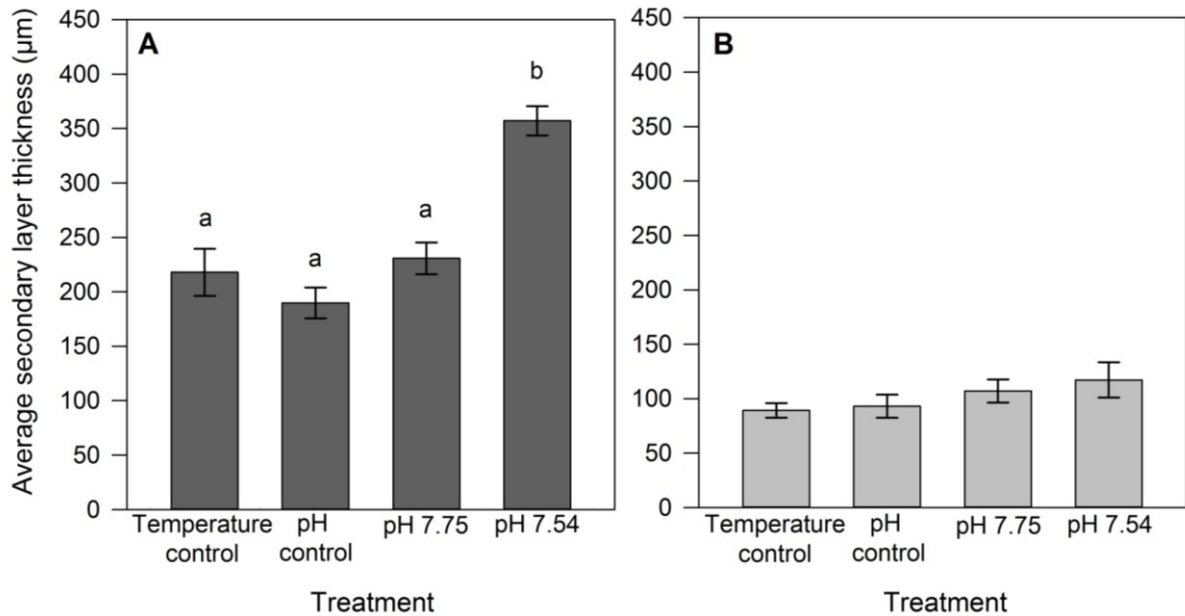


**Figure 4.9 – *L. uva* – Average secondary layer thickness in wild growth (A) and experimental growth (B) in all four treatments. Values plotted are mean  $\pm$  SE. Different letters above columns indicate significant differences ( $p < 0.05$ ).**

*C. inconspicua* secondary layer thickness ranged from 27.9-364.6 µm (whole bars in Appendix Figure B4). In *C. inconspicua* wild growth, secondary layer thickness was not affected by treatment, position or the interaction of these factors (Figure 4.10A and grey bars in Appendix Figure B4A, C, E; Two-way ANOVA - Treatment:  $F_{2,36} = 2.60$ ,  $p = 0.088$ ; Shell position:  $F_{2,36} = 2.04$ ,  $p = 0.145$ ; Interaction:  $F_{4,36} = 0.06$ ,  $p = 0.994$ ). In *C. inconspicua* experimental growth, secondary layer thickness was not affected by treatment or the interaction of treatment and shell position (Figure 4.10B; Two-way ANOVA - Treatment:  $F_{2,36} = 0.33$ ,  $p = 0.718$ ; Interaction:  $F_{4,36} = 0.41$ ,  $p = 0.800$ ). The secondary layer in the youngest position (position 6) was, however, thinner than the older experimental growth (position 4 and 5; grey bars in Appendix Figure B2B, D, F; Two way ANOVA - Shell position:  $F_{2,36} = 15.90$ ,  $p < 0.001$ ).

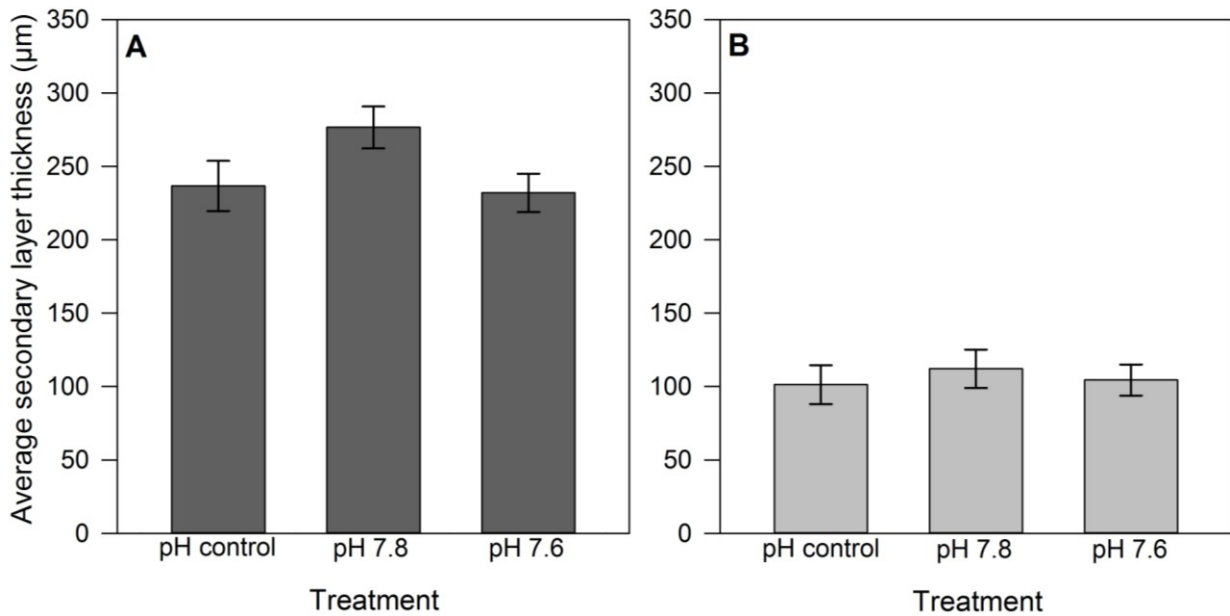


**Figure 4.10 – *C. inconspicua* – Average secondary layer thickness in wild growth (A) and experimental growth (B) in all three treatments. Values plotted are mean  $\pm$  SE.**

#### 4.3.2.3 Total shell thickness

*L. uva* total shell thickness ranged from 84.3-436.5 µm (whole bars in Appendix Figure B3). In *L. uva* wild growth, treatment affected total thickness with pH 7.54 significantly thicker than the other treatments (Figure 4.11A; Two-way ANOVA - Treatment:  $F_{3,45} = 5.66$ ,  $p = 0.002$ ). Shell position and the interaction of treatment and shell position did not, however, affect the thickness of this shell layer (whole bars in Appendix Figure B3A, C, E, G; Two-way ANOVA - Shell position:  $F_{2,45} = 0.53$ ,  $p = 0.592$ ; Interaction:  $F_{6,45} = 0.03$ ,  $p = 1.000$ ). In *L. uva* experimental growth, treatment and the interaction of treatment and shell position did not affect total shell thickness (Figure 4.11B; Two-way ANOVA - Treatment:  $F_{3,45} = 1.76$ ,  $p = 0.168$ ; Interaction:  $F_{6,45} = 0.34$ ,  $p = 0.915$ ). Total shell thickness, however, decreased with the direction of growth (from position 4 to position 6; whole bars in Appendix Figure B3B, D, F, H; Two-way ANOVA - Shell position:  $F_{2,45} = 22.20$ ,  $p < 0.001$ ). Temperature did not affect total shell thickness in *L. uva* wild or experimental growth.

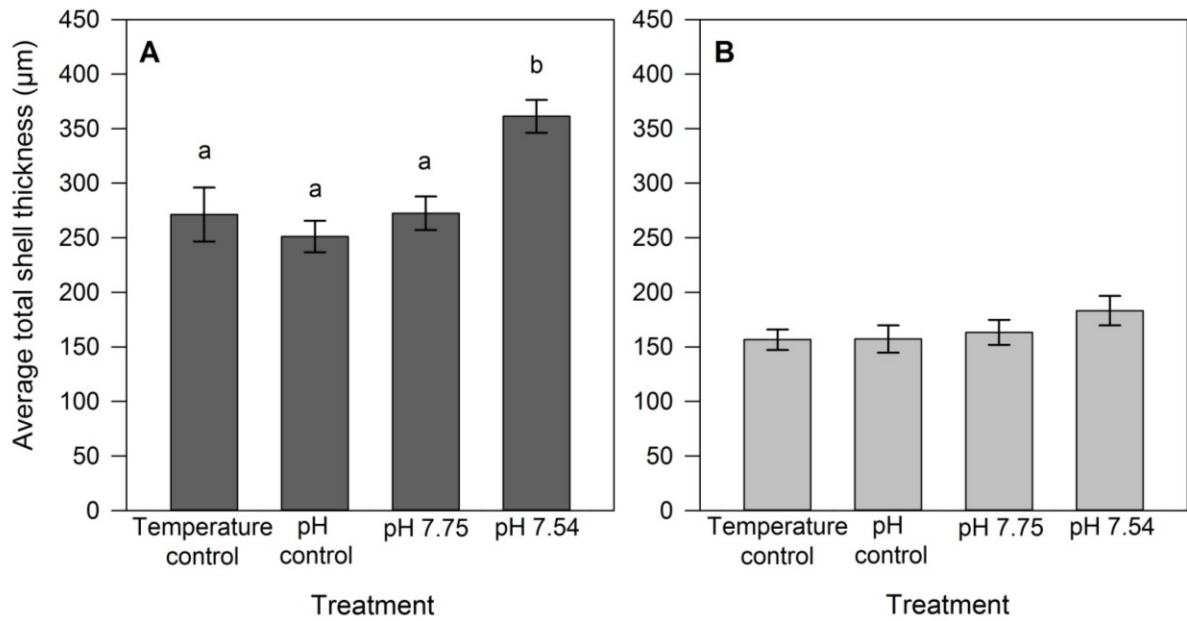


**Figure 4.11 – *L. uva* – Average total shell thickness in wild growth (A) and experimental growth (B) in all four treatments. Values plotted are mean  $\pm$  SE. Different letters above columns indicate significant differences ( $p < 0.05$ ).**

*C. inconspicua* total shell thickness ranged from 42.12-405.5  $\mu\text{m}$  (whole bars in Appendix Figure B4). In *C. inconspicua* wild growth, total shell thickness was not affected by treatment, position or the interaction of the two factors (Figure 4.12A and whole bars in Appendix Figure B4A, C, E; Two-way ANOVA - Treatment:  $F_{2,36} = 2.75$ ,  $p = 0.077$ ; Shell position:  $F_{2,36} = 1.80$ ,  $p = 0.179$ ; Interaction:  $F_{4,36} = 0.06$ ,  $p = 0.993$ ). In *C. inconspicua* experimental growth, total shell thickness was not affected by treatment or the interaction of treatment and shell position (Figure 4.12B; Two-way ANOVA - Treatment:  $F_{2,36} = 0.45$ ,  $p = 0.644$ ; Interaction:  $F_{4,36} = 0.40$ ,  $p = 0.810$ ). Total shell thickness in the youngest position (position 6), however, was thinner than the older parts of the experimental growth (position 4 and 5; whole bars in Appendix Figure B4B, D, F; Two way ANOVA - Shell position:  $F_{2,36} = 14.19$ ,  $p < 0.001$ ).

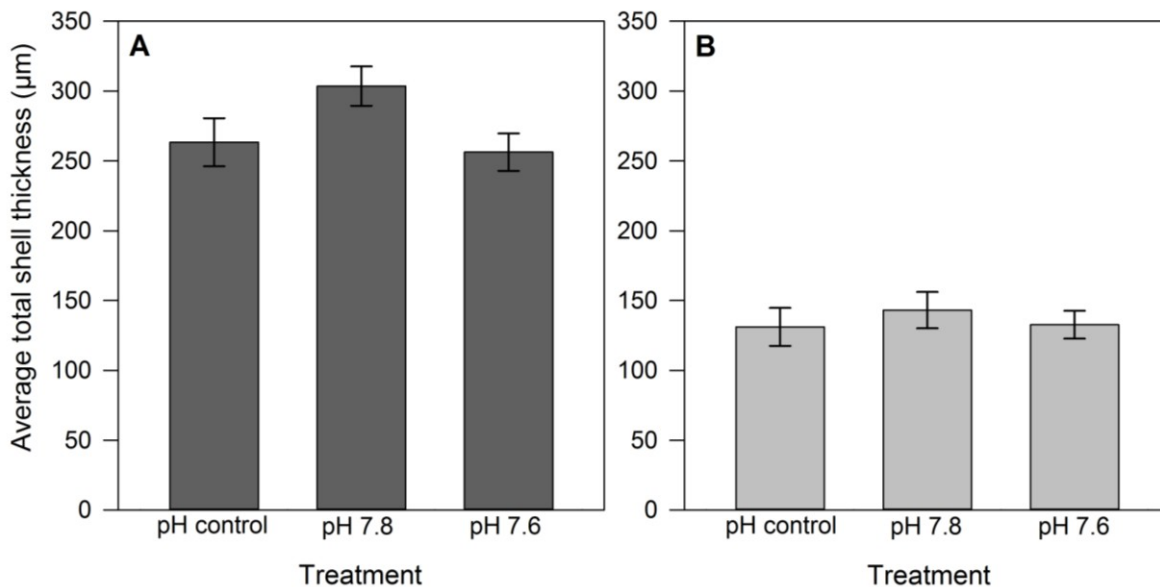


**Figure 4.12 – *C. inconspicua* – Average total shell thickness in wild growth (A) and experimental growth (B) in all three treatments. Values plotted are mean  $\pm$  SE.**

#### 4.4 Discussion

Data presented here show that both the polar *L. uva* and the temperate *C. inconspicua* are susceptible to shell dissolution under predicted end-century acidified conditions as dissolution became more extensive with increasing acidity and no or minimal dissolution was present in the controls. This trend has been widely reported in the ocean acidification literature of several marine calcifiers including coralline algae (e.g. Kamenos et al., 2013; Cornwall et al., 2014), corals (e.g. Andersson et al., 2009; Comeau et al., 2014; Silbiger & Donahue, 2014), echinoderms (e.g. Miles et al., 2007; Dubois, 2014), molluscs (e.g. Hall-Spencer et al. 2008; Marshall et al., 2008; Tunnicliffe et al., 2009; Nienhuis et al., 2010; Thomsen et al., 2010; Milano et al., 2016) and brachiopods (McClintock et al., 2009). These results have been obtained from different methods including laboratory experiments (e.g. Nienhuis et al., 2010; Cornwall et al., 2014; Silbiger & Donahue, 2014; Milano et al., 2016) and field experiments involving mesocosms (e.g. Andersson et al., 2009; Comeau et al., 2014), CO<sub>2</sub> vent sites (e.g. Hall-Spencer et al., 2008; Tunnicliffe et al., 2009; Thomsen et al., 2010) and sampling along natural pH gradients (e.g. Marshall et al., 2008; Bednaršek & Ohman, 2015). A range of time scales are involved in these different approaches indicating that skeletal dissolution can occur after only a few days, in some conditions, and persists throughout an organisms' life. The only other ocean acidification study investigating dissolution in brachiopods found identical results in *L. uva* to those presented in this chapter (McClintock et al., 2009). In their study, deterioration of the primary layer in their most acidified treatment (pH 7.4) occurred after only 35 days and was more extensive after 56 days when calcite fibres were exposed.

McClintock et al. (2009) only used empty dried valves, and it is interesting that in the experiments reported here live specimens exhibited the same dissolution pattern after 7 months exposure to pH 7.54. Exposure of the secondary layer calcite fibres is indicative of structural disintegration that compromises shell integrity and probably strength due to the loss of the hard outer protective primary layer (Scurr & Eichhorn, 2005; McClintock et al., 2009).

Dissolution was more extensive in *L. uva* than *C. inconspicua* as indicated by increased deterioration in the primary layer of *L. uva* than in *C. inconspicua* in the mildly acidified treatments and exposure of the secondary layer only in *L. uva* in the most acidified treatment. Antarctic calcified invertebrates are probably the most vulnerable organisms to ocean acidification due to being weakly calcified (Nicol, 1967, Vermeij, 1978; Watson et al., 2012), the dissolution rates of calcium carbonate being inversely related to temperature (Revelle & Fairbridge, 1957) and the polar regions being predicted to become the first to be undersaturated in aragonite by 2050 (Caldeira & Wickett, 2005; Fabry et al., 2008; Guinotte & Fabry, 2008; McNeil & Matear, 2008). This increased susceptibility partially explains the more severe dissolution in *L. uva* in comparison to *C. inconspicua*. Higher percentage areas of wear (wear stage 1 and 2) were also apparent in *L. uva* wild growth compared to the equivalent growth in *C. inconspicua*. This could potentially be related to the additional stress of ice causing physical abrasion in the polar regions (Cadée, 1999; Harper et al., 2012), however, this is unlikely in the Antarctic brachiopod as it usually lives in protected areas, e.g. crevices and overhangs in shallow sites where the ice persists. Increased wear in *L. uva* is more likely due to its longer lifespan (up to 55-60 years, Peck & Brey, 1996) compared to *C. inconspicua* (up to 14 years, Doherty, 1979), therefore, is exposed to wear for a longer time. *L. uva* also mainly occurs in larger clumps of individuals than *C. inconspicua*, causing more abrasion from the movement of individuals on their pedicle. Subsequently, this increase in wear would have amplified shell dissolution in *L. uva* due to the removal of the periostracum. The presence of this organic protective layer is key in an organism's susceptibility to shell dissolution. Wear was also more extensive in wild growth compared to experimental growth in every treatment in both species which was expected as the experimental growth had only existed for a short time. Another trend is the decrease in wear in the acidified treatments compared to the controls in both species. As this is coupled with increased shell dissolution, it is likely this is a result of the exposed inner shell layers becoming corroded in the acidified treatments whereas no or minimal dissolution occurs in ambient seawater, therefore, only wear persists in the controls. Previous research has illustrated the role of the periostracum in

preventing shell dissolution (Tunnicliffe et al., 2009; Thomsen et al., 2010; Rodolfo-Metalpa et al., 2011; Coleman et al., 2014) including a comprehensive study of 18 benthic marine calcifiers (Ries et al., 2009). Rodolfo-Metalpa et al., (2011) found that dead limpet shells (*Patella caerulea*) which lack periostracum dissolved nine times faster after 21 days exposure to pH<sub>T</sub> 6.8 conditions than dead mussel shells (*Mytilus galloprovincialis*) which have periostracum. Dissolution in closely related live *Mytilus edulis* and *M. galloprovincialis* reportedly only occurs in the umbo region (Thomsen et al., 2010; Rodolfo-Metalpa et al., 2011). The umbo is the oldest part of the shell, and it is often in close contact to other mussels or substrata. It is, therefore, subject to increased damage or removal of the organic cover. Periostracum is only formed at the growing edge and cannot be repaired if damaged. Therefore, thinning or loss of this organic layer through physical or biotic abrasion and epibiont erosion restricts protection from corrosive acidified waters. Increased primary layer dissolution occurred in both *L. uva* and *C. inconspicua* experimental growth in the most acidified treatments. This could be a result of periostracum damage from abrasion of other brachiopods in their conspecific cluster, natural decay of this outer layer or potentially the lowered pH conditions could have disrupted the protective function of the periostracum. Thomsen et al. (2010) suggested this latter possibility as external dissolution was found in newly formed *M. edulis* shell after 2 months exposure to 1400  $\mu$ atm and 4000  $\mu$ atm. The periostracum in brachiopods has been reported to be < 1  $\mu$ m thick (Williams & MacKay, 1979), therefore, suggesting that this thin outer layer might not provide sufficient protection to predicted end-century acidified conditions.

In addition to seawater chemistry and the periostracum, the rate of shell dissolution could be influenced by crystal size and morphology, the magnesium content of calcite and the organic content of shells (Harper, 2000). Crystal size and varying surface area to volume ratios will inevitably affect dissolution rates although individual crystals are rarely completely exposed as they are surrounded by organic matrix. Crystallographic orientation in relation to the dissolution surface may also be important, especially as calcite has been reported to be significantly more soluble along its *c*-axis (Harper, 2000). Magnesium content is also widely reported to affect solubility, with marine calcifiers composed of high magnesium calcite considered more susceptible to dissolution (Morse et al., 2007; Ries et al., 2009). Brachiopods are, however, constructed of low Mg-calcite and results in this chapter demonstrate substantial dissolution, similar in extent to marine calcifiers made of more soluble calcium carbonate polymorphs (McClintock et al., 2009; Nienhuis et al., 2010). McClintock et al.

(2009) found that the Antarctic benthic marine calcifiers, *L. uva*, *Laturnula elliptica*, *Yoldia eightsi* and *Nacella concinna*, are all similarly vulnerable to ocean acidification impacts on shell dissolution despite their different shell microstructures. These species are made of different calcium carbonate polymorphs with no clear trend of calcitic shells being less resistant to dissolution than aragonitic shells even though calcite is 35% less soluble in seawater than aragonite (Morse et al., 1980; Mucci, 1983). This supports the conclusions of Harper (2000) who disputed the common idea that calcitic shells evolved to delay dissolution (Taylor & Reid, 1990; Vermeij, 1993). In addition to the periostracum, the organic matrix is also thought to protect against dissolution by shrouding calcite crystals (Harper, 2000; Melzner et al., 2011). It is thus expected that species or areas of shell with a higher organic content will be less susceptible to dissolution. Data from Harper (2000) support this idea as bivalves with higher organic content microstructures dissolved more slowly in sterile conditions. The same study, however, also found that dissolution in bivalves with higher organic content shells occurred at a faster rate in non-sterile conditions compared to sterile seawater. This suggests that the organic matrix could potentially aid shell degradation via acid release from increased microbial growth on the organic matrix dissolving exposed carbonate crystals. *L. uva* shell organic content is low at 3.46% of its dry weight (Peck et al., 1987a), which could support the suggestion that species with a low organic content dissolve more easily. The organic content of *C. inconspicua* shell remains undetermined, but measurements on other rhynchonelliform brachiopods are also low (e.g. *Terebratulina retusa*: 2.8%, *L. neozelanica*: 1.9%), including *Kraussina rubra* (2.7%) which is in the same suborder as *C. inconspicua* (Copper, 1996). These similarities in shell organic content suggest that organic matrix is not a major factor in the differences in dissolution between *L. uva* and *C. inconspicua*, however, this warrants further investigation.

Increased dissolution at lower pH in *L. uva* wild growth was coupled with decreased thickness of the primary layer. Secondary layer thickness and total shell thickness were significantly increased in the most acidified treatment, indicating that this species can counteract dissolution by laying down more secondary layer and increasing overall shell thickness. The less extensive dissolution in *C. inconspicua* is reflected by no clear impact of acidified conditions on total shell or individual shell layer thicknesses. Despite the widely reported significant effects of dissolution on marine calcifiers in ocean acidification research, few studies report on the compensatory ability of these organisms. New shell deposited by *M. edulis* in a 9 month experiment to 750  $\mu\text{atm}$  and 1000  $\mu\text{atm}$   $p\text{CO}_2$  was rounder and flatter with

a thinner aragonite layer than shell produced in ambient conditions of 380  $\mu\text{atm}$  (Fitzer et al., 2015a). They attributed this new shell shape to a compensatory mechanism to enhance protection from predators and changing environments as these mussels were unable to grow thicker shells in high  $p\text{CO}_2$  conditions. The gastropod *Subnivalia undulata* increased shell thickness and strength after only 25 days exposure to pH 7.7 conditions (Coleman et al., 2014). No differences in shell thickness and reduced shell strength, however, occurred in the mollusc *Austrocochlea porcata* after 3 months exposure to the same pH (Coleman et al., 2014). Decreased shell thickness has also been reported in molluscs in response to lowered pH which is usually a result of internal dissolution of the aragonite layer (Tunnicliffe et al., 2009; Melzner et al., 2011; Fitzer et al., 2015a). This highlights some of the compensatory capacities of marine calcifiers to ocean acidification. For compensatory mechanisms to succeed, they must occur at faster rates than the dissolution. Thicker basal shells in the barnacle *Amphibalanus amphitrite* were produced under pH 7.4 conditions, however, this compensation calcification was insufficient as dissolution rapidly weakened shells as it was deposited (McDonald et al., 2009). The secondary layer of terebratulide brachiopod shells is softer than the harder protective primary layer (Griesshaber et al., 2007; Goetz et al., 2009). However, the ability of *L. uva* to increase secondary layer thickness and the resilience of the thickness of this inner shell layer in *C. inconspicua* under low pH suggests internal dissolution is unlikely in rhynchonelliform brachiopods as suggested to be a problem in molluscs (Tunnicliffe et al., 2009; Melzner et al., 2011; Fitzer et al., 2015a). Furthermore, no external dissolution of the exposed secondary layer of *L. uva* was observed suggesting that the compensatory mechanism of a thicker shell consisting of only secondary layer could provide sufficient protection in predicted pH conditions expected by 2100.

Total shell thickness or individual shell layer thickness of experimental growth of *L. uva* and *C. inconspicua* were not affected by acidified conditions. Both these species, should, therefore, be able to produce the same thickness of shells in 2100, unless the pH or warming conditions go beyond those predicted. The thickness of calcite and aragonite layers in newly formed shell of *M. edulis* were also not affected by elevated  $p\text{CO}_2$  (Thomsen et al., 2010). The resilience of shell thickness in *L. uva* and *C. inconspicua*, in addition to their unaffected shell growth rates (Chapter 2; Cross et al., 2015, 2016), punctal density and calcite fibre size (Chapter 3) under low pH, indicates the robust ability of rhynchonelliform brachiopods to construct shell under acidified conditions.

Temperature has no clear effect on shell dissolution or thickness in *L. uva* as indicated by the lack of, or minimal primary layer dissolution and no change in any thickness measurement in both wild and experimental growth in the temperature control (held at 0°C – current Antarctic summer temperatures) and the pH control (kept at the increased 2°C predicted for 2100). In contrast, temperature and not acidification reduced shell strength in *M. edulis* after 6 months exposure to forecasted end-century pH and warming conditions (Mackenzie et al., 2014), who concluded that warming had an indirect effect on shell strength by shifting the energy budget from shell deposition to increased maintenance costs. Food availability was limited throughout the experiment which could have enhanced the temperature effect as low food levels have also been reported to significantly influence the amount of inner shell dissolution in this species after 7 weeks exposure to varying  $p\text{CO}_2$  levels (Melzner et al., 2011). High  $p\text{CO}_2$  also increased inner shell dissolution highlighting the necessity of full-factorial multistressor ocean acidification research to better understand the abilities of marine calcifiers to maintain shell integrity under future predicted environmental conditions.

The vulnerabilities of *L. uva* and *C. inconspicua* to shell dissolution under predicted acidified conditions for 2100 have been evaluated in this chapter, with more extensive dissolution apparent in the Antarctic brachiopod. Without any counteracting response, dissolution can compromise shell integrity. This could lead to fatal ecological consequences such as reduced protection causing increased susceptibility to bioeroders and microorganisms reaching the soft animal tissues and decreased suitability of brachiopod shells as a habitat for other marine organisms. A compensatory mechanism was identified in *L. uva* as more secondary layer was laid down resulting in a thicker shell under lowered pH levels. The less extensive dissolution in *C. inconspicua* was reflected in the lack of primary layer thinning with increasing acidity, and was probably a function of the higher temperatures in the temperate study and the corresponding lower  $\text{CaCO}_3$  solubility. This suggests that the level of dissolution in *C. inconspicua* after 12 weeks exposure to predicted end-century pH conditions did not require counteracting with increased thickness. This is the first study to examine the effect of acidified conditions on shell dissolution in live brachiopods and also on the compensatory ability of this highly calcium carbonate dependent group. Despite shell dissolution imposing a threat, the apparent compensatory mechanism in *L. uva* and the absence of the requirement of one in *C. inconspicua* suggests that shell integrity in both species will not be compromised with predicted increasing acidity this century. However, this could come at an overall cost to the organism as calcification is energetically expensive, involving the accumulation,

transportation and precipitation of calcium carbonate as seen in the ophiuroid *Amphiura filiformis* (Wood et al., 2008). Metabolic costs of shell deposition in *L. uva* and *C. inconspicua* under future environmental conditions remain to be determined although their apparent resilience to the primary threat of lowered pH levels may prove fundamental in the survival of rhynchonelliform brachiopods to ocean acidification.

# Chapter Five

## Acclimation of *Calloria inconspicua* to environmental change over the last 110 years

### 5.1 Introduction

Since the Industrial Revolution, our oceans have globally become 2°C warmer and 0.1 pH units more acidic as a consequence of increased anthropogenic activities (Caldeira & Wickett, 2003, 2005; Orr et al., 2005; IPCC, 2013). Museum specimens collected in the recent past provide historical records of how organisms have responded to these changes in environmental conditions (Lister, 2011). This approach to understanding the effects of changing environments on marine organisms complements widely used laboratory and field experiments as it provides a historical baseline, allows evaluation of possible long-term adaptation and presents a more complete understanding of species responses.

The long-term ability of a species to adapt to changing environmental conditions is essential to ensure survival (Sunday et al., 2011). Acclimation of *C. inconspicua* to future predicted acidified conditions after 12 weeks exposure has already been demonstrated (Chapter 2, 3 and 4; Cross et al., 2016). However, how this species has responded to increased anthropogenic CO<sub>2</sub> emissions since the Industrial Revolution and its potential for adaptation remain unknown. *C. inconspicua* has a widespread distribution throughout New Zealand and is highly abundant in easily accessible intertidal and subtidal sites (Doherty, 1979). As a result, there are excellent museum collections of this species deposited at regular intervals over the last century making *C. inconspicua* an ideal species to investigate variation in shell characteristics since the Industrial Revolution.

Rhynchonelliform brachiopods are typically found in sheltered waters (Richardson, 1997) making Paterson Inlet, Stewart Island, New Zealand a particularly suitable area for *C. inconspicua* as the entrance is constricted by Ulva Island, Native Island and Bradshaw Peninsula, which added to its position on the east coast, shelter this sampling site from heavy

seas (Figure 5.1; Willan, 1981). Environmental conditions have also been reported at this site at relatively regular intervals with marine biological exploration of Paterson Inlet beginning in the early 1900's (Willan, 1981). Surface seawater temperatures have increased by 0.7°C and the CO<sub>2</sub> concentration has also increased by 90-100 ppm over the last 120 years in New Zealand (Figure 5.2). Therefore, Paterson Inlet is an ideal site to study how a locally common temperate brachiopod has responded to environmental change over the last century. Consequently, the aims of this chapter were to determine if any impacts of change were evident in *C. inconspicua* in its shell morphology, its ability to produce the same shell and maintain shell integrity over the last 110 years. Shell morphology was determined by linear dimensions and a calcification index, variations in producing the same shell determined through shell density, punctal density, punctal width and elemental composition of the shell and shell integrity measured by a shell condition index and thickness.

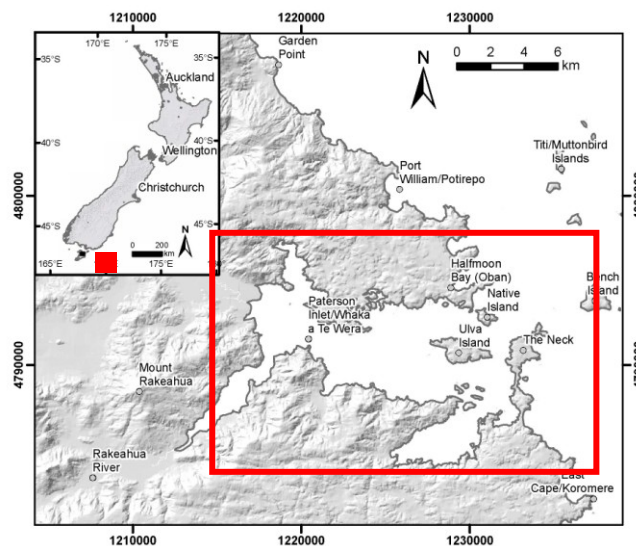


**Figure 5.1 - Location of sampling site (Paterson Inlet, Stewart Island, New Zealand, 46° 58'S, 168° 09'E).**

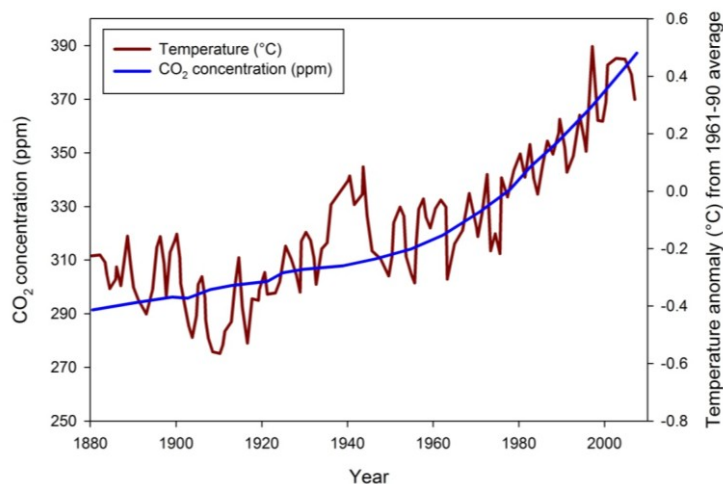


**Figure 5.2 – Temperature and CO<sub>2</sub> concentration changes in New Zealand over the last 120 years (adapted from <http://www.climatechange.govt.nz/science/>).**

## 5.2 Materials and Methods

### 5.2.1 Sampling Collection

Specimens of *C. inconspicua* were evaluated from various museums and research institutions from around New Zealand including Te Papa Museum, National Institute of Water and Atmospheric Research (NIWA), the University of Otago Department of Geology, Canterbury Museum, Auckland Museum and the University of Auckland. Individuals from 2014 were hand collected by Dr Miles Lamare. This data set includes *C. inconspicua* samples from every decade since 1900 to the present day except the 1990's. Non-destructive morphometric measurements were made on all specimens found in the various collections with detailed descriptions of location, date and depth (where possible) of the sample collection site. Depending on the available sample size, three to ten specimens from each decade were donated for further destructive shell analysis (Table 5.1). Only subtidal specimens between 12.1-25.5 mm in length were used in all shell analyses other than the morphometric measurements when all available specimens were measured. Details on the specific location and depth of each sample are given in Appendix Table C1.

### 5.2.2 Morphometrics

Shell length, breadth and height of 624 individuals were measured to the nearest 0.1 mm with Vernier calipers (Figure 5.3). Epibiota were carefully removed with a scalpel where possible. Heavily encrusted shells were excluded from analysis.

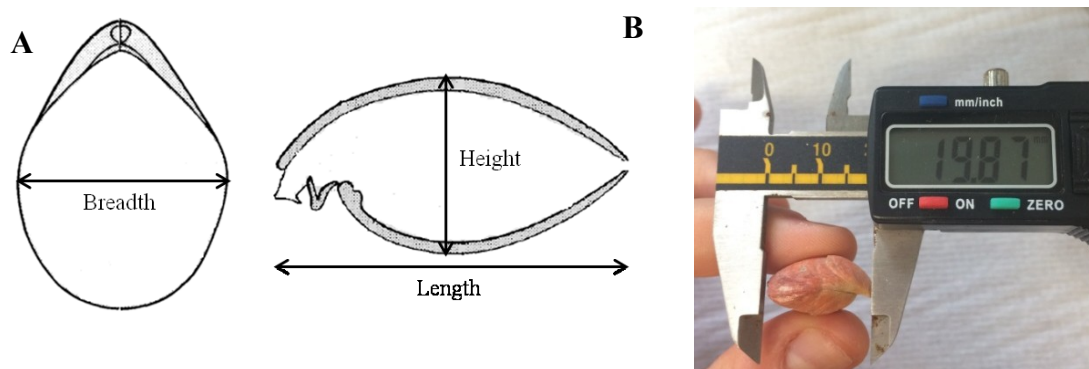


**Figure 5.3 – Measuring morphometrics: (A) schematic of length, breadth and height measurements and (B) an example of measuring the length of an individual with Vernier calipers.**

**Table 5.1 – Specimens selected for calcification index, shell density, punctal density, shell condition index, punctal width, elemental composition and thickness. Initial length is given to indicate size of the individual. Grey cells indicate the use of this specimen in the respective shell analysis.**

Year	Sample ID	Individual Number	Length (mm)	Shell characteristics						
				Whole shell		Pedicule valves		Brachial valves		
				Calcification index	Shell density	Punctal density	Shell condition index	Punctal width	Elemental composition	Thickness
1900	BR000088	1	24.0							
		2	21.8							
		3	21.1							
1914	BR001686	1	18.6							
		2	23.5							
		3	19.6							
1926	BR001062	1	22.0							
		2	21.9							
		3	22.5							
		4	22.1							
		5	22.4							
		6	19.2							
		7	18.0							
		8	18.1							
1934	2006.12.140	58	22.3							
		59	19.7							
		60	19.3							
1935	MA79003	1	22.9							

Year	Sample ID	Individual Number	Length (mm)	Shell characteristics						
				Whole shell		Pedicle valves		Brachial valves		
				Calcification index	Shell density	Punctal density	Shell condition index	Punctal width	Elemental composition	Thickness
1942	MA79298	1	21.3							
		2	17.4							
1942	2005.188.39	10	19.2							
		11	22.1							
		12	19.6							
1947	AU20001	1	20.7							
		2	21.1							
		3	23.0							
		4	22.2							
1955	BR001331	1	20.6							
		2	20.6							
		3	18.9							
1960	NIWA 62858 B243	1	20.0							
		2	18.8							
		3	20.7							
1967	NIWA 62892 E833	1	22.4							
		2	20.1							
		3	23.4							
		4	23.9							
		5	22.5							

Year	Sample ID	Individual Number	Length (mm)	Shell characteristics						
				Whole shell		Pedicel valves		Brachial valves		
				Calcification index	Shell density	Punctal density	Shell condition index	Punctal width	Elemental composition	Thickness
1967	NIWA 62892 E833	6	21.0							
		7	19.4							
		8	18.4							
		9	18.9							
		10	16.9							
		11	16.5							
		12	17.0							
1977	NIWA 62891 K989	1	23.0							
		2	24.4							
		3	25.5							
1980	NIWA 62919 S263	1	22.2							
		2	23.8							
		3	20.0							
		4	25.2							
		5	24.8							
		6	22.6							
		7	20.5							
		8	22.7							
		9	20.4							
2010	Cruise OS15	1	22.1							
		2	21.7							
		3	21.7							
		4	16.1							

Year	Sample ID	Individual Number	Length (mm)	Shell characteristics						
				Whole shell		Pedicle valves		Brachial valves		
				Calcification index	Shell density	Punctal density	Shell condition index	Punctal width	Elemental composition	Thickness
2014	2014	1	21.3							
		2	18.8							
		3	17.0							
		4	18.5							
		5	18.0							
		6	20.0							
		7	19.9							
		8	25.0							
		9	21.7							
		10	22.2							
		11	18.7							
		12	17.1							
		13	23.9							
		14	23.2							
		15	18.4							

### 5.2.3 Calcification Index

Animal tissues were carefully removed through the opening of the valves using a scalpel from the 70 individuals (3-15 specimens per decade except from the 1990's) donated for further destructive analysis. Whole specimens were further cleaned in an ultrasonic bath for 3 minutes and air dried for 24 hours. Individuals with any evidence of shell repair were removed from analysis. Calcification index quantifies the efficiency of calcification. Efficiency is quantified as the amount of internal living space produced per unit of shell material deposited (Graus, 1974). Therefore, the calcification index is calculated from the following equation:

$$\text{Calcification index} = \text{dry weight of the shell (g)} / \text{internal volume of the shell (cm}^3\text{)}$$

For each specimen, the dry weight was measured to 0.001 g on a Sartorius LA3200D weighing balance. The internal volume of the shell was calculated by the total volume minus the shell volume. Volume measurements were made according to Peck (1992). Total volume was measured by sealing the foramen, carefully filling the internal space with distilled water and placing on a suspended tray in a beaker of distilled water which was situated on the weighing balance (Figure 5.4). The given weight was, therefore, of the mass of water displaced which divided by the density of distilled water at room temperature (0.99823 g/cm<sup>3</sup>; Weast, 1975) gave the total volume. To minimise error, the total volume was measured three times with the internal space filled with new distilled water each time, the outer surface of the shell was dabbed dry to remove any excess water and care was taken not to remove any water from the beaker when placing the filled shell on the suspended tray. Mean total volume was used in the calculation of calcification index. The valves were then separated and air dried for 24 hours before measuring shell volume by placing both valves on the suspended tray.

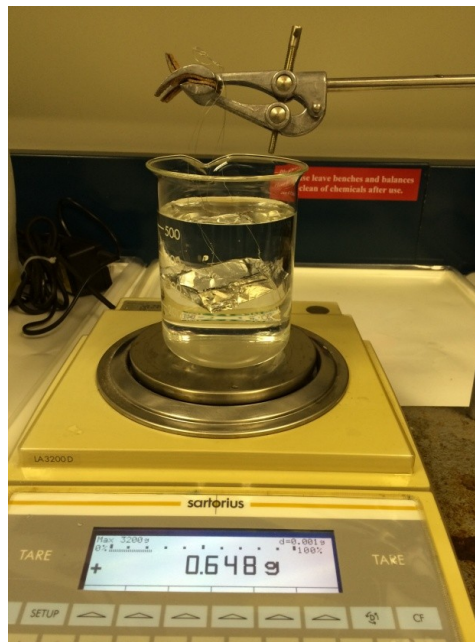


**Figure 5.4 – Calculating calcification index: experimental set up of a suspended tray in beaker of distilled water on a weighing balance.**

#### **5.2.4 Shell density**

Shell density was calculated for the 70 individuals (3-15 specimens per decade except from the 1990's) used in the calcification index analysis using the following equation:

$$\text{Shell density} = \text{dry weight of the shell (g)} / \text{shell volume (cm}^3\text{)}$$

#### **5.2.5 Punctae**

##### **5.2.5.1 Punctal densities**

Punctal densities (see section 3.2.2 for methods) were calculated from SEM micrographs of the outer shell surfaces of 40 pedicle valves (2-3 valves per decade except from the 1990's) at 10 different areas on each specimen (Figure 5.5).

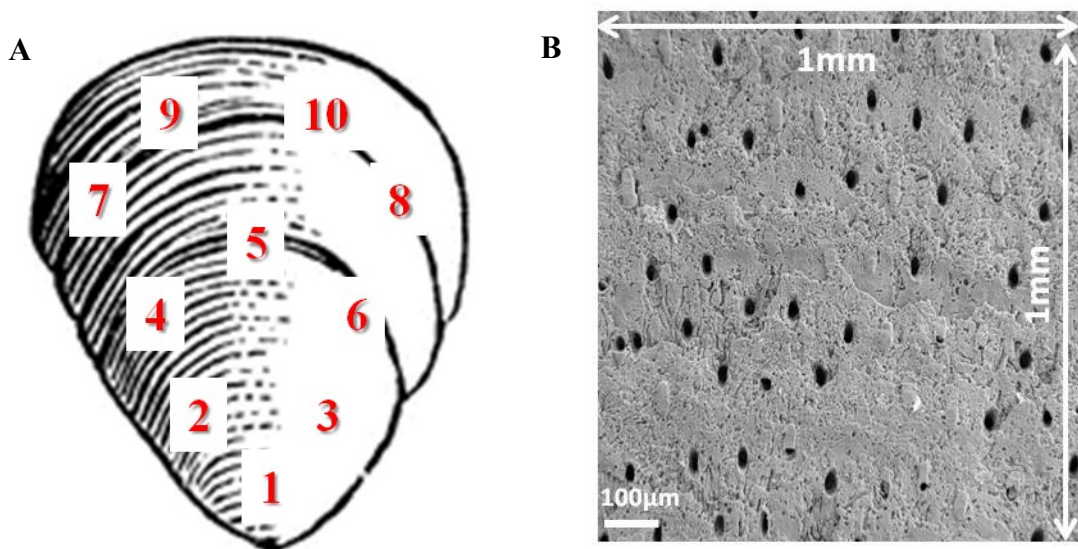


**Figure 5.5 – Calculating punctal densities: (A) schematic of a pedicle valve indicating the 10 areas where SEM micrographs were collected for analysis and (B) an example of a 1 mm<sup>2</sup> SEM micrograph of the outer shell surface collected to count punctal density.**

#### 5.2.5.2 Punctal width

Punctal width was measured in the middle and the top of the punctae (Figure 5.6B) from acetate peels (see section 4.2.4 for details) of cross sections of 40 brachial valves (3-5 valves per decade except the 1990's). Ten punctae were measured per specimen across the length of the individual (Figure 5.6A) to the nearest 0.1 mm on a Swift monocular petrological microscope with fitted micrometer. Punctae were only measured if the whole punctum was visible. Mean punctal width for each position on each individual was then used in the analysis. The percentage of shell that is punctae versus shell matrix was then calculated from the mean area of a punctum for each year by the following equation:

$$\text{Mean area of a punctum } (\mu\text{m}^2) = \pi r^2 = \pi \times (\text{mean punctal width}/2)^2$$

Mean punctal width in the middle of the shell was used in these calculations because punctae are mainly cylindrical with only the top of the punctae near the exterior of the shell branching out. The mean area of a punctum was converted to mm<sup>2</sup> so that the percentage area of shell occupied by punctae for each year could be calculated using the mean punctal density of 152 mm<sup>-2</sup> in the following equation:

Percentage area of shell occupied by punctae =  $(\text{mean area of punctum} \times \text{mean punctal density}) \times 100$

The percentage change in shell occupied by punctae compared to shell matrix was calculated by subtracting the percentage area for 2014 from that for 1900.

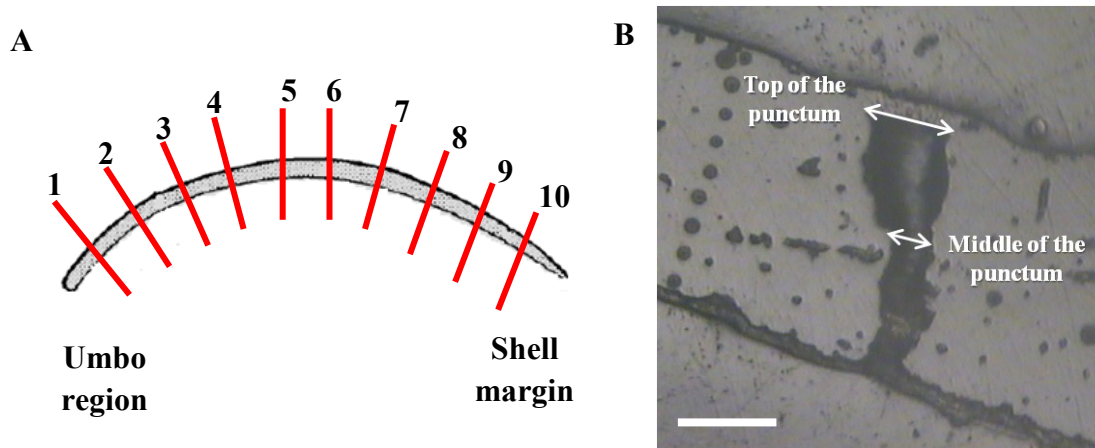


**Figure 5.6 – Punctal width measurements: (A) schematic of a brachial valve cross section indicating the 10 areas where measurements were made and (B) an optical image indicating the middle and top width measurements of a punctum. Scale bar = 10  $\mu\text{m}$ .**

### 5.2.6 Elemental composition

Elemental composition (see section 3.2.5 for methods) of the shell was determined through analysis of cross sections of 20 brachial valves (3 valves per 20 years). Due to time restrictions on use of the Cameca SX100 electron microprobe, only vertical profiles were measured in individuals every 20 years and whole shell thickness was not measured. Identical thicknesses of the secondary layer and 10  $\mu\text{m}$  spacing between points were used to the elemental composition analysis of the experimental specimens (Chapter 3; Figure 5.7B). Three vertical profiles were measured per specimen; near the umbo, in the middle of the shell and near the shell margin (Figure 5.7A). Punctae and other shell perforations were avoided by carefully selecting the start and end points of each profile.

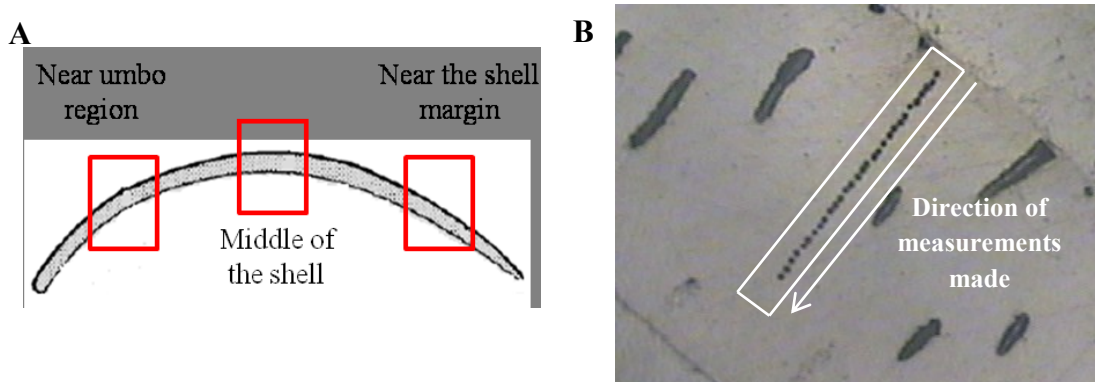


**Figure 5.7 – Elemental composition analysis: (A) schematic of a brachial valve cross section indicating areas where vertical profiles were taken and (B) optical image indicating the points analysed in a vertical profile.**

### 5.2.7 Shell condition index

Shell condition index (see section 4.2.3 for methods) was determined through measuring percentage areas of each shell condition from SEM micrographs of the outer shell surfaces of 40 pedicle valves (2-3 valves per decade except the 1990's) at 10 different areas on each specimen (Figure 5.8).

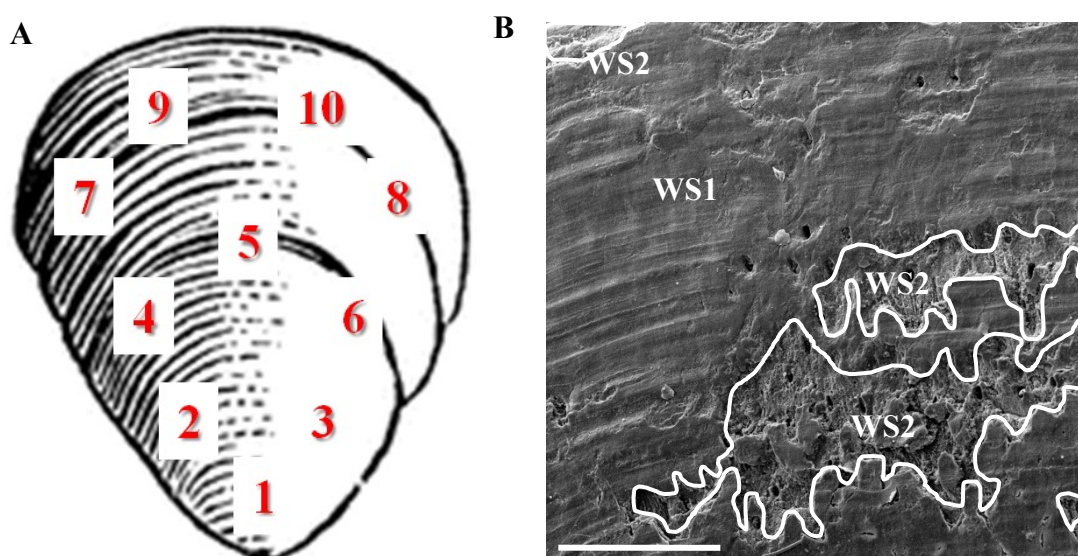


**Figure 5.8 – Shell condition index: (A) schematic of a pedicle valve indicating the 10 areas where SEM micrographs were taken for analysis and (B) an example of a 1 mm<sup>2</sup> SEM micrograph of the outer shell surface used to assess shell condition index. Scale bar = 300  $\mu$ m. WS1 = wear stage 1 and WS2 = wear stage 2.**

### 5.2.8 Shell thickness

Primary layer, secondary layer and total shell thickness measurements (see section 4.2.4 for methods) were made on cross sections of 40 brachial valves (3-5 valves per decade

except the 1990's) near the umbo, in the middle of the shell and near the shell margin on each specimen (Figure 5.9).

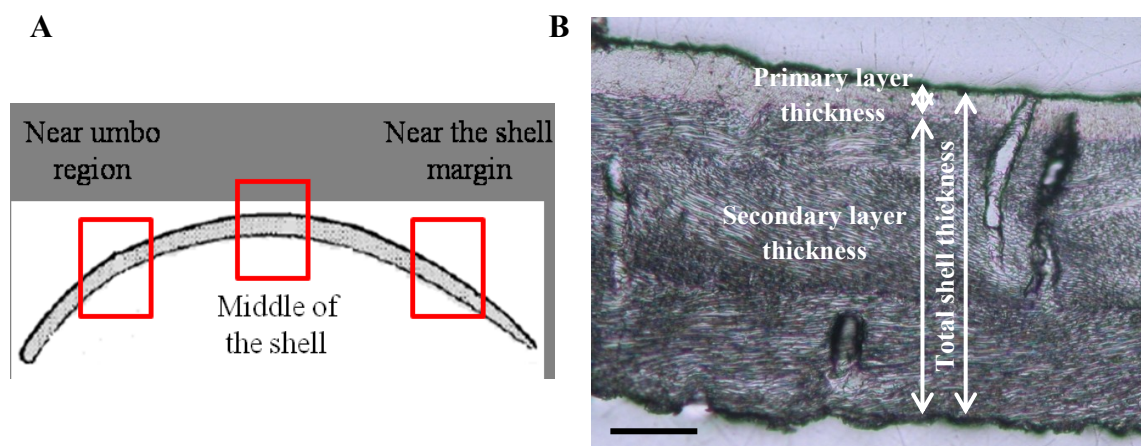


**Figure 5.9 – Thickness measurements: (A) schematic of a brachial valve cross section indicating areas where thickness measurements were made and (B) optical image of the primary and secondary layers. Scale bar = 100  $\mu$ m.**

### 5.2.9 Statistical analyses

All data were analysed using Minitab (Statistical Software™ Version 17). Calcification index, shell density, punctal density, punctal width and shell thickness data were all normally distributed (Anderson-Darling test;  $p > 0.05$ ). Parametric linear regression analyses were, therefore, performed on these characteristics to determine if they changed over the last 110 years. Morphometric and elemental composition raw data were both non-normally distributed even after square-root, log, arcsin, double square-root and double log transformations probably due to the large data sets ( $> 624$  measurements for each morphometric parameter and  $> 973$  points for each element) causing the goodness-of-fit test to become sensitive to very small departures from a normal distribution. Log transformed data in each year for each morphometric measurement were, however, normally distributed (Anderson-Darling test;  $p > 0.05$ ). Therefore, parametric multiple regression analyses were conducted on each morphometric measurement to determine if each relationship with size varied over time. Similarly, raw data in each individual year for Ca, Na and Sr and log transformed data for each individual year for Mg and P were normally distributed (Anderson-Darling test;  $p > 0.05$ ). Therefore, parametric linear regression analyses were performed on each element to determine if elemental composition changed over the last 110 years. Shell condition index data (% area) were arcsin transformed to remove imposed limits, but the transformed data were not normally distributed because of zeros in the dataset (Anderson-Darling test;  $p < 0.05$ ). Non-parametric Kruskal-Wallis tests were, therefore,

used to determine whether treatment and area number affected the proportion of each shell condition. When there were significant differences, a further Kruskal-Wallis Multiple Comparisons test was used to identify differences between treatments.

### 5.3 Results

#### 5.3.1 Morphometrics

Breadth increased almost proportionally to length with size (slope = 1.09) whereas height increased more than length (slope = 1.17) with size (Table 5.2; Figure 5.10). Therefore, shells get taller as they grow and growth is not isometric. Multiple regression analysis revealed that there was no difference between the relationship of length to breadth between years as the regression slopes were not significantly different ( $F_{15,624} = 1.63$ ,  $p = 0.060$ ). There was a difference between relationships of height and length ( $F_{15,623} = 5.45$ ,  $p < 0.001$ ) as 1967 and 2014 had a steeper slope than the other years (1967:  $T = 2.21$ ,  $p = 0.027$ ; 2014:  $T = 2.49$ ,  $p = 0.013$ ). Regression equations of all morphometric relationships in each year are given in Table 5.3.

**Table 5.2 – Regression analysis coefficients on the size and shape of all 624 shells measured.  $b$  = slope, SE = standard error, SEy = standard error about the regression line.**

Independent (x)	Dependent (y)	$b$	SE $b$	Intercept	SEy	R <sup>2</sup>
logLTH	logBTH	1.09	0.009	-0.14	0.01	0.96
logLTH	logHT	1.17	0.018	-0.49	0.01	0.91

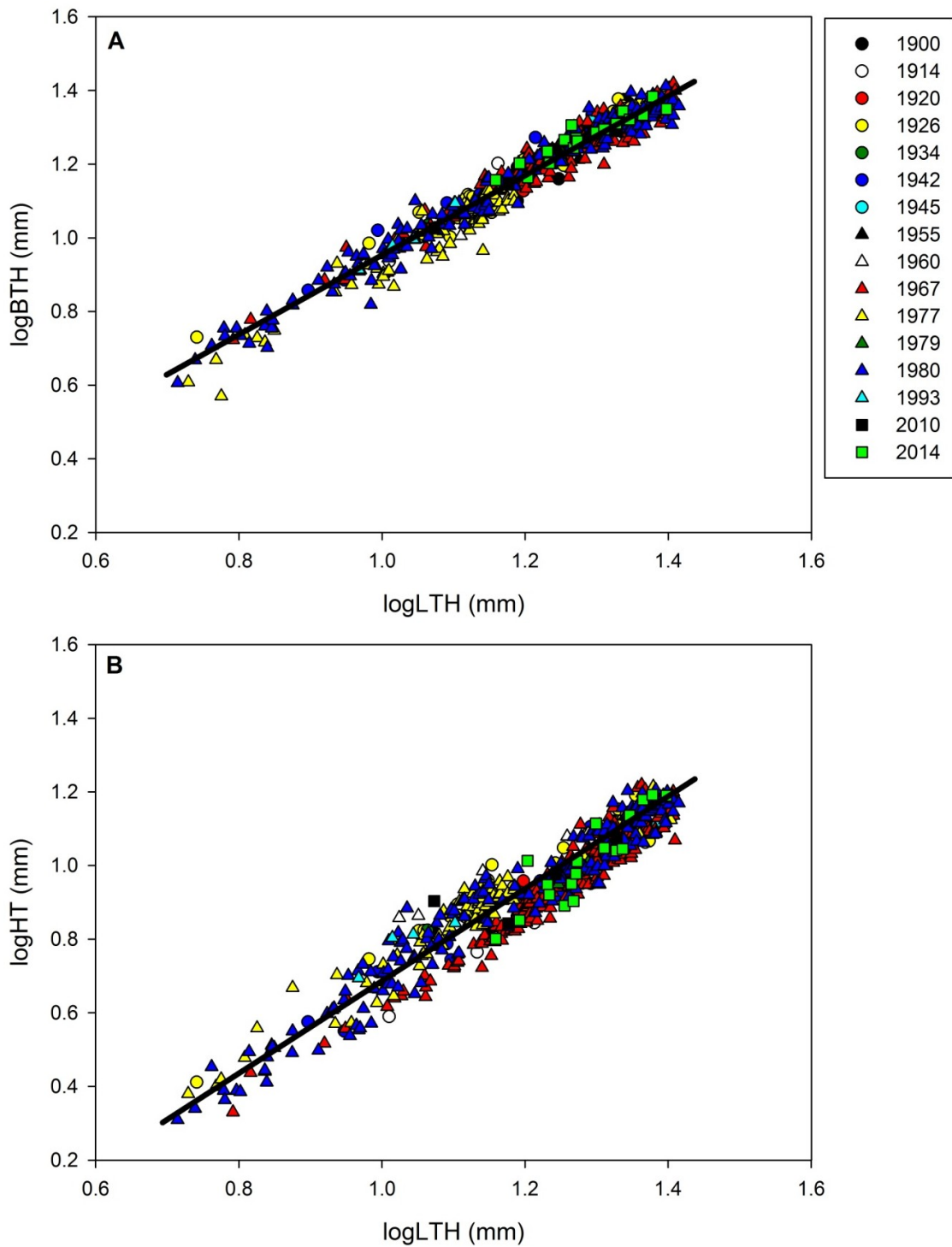


**Figure 5.10 – Relationships between breadth (A) and height (B) with length over the last 110 years. Each different symbol represents a different year (see legend). Regression lines are plotted for all specimens.**

**Table 5.3 – Regression equations for each morphometric relationship for each year. Significantly different years are highlighted in bold.**

Year	Breadth to Length	Height to Length
1900	$\log\text{BTH} = -0.257 + 1.180 \log\text{LTH}$	$\log\text{HT} = -0.344 + 1.064 \log\text{LTH}$
1914	$\log\text{BTH} = -0.158 + 1.119 \log\text{LTH}$	$\log\text{HT} = -0.725 + 1.317 \log\text{LTH}$
1920	$\log\text{BTH} = -0.439 + 1.316 \log\text{LTH}$	$\log\text{HT} = 0.012 + 0.786 \log\text{LTH}$
1926	$\log\text{BTH} = -0.080 + 1.049 \log\text{LTH}$	$\log\text{HT} = -0.260 + 1.013 \log\text{LTH}$
1934	$\log\text{BTH} = -0.007 + 0.975 \log\text{LTH}$	$\log\text{HT} = -0.124 + 0.884 \log\text{LTH}$
1942	$\log\text{BTH} = -0.084 + 1.064 \log\text{LTH}$	$\log\text{HT} = -0.495 + 1.163 \log\text{LTH}$
1945	$\log\text{BTH} = 0.739 + 0.450 \log\text{LTH}$	$\log\text{HT} = -0.010 + 0.805 \log\text{LTH}$
1955	$\log\text{BTH} = -0.115 + 1.064 \log\text{LTH}$	$\log\text{HT} = -0.480 + 1.161 \log\text{LTH}$
1960	$\log\text{BTH} = -0.045 + 1.017 \log\text{LTH}$	$\log\text{HT} = 0.137 + 0.704 \log\text{LTH}$
1967	$\log\text{BTH} = -0.223 + 1.143 \log\text{LTH}$	<b><math>\log\text{HT} = -0.771 + 1.378 \log\text{LTH}</math></b>
1977	$\log\text{BTH} = -0.180 + 1.125 \log\text{LTH}$	$\log\text{HT} = -0.518 + 1.233 \log\text{LTH}$
1979	$\log\text{BTH} = -0.110 + 1.066 \log\text{LTH}$	$\log\text{HT} = -0.680 + 1.310 \log\text{LTH}$
1980	$\log\text{BTH} = -0.361 + 1.315 \log\text{LTH}$	$\log\text{HT} = -0.534 + 1.221 \log\text{LTH}$
1993	$\log\text{BTH} = -1.46 + 1.042 \log\text{LTH}$	$\log\text{HT} = -0.295 + 1.050 \log\text{LTH}$
2010	$\log\text{BTH} = -0.128 + 1.083 \log\text{LTH}$	$\log\text{HT} = 0.059 + 0.739 \log\text{LTH}$
2014	$\log\text{BTH} = 0.101 + 0.913 \log\text{LTH}$	<b><math>\log\text{HT} = -1.030 + 1.590 \log\text{LTH}</math></b>

### 5.3.2 Calcification Index

Calcification index varied from 0.451-1.06 with no significant difference in this index over the last 110 years (Figure 5.11; Linear Regression,  $R^2 = 0.009$ ,  $F_{1,68} = 0.63$ ,  $p = 0.429$ ).

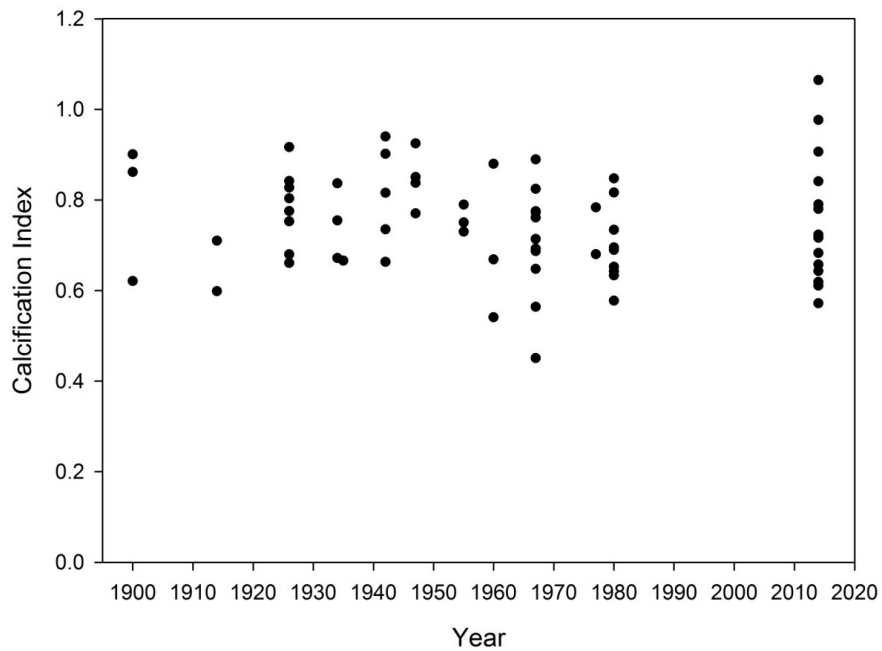


Figure 5.11– Calcification index from each decade over the last 110 years.

### 5.3.3 Shell density

Shell density ranged from 2.21-2.63  $\text{g cm}^{-3}$  (Figure 5.12) and the mean was  $2.43 \pm 0.01 \text{ g cm}^{-3}$ . Shell density significantly increased over the last 110 years by 3.43% from 1900 to 2014 (Figure 5.12; Linear regression:  $R^2 = 0.20$ ,  $F_{1,69} = 17.16$ ,  $p < 0.001$ ).

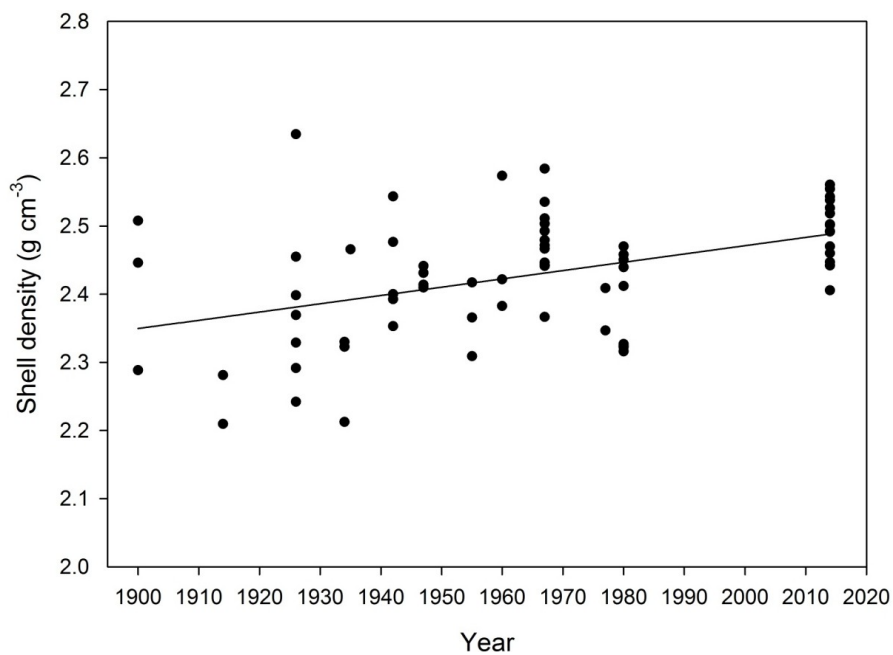
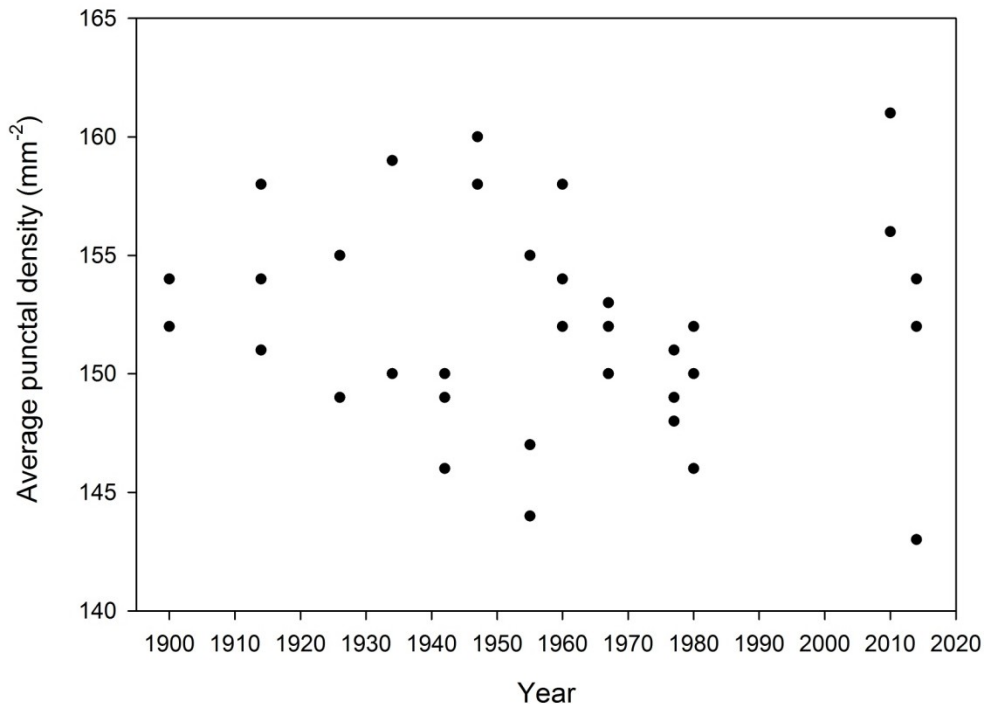


Figure 5.12 – Shell density from each decade over the last 110 years.

### 5.3.4 Punctae

#### 5.3.4.1 Punctal densities

Punctal density ranged from 143-161 mm<sup>-2</sup> (Figure 5.13) and the mean was 152 ± 0.7 mm<sup>-2</sup>. Punctal density did not vary over the last 110 years (Figure 5.13; Linear Regression, R<sup>2</sup> = 0.013, F<sub>1,38</sub> = 0.50, p = 0.485).



**Figure 5.13 – Mean punctal densities from each decade over the last 110 years. Error bars removed for clarity.**

#### 5.3.4.2 Punctal width

Punctal width ranged from 17.7-21.1 µm (mean = 19.6 ± 0.1 µm) in the middle of the punctae (Figure 5.14A) and 28.1-31.9 µm (mean = 30.0 ± 0.2 µm) at the top of the punctae (Figure 5.14B). Punctal width decreased in the middle of the punctae by 8.26% (Linear regression: R<sup>2</sup> = 0.45, F<sub>1,39</sub> = 31.25, p < 0.001) and at the top of the punctae by 7.17% (Linear regression: R<sup>2</sup> = 0.62, F<sub>1,39</sub> = 60.79, p < 0.001) from 1900 to 2014. The area of shell that is punctae compared to shell matrix decreased by 1% over the last 110 years.

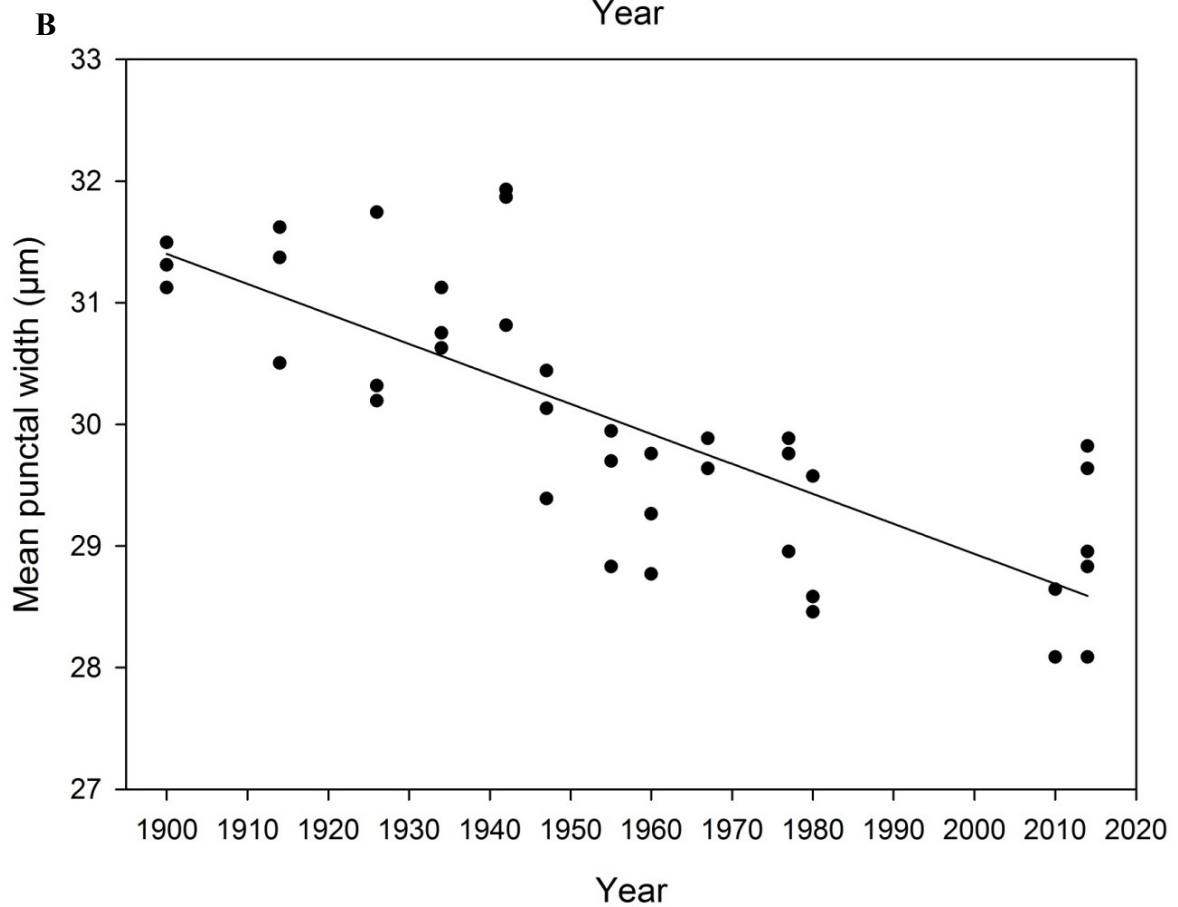
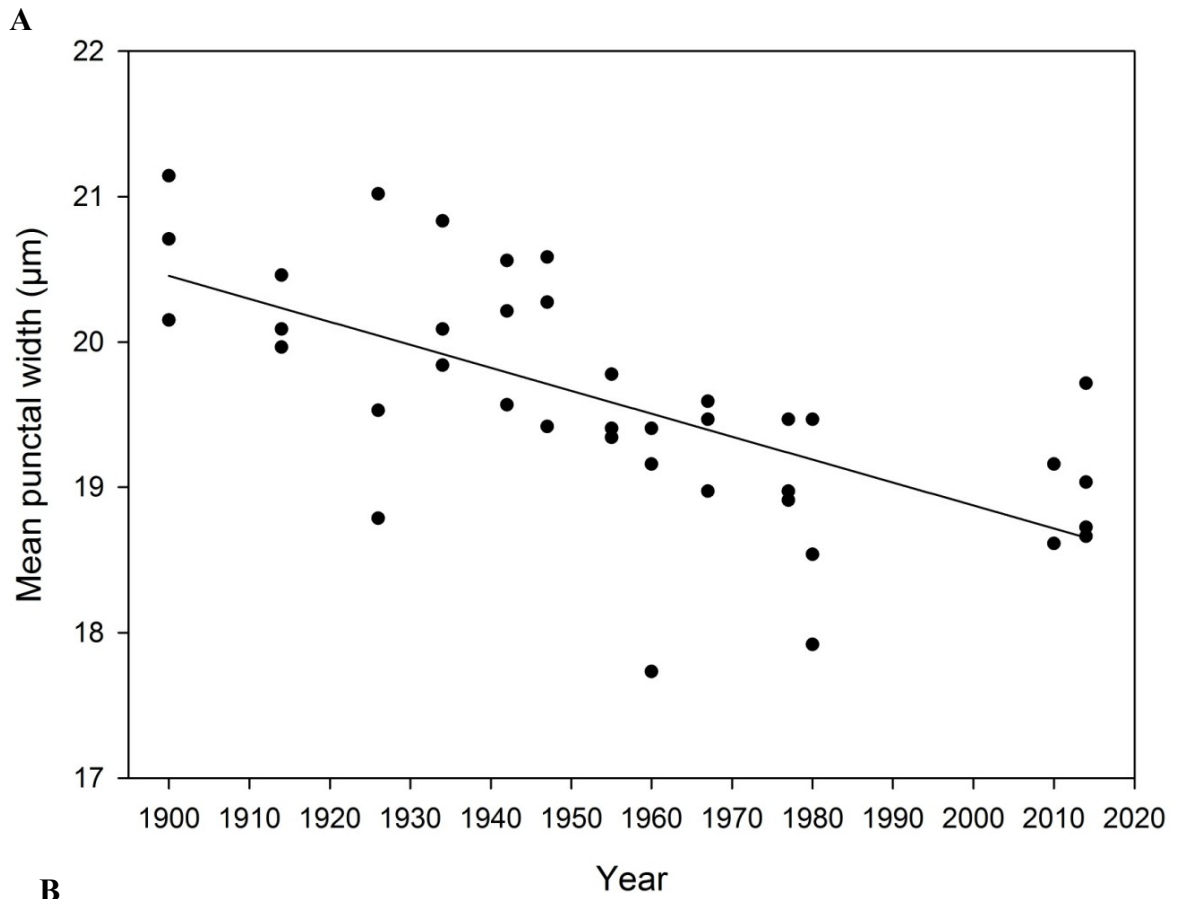


**Figure 5.14 – Mean punctal width from the middle of the punctum (A) and from the top of the punctum (B) from each decade over the last 110 years. Each point represents the mean for an individual. Error bars removed for clarity.**

### 5.3.5 Elemental composition

All major elements (Ca, Mg, Na, Sr and P) were above detection limits of the Electron Microprobe whereas the minor elements (Si, Fe, Mn and Ba) were all consistently below their respective detection limits (Table 5.4). These minor elements were, therefore, excluded from further analysis.

**Table 5.4 – Detection limits for all major and minor elements measured.**

Major elements			Minor elements		
Element	Average (wt %)	SE	Element	Average (wt %)	SE
Ca	0.14	< 0.01	Si	0.03	< 0.01
Mg	0.01	< 0.01	Fe	0.06	< 0.01
Na	0.05	< 0.01	Mn	0.07	< 0.01
Sr	0.04	< 0.01	Ba	0.21	< 0.01
P	0.01	< 0.01			

Overall, Ca concentration ranged from 38.29-40.36 wt %, Mg from 0.01-0.21 wt %, Na from 0.11-0.30 wt %, Sr from 0.06-0.19 wt % and P from 0.01-0.09 wt % (Table 5.5). Concentrations of all elements were more variable in the primary layer. It has been previously reported that the primary layer is not a reliable source of elemental concentrations (Bates & Brand, 1991; Brand et al., 2003; Pérez-Huerta et al., 2008). Data from the primary layer were therefore excluded from further analysis. The primary layer in *C. inconspicua* was defined as data between 0-30  $\mu\text{m}$  from the exterior as 30  $\mu\text{m}$  was determined as the mean primary layer thickness for this species in Chapter 4. None of the elemental concentrations varied over the last 110 years (Figure 5.15 and Appendix Figures C1-5; Ca linear regression:  $R^2 = 0.002$ ,  $F_{1,1162} = 1.87$ ,  $p = 0.171$ ; Mg linear regression:  $R^2 = 0.000$ ,  $F_{1,1093} = 0.11$ ,  $p = 0.736$ ; Na linear regression:  $R^2 = 0.003$ ,  $F_{1,1162} = 3.51$ ,  $p = 0.061$ ; Sr linear regression:  $R^2 = 0.000$ ,  $F_{1,1132} = 0.18$ ,  $p = 0.671$ ; P linear regression:  $R^2 = 0.001$ ,  $F_{1,990} = 0.99$ ,  $p = 0.321$ ).

**Table 5.5 - Minimum, maximum and mean weight % and standard error of each element from each year.**

Year	Element	Minimum (wt %)	Maximum (wt %)	Mean (wt %)	S.E.	Year	Element	Minimum (wt %)	Maximum (wt %)	Mean (wt %)	S.E.
1900	Ca	38.40	40.36	39.43	0.03	1926	Ca	38.29	40.21	39.26	0.03
	Mg	0.01	0.19	0.06	< 0.01		Mg	0.02	0.17	0.07	< 0.01
	Na	0.11	0.28	0.19	< 0.01		Na	0.11	0.28	0.20	< 0.01
	Sr	0.07	0.19	0.11	< 0.01		Sr	0.06	0.18	0.11	< 0.01
	P	0.01	0.08	0.03	< 0.01		P	0.01	0.06	0.03	< 0.01
1942	Ca	38.42	40.42	39.40	0.03	1960	Ca	38.39	40.17	39.27	0.03
	Mg	0.02	0.21	0.06	< 0.01		Mg	0.02	0.20	0.10	< 0.01
	Na	0.11	0.30	0.19	< 0.01		Na	0.11	0.30	0.18	< 0.01
	Sr	0.08	0.19	0.11	< 0.01		Sr	0.06	0.17	0.11	< 0.01
	P	0.01	0.08	0.03	< 0.01		P	0.01	0.08	0.03	< 0.01
1980	Ca	38.83	40.35	39.52	0.03	2010	Ca	38.91	40.12	39.50	0.03
	Mg	0.02	0.20	0.07	< 0.01		Mg	0.02	0.20	0.08	< 0.01
	Na	0.12	0.26	0.19	< 0.01		Na	0.11	0.25	0.18	< 0.01
	Sr	0.06	0.17	0.11	< 0.01		Sr	0.07	0.19	0.11	< 0.01
	P	0.01	0.09	0.03	< 0.01		P	0.01	0.07	0.03	< 0.01
2014	Ca	38.41	39.95	39.33	0.03						
	Mg	0.01	0.15	0.05	< 0.01						
	Na	0.13	0.26	0.19	< 0.01						
	Sr	0.07	0.16	0.11	< 0.01						
	P	0.01	0.06	0.03	0.00						

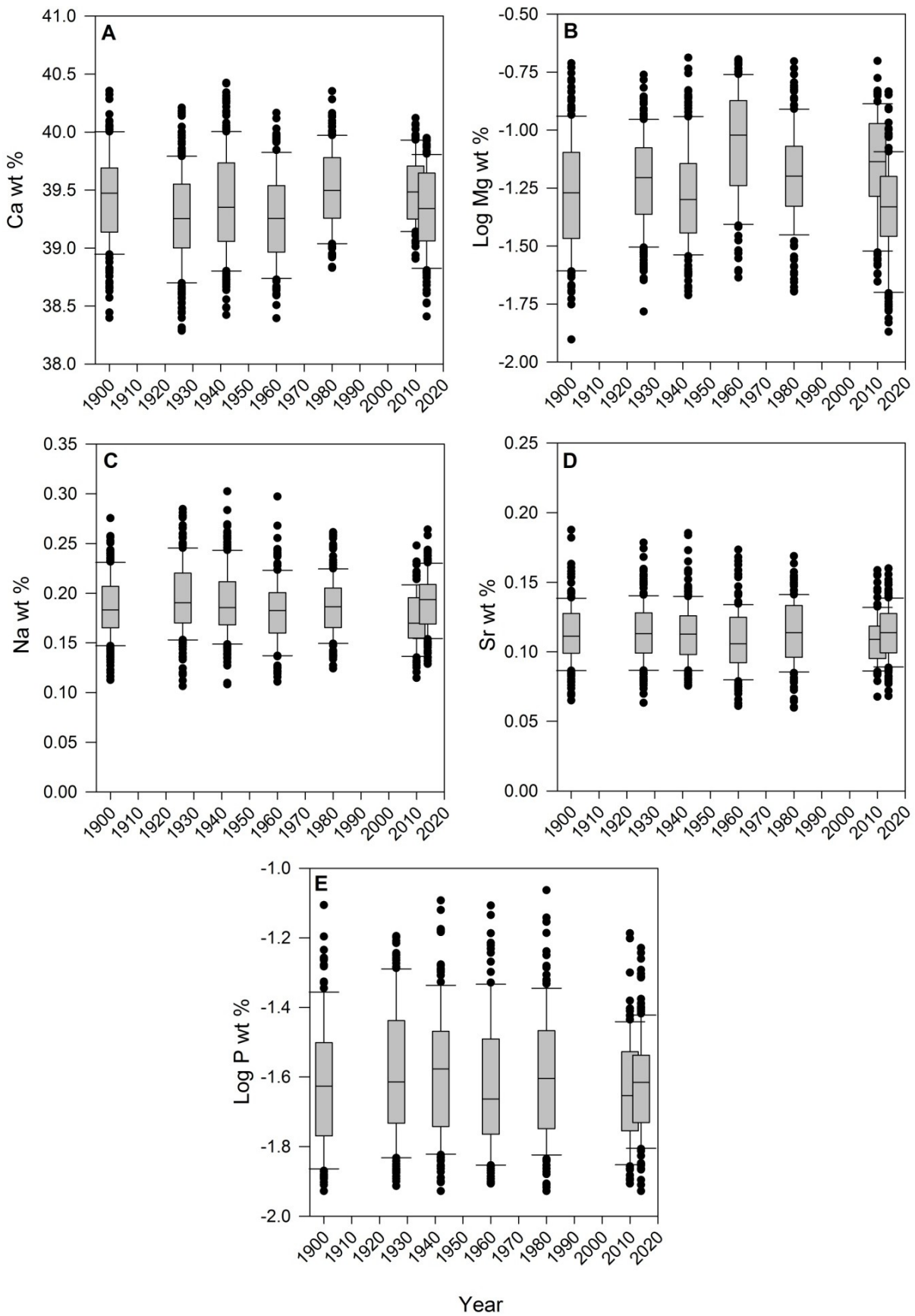
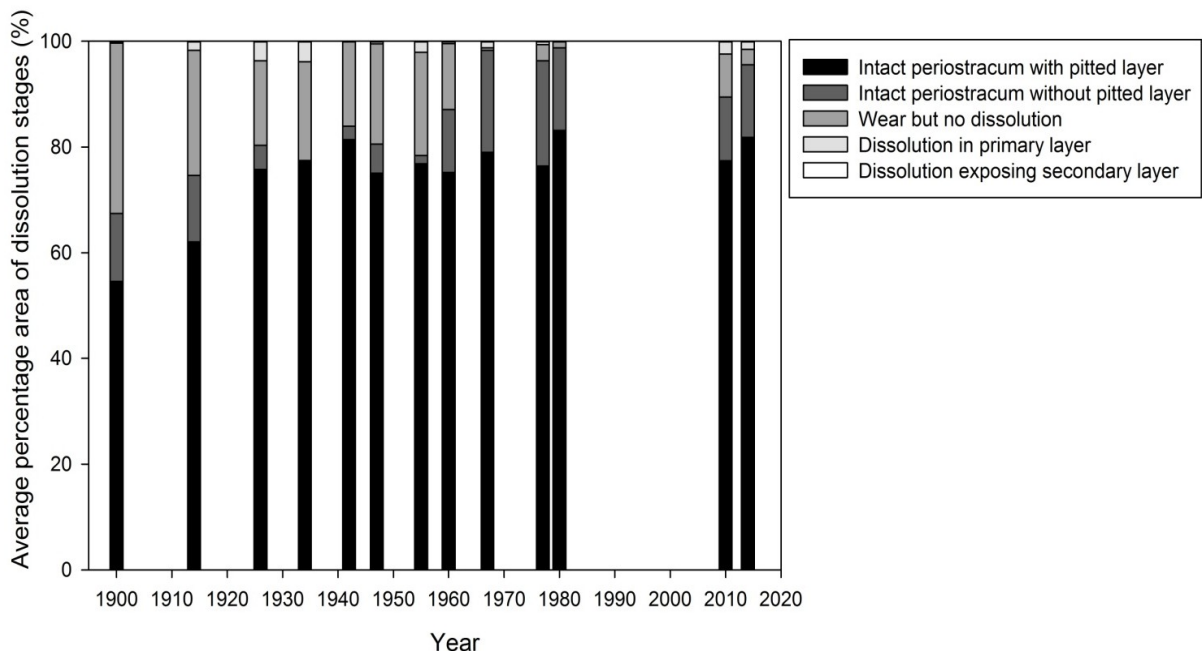


Figure 5.15 – Ca (a), log Mg (b), Na (c), Sr (d) and log P (e) concentrations in the secondary layer over the last 110 years.

### 5.3.6 Shell condition index

Shell surfaces in all years mainly showed intact periostracum with pitted layer (stage 0) with > 55% of all areas classified as this type of shell condition (Figures 5.16 and 5.17 and Appendix Figure C6). The percentage cover of stage 0 changed significantly over time (Kruskal-Wallis;  $H = 42.31$ ,  $p < 0.001$ ). A further Kruskal-Wallis Multiple Comparison test indicated that 1900 and 1914 had lower percentage cover than most other years (Table 5.6). The less severe type of wear (intact periostracum without pitted layer) is more variable, with a significant difference between years (Kruskal-Wallis,  $H = 68.18$ ,  $p < 0.001$ ). A further Kruskal-Wallis Multiple Comparison test revealed that percentage cover of wear stage 1 generally increased from 1967 onwards (Table 5.6). The more severe type of wear (wear but no dissolution) has the opposite trend to wear stage 1 with percentage cover of this type of wear decreasing from 1900 to 2014 (Kruskal-Wallis;  $H = 96.0$ ,  $p < 0.001$ ; Table 5.6). Despite significant differences between years in the percentage cover of both types of wear, only minimal dissolution occurred in the primary layer (dissolution stage 1; 0–12.7%) and this did not vary over the 110 year time period (Figure 5.16, Figure 5.17 and Appendix Figure C6; Kruskal-Wallis,  $H = 19.37$ ,  $p = 0.080$ ). Dissolution exposing the secondary layer (dissolution stage 2) also did not occur in any year (Figure 5.16 and Figure 5.17).



**Figure 5.16 - Mean percentage area of the different types of shell conditions over the last 110 years. Lighter grey tones indicate an increase in wear and/or shell dissolution (see legend).**

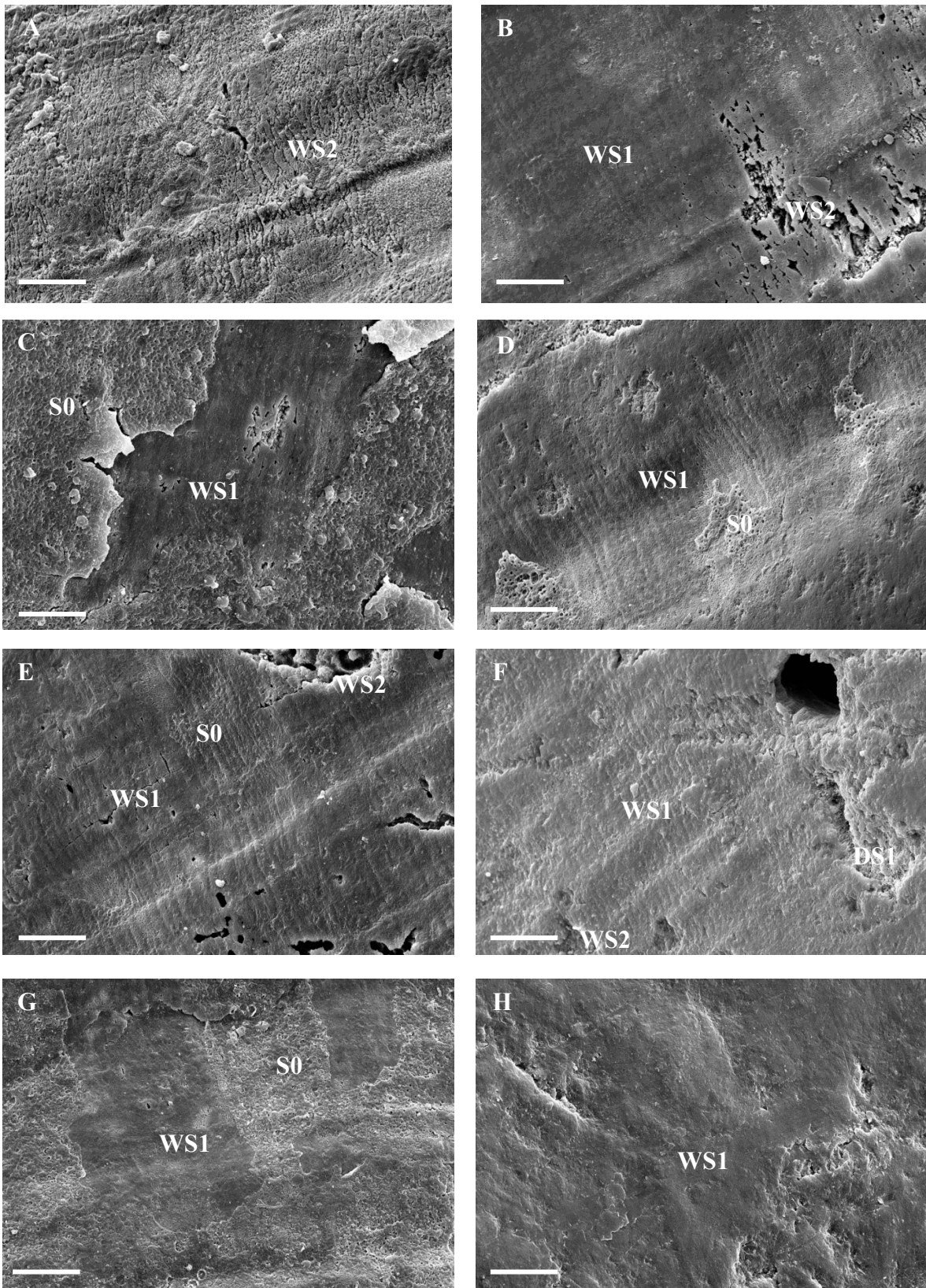


**Figure 5.17a - SEM micrographs of shell surfaces in 1900 (A), 1914 (B), 1926 (C), 1934 (D), 1942 (E) and 1947 (F), 1955 (G) and 1960 (H). S0 = stage 0, WS1 = wear stage 1, WS2 = wear stage 2 and DS1 = dissolution stage 1. Scale bar = 20  $\mu$ m.**

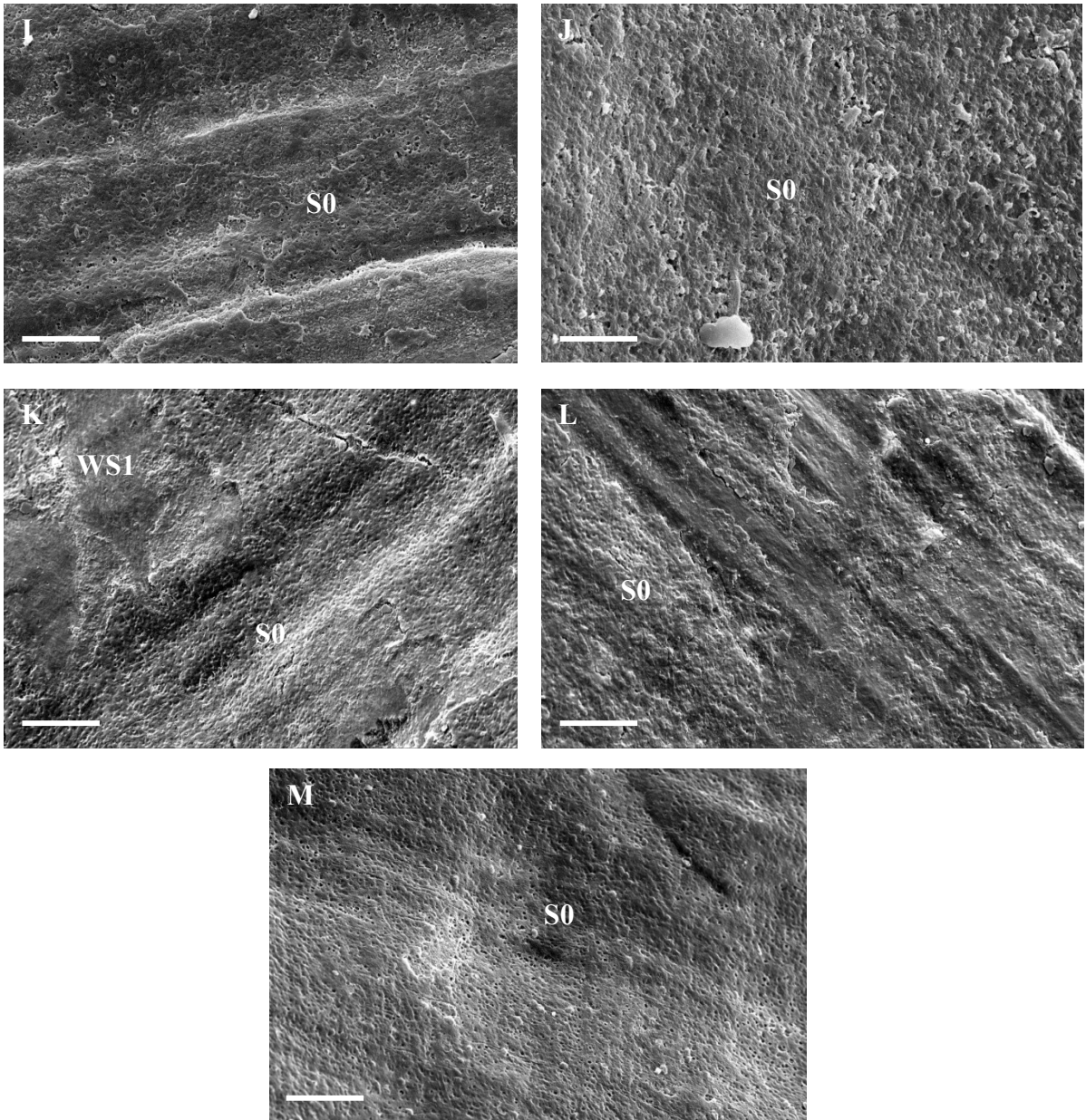


**Figure 5.17b - SEM micrographs of shell surfaces in 1967 (I), 1977 (J), 1980 (K), 2010 (L) and 2014 (M). S0 = stage 0, WS1 = wear stage 1, WS2 = wear stage 2 and DS1 = dissolution stage 1. Scale bar = 20  $\mu$ m.**

**Table 5.6 – Statistical results from Kruskal-Wallis Multiple Comparison Tests on each type of shell condition. Only significant differences are shown with the year with the higher percentage cover highlighted in bold.**

Intact periostracum with pitted layer (stage 0)			Intact periostracum without pitted layer (wear stage 1)			Wear but no dissolution (wear stage 2)		
Years	Z value	p value	Years	Z value	p value	Years	Z value	p value
1900 vs <b>1926</b>	3.018	0.003	<b>1900</b> vs 1934	3.895	0.001	<b>1900</b> vs 1967	5.872	0.001
1900 vs <b>1934</b>	3.731	0.001	<b>1900</b> vs 1955	3.372	0.001	<b>1900</b> vs 1977	4.979	0.001
1900 vs <b>1942</b>	4.271	0.001	<b>1914</b> vs 1934	3.360	0.001	<b>1900</b> vs 1980	5.465	0.001
1900 vs <b>1947</b>	3.306	0.001	1926 vs <b>1967</b>	3.114	0.002	<b>1900</b> vs 2010	3.812	0.001
1900 vs <b>1955</b>	3.018	0.003	1926 vs <b>1977</b>	3.564	0.001	<b>1900</b> vs 2014	5.026	0.001
1900 vs <b>1967</b>	4.220	0.001	1934 vs <b>1960</b>	3.531	0.001	<b>1914</b> vs 1967	5.578	0.001
1900 vs <b>1977</b>	3.101	0.002	1934 vs <b>1967</b>	4.624	0.001	<b>1914</b> vs 1977	4.685	0.001
1900 vs <b>1980</b>	4.496	0.001	1934 vs <b>1977</b>	5.075	0.001	<b>1914</b> vs 1980	5.172	0.001
1900 vs <b>2010</b>	3.274	0.001	1934 vs <b>1980</b>	4.099	0.001	<b>1914</b> vs 2010	3.518	0.001
1900 vs <b>2014</b>	4.102	0.001	1934 vs <b>2010</b>	3.627	0.001	<b>1914</b> vs 2014	4.732	0.001
1914 vs <b>1942</b>	3.466	0.001	1934 vs <b>2014</b>	3.928	0.001	<b>1926</b> vs 1967	3.592	0.001
1914 vs <b>1967</b>	3.416	0.001	1942 vs <b>1967</b>	3.540	0.001	<b>1926</b> vs 1980	3.185	0.001
1914 vs <b>1980</b>	3.692	0.001	1942 vs <b>1977</b>	3.991	0.001	<b>1934</b> vs 1967	4.248	0.001
1914 vs <b>2014</b>	3.297	0.001	1947 vs <b>1967</b>	3.576	0.001	<b>1934</b> vs 1977	3.355	0.001
			1947 vs <b>1977</b>	4.027	0.001	<b>1934</b> vs 1980	3.842	0.001
			1955 vs <b>1967</b>	4.102	0.001	<b>1934</b> vs 2014	3.402	0.001
			1955 vs <b>1977</b>	4.552	0.001	<b>1942</b> vs 1967	4.014	0.001
			1955 vs <b>1980</b>	3.576	0.001	<b>1942</b> vs 1977	3.120	0.002
			1955 vs <b>2014</b>	3.405	0.001	<b>1942</b> vs 1980	3.607	0.001
						<b>1942</b> vs 2014	3.168	0.002
						<b>1947</b> vs 1967	4.210	0.001
						<b>1947</b> vs 1977	3.316	0.001
						<b>1947</b> vs 1980	3.803	0.001
						<b>1947</b> vs 2014	3.364	0.001
						<b>1955</b> vs 1967	4.750	0.001
						<b>1955</b> vs 1977	3.856	0.001
						<b>1955</b> vs 1980	4.343	0.001
						<b>1955</b> vs 2014	3.904	0.001
						<b>1960</b> vs 1967	3.126	0.002

### 5.3.7 Shell thickness

Primary layer thickness ranged from 17-52  $\mu\text{m}$  (Figure 5.18A & black bars in Appendix Figure C7), secondary layer thickness ranged from 311-889  $\mu\text{m}$  (Figure 5.18B & grey bars in Appendix Figure C7) and total shell thickness ranged from 328-941  $\mu\text{m}$  (Figure 5.18C & whole bars in Appendix Figure C7) across all years. Primary layer thickness increased from 1900 to 2014 by 20.56% (Linear Regression,  $R^2 = 0.039$ ,  $F_{1,119} = 4.80$ ,  $p = 0.030$ ) whereas secondary layer and total shell thickness did not vary over the last 110 years (Secondary layer: Linear Regression,  $R^2 = 0.014$ ,  $F_{1,119} = 1.73$ ,  $p = 0.191$ ; Total shell: Linear Regression,  $R^2 = 0.008$ ,  $F_{1,119} = 0.95$ ,  $p = 0.331$ ).

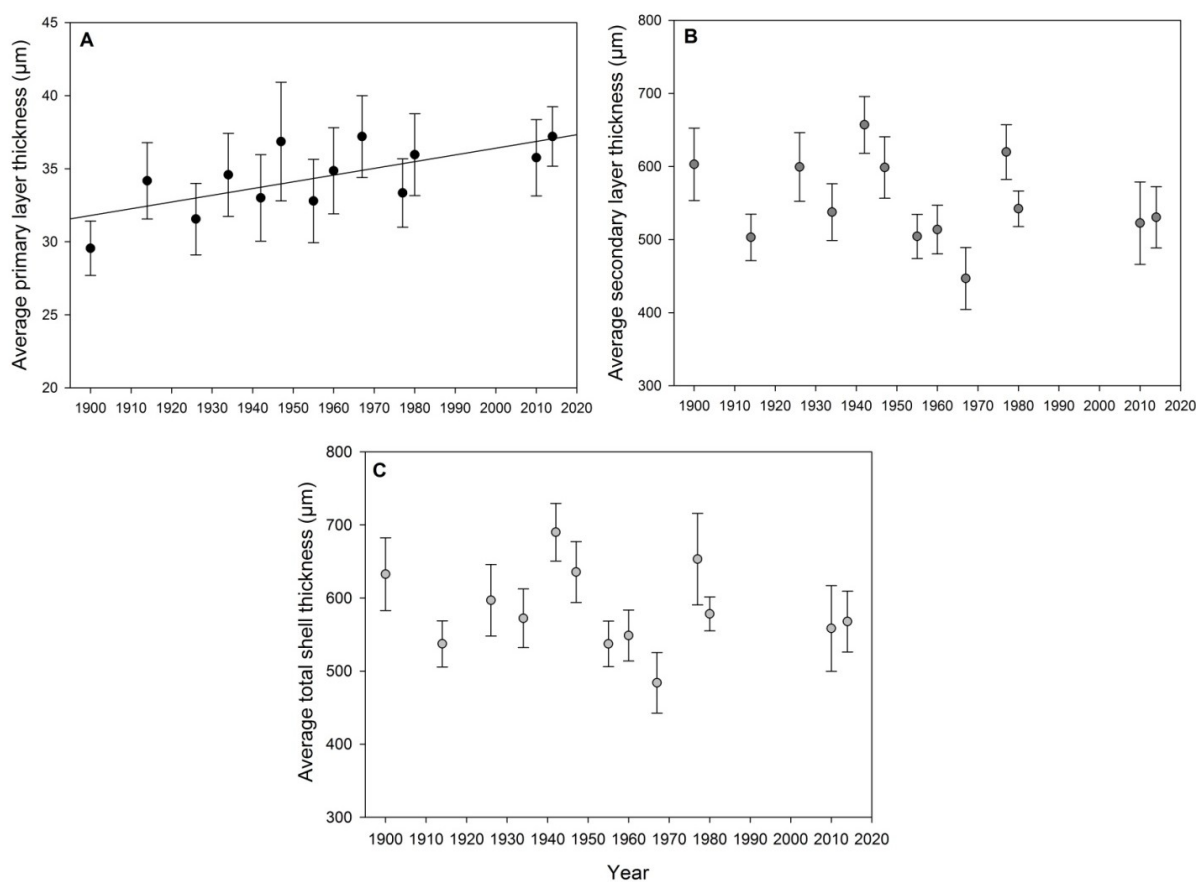


**Figure 5.18 – Primary layer (A), secondary layer (B) and total shell thickness (C) from each decade over the last 110 years. Values plotted as mean  $\pm$  SE.**

### 5.4 Discussion

The resilience of *C. inconspicua* to environmental change since the Industrial Revolution is clear from the data on various shell characteristics in this chapter. Six key aspects of the shells of this high calcium carbonate content species did not change since 1900 despite significant shifts in its natural habitat of a 0.7°C temperature increase and 90-100 ppm increase in CO<sub>2</sub> concentration (<http://www.climatechange.govt.nz/science/>).

As *C. inconspicua* grows, breadth increases almost proportionally to length, but height increases more than length. A similar relationship was found in Aldridge & Gaspard (2011) who also reported an anterior change in shell shape in *C. inconspicua* once an individual reaches 20 mm in length as animals slowed growth in the length direction but continued to increase in height. Evidence of this trend were crowded growth lines, a more gibbous appearance and valves growing inwards towards the umbo only in larger specimens. Morphometric relationships mainly did not differ over the last 110 years with only individuals from 1967 and 2014 being taller than all other years. All specimens from 2014 were large individuals (14.4-25.0 mm length), which coincides with the size of sexual maturity in *C. inconspicua* (14-16 mm length; Doherty, 1979, Lee & Wilson, 1979). Growth rate slows appreciably with the onset of breeding as energy is reallocated to reproduction (Rickwood, 1977). However, shells continue to increase in height to increase the volume of the mantle cavity to allow space for larger gonads and larval brooding as well as for the increasing size of the plectolophus lophophore (Rickwood, 1977). The significantly taller individuals in 2014 are thus most likely due to the size range of specimens available and it is unlikely that environmental parameters caused a different shell shape to all other years studied. Phenotypic plasticity of shell morphology has been reported in other shell-bearing animals in response to changing environmental conditions (Peyer et al., 2010; Fitzer et al., 2015a). Temperature had the greatest effect on shell morphology in the mussel *Dreissena polymorpha* in comparison to food quantity and water motion (Peyer et al., 2010). Higher temperatures (~18-20°C) caused more rotund shells to be produced whereas lower temperatures (~6-8°C) caused more laterally flattened shells. Increased  $p\text{CO}_2$  conditions (750  $\mu\text{atm}$  and 1000  $\mu\text{atm}$ ) resulted in rounder and flatter *M. edulis* shells which also had a thinner aragonite layer compared to ambient conditions (380  $\mu\text{atm}$ ) (Fitzer et al., 2015a). This new shell shape was explained as a compensatory mechanism to enhance protection from predators and changing environments due to the inability of this species to produce thicker shells under increased ocean acidity. The lack of a change in shell morphology of *C. inconspicua* over the last 110 years demonstrates the tolerance of this species to altered abiotic conditions.

Shell density increased by 3.43% from 1900 to 2014, which cannot be explained by a change in calcification index, elemental composition, punctal density and/or shell thickness as none of these shell characteristics varied over this period. Punctal width significantly decreased by 8.26% in the middle of the punctae and by 7.17% at the top of the punctae. This equates to a

1% decrease in shell occupied by punctae, which explains part of the 3.43% increase in shell density. Therefore, *C. inconspicua* has not changed its shell morphology, elemental concentrations, shell thickness or the number of punctae in response to changing environmental conditions over the last 110 years. Instead this species appears to lay down more shell by constructing thinner punctae. This response may also increase protection from their changing habitat by reinforcing the shell structure. Producing thinner punctae, however, could have physiological implications for rhynchonelliform brachiopods as there is less space for the caeca. As the function of punctae is still under debate, the extent, if any, of the impact to the organism remains unknown. Other historical studies have demonstrated varying responses of marine calcifiers to changing environmental conditions over a wide range of time scales. Pfister et al. (2016) discovered modern shells from 2009-2011 and 1960s-1970s of *Mytilus californianus* were thinner than shells from Native American midden sites dating back to ~1000-2420 years BP. There was no decline, however, in shell thickness over the last 40 years. The authors suggested that declining ocean pH was a likely explanation for the shell thinning on the millennial scale as it is known to affect calcification. Caution is required, however, when interpreting results over such long time periods as multiple abiotic and biotic changes will have occurred in the environment. Certain reef-building corals have the potential to provide information about coral growth and climate over the past several centuries (Lough & Barnes, 1997; Bessat & Buigues, 2001). Coral growth measurements, including linear extension, density and calcification measurements, in *Porites* colonies dating back 49-507 years from the Great Barrier Reef indicated that calcification increased by 3.5% with a 1°C increase from 20-21°C (Lough & Barnes, 1997, 2000). A similar study on the same reef-building coral from 1800-1900 in Moorea, French Polynesia also demonstrated a 4.5% increase in calcification with a 1°C rise in temperature (Bessat & Buigues, 2001). These studies demonstrate the usefulness of historical studies to providing a more complete understanding of organisms' responses to environmental change.

The majority of the shell surfaces throughout the 110 year time period remained intact with the protective periostracum layer undamaged and the pitted layer present. Although, the percentage cover of wear decreased from 1900 to 2014, which was associated with a parallel increase in the thickness of the primary layer. This is most likely a result of post collection wear in museum storage and the trend is most likely correlated with the time spent in museum collections. The most common cause of the deterioration of museum specimens is through movement in storage cabinets and/or against the wadding they are packed in and also the

build up of abrasive particulates such as dirt and dust (Stansfield, 2012). Dust can also attract pests and removing it can cause damage to any fragile stored sample. Calcareous shells are also susceptible to damage if they are stored in environments with acid vapours, which could result from unsuitable woods in the construction of storage cabinets (Thickett & Lee, 2004; Stansfield, 2012). These highlight limitations of museum storage and should be taken into consideration when using historic specimens to determine impacts of the natural environment on shell-bearing organisms. Only low levels of dissolution in the primary layer occurred through the time series and the secondary layer was not exposed in any specimen. This indicates that the 90-100 ppm increase in CO<sub>2</sub> concentration from 290-380 ppm did not cause extensive dissolution. As only minimal dissolution in the primary layer was seen throughout all years and there was no change in the secondary layer and overall thickness of shells, it is likely that *C. inconspicua* maintained its shell integrity in response to environmental change since 1900.

Historical data can be used to test predictions from laboratory and comparative spatial analyses. This enables us to better understand the responses of marine calcifiers to increasing anthropogenic CO<sub>2</sub> emissions. Experiments in chapters 2, 3 and 4 illustrate the resilience of *C. inconspicua* to future ocean acidification as punctal density, elemental composition, shell condition and shell thickness were not impacted by exposure to predicted future change. Shell growth rates, ability to repair shell and shell microstructure were similarly not affected. Despite the usefulness of museum collections, there are limitations to using this approach. These include relying on repeated sampling from the same site, sample bias towards larger individuals, a lack of collection details prohibiting the use of all available specimens, accuracy of the collection details that are given and the inability to identify environmental parameters affecting organism traits. This chapter presents unique and valuable data for a wide range of shell characteristics of locally abundant *C. inconspicua* from the same site every decade since 1900. Six out of eight key shell characteristics measured in this unique collection were not affected by environmental change. The only change observed was a decrease in punctal width which partially explained the increase in shell density. This is suggested to reinforce the structure of the shell. This indicates the resilience of this highly calcium carbonate dependent species to environmental conditions that have already changed over the last 110 years and provides an insight into how this species might react to future change and its possible ability to adapt.



# Chapter Six

## General Discussion

### 6.1 Summary

Ocean acidification research on the effects of future pH conditions on marine organisms is currently largely based on predictions from short to medium term laboratory and field experiments. Long-term experiments are crucial to be able to evaluate the ability of organisms to acclimate and possibly adapt over multiple generations to ocean acidification (Collins et al., 2014; Andersson et al., 2015). Assessing how organisms have coped with past environmental change through the use of museum specimens is also an invaluable technique to provide a historical reference for future climate change responses (Hoeksema et al., 2011; Lister, 2011). A combination of approaches provides data and information that allows a mechanistic understanding of the impacts of excess CO<sub>2</sub> through anthropogenic activities and the necessary predictive power for future change (Dupont & Pörtner, 2013; Andersson et al., 2015). Previous ocean acidification research has also focused on the impacts on other vulnerable marine calcifiers such as corals and molluscs. Rhynchonelliform brachiopods have persisted throughout the last 550 million years (Rudwick, 1970; Richardson, 1981a; Rhodes & Thompson, 1992), inhabit all of the world's oceans (James et al., 1992; Peck, 2001a) and have a high calcium carbonate requirement (Peck, 1993, 2008), however, little is known about the effects of end-century pH and temperature conditions on these taxa. This thesis, therefore, exploited long-term laboratory experiments and the use of historic specimens from museum collections to provide a more complete understanding into how possibly one of the most calcium carbonate dependent groups of organisms has and will be able to tolerate our acidifying and warming oceans.

*Will predicted end-century decreased pH and elevated temperature have a negative effect on their ability to repair shell?*

Both *L. uva* and *C. inconspicua* will be able to repair damage to their shells and continue to produce shell in the natural environment in the next 84 years. The majority of damaged *L. uva*

also continued shell production after the completion of repair, further demonstrating the tolerance of this species. None of the *C. inconspicua* specimens laid down new shell after repairing their notch, even though the majority of the damaged individuals managed to fully repair their shell. The difference between *L. uva* and *C. inconspicua* was probably because a wider size range (5.0-37.0 mm) of *L. uva* was used in comparison to the limited size range of *C. inconspicua* individuals in each treatment where only large individuals (> 14 mm) were used. This is the size of sexual maturity in *C. inconspicua* (Doherty, 1976; Lee & Wilson, 1979) and growth rates were thus already low in these individuals due to a transfer of resources from somatic growth to reproduction. Therefore, once the critical process of repair was complete, these individuals were much less likely to grow than the juvenile specimens included in the Antarctic experiment.

*Does lowered pH and warming conditions predicted by 2100 decrease growth rates?*

Shell growth rates in both undamaged and damaged *L. uva* were not different among any of the experimental treatments indicating that *L. uva* has the phenotypic plasticity to make shell in predicted end-century pH conditions without any of the genetic adaptation that may occur in the next 84 years. This species should, therefore, be able to continue shell production in the predicted future ocean conditions, including acidification, even after disturbance events that cause minor to moderate shell damage. Shell production in *C. inconspicua* should also be unaffected by changing pH levels in the natural environment up to 2100, as growth rates in undamaged individuals were either not affected (> 3 mm) or positively affected (< 3 mm) by acidified conditions. This ability of both species to continue shell production in low pH indicates that this species can generate suitable conditions at the site of calcification (Ries, 2011; Gazeau et al., 2013; Wittmann & Pörtner, 2013). Elevated temperature to the predicted 2°C increase alongside ocean acidification by 2100 positively affected shell growth rate in the Antarctic brachiopod. Shell deposition, therefore, could occur at a faster rate in 50-100 years as a consequence of warming despite the predicted acidity of the oceans. Although, other factors such as changes in food availability from altered phytoplankton blooms will also affect future growth rates.

*Does decreased pH and increased temperature alter the shell microstructure and elemental composition?*

Punctal density, calcite fibre size and elemental composition were not affected by acidified conditions in either species, or also by warming in *L. uva*. Over the next 84 years, both the polar and temperate brachiopod, therefore, will have the ability to produce the same shell structure, in terms of punctal density and calcite fibre size, and shell consisting of the same elemental composition, in terms of the major elements (Ca, Mg, Na, Sr, P) measured here. Other shell structure characteristics, including crystal morphology, shell texture and hardness, as well as other elements, including trace elements, requires further investigation to determine the extent of the these species' tolerance to maintain the production of a robust shell under future environmental change.

*Will forecasted end-century pH and warming affect shell dissolution?*

Predicted pH conditions for 2050 and 2100 caused shell dissolution in both *L. uva* and *C. inconspicua* with dissolution becoming more extensive with increasing acidity. The polar brachiopod also exhibited more extensive dissolution than the temperate species. Increased susceptibility of Antarctic calcified invertebrates is due to being weakly calcified (Nicol, 1967, Vermeij, 1978; Watson et al., 2012), dissolution rates of calcium carbonate being inversely related to temperature (Revelle & Fairbridge, 1957) and the polar regions being predicted to become the first to be undersaturated in aragonite by 2050 (Caldeira & Wickett, 2005; Fabry et al., 2008; Guinotte & Fabry, 2008; McNeil & Matear, 2008). Shell laid down in the wild appeared more worn in *L. uva* compared to *C. inconspicua*, which was potentially related to their longer life span (Doherty, 1979; Peck & Brey, 1996), with *L. uva* being subjected to wear over a longer time scale. Increased abrasion also occurs through other individuals in the larger *L. uva* clumps. This removal of the periostracum would have amplified dissolution in *L. uva* as the presence of this organic protective layer reduces an organism's susceptibility to shell dissolution (Ries et al., 2009; Tunnicliffe et al., 2009; Thomsen et al., 2010; Rodolfo-Metalpa et al., 2011; Coleman et al., 2014). Temperature had no effect on dissolution in *L. uva*.

*Will rhynchonelliform brachiopods be able to counteract shell loss through dissolution?*

The more extensive dissolution in *L. uva* was counteracted by laying down more secondary layer and increasing overall shell thickness, thus overcompensating the loss of shell. The less extensive dissolution in *C. inconspicua* did not require any extra resources being diverted to increase secondary layer thickness to compensate minor losses in the primary layer. As exposed *L. uva* secondary layer did not exhibit any external dissolution after long-term (7 months) exposure to predicted 2100 pH conditions, the compensatory mechanism of a thicker shell of only secondary layer could provide sufficient protection over the next 84 years to acidifying oceans.

*Has environmental change over the last century negatively impacted shell characteristics?*

Since 1900, temperature has risen by 0.7°C and CO<sub>2</sub> concentration has increased by 90-100 ppm in New Zealand (<http://www.climatechange.govt.nz/science/>). The resilience of *C. inconspicua* to this environmental change over the last 110 years was demonstrated by six key shell characteristics being unaffected over this time. These were: morphometrics, calcification index, punctal density, elemental composition, shell condition index and shell thickness. Shell density, however, increased by 3.43% over the last 110 years, which was partially explained by a 1% decrease in the area of shell occupied by punctae. This species, therefore, appears to lay down more shell fabric by constructing thinner punctae, which could increase protection from their changing environment by reinforcing the shell structure. This alternative approach to understanding the effects of changing environments on marine organisms complemented data emphasising the resilience of *C. inconspicua* in the laboratory experiments. The use of museum specimens has provided a unique and valuable historical record of how a highly calcium carbonate dependent species has responded to environmental change over the last century and also provides an insight into how this species might react to future change and its possible ability to adapt.

## **6.2 Future Research**

This thesis has explored many different shell characteristics of rhynchonelliform brachiopods to address outstanding questions on how marine calcifiers have, and will be affected by environmental change. A wide range of shell properties were investigated, however, there are others that warrant further research to fully understand the impact of ocean acidification and warming on the protective shell crucial to the existence of these organisms. Ocean

acidification has been reported to affect shell texture in bivalve molluscs (Hahn et al., 2012; Fitzer et al., 2014b, 2016). Electron Backscatter Diffraction (EBSD) further revealed that increased  $p\text{CO}_2$  reduces crystallographic control of shell formation (Fitzer et al., 2014b, 2016). Valve texture of rhynchonelliform brachiopods, including *L. uva*, has been previously determined (Cusack et al., 2008; Griesshaber et al., 2007, 2008; Schmahl et al., 2008a,b; Goetz et al., 2009), although none of these studies incorporated any effect of environmental parameters. Valve hardness has also been reported to be affected by acidified conditions in molluscs (Landes & Zimmer, 2012; Goffredo et al., 2014; Fitzer et al., 2015b). Fitzer et al. (2015b) found that high  $p\text{CO}_2$  (750  $\mu\text{atm}$ ) caused *Mytilus edulis* to produce shell calcite that is stiffer and harder than their aragonite and calcite shells produced in control conditions (380  $\mu\text{atm}$ ). This implied that *M. edulis* has a threshold above which it alters the characteristics of calcite it produces although when increased  $p\text{CO}_2$  was combined with a 2°C increase in temperature, the impact of  $p\text{CO}_2$  on hardness was reduced. Valve hardness has previously been determined in rhynchonelliform brachiopods, including *L. uva* (Griesshaber et al., 2007; Pérez-Huerta et al., 2007; Schmahl et al., 2008a,b; Goetz et al., 2009), however, the impact of environmental change has never been included. Goetz et al. (2009) found that the Antarctic *L. uva* has one of the hardest brachiopod shells with the outer primary layer being harder ( $464 < \text{HV} < 521$ ) than the inner secondary layer ( $269 < \text{HV} < 272$ ). The hardness gradient was also less pronounced in *L. uva* than other brachiopods, e.g. *Megerlia truncata*. As previously demonstrated (Chapter 4), *L. uva* experienced extensive dissolution under predicted end-century acidified conditions that exposed the secondary layer. The compensation mechanism employed by this species was laying down more secondary layer and increasing overall shell thickness. As the secondary layer is softer than the primary layer, there could be long-term implications of this compensatory mechanism as a shell only consisting of secondary layer potentially might not provide a strong enough support or maybe needs to be thicker to meet the biomechanical requirements, e.g. defence against predators and valve snapping to eject faeces and pseudofaeces.

In addition to shell characteristics, it is also crucial to discover how other biological aspects of rhynchonelliform brachiopods might be impacted by future environmental change. Physiological processes such as metabolic rate, respiration and reproduction, ecological factors such as behaviour and predator-prey interactions as well as genomics and epigenetics are key to determine the complete response of this highly calcium carbonate dependent group of organisms. The impact of ocean acidification and temperature on these biological processes

has been widely investigated in molluscs with positive, negative and no effects being reported (see reviews by Fabry et al., 2008; Doney et al., 2009; Gattuso et al., 2013; Gazeau et al., 2013; Kelly & Hofmann, 2013). The majority of shell characteristics remained unaffected in *L. uva* and *C. inconspicua*, however, shell dissolution was counteracted by laying down more shell in *L. uva*. It remains unknown whether this compensatory mechanism is present in *C. inconspicua* if more extensive dissolution occurs. Increasing shell costs will shift their energy budget and decrease allocation to other essential processes such as growth and reproduction. This requires further investigation as it is crucial that we determine what level of acidification and warming will critically impact energy required for critical physiological processes.

Ocean acidification research is evolving to incorporate more multistressors into experiments (see reviews by Byrne & Przeslawski, 2013; Riebesell & Gattuso, 2015), which this thesis has touched on by including temperature in the polar experiment. A fully multifactorial experiment including many different combinations of temperature and pH would be beneficial to the polar experiment as well as adding temperature as another stressor in the temperate experiment. In addition, other environmental variables have been included in other multiple stressor ocean acidification studies such as food availability (e.g. Thomsen et al., 2013), hypoxia (e.g. Rosa & Siebel, 2008) and pollution (e.g. Lewis et al., 2016) which have often been shown to have a greater effect on marine organisms than lowered pH. Incorporation of more stressors to the experimental approach increases the environmental relevance of the organism's responses.

Investigating more brachiopod species would be advantageous as this is the first ocean acidification study to involve live brachiopods. It would be particularly interesting to involve the other brachiopod orders, the thecids and the rhynchonellids, within the rhynchonelliforms due to their micromorphic size and different shell characteristics, respectively, as well as increasing the number of terebratulides to determine the extent of resilience in this order. Further to this, it would be a good avenue to investigate the two other subphyla of brachiopods, the linguliform and craniiform brachiopods due to their different shell structures. Shells of linguliform brachiopods also have a very different elemental composition as they have a calcium phosphate shell and they are typically infaunal species, therefore, probably already living in lowered pH conditions (Williams, 1997). As calcium carbonate is known to be a vulnerable chemical compound in our acidifying oceans and shells are mainly under

threat when the periostracum is damaged exposing underlying shell when in direct contact with seawater, I would expect minimal, if any, impact of environmental change on the linguliforms.

As brachiopods have persisted for > 550 million years, fossils can be assessed to determine how this phylum has survived through several geological periods with fluctuating environmental conditions. Ocean carbonate chemistry has changed throughout the Phanerozoic (past 540 Ma) with periods of high atmospheric CO<sub>2</sub> concentrations common in the geological record (Doney et al., 2009). The most catastrophic and abrupt ocean acidification event prior to the present day was the Permo-Triassic mass extinction 245 million years ago where the second extinction pulse involved a rapid, large injection of carbon that caused a major loss of heavily calcified marine species including brachiopods (Thayer, 1986; Pennington & Stricker, 2001; Clarkson et al., 2015). Another prominent acidification event was the Paleocene-Eocene thermal maximum (PETM) 55 million years ago which is considered to be the most comparable to current ocean acidification (Zachos et al., 2005, 2008; Widdicombe & Spicer, 2008; Doney et al., 2009). There are limitations to this method though, including unclear rates of change, for example the carbon addition at the PETM might not be as rapid as the present day increase. Environmental conditions were also different to the present day, for example, the PETM carbon excursion occurred within a background of already high CO<sub>2</sub> and temperature. It is also not possible to definitively attribute any identified biological impacts to only ocean acidification as lowered pH often occurred with warming and anoxia (Andersson et al., 2015). These acidification events also occurred over much longer time scales and at slower rates than the current anthropogenic ocean acidification (Zachos et al., 2005; Hönlisch et al., 2012). It is thus possible that impacts of current ocean acidification may be more severe than fluctuations in the geological past (Hoegh-Guldberg et al., 2007; Pelejero et al., 2010). These differences between past geological periods and the present day need to be considered when using fossil specimens to assist predictions of modern day species responses, however, this approach would still be useful to assess how marine organisms coped with acidification events in the geological past.

### **6.3 Conclusions**

Overall, this thesis has indicated the robust ability of shell production and maintenance in a polar and a temperate brachiopod to recent past and predicted end-century acidified and

warming conditions. The majority of shell characteristics have remained unchanged over the last 110 years and will also continue to be unaffected by environmental change over the next 84 years. Shell density in *C. inconspicua*, however, increased from 1900 to 2014 as this species laid down more shell partly by constructing thinner punctae. Shell dissolution will also impose a threat to both *L. uva* and *C. inconspicua*, however, *L. uva* has demonstrated the ability to counteract this by increasing secondary layer and thus total shell thickness. If shell dissolution becomes more extensive in *C. inconspicua* than observed in this study, this compensatory mechanism could occur in this temperate brachiopod. The shell is crucial to the existence of rhynchonelliform brachiopods and other shell-bearing organisms (Harper et al., 2012), therefore, the resilience of these marine calcifiers to maintain production, integrity and repair of this protective barrier will be a key aspect to their survival through predicted environmental change up to 2100. The main mechanisms that organisms can use to respond to environmental change are acclimation and genetic adaptation (Somero, 2010; Peck, 2011). Long-term laboratory experiments and historical specimens used here have produced insights into how these species can acclimate and their possible capacity to adapt to future change.

This thesis adds the responses of the less studied brachiopods to the existing literature on how marine calcifiers will be impacted by future ocean acidification and warming. The tolerance of possibly the most calcium carbonate dependent group of organisms to the fastest rate of environmental change ever experienced on Earth has highlighted the need for more environmentally relevant long-term experiments. Incorporating the use of museum specimens to determine how marine calcifiers have responded to recent past change with long-term laboratory experiments investigating future impacts using the same species is rare. This multi-method approach has enabled a more complete understanding of the effects of forecasted environmental change on locally important rhynchonelliform brachiopods that have persisted over the last 550 million years and survived several geological periods of fluctuating conditions. Comparable long-term studies on other species from polar to tropical environments are essential to increase our knowledge of the capability of these integral organisms to succeed under changing environmental conditions.

# References

- Al-Horani, F. A., Al-Moghrabi, S. M., & Beer, D. 2003. The mechanism of calcification and its relation to photosynthesis and respiration in the scleractinian coral *Galaxea fascicularis*. *Marine Biology*, 142: 419-426.
- Aldridge, A. E. 1981. Intraspecific variation of shape and size in subtidal populations of two Recent New Zealand articulate brachiopods. *New Zealand Journal of Zoology*, 8: 169-174.
- Aldridge, A. E., & Gaspard, D. 2011. Brachiopod life histories from spiral deviations in shell shape and microstructural signature – preliminary report. *Memoirs of the Association of Australasian Palaeontologists*, 41: 257-268.
- Alexander, R. R., James, M. A., & Ansell, A. D. 1992. Survival and repair of surgical and natural shell damage in the articulate brachiopod *Terebratulina retusa* (Linnaeus). *Historical Biology*, 6: 221-231.
- Almada-Vilela, P. C., Davenport, J., & Gruffydd, L. D. 1982. The effects of temperature on the shell growth of young *Mytilus edulis* L. *Journal of Experimental Marine Biology and Ecology*, 59: 275-288.
- Andersson, A. J., Kline, D. I., Edmunds, P. J., Archer, S., Bednaršek, N., Carpenter, R. C., Chadsey, M., Goldstein, P., Grottole, A., Hurst, T., King, A., Kübler, J., Kuffner, I. B., Mackey, K., Menge, B. A., Paytan, A., Riebesell, U., Schnetzer, A., Warner, M., & Zimmerman, R. 2015. Understanding ocean acidification impacts on organismal to ecological scales. *Oceanography*, 25: 16-27.
- Andersson, A. J., Kuffner, I. B., MacKenzie, F. T., Jokiel, P. L., Rodgers, K. S., & Tan, A. 2009. Net loss of CaCO<sub>3</sub> from a subtropical calcifying community due to seawater acidification: mesocosm-scale experimental evidence. *Biogeosciences*, 6: 1811-1823.
- Andersson, A. J., Mackenzie, F. T., & Bates, N. R. 2008. Life on the margin: implications of ocean acidification on Mg-calcite, high latitude and cold-water marine calcifiers. *Marine Ecology Progress Series*, 373: 265-273.
- Arntz, W. E., Brey, T., & Gallardo, V. A. 1994. Antarctic zoobenthos. *Oceanography and Marine Biology: An Annual Review*, 32: 251-303.

- Aronson, R. B., Thatje, S., Clarke, A., Peck, L. S., Blake, D. B., Wilga, C. D., & Seibel, B. A. 2007. Climate change and invasibility of the Antarctic benthos. *Annual Review of Ecology, Evolution and Systematics*, 38: 129-154.
- Asnaghi, V., Mangialajo, L., Gattuso, J.-P., Francour, P., Privitera, D., & Chiantore, M. 2014. Effects of ocean acidification and diet on thickness and carbonate elemental composition of the test of juvenile sea urchins. *Marine Environmental Research*, 93: 78-84.
- Baird, M. J., Lee, D. E., & Lamare, M. D. 2013. Reproduction and growth of the terebratulid brachiopod *Liothyrella neozelanica* Thomson, 1918 from Doubtful Sound, New Zealand. *The Biological Bulletin*, 225: 125-136.
- Barnes, D. K. A., & Peck, L. S. 1996. Epibiota and attachment substrata of deep-water brachiopods from Antarctica and New Zealand. *Philosophical Transactions of the Royal Society of London, Series B: Biological Sciences*, 351: 677-687.
- Barry, J. P., Lovera, C., Buck, K. R., Peltzer, E. T., Taylor, J. R., Walz, P., Whaling, P. J., & Brewer, P. G. 2014. Use of a free ocean CO<sub>2</sub> enrichment (FOCE) system to evaluate the effects of ocean acidification on the foraging behavior of a deep-sea urchin. *Environmental Science & Technology*, 48: 9890-9897.
- Barry, J. P., Tyrell, T., Hansson, L., Plattner, G. K., & Gattuso, J.-P. 2010. Atmospheric CO<sub>2</sub> targets for ocean acidification perturbation experiments. *In: Guide to best practices for ocean acidification research and data reporting*, pp. 53-66. Ed. by U. Riebesell, V. F. Fabry, L. Hansson, & J.-P. Gattuso. Publications Office of the European Union.
- Bates, N. R., & Brand, U. 1991. Environmental and physiological influences on isotopic and elemental compositions of brachiopod shell calcite: Implications for the isotopic evolution of Paleozoic oceans. *Chemical Geology*, 94: 67-78.
- Bednaršek, N., & Ohman, M. D. 2015. Changes in pteropod distributions and shell dissolution across a frontal system in the California Current System. *Marine Ecology Progress Series*, 523: 93-103.
- Beniash, E., Ivanina, A., Lieb, N. S., Kurochkin, I., & Sokolova, I. M. 2010. Elevated level of carbon dioxide affects metabolism and shell formation in oysters *Crassostrea virginica*. *Marine Ecology Progress Series*, 419: 95-108.
- Berge, J. A., Bjerkeng, B., Pettersen, O., Schaanning, M. T., & Oxnevad, S. 2006. Effects of increased sea water concentrations of CO<sub>2</sub> on growth of the bivalve *Mytilus edulis* L. *Chemosphere*, 62: 681-687.

- Bessat, F., & Buigues, D. 2001. Two centuries of variation in coral growth in a massive *Porites* colony from Moorea (French Polynesia): a response of ocean-atmosphere variability from south central Pacific. *Palaeogeography, Palaeoclimatology, Palaeoecology*, 175: 381-392.
- Bickmore, M. G., Lohmann, K. C., & Thayer, C. W. 1994. Intra-annual, seasonal variations in the isotopic and minor element composition of brachiopod calcite (*Terebratalia transversa*). In: Geological Society of America, Abstracts with Programs, p. 421.
- Brand, U., Azmy, K., Bitner, M. A., Logan, A., Zuschin, M., Came, R., & Ruggiero, E. 2013. Oxygen isotopes and MgCO<sub>3</sub> in brachiopod calcite and a new paleotemperature equation. *Chemical Geology*, 359: 23-31.
- Brand, U., Logan, A., Hiller, N., & Richardson, J. R. 2003. Geochemistry of modern brachiopods: applications and implications for oceanography and paleoceanography. *Chemical Geology*, 198: 305-334.
- Bray, L., Pancucci-Papadopoulou, M. A., & Hall-Spencer, J. M. 2014. Sea urchin response to rising *p*CO<sub>2</sub> shows ocean acidification may fundamentally alter the chemistry of marine skeletons. *Mediterranean Marine Science*, 15: 510-519.
- Brewer, P. G. 1997. Ocean chemistry of the fossil fuel CO<sub>2</sub> signal: the haline signal of “business as usual”. *Geophysical Research Letters*, 24: 1367-1369.
- Brönmark, C., Lakowitz, T., & Hollander, J. 2011. Predator-induced morphological plasticity across local populations of a freshwater snail. *PLoS ONE*, 6: e21773.
- Buening, N., & Carlson, S. J. 1992. Geochemical investigation of growth in selected Recent articulate brachiopods. *Lethaia*, 25: 331-345.
- Busenberg, E., & Plummer, L. N. 1985. Kinetic and thermodynamic factors controlling the distribution of SO<sub>4</sub><sup>2-</sup> and Na<sup>+</sup> in calcites and selected aragonites. *Geochimica et Cosmochimica Acta*, 49: 713-725.
- Byrne, M. 2011. Impact of ocean warming and ocean acidification on marine invertebrate life history stages: vulnerabilities and potential for persistence in a changing ocean. *Oceanography and Marine Biology: An Annual Review*, 49: 1-42.
- Byrne, M., & Przeslawski, R. 2013. Multistressor impacts of warming and acidification of the ocean on marine invertebrates' life histories. *Integrative and Comparative Biology*, 53: 582-596.
- Cadée, G. C. 1999. Shell damage and shell repair in the Antarctic limpet *Nacella concinna* from King George Island. *Journal of Sea Research*, 41: 149-161.
- Caldeira, K., & Wickett, M. E. 2003. Anthropogenic carbon and ocean pH. *Nature*, 425: 365.

- Caldeira, K., & Wickett, M. E. 2005. Ocean model predictions of chemistry changes from carbon dioxide emissions to the atmosphere and ocean. *Journal of Geophysical Research*, 110: C09S04.
- Carpenter, S. J., & Lohmann, K. C. 1992. Sr/Mg ratios of modern marine calcite: Empirical indicators of ocean chemistry and precipitation rate. *Geochimica et Cosmochimica Acta*, 56: 1837-1849.
- Chave, K. E. 1952. A solid solution between calcite and dolomite. *The Journal of Geology*, 60: 190-192.
- Chuang, S. H. 1996. The embryonic, larval and early postlarval development of the terebratellid brachiopod *Calloria inconspicua* (Sowerby). *Journal of the Royal Society of New Zealand*, 26: 119-137.
- Ciais, P., Gasser, T., Paris, J. D., Caldeira, K., Raupach, M. R., Canadell, J. G., Patwardhan, A., Friedlingstein, P., Piao, S. L., & Gitz, V. 2013. Attributing the increase in atmospheric CO<sub>2</sub> to emitters and absorbers. *Nature Climate Change*, 3: 926-930.
- Clark, D., Lamare, M., & Barker, M. 2009. Response of sea urchin pluteus larvae (Echinodermata: Echinoidea) to reduced seawater pH: a comparison among a tropical, temperate, and a polar species. *Marine Biology*, 156: 1125-1137.
- Clark, M. S., Sommer, U., Sihra, J. K., Thorne, M. A., Morley, S. A., King, M., Viant, M. R., & Peck, L. S. 2016. Biodiversity in marine invertebrate responses to acute warming revealed by a comparative multi-omics approach. *Global Change Biology*: doi: 10.1111/gcb.13357.
- Clarke, A. 1990. Temperature and evolution: Southern Ocean cooling and the Antarctic marine fauna. *In: Antarctic ecosystems*, pp. 9-22. Springer Berlin Heidelberg.
- Clarke, A. 1993. Seasonal acclimatisation and latitudinal compensation in metabolism: Do they exist? *Functional Ecology*, 7: 139-149.
- Clarke, A., Meredith, M. P., Wallace, M. I., Brandon, M. A., & Thomas, D. N. 2008. Seasonal and interannual variability in temperature, chlorophyll and macronutrients in northern Marguerite Bay, Antarctica. *Deep-Sea Research Part II: Topical Studies in Oceanography*, 55: 1988-2006.
- Clarkson, M. O., Kasemann, S. A., Wood, R. A., Lenton, T. M., Daines, S. J., Richoz, S., Ohnemueeller, F., Meixner, A., Poulton, S. W., & Tipper, E. T. 2015. Ocean acidification and the Permo-Triassic mass extinction. *Science*, 348: 229-232.
- Cohen, A. L., & McConnaughey, T. A. 2003. Geochemical perspectives on coral mineralization. *Reviews in Mineralogy & Geochemistry*, 54: 151-187.

- Cohen, A. L., McCorkle, D. C., de Putron, S., Gaetani, G. A., & Rose, K. A. 2009. Morphological and compositional changes in the skeletons of new coral recruits reared in acidified seawater: Insights into the biomineralization response to ocean acidification. *Geochemistry, Geophysics, Geosystems*, 10: Q07005.
- Cohen, B. L., Bitner, M. A., Harper, E. M., Lee, D. E., Mutschke, E., & Sellanes, J. 2011. Vicariance and convergence in Magellanic and New Zealand long-looped brachiopod clades (Pan-Brachiopoda: Terebratelloidea). *Zoological Journal of the Linnean Society*, 162: 631-645.
- Coleman, D. W., Byrne, M., & Davis, A. R. 2014. Molluscs on acid: gastropod shell repair and strength in acidifying oceans. *Marine Ecology Progress Series*, 509: 203-211.
- Collins, S., Rost, B., & Rynearson, T. A. 2014. Evolutionary potential of marine phytoplankton under ocean acidification. *Evolutionary Applications*, 7: 140-155.
- Comeau, S., Carpenter, R. C., Lantz, C. A., & Edmunds, P. J. 2014. Ocean acidification accelerates dissolution of experimental coral reef communities. *Biogeosciences Discussions*, 11: 12323-12339.
- Cooper, G. A., & Lee, D. E. 1993. *Calloria*, a replacement name for the Recent brachiopod genus *Waltonia* from New Zealand. *Journal of the Royal Society of New Zealand*, 23: 257-270.
- Copper, P. 1996. Brachiopods, A. A. Balkema Publishers, Rotterdam, Netherlands. 356 pp.
- Cornwall, C. E., Boyd, P. W., McGraw, C. M., Hepburn, C. D., Pilditch, C. A., Morris, J. N., Smith, A. M., & Hurd, C. L. 2014. Diffusion boundary layers ameliorate the negative effects of ocean acidification on the temperate coralline macroalga *Arthrocardia corymbosa*. *PLoS ONE*, 9: e97235.
- Courtney, T., Westfield, I., & Ries, J. B. 2013. CO<sub>2</sub>-induced ocean acidification impairs calcification in the tropical urchin *Echinometra viridis*. *Journal of Experimental Marine Biology and Ecology*, 440: 169-175.
- Cowen, R. 1966. The distribution of punctae on the brachiopod shell. *Geological Magazine*, 103: 269-275.
- Cross, E. L., Peck, L. S., & Harper, E. M. 2015. Ocean acidification does not impact shell growth or repair of the Antarctic brachiopod *Liothyrella uva* (Broderip, 1833). *Journal of Experimental Marine Biology and Ecology*, 462: 29-35.
- Cross, E. L., Peck, L. S., Lamare, M. D., & Harper, E. M. 2016. No ocean acidification effects on shell growth and repair in the New Zealand brachiopod *Calloria inconspicua* (Sowerby, 1846). *ICES Journal of Marine Science*, 73: 920-926.

- Cummings, V., Hewitt, J., Van Rooyen, A., Currie, K., Beard, S., Thrush, S., Norkko, J., Barr, N., Heath, P., Halliday, N. J., Sedcole, R., Gomez, A., McGraw, C., & Metcalf, V. 2011. Ocean acidification at high latitudes: potential effects on functioning of the Antarctic bivalve *Laternula elliptica*. *PLoS ONE*, 6: e16069.
- Cunningham, S. C., Smith, A. M., & Lamare, M. D. 2016. The effects of elevated  $p\text{CO}_2$  on growth, shell production and metabolism of cultured juvenile abalone, *Haliotis iris*. *Aquaculture Research*, 47: 2375-2392.
- Curry, G. B. 1983a. Ecology of the Recent deep-water rhynchonellid brachiopod *Cryptopora* from the Rockall Trough. *Palaeogeography, Palaeoclimatology, Palaeoecology*, 44: 93-102.
- Curry, G. B. 1983b. Microborings in Recent brachiopods and the functions of caeca. *Lethaia*, 16: 119-127.
- Curry, G. B., & Ansell, A. D. 1986. Tissue mass in living brachiopods. In: Les brachiopodes fossiles et actuels: actes du 1er Congrès international sur les brachiopodes, Brest 1985. Series: Collection "Biostratigraphie du Paléozoïque" pp. 231-241. Ed. by P. R. Racheboeuf, & C. C. Emig. Université de Bretagne Occidentale, Brest, Bretagne, France.
- Curry, G. B., Ansell, A. D., James, M., & Peck, L. S. 1989. Physiological constraints on living and fossil brachiopods. *Earth and Environmental Science Transactions of the Royal Society of Edinburgh*, 80: 255-262.
- Cusack, M., Dauphin, Y., Chung, P., Pérez-Huerta, A., & Cuif, J. P. 2008. Multiscale structure of calcite fibres of the shell of the brachiopod *Terebratulina retusa*. *Journal of Structural Biology*, 164: 96-100.
- Dawson, E. W. 1991. The systematics and biogeography of the living Brachiopoda of New Zealand. In: Brachiopods through time, pp. 431-437. Ed. by D. I. MacKinnon, D. E. Lee, & J. D. Campbell. A. A. Balkema, Rotterdam.
- Dickson, A. G., & Millero, F. J. 1987. A comparison of the equilibrium-constants for the dissociation of carbonic-acid in seawater media. *Deep-Sea Research Part A Oceanographic Research Papers*, 34: 1733-1743.
- Dickson, A. G., Sabine, C. L., & Christian, J. R. 2007. Guide to best practices for Ocean  $\text{CO}_2$  Measurements. IOCCP report No. 8.
- Doherty, P. J. 1979. A demographic study of a subtidal population of the New Zealand articulate brachiopod *Terebratella inconspicua*. *Marine Biology*, 52: 331-342.

- Doney, S. C., Fabry, V. J., Feely, R. A., & Kleypas, J. A. 2009. Ocean acidification: the other CO<sub>2</sub> problem. *Annual Review of Marine Science*, 1: 169-192.
- Doney, S. C., & Schimel, D. S. 2007. Carbon and climate system coupling on timescales from the Precambrian to the Anthropocene. *Annual Review of Environment and Resources*, 32: 31-66.
- Dubois, P. 2014. The skeleton of postmetamorphic echinoderms in a changing world. *The Biological Bulletin*, 226: 223-236.
- Dupont, S., & Pörtner, H. 2013. Marine science: Get ready for ocean acidification. *Nature*, 498: 429-429.
- Emig, C. C. 2009. Brachiopods. In: Marine Biodiversity of Costa Rica, Central America. Monographiae Biologicae. Ed. by I. S. Wehrtmann, & J. Cortés. Springer, Netherlands.
- Enochs, I. C., Manzello, D. P., Donham, E. M., Kolodziej, G., Okano, R., Johnston, L., Young, C., Iguel, J., Edwards, C. B., Fox, M. D., Valentino, L., Johnson, S., Benavente, D., Clark, S. J., Carlton, R., Burton, T., Eynaud, Y., & Price, N. N. 2015. Shift from coral to macroalgae dominance on a volcanically acidified reef. *Nature Climate Change*, 5: 1083-1089.
- Ericson, J. A., Ho, M. A., Miskelly, A., King, C. K., Virtue, P., Tilbrook, B., & Byrne, M. 2012. Combined effects of two ocean change stressors, warming and acidification, on fertilization and early development of the Antarctic echinoid *Sterechinus neumayeri*. *Polar Biology*, 35: 1027-1034.
- Fabricius, K. E., Langdon, C., Uthicke, S., Humphrey, C., Noonan, S., De'ath, G., Okazaki, R., Muehllehner, N., Glas, M. S., & Lough, J. M. 2011. Losers and winners in coral reefs acclimatized to elevated carbon dioxide concentrations. *Nature Climate Change*, 1: 165-169.
- Fabry, V. J., McClintock, J. B., Mathis, J. T., & Grebmeier, J. M. 2009. Ocean acidification at high latitudes: the bellwether. *Oceanography*, 22: 160-171.
- Fabry, V. J., Seibel, B. A., Feely, R. A., & Orr, J. C. 2008. Impacts of ocean acidification on marine fauna and ecosystem processes. *ICES Journal of Marine Science*, 65: 414-432.
- Feely, R. A., Sabine, C. L., Lee, K., Berelson, W., Kleypas, J., Fabry, V. J., & Millero, F. J. 2004. Impact of anthropogenic CO<sub>2</sub> on the CaCO<sub>3</sub> system in the oceans. *Science*, 305: 362-366.

- Findlay, H. S., Kendall, M. A., Spicer, J. I., Turley, C., & Widdicombe, S. 2008. Novel microcosm system for investigating the effects of elevated carbon dioxide and temperature on intertidal organisms. *Aquatic Biology*, 3: 51-62.
- Fisher, J. A., Rhile, E. C., Liu, H., & Petraitis, P. S. 2009. An intertidal snail shows a dramatic size increase over the past century. *Proceedings of the National Academy of Sciences of the United States of America*, 106: 5209-5212.
- Fitzer, S. C., Chung, P., Maccherozzi, F., Dhési, S. S., Kamenos, N. A., Phoenix, V. R., & Cusack, M. 2016. Biomineral shell formation under ocean acidification: a shift from order to chaos. *Scientific Reports*, 6: 21076.
- Fitzer, S. C., Cusack, M., Phoenix, V. R., & Kamenos, N. A. 2014b. Ocean acidification reduces the crystallographic control in juvenile mussel shells. *Journal of Structural Biology*, 188: 39-45.
- Fitzer, S. C., Phoenix, V. R., Cusack, M., & Kamenos, N. A. 2014a. Ocean acidification impacts mussel control on biomineralisation. *Scientific Reports*, 4: 6218.
- Fitzer, S. C., Vittert, L., Bowman, A., Kamenos, N. A., Phoenix, V. R., & Cusack, M. 2015a. Ocean acidification and temperature increase impact mussel shell shape and thickness: problematic for protection? *Ecology and Evolution*, 5: 4875-4884.
- Fitzer, S. C., Zhu, W., Tanner, K. E., Phoenix, V. R., Kamenos, N. A., & Cusack, M. 2015b. Ocean acidification alters the material properties of *Mytilus edulis* shells. *Journal of the Royal Society Interface*, 12: 20141227.
- Form, A. U., & Riebesell, U. 2012. Acclimation to ocean acidification during long-term CO<sub>2</sub> exposure in the cold-water coral *Lophelia pertusa*. *Global Change Biology*, 18: 843-853.
- Forster, P., Ramaswamy, V., Artaxo, P., Berntsen, T., Betts, R., Fahey, D. W., Haywood, J., Lean, J., Lowe, D. C., Myhre, G., Nganga, J., Prinn, R., Raga, G., Schulz, M., & Van Dorland, R. 2007. Changes in atmospheric constituents and in radiative forcing. *In: Climate Change 2007: the Physical Science Basis. Contribution of Working Group I to the Fourth Assessment Report of the Intergovernmental Panel on Climate Change*, pp. 129–234. Ed. by S. Solomon, D. Qin, M. Manning, Z. Chen, M. Marquis, K. B. Averyt, M. Tignor, & H. L. Miller. Cambridge University Press, Cambridge.
- Foster, M. W. 1974. Recent Antarctic and subantarctic brachiopods, American Geophysical Union, Washington D.C., USA. 189 pp.
- Freeman, A. S., & Byers, J. E. 2006. Divergent induced responses to an invasive predator in marine mussel populations. *Science*, 313: 831-834.

- Garibotti, I. A., Vernet, M., & Ferrario, M. E. 2005. Annually recurrent phytoplanktonic assemblages during summer in the seasonal ice zone west of the Antarctic Peninsula (Southern Ocean). *Deep-sea Research Part I: Oceanographic Research Papers*, 52: 1823-1841.
- Garibotti, I. A., Vernet, M., Ferrario, M. E., Smith, R. C., Ross, R. M., & Quentin, L. B. 2003. Phytoplankton spatial distribution patterns along the western Antarctic Peninsula (Southern Ocean). *Marine Ecology Progress Series*, 261: 21-39.
- Gattuso, J.-P., Frankignoulle, M., Bourge, I., Romaine, S., & Buddemeier, R. W. 1998. Effect of calcium carbonate saturation of seawater on coral calcification. *Global and Planetary Change*, 18: 37-46.
- Gattuso, J.-P., & Hansson, L. 2011. *Ocean Acidification*, Oxford University Press, Oxford.
- Gattuso, J.-P., Kirkwood, W., Barry, J. P., Cox, E., Gazeau, F., Hansson, L., Hendriks, I., Kline, D. I., Mahacek, P., Martin, S., McElhany, P., Peltzer, E. T., Reeve, J., Roberts, D., Saderne, V., Tait, K., Widdicombe, S., & Brewer, P. G. 2014. Free-ocean CO<sub>2</sub> enrichment (FOCE) systems: present status and future developments. *Biogeosciences*, 11: 4057-4075.
- Gattuso, J.-P., Mach, K. J., & Morgan, G. 2013. Ocean acidification and its impacts: an expert survey. *Climatic Change*, 117: 725-738.
- Gazeau, F., Parker, L. M., Comeau, S., Gattuso, J.-P., O'Connor, W. A., Martin, S., Pörtner, H.-O., & Ross, P. M. 2013. Impacts of ocean acidification on marine shelled molluscs. *Marine Biology*, 160: 2207-2245.
- Ghedini, G., & Connell, S. D. 2016. Organismal homeostasis buffers the effects of abiotic change on community dynamics. *Ecology*: doi: 10.1002/ecy.1488.
- Gobler, C. J., DePasquale, E. L., Griffith, A. W., & Baumann, H. 2014. Hypoxia and acidification have additive and synergistic negative effects on the growth, survival, and metamorphosis of early life stage bivalves. *PLoS ONE*, 9: e83648.
- Goetz, A. J., Griesshaber, E., Neuser, R. D., Lüter, C., Hühner, M., Harper, E. M., & Schmahl, W. W. 2009. Calcite morphology, texture and hardness in the distinct layers of rhynchonelliform brachiopod shells. *European Journal of Mineralogy*, 21: 303-315.
- Goffredo, S., Prada, F., Caroselli, E., Capaccioni, B., Zaccanti, F., Pasquini, L., Fantazzini, P., Fermani, S., Reggi, M., Levy, O., Fabricius, K. E., Dubinsky, Z., & Falini, G. 2014. Biomineralization control related to population density under ocean acidification. *Nature Climate Change*, 4: 593-597.

- Gould, S. J., & Calloway, C. B. 1980. Clams and brachiopods - Ships that pass in the night. *Paleobiology*, 6: 383-396.
- Grange, K. R., Singleton, R. I., Richardson, J. R., Hill, P. J., & Main, W. d. 1981. Shallow rock-wall biological associations of some southern fiords of New Zealand. *New Zealand Journal of Zoology*, 8: 209-227.
- Grange, K. R., & Singleton, R. J. 1988. Population structure of black coral, *Antipathes aperta*, in the southern fiords of New Zealand. *New Zealand Journal of Zoology*, 15: 481-489.
- Graus, R. R. 1974. Latitudinal trends in the shell characteristics of marine gastropods. *Lethaia*, 7: 303-314.
- Greig, M. J., Ridgway, N. M., & Shakespeare, B. S. 1988. Sea surface temperature variations at coastal sites around New Zealand. *New Zealand Journal of Marine and Freshwater Research*, 22: 391-400.
- Griesshaber, E., Neuser, R. D., Brand, U., & Schmahl, W. W. 2008. Texture and microstructure of modern rhynchonellide brachiopod shells - an ontogenetic study. *Applications of Texture Analysis: Ceramic Transactions*, 201: 605-617.
- Griesshaber, E., Schmahl, W. W., Neuser, R., Pettke, T., Blüm, M., Mutterlose, J., & Brand, U. 2007. Crystallographic texture and microstructure of terebratulide brachiopod shell calcite: An optimized materials design with hierarchical architecture. *American Mineralogist*, 92: 722-734.
- Grossman, E. L., Mii, H.-S., Zhang, C., & Yancey, T. E. 1996. Chemical variation in Pennsylvanian brachiopod shells - diagenetic, taxonomic, microstructural, and seasonal effects. *Journal of Sedimentary Research*, 66: 1011-1022.
- Guinotte, J. M., & Fabry, V. J. 2008. Ocean acidification and its potential effects on marine ecosystems. *Annals of the New York Academy of Sciences*, 1134: 320-342.
- Hahn, S., Griesshaber, E., Schmahl, W. W., Neuser, R. D., Ritter, A.-C., Hoffmann, R., Buhl, D., Niedermayr, A., Geske, A., Immenhauser, A., & Pufahl, P. 2014. Exploring aberrant bivalve shell ultrastructure and geochemistry as proxies for past sea water acidification. *Sedimentology*, 61: 1625-1658.
- Hahn, S., Rodolfo-Metalpa, R., Griesshaber, E., Schmahl, W. W., Buhl, D., Hall-Spencer, J. M., Baggini, C., Fehr, K. T., & Immenhauser, A. 2012. Marine bivalve shell geochemistry and ultrastructure from modern low pH environments: environmental effect versus experimental bias. *Biogeosciences*, 9: 1897-1914.

- Hall-Spencer, J. M., Rodolfo-Metalpa, R., Martin, S., Ransome, E., Fine, M., Turner, S. M., Rowley, S. J., Tedesco, D., & Buia, M. C. 2008. Volcanic carbon dioxide vents show ecosystem effects of ocean acidification. *Nature*, 454: 96-99.
- Hardy, N. A., & Byrne, M. 2014. Early development of congeneric sea urchins (*Heliocidaris*) with contrasting life history modes in a warming and high CO<sub>2</sub> ocean. *Marine Environmental Research*, 102: 78-87.
- Harper, E. M. 1997. The molluscan periostracum: an important constraint in bivalve evolution. *Palaeontology*, 40: 71-97.
- Harper, E. M. 2000. Are calcitic layers an effective adaptation against shell dissolution in the Bivalvia? *Journal of Zoology*, 251: 179-186.
- Harper, E. M., Clark, M. S., Hoffman, J. I., Philipp, E. E., Peck, L. S., & Morley, S. A. 2012. Iceberg scour and shell damage in the Antarctic bivalve *Laternula elliptica*. *PLoS ONE*, 7: e46341.
- Harper, E. M., & Peck, L. S. 2016. Latitudinal and depth gradients in marine predation pressure. *Global Ecology and Biogeography*, 25: 670-678.
- Harper, E. M., Peck, L. S., & Hendry, K. R. 2009. Patterns of shell repair in articulate brachiopods indicate size constitutes a refuge from predation. *Marine Biology*, 156: 1993-2000.
- Harper, E. M., Robinson, J. H., & Lee, D. E. 2011. Drill hole analysis reveals evidence of targeted predation on modern brachiopods. *Palaeogeography, Palaeoclimatology, Palaeoecology*, 305: 162-171.
- Hazan, Y., Wangensteen, O. S., & Fine, M. 2014. Tough as a rock-boring urchin: adult *Echinometra* sp. EE from the Red Sea show high resistance to ocean acidification over long-term exposures. *Marine Biology*, 161: 2531-2545.
- Hennige, S. J., Wicks, L. C., Kamenos, N. A., Bakker, D. C. E., Findlay, H. S., Dumousseaud, C., & Roberts, J. M. 2014. Short-term metabolic and growth responses of the cold-water coral *Lophelia pertusa* to ocean acidification. *Deep Sea Research Part II: Topical Studies in Oceanography*, 99: 27-35.
- Hiebenthal, C., Philipp, E. E. R., Eisenhauer, A., & Wahl, M. 2012. Effects of seawater pCO<sub>2</sub> and temperature on shell growth, shell stability, condition and cellular stress of Western Baltic Sea *Mytilus edulis* (L.) and *Arctica islandica* (L.). *Marine Biology*, 160: 2073-2087.

- Hiller, N., Robinson, J. H., & Lee, D. E. 2008. The micromorphic brachiopod *Argyrotheca* (Terebratulida: Megathyridoidea) in Australia and New Zealand. *Proceedings of the Royal Society of Victoria*, 120: 167-183.
- Hoegh-Guldberg, O., Mumby, P. J., Hooten, A. J., Steneck, R. S., Greenfield, P., Gomez, E., Harvell, C. D., Sale, P. F., Edwards, A. J., Caldeira, K., Knowlton, N., Eakin, C. M., Iglesias-Prieto, R., Muthiga, N., Bradbury, R. H., Dubi, A., & Hatziolos, M. E. 2007. Coral reefs under rapid climate change and ocean acidification. *Science*, 318: 1737-1742.
- Hoeksema, B. W., van der Land, J., van der Meij, S. E. T., van Ofwegen, L. P., Reijnen, B. T., van Soest, R. W. M., & de Voogd, N. J. 2011. Unforeseen importance of historical collections as baselines to determine biotic change of coral reefs: the Saba Bank case. *Marine Ecology*, 32: 135-141.
- Hofmann, G. E., Barry, J. P., Edmunds, P. J., Gates, R. D., Hutchins, D. A., Klinger, T., & Sewell, M. A. 2010. The effect of ocean acidification on calcifying organisms in marine ecosystems: An organism-to-ecosystem perspective. *Annual Review of Ecology, Evolution, and Systematics*, 41: 127-147.
- Hönisch, B., Ridgwell, A., Schmidt, D. N., Thomas, E., Gibbs, S. J., Sluijs, A., Zeebe, R. E., Kump, L., Martindale, R. C., Greene, S. E., Kiessling, W., Ries, J., & Zachos, J. C. 2012. The geological record of ocean acidification. *Science*, 335: 1058-1063.
- Hyun, B., Choi, K.-H., Jang, P.-G., Jang, M.-C., Lee, W.-J., Moon, C.-H., & Shin, K. 2014. Effects of increased CO<sub>2</sub> and temperature on the growth of four diatom species (*Chaetoceros debilis*, *Chaetoceros didymus*, *Skeletonema costatum* and *Thalassiosira nordenskiöldii*) in laboratory experiments. *Journal of Environmental Science International*, 23: 1003-1012.
- IPCC 2013. Climate Change 2013: The Physical Science Basis. In: Working Group I Contribution to the Fifth Assessment Report of the Intergovernmental Panel on Climate Change, p. 1552. Ed. by T. F. Stocker, D. Qin, G.-K. Plattner, M. Tignor, S. K. Allen, J. Boschung, A. Nauels, Y. Xia, V. Bex, & P. M. Midgley. Cambridge, United Kingdom and New York, NY, USA.
- James, M. A., Ansell, A. D., Collins, M. J., Curry, G. B., Peck, L. S., & Rhodes, M. C. 1992. Biology of Living Brachiopods. In: *Advances in Marine Biology*, pp. 175-387.
- James, M. A., Ansell, A. D., & Curry, G. B. 1991. Functional morphology of the gonads of the articulate brachiopod *Terebratulina retusa*. *Marine Biology*, 111: 401-410.

- Kamenos, N. A., Burdett, H. L., Aloisio, E., Findlay, H. S., Martin, S., Longbone, C., Dunn, J., Widdicombe, S., & Calosi, P. 2013. Coralline algal structure is more sensitive to rate, rather than the magnitude, of ocean acidification. *Global Change Biology*, 19: 3621-3628.
- Kelly, M. W., & Hofmann, G. E. 2013. Adaptation and the physiology of ocean acidification. *Functional Ecology*, 27: 980-990.
- Kinsman, D. J. J., & Holland, H. D. 1969. The co-precipitation of cations with CaCO<sub>3</sub>-IV. The co-precipitation of Sr<sup>2+</sup> with aragonite between 16° and 96°C. *Geochimica et Cosmochimica Acta*, 33: 1-17.
- Kirkwood, W. J., Walz, P. M., Peltzer, E. T., Barry, J. P., Herlien, R. A., Headley, K. L., Key, C., Matsumoto, G. I., Maughan, T., O'Reilly, T. C., Salamy, K. A., Shane, F., & Brewer, P. G. 2015. Design, construction, and operation of an actively controlled deep-sea CO<sub>2</sub> enrichment experiment using a cabled observatory system. *Deep Sea Research Part I: Oceanographic Research Papers*, 97: 1-9.
- Kline, D. I., Teneva, L., Schneider, K., Miard, T., Chai, A., Marker, M., Headley, K., Opdyke, B., Nash, M., Valetich, M., Caves, J. K., Russell, B. D., Connell, S. D., Kirkwood, B. J., Brewer, P., Peltzer, E., Silverman, J., Caldeira, K., Dunbar, R. B., Koseff, J. R., Monismith, S. G., Mitchell, B. G., Dove, S., & Hoegh-Guldberg, O. 2012. A short-term in situ CO<sub>2</sub> enrichment experiment on Heron Island (GBR). *Scientific Reports*, 2: 413.
- Ko, G. W., Dineshram, R., Campanati, C., Chan, V. B., Havenhand, J., & Thiyagarajan, V. 2014. Interactive effects of ocean acidification, elevated temperature, and reduced salinity on early-life stages of the pacific oyster. *Environmental Science & Technology*, 48: 10079-10088.
- Kroeker, K. J., Gaylord, B., Hill, T. M., Hosfelt, J. D., Miller, S. H., & Sanford, E. 2014. The role of temperature in determining species' vulnerability to ocean acidification: A case study using *Mytilus galloprovincialis*. *PLoS ONE*, 9: e100353.
- Kroeker, K. J., Kordas, R. L., Crim, R., Hendriks, I. E., Ramajo, L., Singh, G. S., Duarte, C. M., & Gattuso, J.-P. 2013. Impacts of ocean acidification on marine organisms: quantifying sensitivities and interaction with warming. *Global Change Biology*, 19: 1884-1896.
- Kurihara, H., Shimode, S., & Shirayama, Y. 2004. Sub-lethal effects of elevated concentration of CO<sub>2</sub> on planktonic copepods and sea urchins. *Journal of Oceanography*, 60: 743-750.

- Landes, A., & Zimmer, M. 2012. Acidification and warming affect both a calcifying predator and prey, but not their interaction. *Marine Ecology Progress Series*, 450: 1-10.
- LaVigne, M., Hill, T. M., Sanford, E., Gaylord, B., Russell, A. D., Lenz, E. A., Hosfelt, J. D., & Young, M. K. 2013. The elemental composition of purple sea urchin (*Strongylocentrotus purpuratus*) calcite and potential effects of  $p\text{CO}_2$  during early life stages. *Biogeosciences*, 10: 3465-3477.
- Le Quéré, C., Andres, R. J., Boden, T., Conway, T., Houghton, R. A., House, J. I., Marland, G., Peters, G. P., van der Werf, G. R., Ahlström, A., Andrew, R. M., Bopp, L., Canadell, J. G., Ciais, P., Doney, S. C., Enright, C., Friedlingstein, P., Huntingford, C., Jain, A. K., Jourdain, C., Kato, E., Keeling, R. F., Klein Goldewijk, K., Levis, S., Levy, P., Lomas, M., Poulter, B., Raupach, M. R., Schwinger, J., Sitch, S., Stocker, B. D., Viovy, N., Zaehle, S., & Zeng, N. 2013. The global carbon budget 1959–2011. *Earth System Science Data*, 5: 165-185.
- Lee, D. E. 1991. Aspects of the ecology and distribution of the living Brachiopoda of New Zealand. In: *Brachiopods Through Time*, pp. 273-279. Ed. by D. I. MacKinnon, D. E. Lee, & J. D. Campbell. A.A Balkema Publishers, Rotterdam, Netherlands.
- Lee, D. E. 2008. The terebratulides: the supreme brachiopod survivors. *Fossils and Strata*, 54: 241-249.
- Lee, D. E., Robinson, J. H., Witman, J. D., Copeland, S. E., Harper, E. M., Smith, F., & Lamare, M. D. 2010. Observations on recruitment, growth and ecology in a diverse living brachiopod community, Doubtful Sound, Fiordland, New Zealand. *Special Papers in Palaeontology*, 84: 177-191.
- Lee, D. E., & Wilson, J. B. 1979. Cenozoic and recent rhynchonellide brachiopods of New Zealand: Systematics and variation in the genus *Notosaria*. *Journal of the Royal Society of New Zealand*, 9: 437-463.
- Lewis, C., Ellis, R. P., Vernon, E., Elliot, K., Newbatt, S., & Wilson, R. W. 2016. Ocean acidification increases copper toxicity differentially in two key marine invertebrates with distinct acid-base responses. *Scientific Reports*, 6: 21554.
- Lewis, D. E., & Cerrato, R. M. 1997. Growth uncoupling and the relationship between shell growth and metabolism in the soft shell clam *Mya arenaria*. *Marine Ecology Progress Series*, 158: 177-189.
- Lewis, E., Wallace, D. W. R., & Allison, L. J. 1998. Program developed for  $\text{CO}_2$  system calculations, Carbon Dioxide Information Analysis Center, Oak Ridge National Laboratory, US Department of Energy, Oak Ridge, Tennessee, US.

- Lister, A. M. 2011. Natural history collections as sources of long-term datasets. *Trends in Ecology & Evolution*, 26: 153-154.
- Lough, J. M., & Barnes, D. J. 1997. Several centuries of variation in skeletal extension, density and calcification in massive *Porites* colonies from the Great Barrier Reef: A proxy for seawater temperature and a background of variability against which to identify unnatural change. *Journal of Experimental Marine Biology and Ecology*, 211: 29-67.
- Lough, J. M., & Barnes, D. J. 2000. Environmental controls on growth of the massive coral *Porites*. *Journal of Experimental Marine Biology and Ecology*, 245: 225-243.
- Lowenstam, H. A. 1961. Mineralogy,  $O^{18}/O^{16}$  ratios, and strontium and magnesium contents of Recent and fossil brachiopods and their bearing on the history of the oceans. *The Journal of Geology*, 69: 241-260.
- Lüter, C. 1998. Note: Embryonic and larval development of *Calloria inconspicua* (Brachiopoda, Terebratulidae). *Journal of the Royal Society of New Zealand*, 28: 165-167.
- MacFarlan, D. A. B., Bradshaw, M. A., Campbell, H. J., Cooper, R. A., Lee, D. E., MacKinnon, D. I., Waterhouse, J. B., Wright, A. J., & Robinson, J. H. 2009. Phylum Brachiopoda – Lampshells. In: *The New Zealand inventory of biodiversity*, vol. 1. Kingdom Animalia: Radiata, Lophotrochozoa, and Deuterostomia., p. 566. Ed. by D. P. Gordon. Canterbury University Press, Christchurch.
- Mackenzie, C. L., Ormondroyd, G. A., Curling, S. F., Ball, R. J., Whiteley, N. M., & Malham, S. K. 2014. Ocean warming, more than acidification, reduces shell strength in a commercial shellfish species during food limitation. *PLoS ONE*, 9: e86764.
- MacKinnon, D. I., & Williams, A. 1974. Shell structure of terebratulid brachiopods. *Palaeontology*, 17: 179-202.
- Marshall, D. J., Santos, J. H., Leung, K. M., & Chak, W. H. 2008. Correlations between gastropod shell dissolution and water chemical properties in a tropical estuary. *Marine Environmental Research*, 66: 422-429.
- Martin, S., & Gattuso, J.-P. 2009. Response of Mediterranean coralline algae to ocean acidification and elevated temperature. *Global Change Biology*, 15: 2089-2100.
- Martin, S., Rodolfo-Metalpa, R., Ransome, E., Rowley, S., Buia, M.-C., Gattuso, J.-P., & Hall-Spencer, J. 2008. Effects of naturally acidified seawater on seagrass calcareous epibionts. *Biology Letters*, 4: 689-692.
- Marubini, F., & Atkinson, M. J. 1999. Effects of lowered pH and elevated nitrate on coral calcification. *Marine Ecology Progress Series*, 188: 117-121.

- McClintock, J. B., Angus, R. A., McDonald, M. R., Amsler, C. D., Catledge, S. A., & Vohra, Y. K. 2009. Rapid dissolution of shells of weakly calcified Antarctic benthic macroorganisms indicates high vulnerability to ocean acidification. *Antarctic Science*, 21: 449-456.
- McConnaughey, T. A., & Falk, R. H. 1991. Calcium-proton exchange during algae calcification. *Biological Bulletin*, 180: 185-195.
- McConnaughey, T. A., & Whelan, J. F. 1997. Calcification generates protons for nutrient and bicarbonate uptake. *Earth-Science Reviews*, 42: 95-117.
- McCulloch, M., Falter, J., Trotter, J., & Montagna, P. 2012. Coral resilience to ocean acidification and global warming through pH up-regulation *Nature Climate Change*, 2: 623-627.
- McDonald, M. R., McClintock, J. B., Amsler, C. D., Rittschof, D., Angus, R. A., Orihuela, B., & Lutostanski, K. 2009. Effects of ocean acidification over the life history of the barnacle *Amphibalanus amphitrite*. *Marine Ecology Progress Series*, 385: 179-187.
- McNeil, B. I., & Matear, R. J. 2008. Southern Ocean acidification: a tipping point at 450-ppm atmospheric CO<sub>2</sub>. *Proceedings of the National Academy of Sciences of the United States of America*, 105: 18860-18864.
- Mehrbach, C., Culberson, C. H., Hawley, J. E., & Pytkowicz, R. M. 1973. Measurement of apparent dissociation constants of carbonic acid in seawater at atmospheric pressure. *Limnology and Oceanography*, 18: 897-907.
- Meidlinger, K., Tyler, P. A., & Peck, L. S. 1998. Reproductive patterns in the Antarctic brachiopod *Liothyrella uva*. *Marine Biology*, 132: 153-162.
- Melzner, F., Stange, P., Trubenbach, K., Thomsen, J., Casties, I., Panknin, U., Gorb, S. N., & Gutowska, M. A. 2011. Food supply and seawater pCO<sub>2</sub> impact calcification and internal shell dissolution in the blue mussel *Mytilus edulis*. *PLoS ONE*, 6: e24223.
- Michaelidis, B., Ouzounis, C., Palaras, A., & Pörtner, H. O. 2005. Effects of long-term moderate hypercapnia on acid-base balance and growth rate in marine mussels *Mytilus galloprovincialis*. *Marine Ecology Progress Series*, 293: 109-118.
- Mii, H.-S., & Grossman, E. L. 1994. Late Pennsylvanian seasonality reflected in the <sup>18</sup>O and elemental composition of a brachiopod shell. *Geology*, 22: 661-664.
- Milano, S., Schöne, B. R., Wang, S., & Müller, W. E. 2016. Impact of high pCO<sub>2</sub> on shell structure of the bivalve *Cerastoderma edule*. *Marine Environmental Research*, 119: 144-155.

- Miles, H., Widdicombe, S., Spicer, J. I., & Hall-Spencer, J. 2007. Effects of anthropogenic seawater acidification on acid-base balance in the sea urchin *Psammechinus miliaris*. *Marine Pollution Bulletin*, 54: 89-96.
- Mitchell, J. F. B., Senior, C. A., & Johns, T. C. 1998. Transient response to increasing greenhouse gases using models with and without flux adjustment, Metrological Office.
- Morse, J. W., Arvidson, R. S., & Lüttge, A. 2007. Calcium carbonate formation and dissolution. *Chemical Reviews*, 107: 342-381.
- Morse, J. W., Mucci, A., & Millero, F. J. 1980. The solubility of calcite and aragonite in seawater of 35‰ salinity at 25°C and atmospheric pressure. *Geochimica et Cosmochimica Acta*, 44: 85-94.
- Mucci, A. 1983. The solubility of calcite and aragonite in seawater at various salinities, temperatures, and one atmosphere total pressure. *American Journal of Science*, 283: 780-799.
- Nagelkerken, I., & Connell, S. D. 2015. Global alteration of ocean ecosystem functioning due to increasing human CO<sub>2</sub> emissions. *Proceedings of the National Academy of Sciences*, 112: 13272-13277.
- Nagelkerken, I., & Munday, P. L. 2015. Animal behaviour shapes the ecological effects of ocean acidification and warming: moving from individual to community-level responses. *Global Change Biology*, 22: 974-989.
- Nickell, L. A., Black, K. D., Hughes, D. J., Overnell, J., Brand, T., Nickell, T. D., Breuer, E., & Martyn Harvey, S. 2003. Bioturbation, sediment fluxes and benthic community structure around a salmon cage farm in Loch Creran, Scotland. *Journal of Experimental Marine Biology and Ecology*, 285-286: 221-233.
- Nicol, D. 1967. Some characteristics of cold-water marine pelecypods. *Journal of Paleontology*, 41: 1330-1340.
- Nienhuis, S., Palmer, A. R., & Harley, C. D. 2010. Elevated CO<sub>2</sub> affects shell dissolution rate but not calcification rate in a marine snail. *Proceedings of the Royal Society of London, Series B: Biological Sciences*, 277: 2553-2558.
- Orr, J. C. 2011. Recent and future changes in ocean carbonate chemistry. *In: Ocean Acidification*, pp. 41-66. Ed. by J.-P. Gattuso, & L. Hansson. Oxford University Press, Oxford.
- Orr, J. C., Fabry, V. J., Aumont, O., Bopp, L., Doney, S. C., Feely, R. A., Gnanadesikan, A., Gruber, N., Ishida, A., Joos, F., Key, R. M., Lindsay, K., Maier-Reimer, E., Matear, R., Monfray, P., Mouchet, A., Najjar, R. G., Plattner, G. K., Rodgers, K. B., Sabine,

- C. L., Sarmiento, J. L., Schlitzer, R., Slater, R. D., Totterdell, I. J., Weirig, M. F., Yamanaka, Y., & Yool, A. 2005. Anthropogenic ocean acidification over the twenty-first century and its impact on calcifying organisms. *Nature*, 437: 681-686.
- Owen, G., & Williams, A. 1969. The caecum of articulate Brachiopoda. *Proceedings of the Royal Society of London. Series B, Biological Sciences*, 172: 187-201.
- Palmer, A. R. 1983. Relative cost of producing skeletal organic matrix versus calcification: Evidence from marine gastropods. *Marine Biology*, 75: 287-292.
- Pan, C.-M., & Watabe, N. 1988. Uptake and transport of shell minerals in *Glottidia pyramidata* Stimpson (Brachiopoda: Inarticulata). *Journal of Experimental Marine Biology and Ecology*, 118: 257-268.
- Parker, L. M., Ross, P. M., O'Connor, W. A., Pörtner, H. O., Scanes, E., & Wright, J. M. 2013. Predicting the response of molluscs to the impact of ocean acidification. *Biology*, 2: 651-692.
- Parkinson, D., Curry, G. B., Cusack, M., & Fallick, A. E. 2005. Shell structure, patterns and trends of oxygen and carbon stable isotopes in modern brachiopod shells. *Chemical Geology*, 219: 193-235.
- Peake, B. M., Walls, D. J., & Gibbs, M. T. 2001. Spatial variations in the levels of nutrients, chlorophyll *a*, and dissolved oxygen in summer and winter in Doubtful Sound, New Zealand. *New Zealand Journal of Marine and Freshwater Research*, 35: 681-694.
- Pearse, J. S., McClintock, J. B., & Bosch, I. 1991. Reproduction of Antarctic benthic marine invertebrates: Tempos, modes and timing. *American Zoologist*, 31: 65-80.
- Peck, L. S. 1989. Temperature and basal metabolism in two Antarctic marine herbivores. *Journal of Experimental Marine Biology and Ecology*, 127: 1-12.
- Peck, L. S. 1992. Body volumes and internal space constraints in articulate brachiopods. *Lethaia*, 25: 383-390.
- Peck, L. S. 1993. The tissues of articulate brachiopods and their value to predators. *Philosophical Transactions of the Royal Society of London, Series B: Biological Sciences*, 339: 17-32.
- Peck, L. S. 1996. Metabolism and feeding in the Antarctic brachiopod *Liothyrella uva*: a low energy lifestyle species with restricted metabolic scope. *Proceedings of the Royal Society B: Biological Sciences*, 263: 223-228.
- Peck, L. S. 2001a. Ecology. *In: Brachiopods ancient and modern: a tribute to G. Arthur Cooper. The Paleontology Society Papers*, pp. 171-183. Ed. by S. Carlson, & M. Sandy, New Haven, CT: Yale University.

- Peck, L. S. 2001b. Physiology. *In: Brachiopods ancient and modern: a tribute to G. Arthur Cooper*. The Paleontology Society Papers, pp. 89-104. Ed. by S. Carlson, & M. Sandy, New Haven, CT: Yale University.
- Peck, L. S. 2008. Brachiopods and climate change. *Earth and Environmental Science Transactions of the Royal Society of Edinburgh*, 98: 451-456.
- Peck, L. S. 2011. Organisms and responses to environmental change. *Marine Genomics*, 4: 237-243.
- Peck, L. S. 2016. A cold limit to adaptation in the sea. *Trends in Ecology & Evolution*, 31: 13-26.
- Peck, L. S., Barnes, D. K. A., & Willmott, J. 2005. Responses to extreme seasonality in food supply: diet plasticity in Antarctic brachiopods. *Marine Biology*, 147: 453-463.
- Peck, L. S., & Brey, T. 1996. Bomb signals in old Antarctic brachiopods. *Nature*, 380: 207-208.
- Peck, L. S., Brockington, S., & Brey, T. 1997. Growth and metabolism in the Antarctic brachiopod *Liothyrella uva*. *Philosophical Transactions of the Royal Society of London. Series B: Biological Sciences*, 352: 851-858.
- Peck, L. S., Clark, M. S., Morley, S. A., Massey, A., & Rossetti, H. 2009. Animal temperature limits and ecological relevance: effects of size, activity and rates of change. *Functional Ecology*, 23: 248-256.
- Peck, L. S., Clark, M. S., Power, D., Reis, J., Batista, F. M., & Harper, E. M. 2015. Acidification effects on biofouling communities: winners and losers. *Global Change Biology*, 21: 1907-1913.
- Peck, L. S., Clarke, A., & Holmes, L. J. 1987a. Size, shape and the distribution of organic matter in the Recent Antarctic brachiopod *Liothyrella uva*. *Lethaia*, 20: 33-40.
- Peck, L. S., Clarke, A., & Holmes, L. J. 1987b. Summer metabolism and seasonal changes in biochemical composition of the Antarctic brachiopod *Liothyrella uva* (Broderip, 1833). *Journal of Experimental Marine Biology and Ecology*, 114: 85-97.
- Peck, L. S., & Conway, L. Z. 2000. The myth of metabolic cold adaptation: oxygen consumption in stenothermal Antarctic bivalves. *Geological Society, London, Special Publications*, 177: 441-450.
- Peck, L. S., & Harper, E. M. 2010. Variation in size of living articulated brachiopods with latitude and depth. *Marine Biology*, 157: 2205-2213.

- Peck, L. S., & Holmes, L. J. 1989a. Scaling patterns in the Antarctic brachiopod *Liothyrella uva* (Broderip, 1833). *Journal of Experimental Marine Biology and Ecology*, 133: 141-150.
- Peck, L. S., & Holmes, L. J. 1989b. Seasonal and ontogenetic changes in tissue size in the Antarctic brachiopod *Liothyrella uva* (Broderip, 1833). *Journal of Experimental Marine Biology and Ecology*, 134: 25-36.
- Peck, L. S., Meidlinger, K., & Tyler, P. A. 2001. Developmental and settlement characteristics of the Antarctic brachiopod *Liothyrella uva* (Broderip 1833). In: *Brachiopods Past and Present*. Ed. by C. H. C. Brunton, L. R. Cocks, & S. L. Long. Taylor and Francis, London and New York.
- Peck, L. S., Morley, S. A., Pörtner, H., & Clark, M. S. 2007. Thermal limits of burrowing capacity are linked to oxygen availability and size in the Antarctic clam *Laternula elliptica*. *Oecologia*, 154: 479-484.
- Peck, L. S., Morris, D. J., & Clarke, A. 1986a. The caeca of punctate brachiopods: a respiring tissue not a respiratory organ. *Lethaia*, 19: 232-232.
- Peck, L. S., Morris, D. J., Clarke, A., & Holmes, L. J. 1986b. Oxygen consumption and nitrogen excretion in the Antarctic brachiopod *Liothyrella uva* (Jackson, 1912) under simulated winter conditions. *Journal of Experimental Marine Biology and Ecology*, 104: 203-213.
- Peck, L. S., & Robinson, K. 1994. Pelagic larval development in the brooding Antarctic brachiopod *Liothyrella uva*. *Marine Biology*, 120: 279-286.
- Pelejero, C., Calvo, E., & Hoegh-Guldberg, O. 2010. Paleo-perspectives on ocean acidification. *Trends in Ecology & Evolution*, 25: 332-344.
- Pennington, J. T., & Stricker, S. A. 2001. Phylum Brachiopoda. In: *Atlas of Marine Invertebrate Larval Forms*, pp. 441-461. Ed. by C. M. Young. Academic Press, New York.
- Percival, E. 1944. A contribution to the life history of the brachiopod *Terebratella inconspicua* Sowerby. *Transactions of the Royal Society of New Zealand*, 74: 1-23.
- Pérez-Huerta, A., & Cusack, M. 2008. Common crystal nucleation mechanism in shell formation of two morphologically distinct calcite brachiopods. *Zoology*, 111: 9-15.
- Pérez-Huerta, A., Cusack, M., Ball, A., Williams, C. T., & MacKay, S. 2008. Deciphering the distribution of organic components in brachiopod shells by confocal laser scanning microscopy. *Journal of Microscopy*, 230: 94-99.

- Pérez-Huerta, A., Cusack, M., McDonald, S., Marone, F., Stampanoni, M., & MacKay, S. 2009. Brachiopod punctae: a complexity in shell biomineralisation. *Journal of Structural Biology*, 167: 62-67.
- Pérez-Huerta, A., Cusack, M., Zhu, W., England, J., & Hughes, J. 2007. Material properties of brachiopod shell ultrastructure by nanoindentation. *Journal of the Royal Society Interface*, 4: 33-39.
- Peyer, S. M., Hermanson, J. C., & Lee, C. E. 2010. Developmental plasticity of shell morphology of quagga mussels from shallow and deep-water habitats of the Great Lakes. *Journal of Experimental Biology*, 213: 2602-2609.
- Pfister, C. A., Roy, K., Wootton, J. T., McCoy, S. J., Paine, R. T., Suchanek, T. H., & Sanford, E. 2016. Historical baselines and the future of shell calcification for a foundation species in a changing ocean. *Proceedings of the Royal Society B: Biological Sciences*, 283: 20160392.
- Pörtner, H. 2008. Ecosystem effects of ocean acidification in times of ocean warming: a physiologist's view. *Marine Ecology Progress Series*, 373: 203-217.
- Pouchou, J. L., & Pichoir, F. 1984. A new model for quantitative x-ray microanalysis. 2. Application to in-depth analysis of heterogenous samples. *Recherche Aerospatiale*, 5: 349-367.
- Queirós, A. M., Fernandes, J. A., Faulwetter, S., Nunes, J., Rastrick, S. P., Mieszkowska, N., Artioli, Y., Yool, A., Calosi, P., Arvanitidis, C., Findlay, H. S., Barange, M., Cheung, W. W., & Widdicombe, S. 2015. Scaling up experimental ocean acidification and warming research: from individuals to the ecosystem. *Global Change Biology*, 21: 130-143.
- Reed, S. J. B. 1993. *Electron Microprobe Analysis*, University of Cambridge Press, Cambridge.
- Reeder, R. J. 1983. Crystal chemistry of the rhombohedral carbonates. *Reviews in Mineralogy and Geochemistry*, 11: 1-47.
- Revelle, R. R., & Fairbridge, R. W. 1957. Carbonates and carbon dioxide. *In: Geological Society of America Memoirs*, pp. 239-296.
- Reymond, C. E., Lloyd, A., Kline, D. I., Dove, S. G., & Pandolfi, J. M. 2013. Decline in growth of foraminifer *Marginopora rossi* under eutrophication and ocean acidification scenarios. *Global Change Biology*, 19: 291-302.

- Reynaud, S., Leclercq, N., Romaine-Lioud, S., Ferrier-Pages, C., Jaubert, J., & Gattuso, J.-P. 2003. Interacting effects of CO<sub>2</sub> partial pressure and temperature on photosynthesis and calcification in a scleractinian coral. *Global Change Biology*, 9: 1660-1668.
- Rhodes, M. C., & Thompson, R. J. 1992. Clearance rate of the articulate brachiopod *Neothyris lenticularis* (Deshayes, 1839). *Journal of Experimental Marine Biology and Ecology*, 163: 77-89.
- Rhodes, M. C., & Thompson, R. J. 1993. Comparative physiology of suspension-feeding in living brachiopods and bivalves: Evolutionary implications. *Paleobiology*, 19: 322-334.
- Richardson, C. A., Crisp, D. J., & Runham, N. W. 1979. Tidally deposited growth bands in the shell of the common cockle, *Cerastoderma edula* (L.). *Malacologia*, 18: 277-290.
- Richardson, J. R. 1981a. Recent brachiopods from New Zealand - background to the study cruises of 1977-79. *New Zealand Journal of Zoology*, 8: 133-143.
- Richardson, J. R. 1981b. Distribution and orientation of six articulate brachiopod species from New Zealand. *New Zealand Journal of Zoology*, 8: 189-196.
- Richardson, J. R. 1986. Brachiopods. *Scientific American*, 255: 100-106.
- Richardson, J. R. 1997. Ecology of articulated brachiopods. In: *Treatise on Invertebrate Paleontology, Part H, Brachiopods (Revised)*, pp. 441-462. Ed. by R. L. Kaesler. The Geological Society of America and The University of Kansas Press, Boulder, Colorado, and Lawrence, Kansas.
- Richter, K. D., Götze, T., Götze, J., & Neuser, D. R. 2003. Progress in application of cathodoluminescence (CL) in sedimentary petrology. *Mineralogy and Petrology*, 79: 127-166.
- Rickwood, A. E. 1977. Age, growth and shape of the intertidal brachiopod *Waltonia inconspicua* Sowerby, from New Zealand. *American Zoologist*, 17: 63-73.
- Riebesell, U., Czerny, J., von Bröckel, K., Boxhammer, T., Büdenbender, J., Deckelnick, M., Fischer, M., Hoffmann, D., Krug, S. A., Lentz, U., Ludwig, A., Mücke, R., & Schulz, K. G. 2013. Technical Note: A mobile sea-going mesocosm system – new opportunities for ocean change research. *Biogeosciences*, 10: 1835-1847.
- Riebesell, U., & Gattuso, J.-P. 2015. Lessons learned from ocean acidification research. *Nature Climate Change*, 5: 12-14.
- Riebesell, U., Zondervan, I., Rost, B., Tortell, P. D., Zeebe, R. E., & Morel, F. M. M. 2000. Reduced calcification of marine plankton in response to increased atmospheric CO<sub>2</sub>. *Nature*, 407: 364-367.

- Ries, J. B. 2011. A physicochemical framework for interpreting the biological calcification response to CO<sub>2</sub>-induced ocean acidification. *Geochimica et Cosmochimica Acta*, 75: 4053-4064.
- Ries, J. B., Cohen, A. L., & McCorkle, D. C. 2009. Marine calcifiers exhibit mixed responses to CO<sub>2</sub>-induced ocean acidification. *Geology*, 37: 1131-1134.
- Riisgård, H. U., & Randløv, A. 1981. Energy budgets, growth and filtration rates in *Mytilus edulis* at different algal concentrations. *Marine Biology*, 61: 227-234.
- Ringwood, A. H., & Keppler, C. J. 2002. Water quality variation and clam growth: Is pH really a non-issue in estuaries? *Estuaries*, 25: 901-907.
- Robbins, L. L., Hansen, M. E., Kleypas, J. A., & Meylan, S. C. 2010. CO<sub>2</sub>calc: a user-friendly carbon calculator for windows, Mac OS X, and iOS (iPhone). *In*: U.S. Geological Survey Open File Report 2010–1280.
- Rodolfo-Metalpa, R., Houlbreque, F., Tambutte, E., Boisson, F., Baggini, C., Patti, F. P., Jeffree, R., Fine, M., Foggo, A., Gattuso, J.-P., & Hall-Spencer, J. M. 2011. Coral and mollusc resistance to ocean acidification adversely affected by warming. *Nature Climate Change*, 1: 308-312.
- Roleda, M. Y., Boyd, P. W., & Hurd, C. L. 2012. Before ocean acidification: Calcifier chemistry lessons. *Journal of Phycology*, 48: 840-843.
- Roper, D. S., & Jillett, J. B. 1981. Seasonal occurrence and distribution of flatfish (Pisces: Pleuronectiformes) in inlets and shallow water along the Otago coast. *New Zealand Journal of Marine and Freshwater Research*, 15: 1-13.
- Rosa, R., & Seibel, B. A. 2008. Synergistic effects of climate-related variables suggest future physiological impairment in a top oceanic predator. *Proceedings of the National Academy of Sciences of the United States of America*, 105: 20776-20780.
- Rudwick, M. J. S. 1962. Notes on the ecology of brachiopods in New Zealand. *Transactions of the Royal Society of New Zealand (Zoology)*, 1: 327-355.
- Rudwick, M. J. S. 1970. Living and Fossil Brachiopods, Hutchinson & Co LTD, London. 199 pp.
- Sabine, C. L., Feely, R. A., Gruber, N., Key, R. M., Lee, K., Bullister, J. L., Wanninkhof, R., Wong, C. S., Wallace, D. W. R., Tilbrook, B., Millero, F. J., Peng, T.-H., Kozyr, A., Ono, T., & Rios, A. F. 2004. The oceanic sink for anthropogenic CO<sub>2</sub>. *Science*, 305: 367-371.
- Schmahl, W. W., Griesshaber, E., Merkel, C., Kelm, K., Deuschle, J., Neuser, R. D., Götz, A. J., Sehrbrock, A., & Mader, W. 2008a. Hierarchical fibre composite structure and

- micromechanical properties of phosphatic and calcitic brachiopod shell biomaterials – an overview. *Mineralogical Magazine*, 72: 541-562.
- Schmahl, W. W., Griesshaber, E., Neuser, R., Lenze, A., Job, R., & Brand, U. 2004. The microstructure of the fibrous layer of terebratulide brachiopod shell calcite. *European Journal of Mineralogy*, 16: 693-697.
- Schmahl, W. W., Griesshaber, E., Neuser, R. D., Goetz, A. J., & Lüter, C. 2008b. Electron backscatter diffraction study of brachiopod shell calcite - microscale phase and texture analysis of a polycrystalline biomaterial. *Particle & Particle Systems Characterization*, 25: 474-478.
- Scurr, D. J., & Eichhorn, S. J. 2005. Structure/property relationships in seashells. In: *Mechanical Properties of Bioinspired Materials* pp. 87–92. Ed. by C. Viney, K. Katti, F.-J. Ulm, & C. Hellmich. Materials Research Society Symposium Proceedings, Warrendale, PA.
- Shumway, S. E. 1982. Oxygen consumption in brachiopods and the possible role of punctae. *Journal of Experimental Marine Biology and Ecology*, 58: 207-220.
- Siegenthaler, U., & Sarmiento, J. L. 1993. Atmospheric carbon dioxide and the ocean. *Nature*, 365: 119-125.
- Siegenthaler, U., Stocker, T. F., Monnin, E., Lüthi, D., Schwander, J., Stauffer, B., Raynaud, D., Barnola, J.-M., Fischer, H., Masson-Delmotte, V., & Jouzel, J. 2005. Stable carbon cycle-climate relationship during the Late Pleistocene. *Science*, 310: 1313-1317.
- Silbiger, N. J., & Donahue, M. J. 2014. Secondary calcification and dissolution respond differently to future ocean conditions. *Biogeosciences Discussions*, 11: 12799-12831.
- Sollas, W. J. 1886. The 'caecal processes' of the shells of brachiopods interpreted as sense organs. *The Scientific Proceedings of the Royal Dublin Society*, 5: 318-320.
- Somero, G. N. 2010. The physiology of climate change: how potentials for acclimatization and genetic adaptation will determine ‘winners’ and ‘losers’. *Journal of Experimental Biology*, 213: 912-920.
- Stansfield, G. 2012. *Conservation and storage: zoological collections*, Routledge, New York. 775 pp.
- Stewart, I. R. 1981. Population structure of articulate brachiopod species from soft and hard substrates. *New Zealand Journal of Zoology*, 8: 197-207.
- Stor, J. F., Costa, A. L., & Prawel, D. A. 1982. Effects of temperature on calcium deposition in the hard-shelled clam, *Mercenaria mercenaria*. *Journal of Thermal Biology*, 7: 57-61.

- Suckling, C. C. 2012. Calcified marine invertebrates: The effects of ocean acidification. *In*: PhD Thesis, Department of Earth Sciences, p. 162. University of Cambridge, Gonville and Caius College, Cambridge.
- Suckling, C. C., Clark, M. S., Richard, J., Morley, S. A., Thorne, M. A., Harper, E. M., & Peck, L. S. 2014. Adult acclimation to combined temperature and pH stressors significantly enhances reproductive outcomes compared to short-term exposures. *Journal of Animal Ecology*, 84: 773-784.
- Sunday, J. M., Crim, R. N., Harley, C. D., & Hart, M. W. 2011. Quantifying rates of evolutionary adaptation in response to ocean acidification. *PLoS ONE*, 6: e22881.
- Taylor, J. D., & Reid, D. G. 1990. Shell microstructure and mineralogy of the Littorinidae: ecological and evolutionary significance. *Hydrobiologia*, 193: 199-215.
- Thayer, C. W. 1986. Respiration and the function of brachiopod punctae. *Lethaia*, 19: 23-31.
- Thickett, D., & Lee, L. R. 2004. Selection of materials for the storage or display of museum objects, British Museum, London. 31 pp.
- Thomsen, J., Casties, I., Pansch, C., Kortzinger, A., & Melzner, F. 2013. Food availability outweighs ocean acidification effects in juvenile *Mytilus edulis*: laboratory and field experiments. *Global Change Biology*, 19: 1017-1027.
- Thomsen, J., Gutowska, M. A., Saphörster, J., Heinemann, A., Trübenbach, K., Fietzke, J., Hiebenthal, C., Eisenhauer, A., Kortzinger, A., Wahl, M., & Melzner, F. 2010. Calcifying invertebrates succeed in a naturally CO<sub>2</sub>-rich coastal habitat but are threatened by high levels of future acidification. *Biogeosciences*, 7: 3879-3891.
- Tribble, J. S., Arvidson, R. S., Lane, M., & MacKenzie, F. T. 1995. Crystal chemistry, and thermodynamic and kinetic properties of calcite, dolomite, apatite, and biogenic silica: applications to petrological problems. *Sedimentary Geology*, 95: 11-37.
- Tunnicliffe, V., Davies, K. T. A., Butterfield, D. A., Embley, R. W., Rose, J. M., & Chadwick Jr, W. W. 2009. Survival of mussels in extremely acidic waters on a submarine volcano. *Nature Geoscience*, 2: 344-348.
- Uthicke, S., Ebert, T., Liddy, M., Johansson, C., Fabricius, K. E., & Lamare, M. 2016. *Echinometra* sea urchins acclimated to elevated pCO<sub>2</sub> at volcanic vents outperform those under present-day pCO<sub>2</sub> conditions. *Global Change Biology*, 22: 2451-2461.
- Veizer, J., Ala, D., Azmy, K., Bruckschen, P., Buhl, D., Bruhn, F., Carden, G. A. F., Diener, A., Ebner, S., Godderis, Y., Jasper, T., Korte, C., Pawellek, F., Podlaha, O. G., & Strauss, H. 1999. <sup>87</sup>Sr/<sup>86</sup>Sr,  $\delta^{13}\text{C}$  and  $\delta^{18}\text{O}$  evolution of Phanerozoic seawater. *Chemical Geology*, 161: 59-88.

- Veizer, J., Fritz, P., & Jones, B. 1986. Geochemistry of brachiopods: Oxygen and carbon isotopic records of Paleozoic oceans. *Geochimica et Cosmochimica Acta*, 50: 1679-1696.
- Vermeij, G. J. 1977. The Mesozoic marine revolution: evidence from snails, predators and grazers. *Paleobiology*, 3: 245-258.
- Vermeij, G. J. 1978. Biogeography and adaptation: patterns of marine life, Harvard University Press, Cambridge, Massachusetts, USA. 332 pp.
- Vermeij, G. J. 1982. Phenotypic evolution in a poorly dispersing snail after arrival of a predator. *Nature*, 299: 349-350.
- Vermeij, G. J. 1983. Traces and trends of predation, with special reference to bivalved animals. *Palaeontology Review*, 26: 455-465.
- Vermeij, G. J. 1993. A natural history of shells, Princeton University Press, Princeton, NJ. 207 pp.
- Wanninkhof, R., Lewis, E., Feely, R. A., & Millero, F. J. 1999. The optimal carbonate dissociation constants for determining surface water  $p\text{CO}_2$  from alkalinity and total inorganic carbon. *Marine Chemist*, 65: 291-301.
- Watson, S.-A., Peck, L. S., Tyler, P. A., Southgate, P. C., Tan, K. S., Day, R. W., & Morley, S. A. 2012. Marine invertebrate skeleton size varies with latitude, temperature and carbonate saturation: implications for global change and ocean acidification. *Global Change Biology*, 18: 3026-3038.
- Weast, R. C. 1975. Handbook of Chemistry and Physics, The Chemical Rubber Co., Cleveland. 2528 pp.
- Widdicombe, S., & Spicer, J. I. 2008. Predicting the impact of ocean acidification on benthic biodiversity: What can animal physiology tell us? *Journal of Experimental Marine Biology and Ecology*, 366: 187-197.
- Wilbur, K. M. 1960. Shell structure and mineralization in molluscs. *In: Calcification in Biological Systems*, pp. 15-40. Ed. by R. F. Sognaes. AAAS, Washington.
- Willan, R. C. 1981. Soft-bottom assemblages of Paterson Inlet, Stewart Island. *New Zealand Journal of Zoology*, 8: 229-248.
- Williams, A. 1956. The calcareous shell of the Brachiopoda and its importance to their classification. *Biological Reviews*, 31: 243-287.
- Williams, A. 1966. Growth and structure of the shell of living articulate brachiopods. *Nature*, 211: 1146-1148.

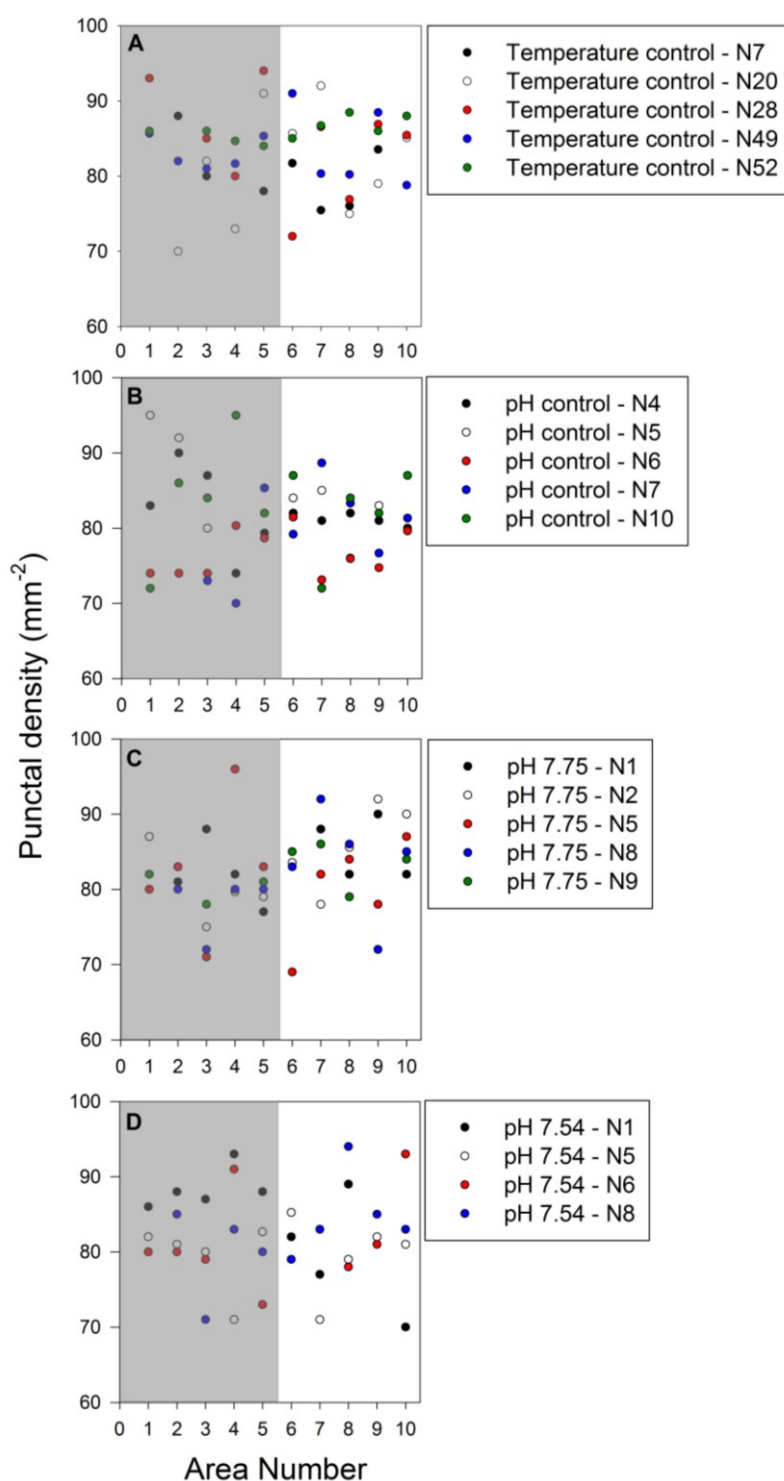
- Williams, A. 1968a. Evolution of the shell structure of articulate brachiopods. *Special Papers in Palaeontology*, 2: 1-55.
- Williams, A. 1968b. A history of skeletal secretion among articulate brachiopods *Lethaia*, 1: 268-287.
- Williams, A. 1968c. Significance of the structure of the brachiopod periostracum. *Nature*, 218: 551-554.
- Williams, A. 1973. The secretion and structural evolution of the shell of thecideidine brachiopods. *Philosophical Transactions of the Royal Society of London. Series B, Biological Sciences*, 264: 439-478.
- Williams, A. 1997. Shell structure. *In: Treatise on Invertebrate Paleontology, Part H, Brachiopods (Revised)*, pp. 267-320. Ed. by R. L. Kaesler. The Geological Society of America and The University of Kansas Press, Boulder, Colorado, and Lawrence, Kansas.
- Williams, A., Brunton, C. H. C., & MacKinnon, D. I. 1997. Morphology. *In: Treatise on Invertebrate Paleontology, Part H, Brachiopods (Revised)*, pp. 321-422. Ed. by R. L. Kaesler. The Geological Society of America and The University of Kansas Press, Boulder, Colorado, and Lawrence, Kansas.
- Williams, A., Carlson, S. J., Brunton, H. C., Holmer, L. E., & Popov, L. 1996. A supra-ordinal classification of the Brachiopoda. *Philosophical Transactions: Biological Sciences*, 351: 1171-1193.
- Williams, A., & Mackay, S. 1978. Secretion and ultrastructure of the periostracum of some terebratulide brachiopods. *Proceedings of the Royal Society of London, Series B: Biological Sciences*, 202: 191-209.
- Williams, A., & MacKay, S. 1979. Differentiation of the brachiopod periostracum. *Palaeontology*, 22: 721-736.
- Williams, A., & Rowell, A. J. 1965. Morphology. *In: Treatise on Invertebrate Paleontology. Part H, Brachiopoda*, pp. 57-138. Ed. by R. C. Moore. Geological Society of America & University of Kansas Press, New York & Lawrence.
- Williams, A., & Wright, A. D. 1970. Shell structure of the Craniacea and other calcareous inarticulate brachiopods. *Special Papers in Palaeontology*, 7: 1-51.
- Wittmann, A. C., & Pörtner, H. 2013. Sensitivities of extant animal taxa to ocean acidification. *Nature Climate Change*, 3: 995-1001.

- Wolfe, K., Dworjanyn, S. A., & Byrne, M. 2013. Effects of ocean warming and acidification on survival, growth and skeletal development in the early benthic juvenile sea urchin (*Heliocidaris erythrogramma*). *Global Change Biology*, 19: 2698-2707.
- Wood, H. L., Spicer, J. I., & Widdicombe, S. 2008. Ocean acidification may increase calcification rates, but at a cost. *Proceedings of the Royal Society of London, Series B: Biological Sciences*, 275: 1767-1773.
- Wootton, J. T., Pfister, C. A., & Forester, J. D. 2008. Dynamic patterns and ecological impacts of declining ocean pH in a high- resolution multi-year dataset. *Proceedings of the National Academy of Sciences*, 105: 18848-18853.
- Zachos, J. C., Dickens, G. R., & Zeebe, R. E. 2008. An early Cenozoic perspective on greenhouse warming and carbon-cycle dynamics. *Nature*, 451: 279-283.
- Zachos, J. C., Rohl, U., Schellenberg, S. A., Sluijs, A., Hodell, D. A., Kelly, D. C., Thomas, E., Nicolo, M., Raffi, I., Lourens, L. J., McCarren, H., & Kroon, D. 2005. Rapid acidification of the ocean during the Paleocene-Eocene Thermal Maximum. *Science*, 308: 1611-1615.
- Zeina, O. N. 2008. Biogeography of the Recent brachiopods. *Paleontological Journal*, 42: 830-858.
- Zondervan, I., Zeebe, R. E., Rost, B., & Riebesell, U. 2001. Decreasing marine biogenic calcification: A negative feedback on rising atmospheric  $p\text{CO}_2$ . *Global Biogeochemical Cycles*, 15: 507-516.

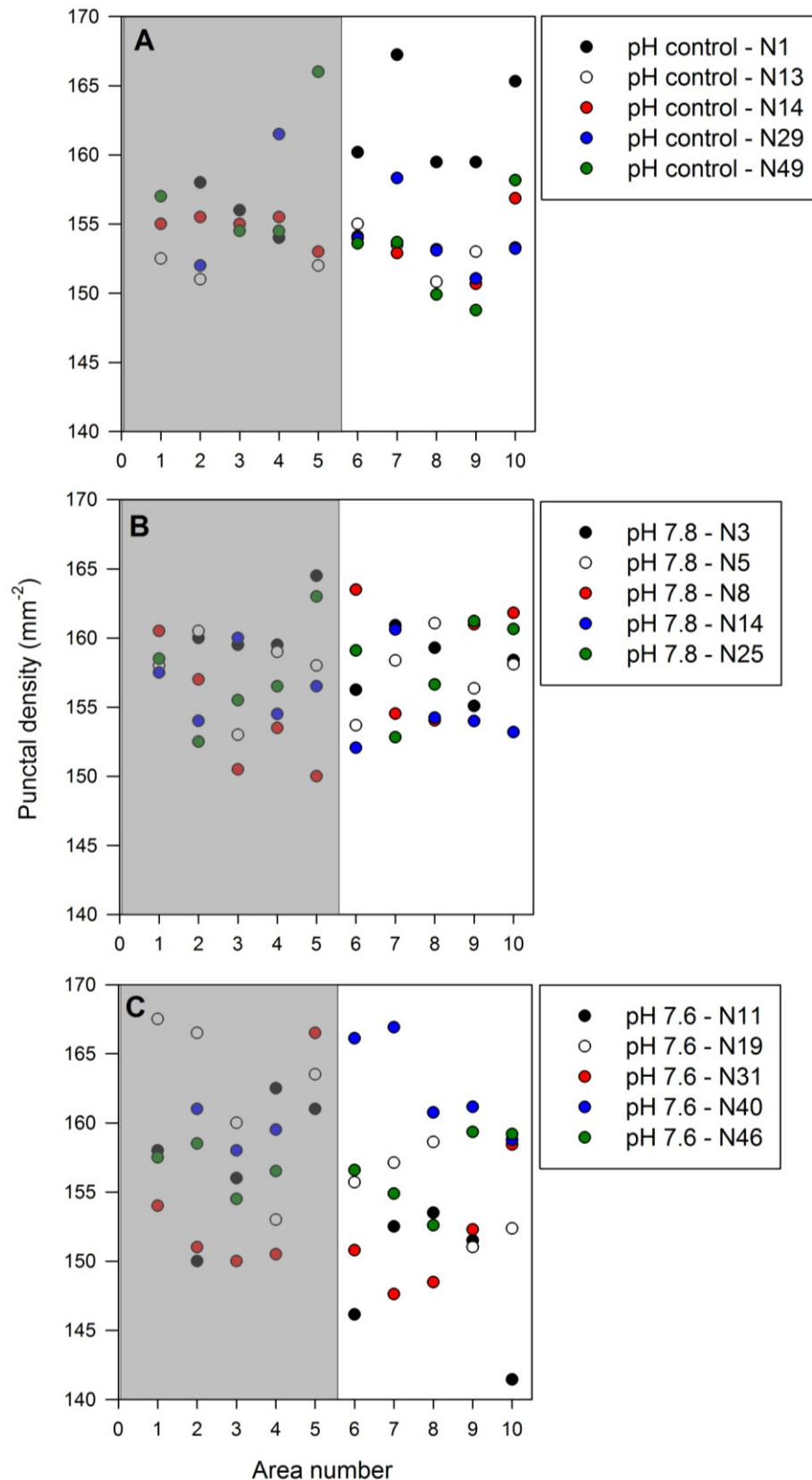
# APPENDICES

## Appendix A

Supporting material for Chapter 3 (Do polar and temperate brachiopods produce the same shell structurally and elementally under forecasted end-century acidified conditions?)



**Appendix Figure A1– *L. uva* - punctal densities from each of the 10 different areas throughout the shell in (A) Temperature control (B) pH control (C) pH 7.75 and (D) pH 7.54 treatments. Each coloured symbol refers to an individual in that treatment. The grey area indicates shell growth laid down in the natural environment and the white area refers to growth laid down in the experiment.**



**Appendix Figure A2 – *C. inconspicua* - punctal densities from each of the 10 different areas throughout the shell in (A) pH control (B) pH 7.8 and (C) pH 7.6 treatments. Each coloured symbol refers to an individual in that treatment. The grey area indicates areas of shell growth laid down in the natural environment and the white area refers to growth laid down in the experiment.**

**Appendix Table A1 – *L. uva* - Statistical analysis results comparing the elemental composition data from each method.**

Treatment	Element	Wild growth			Experimental growth		
		Average wt % of spot point method	Average wt % of vertical profiles	Statistical analysis results (One-way ANOVA)	Average wt % of spot point method	Average wt % of vertical profiles	Statistical analysis results (One-way ANOVA)
Temperature control	Ca	39.10	39.05	$F_{1,83} = 0.14, p = 0.709$	39.21	39.17	$F_{1,54} = 0.03, p = 0.858$
	Mg	0.24	0.21	$F_{1,80} = 0.79, p = 0.377$	0.29	0.26	$F_{1,54} = 0.43, p = 0.514$
	Na	0.31	0.31	$F_{1,83} = 0.45, p = 0.506$	0.32	0.32	$F_{1,54} = 0.08, p = 0.781$
	Sr	0.16	0.17	$F_{1,83} = 0.65, p = 0.423$	0.18	0.19	$F_{1,54} = 0.43, p = 0.515$
	P	0.03	0.03	$F_{1,56} = 0.49, p = 0.487$	0.03	0.02	$F_{1,28} = 0.01, p = 0.927$
pH control	Ca	39.12	38.91	$F_{1,57} = 2.06, p = 0.157$	39.25	39.11	$F_{1,45} = 0.75, p = 0.393$
	Mg	0.23	0.23	$F_{1,53} = 0.00, p = 0.991$	0.26	0.30	$F_{1,41} = 0.28, p = 0.601$
	Na	0.31	0.34	$F_{1,57} = 3.33, p = 0.074$	0.31	0.33	$F_{1,45} = 2.59, p = 0.115$
	Sr	0.16	0.18	$F_{1,57} = 0.74, p = 0.393$	0.17	0.18	$F_{1,45} = 0.29, p = 0.595$
	P	0.02	0.03	$F_{1,44} = 1.73, p = 0.195$	0.02	0.02	$F_{1,33} = 0.01, p = 0.943$
pH 7.75	Ca	39.09	39.31	$F_{1,76} = 1.60, p = 0.029$	39.20	39.21	$F_{1,97} = 0.00, p = 0.945$
	Mg	0.22	0.28	$F_{1,76} = 1.62, p = 0.207$	0.25	0.20	$F_{1,96} = 1.57, p = 0.214$
	Na	0.32	0.34	$F_{1,77} = 1.43, p = 0.236$	0.32	0.31	$F_{1,97} = 1.87, p = 0.175$
	Sr	0.17	0.17	$F_{1,77} = 0.18, p = 0.677$	0.16	0.16	$F_{1,97} = 0.22, p = 0.638$
	P	0.03	0.03	$F_{1,58} = 0.94, p = 0.336$	0.02	0.02	$F_{1,73} = 0.00, p = 0.962$
pH 7.54	Ca	39.02	39.26	$F_{1,55} = 2.85, p = 0.097$	39.18	38.98	$F_{1,59} = 1.18, p = 0.283$
	Mg	0.27	0.32	$F_{1,49} = 1.29, p = 0.262$	0.25	0.32	$F_{1,58} = 1.53, p = 0.221$
	Na	0.32	0.32	$F_{1,54} = 0.01, p = 0.926$	0.31	0.32	$F_{1,57} = 0.34, p = 0.560$
	Sr	0.17	0.15	$F_{1,55} = 2.84, p = 0.098$	0.16	0.16	$F_{1,59} = 0.00, p = 0.998$
	P	0.03	0.03	$F_{1,47} = 2.84, p = 0.099$	0.02	0.03	$F_{1,51} = 1.46, p = 0.232$

Appendix Table A2 – *C. inconspicua* – Statistical analysis results comparing the elemental composition data from each method.

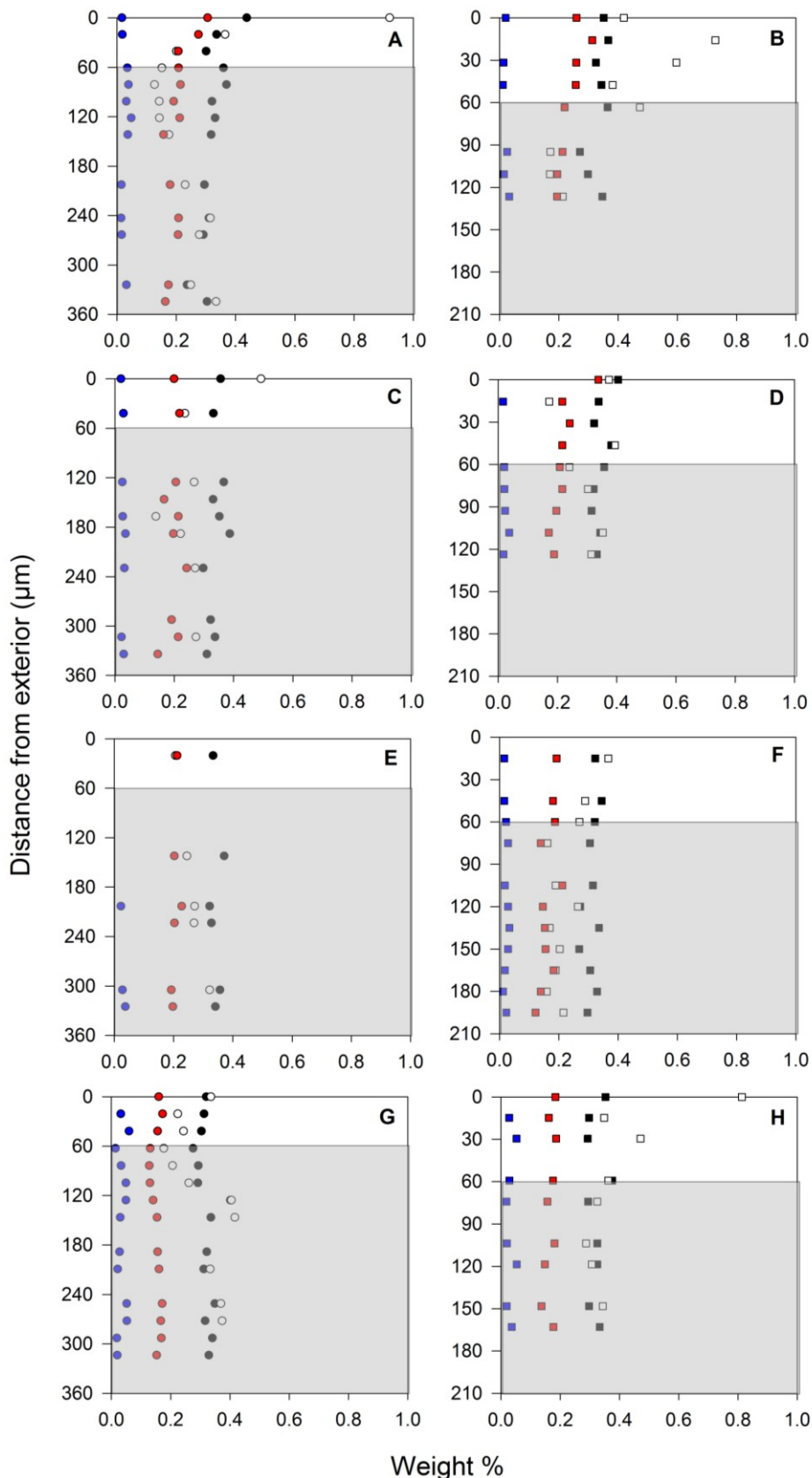
Treatment	Element	Wild growth			Experimental growth		
		Average wt % of spot point method	Average wt % of vertical profiles	Statistical analysis results (One-way ANOVA)	Average wt % of spot point method	Average wt % of vertical profiles	Statistical analysis results (One-way ANOVA)
pH control	Ca	39.25	39.05	$F_{1,88} = 3.09, p = 0.082$	39.18	39.12	$F_{1,59} = 0.11, p = 0.744$
	Mg	0.10	0.10	$F_{1,88} = 0.76, p = 0.387$	0.13	0.13	$F_{1,56} = 0.05, p = 0.816$
	Na	0.22	0.21	$F_{1,88} = 1.42, p = 0.237$	0.22	0.22	$F_{1,47} = 0.19, p = 0.661$
	Sr	0.12	0.12	$F_{1,85} = 0.00, p = 0.953$	0.12	0.11	$F_{1,59} = 0.30, p = 0.585$
	P	0.02	0.02	$F_{1,73} = 0.89, p = 0.348$	0.03	0.02	$F_{1,54} = 3.39, p = 0.071$
pH 7.8	Ca	39.24	39.30	$F_{1,76} = 0.23, p = 0.632$	39.28	39.24	$F_{1,58} = 0.09, p = 0.771$
	Mg	0.11	0.11	$F_{1,79} = 0.00, p = 0.960$	0.13	0.13	$F_{1,57} = 0.00, p = 0.972$
	Na	0.21	0.21	$F_{1,77} = 0.01, p = 0.920$	0.22	0.21	$F_{1,55} = 1.14, p = 0.291$
	Sr	0.11	0.11	$F_{1,79} = 0.10, p = 0.756$	0.11	0.11	$F_{1,58} = 0.23, p = 0.633$
	P	0.02	0.02	$F_{1,65} = 0.98, p = 0.327$	0.03	0.02	$F_{1,52} = 3.20, p = 0.080$
pH 7.6	Ca	39.22	39.19	$F_{1,70} = 0.05, p = 0.831$	39.16	39.16	$F_{1,82} = 0.00, p = 0.962$
	Mg	0.10	0.11	$F_{1,70} = 0.05, p = 0.827$	0.12	0.12	$F_{1,80} = 0.00, p = 0.992$
	Na	0.20	0.21	$F_{1,69} = 0.02, p = 0.900$	0.22	0.20	$F_{1,82} = 2.53, p = 0.116$
	Sr	0.11	0.12	$F_{1,70} = 0.91, p = 0.343$	0.11	0.11	$F_{1,83} = 0.01, p = 0.922$
	P	0.02	0.03	$F_{1,57} = 0.96, p = 0.333$	0.02	0.02	$F_{1,77} = 3.04, p = 0.085$

**Appendix Table A3 – *L. uva* - Statistical analysis results of elemental composition data from the vertical profiles. Two-way ANOVA and post-hoc Tukey tests were used to determine any significant effects of treatment, growth period and interaction of these two factors.**

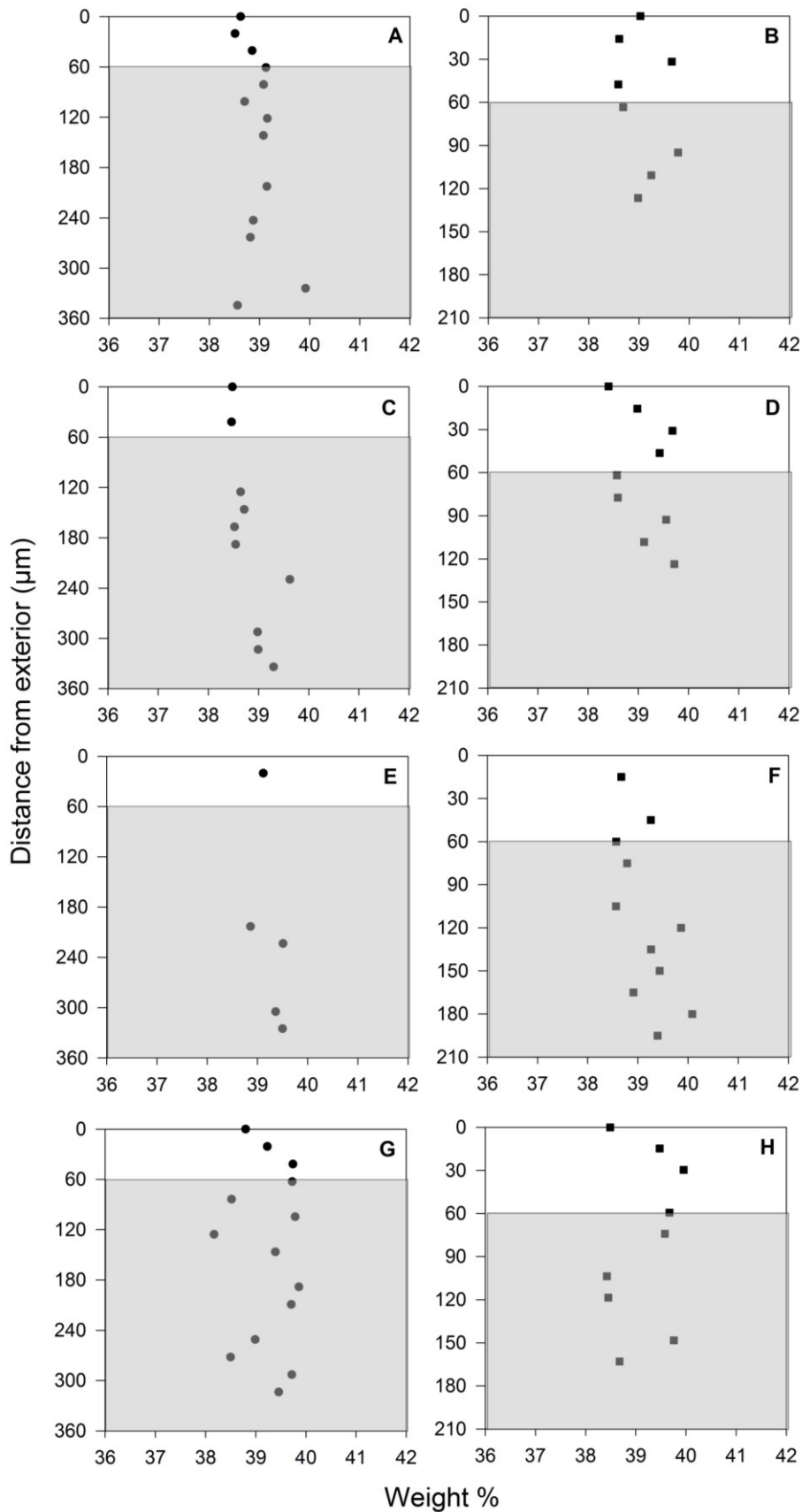
Element	Vertical Profiles			
	Two-way ANOVA results (Response: weight%, Factors: treatment, wild vs experimental growth)			Post-hoc Tukey results
	Treatment	Wild vs Experimental growth	Interaction	
Ca	$F_{3,55} = 0.47$ , $p = 0.708$	$F_{1,55} = 0.01$ , $p = 0.919$	$F_{3,55} = 0.60$ , $p = 0.618$	N/A
Mg	$F_{3,47} = 2.83$ , $p = 0.050$	$F_{1,47} = 0.16$ , $p = 0.691$	$F_{3,47} = 1.90$ , $p = 0.145$	N/A
Na	$F_{3,56} = 0.97$ , $p = 0.416$	$F_{1,56} = 1.58$ , $p = 0.215$	$F_{3,56} = 1.26$ , $p = 0.297$	N/A
Sr	$F_{3,56} = 2.87$ , $p = 0.046$	$F_{1,56} = 0.13$ , $p = 0.721$	$F_{3,56} = 1.11$ , $p = 0.353$	N/A
P	$F_{3,50} = 0.66$ , $p = 0.579$	$F_{1,50} = 1.50$ , $p = 0.228$	$F_{3,50} = 0.02$ , $p = 0.996$	N/A

**Appendix Table A4 – *C. inconspicua* – Statistical analysis results of elemental composition data from the vertical profiles. Two-way ANOVA and post-hoc Tukey tests were used to determine any significant effects of treatment, growth period and interaction of these two factors. Significant differences are highlighted in bold.**

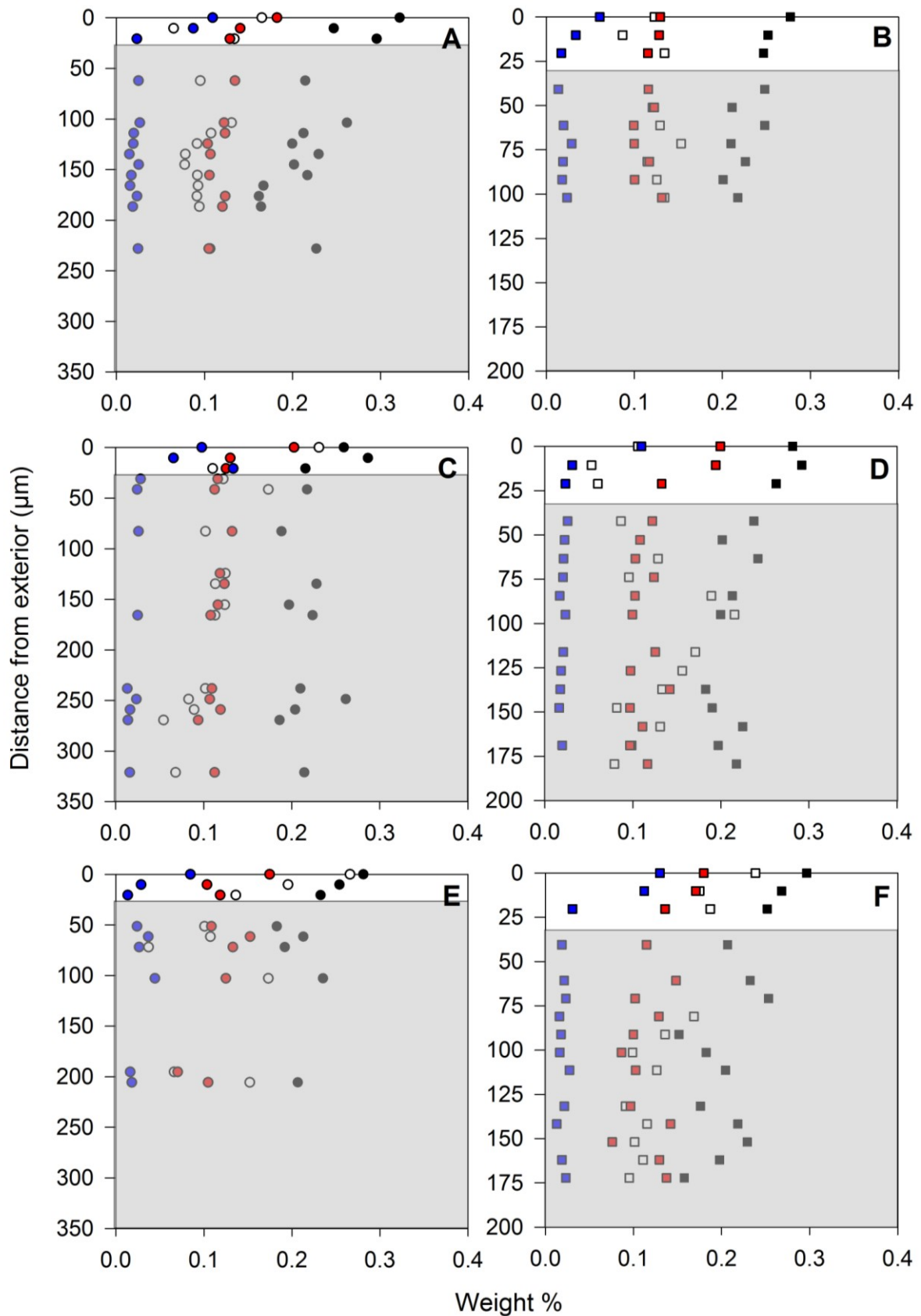
Element	Vertical Profiles			
	Two-way ANOVA results (Response: weight%, Factors: treatment, wild vs experimental growth)			Post-hoc Tukey results
	Treatment	Wild vs Experimental growth	Interaction	
Ca	$F_{2,56} = 1.79$ , $p = 0.178$	$F_{1,56} = 0.00$ , $p = 0.964$	$F_{2,56} = 0.22$ , $p = 0.800$	N/A
Mg	$F_{2,55} = 0.24$ , $p = 0.785$	<b><math>F_{1,55} = 6.17</math></b> , <b><math>p = 0.016</math></b>	$F_{2,55} = 0.51$ , $p = 0.607$	Experimental growth has a higher concentration than wild growth.
Na	$F_{2,53} = 0.71$ , $p = 0.494$	$F_{1,53} = 0.24$ , $p = 0.629$	$F_{2,53} = 1.01$ , $p = 0.372$	N/A
Sr	$F_{2,58} = 0.09$ , $p = 0.915$	$F_{1,58} = 0.39$ , $p = 0.535$	$F_{2,58} = 0.01$ , $p = 0.991$	N/A
P	$F_{1,53} = 1.76$ , $p = 0.183$	$F_{1,53} = 3.54$ , $p = 0.066$	$F_{2,53} = 2.69$ , $p = 0.078$	N/A



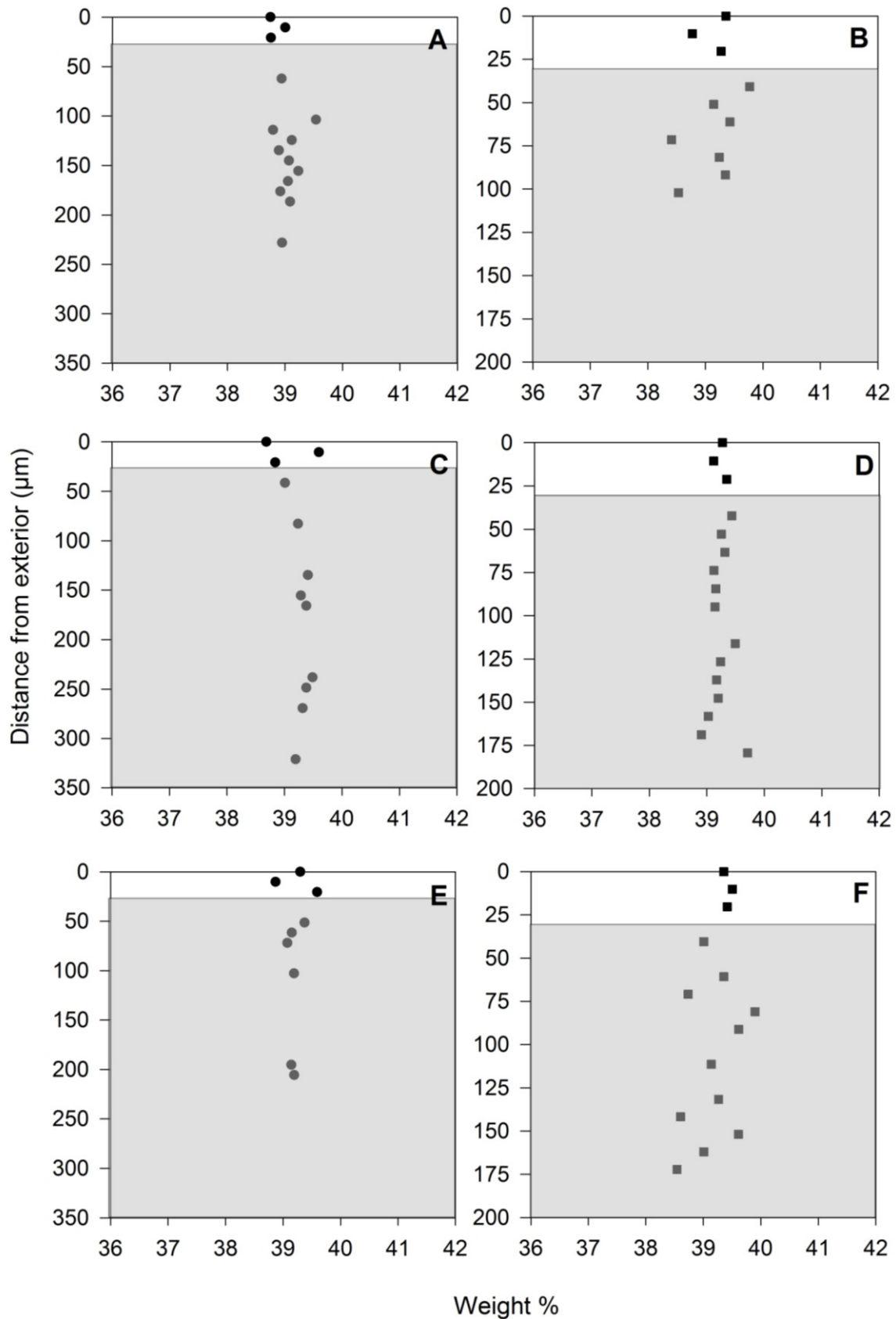
Appendix Figure A3 – *L. uva* - Vertical profiles of Na (black symbols), Mg (white symbols), Sr (red symbols), P (blue symbols) from wild growth (circle symbols) and experimental growth (square symbols) in the temperature control (A, B), pH control (C, D), pH 7.75 treatment (E, F) and pH 7.54 treatment (G, H). White area is the primary layer and grey area is the secondary layer.



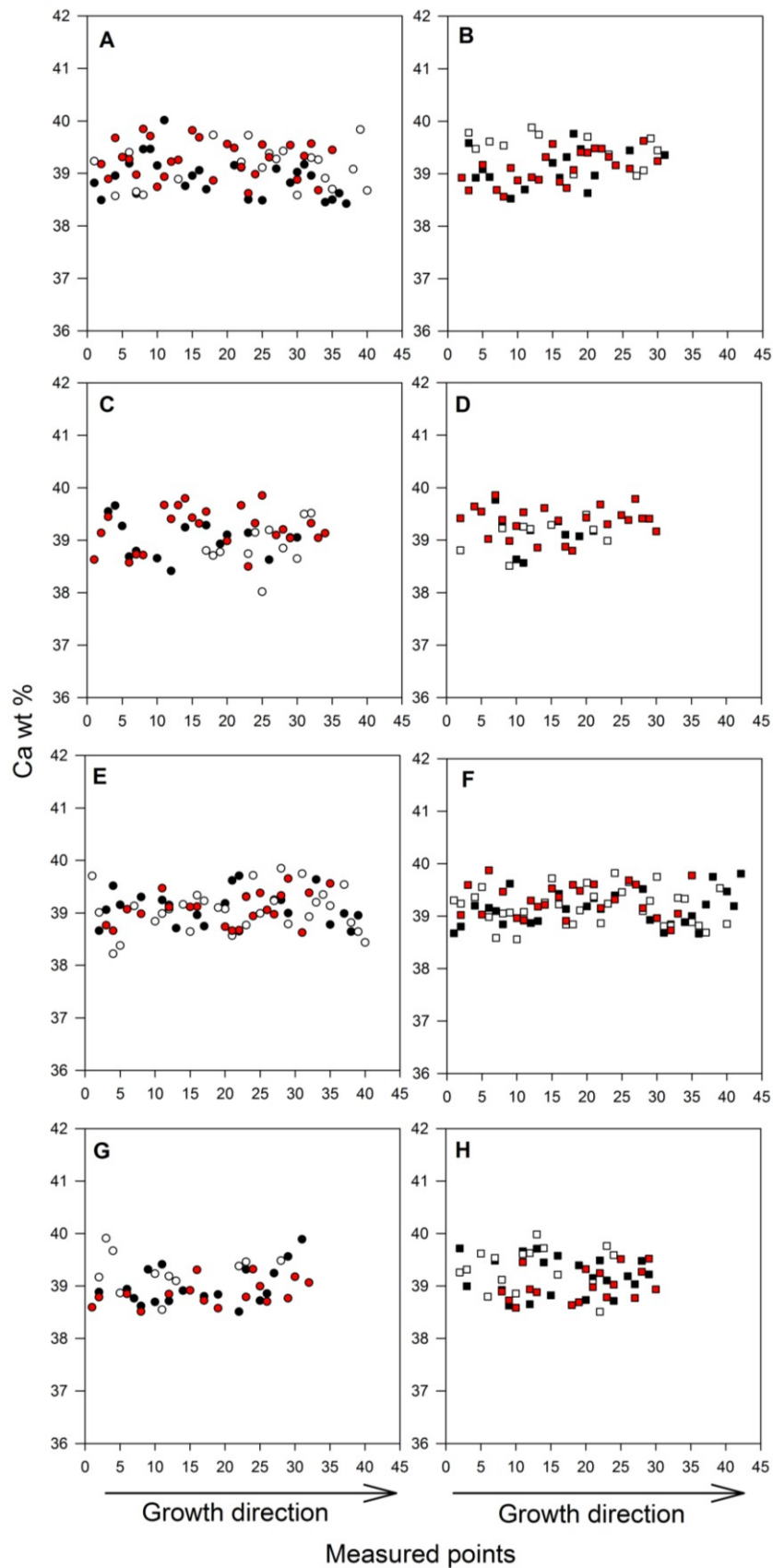
**Appendix Figure A4 – *L. uva* - Vertical profiles of Ca from wild growth (circle symbols) and experimental growth (square symbols) in the temperature control (A, B), pH control (C, D), pH 7.75 treatment (E, F) and pH 7.54 treatment (G, H). White area is the primary layer and grey area is the secondary layer.**



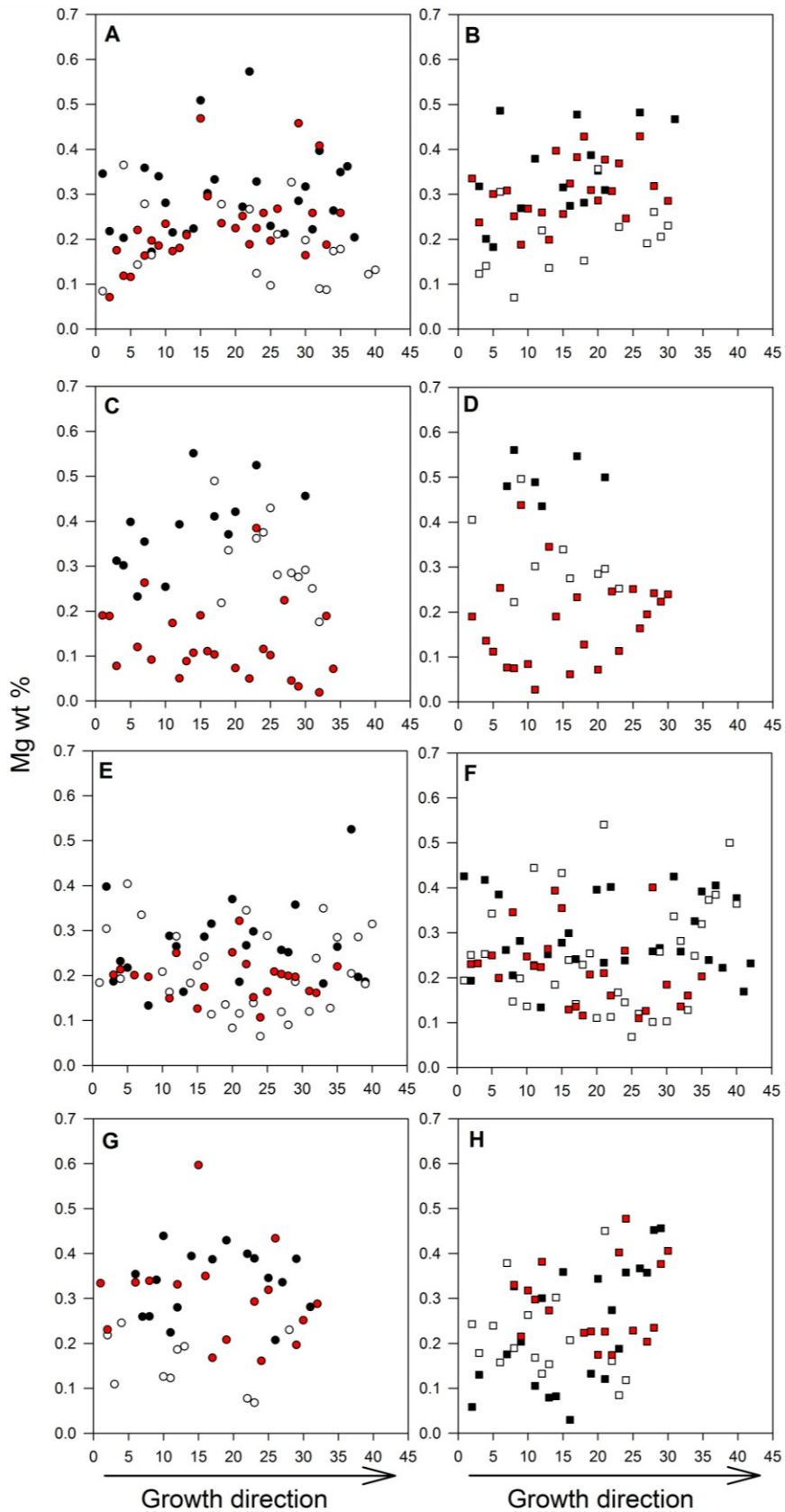
**Appendix Figure A5 – *C. inconspicua* - Vertical profiles of Na (black symbols), Mg (white symbols), Sr (red symbols), P (blue symbols) from wild growth (circle symbols) and experimental growth (square symbols) in the pH control (A, B), pH 7.8 (C, D) and pH 7.6 treatment (E, F). White area is the primary layer and grey area is the secondary layer.**



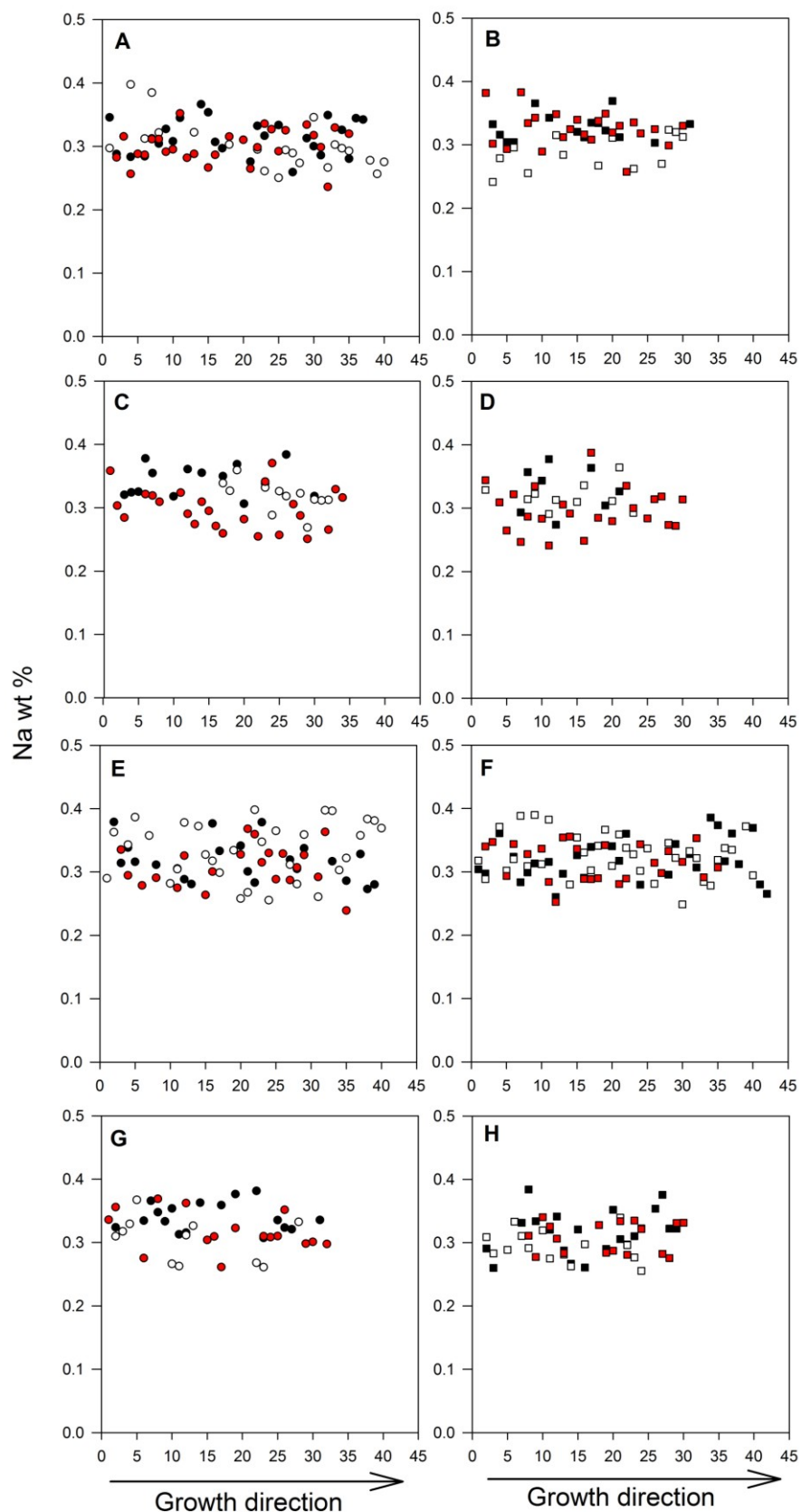
Appendix Figure A6 – *C. inconspicua* - Vertical profiles of Ca from wild growth (circle symbols) and experimental growth (square symbols) in the pH control (A, B), pH 7.8 (C, D) and pH 7.6 treatment (E, F). White area is the primary layer and grey area is the secondary layer.



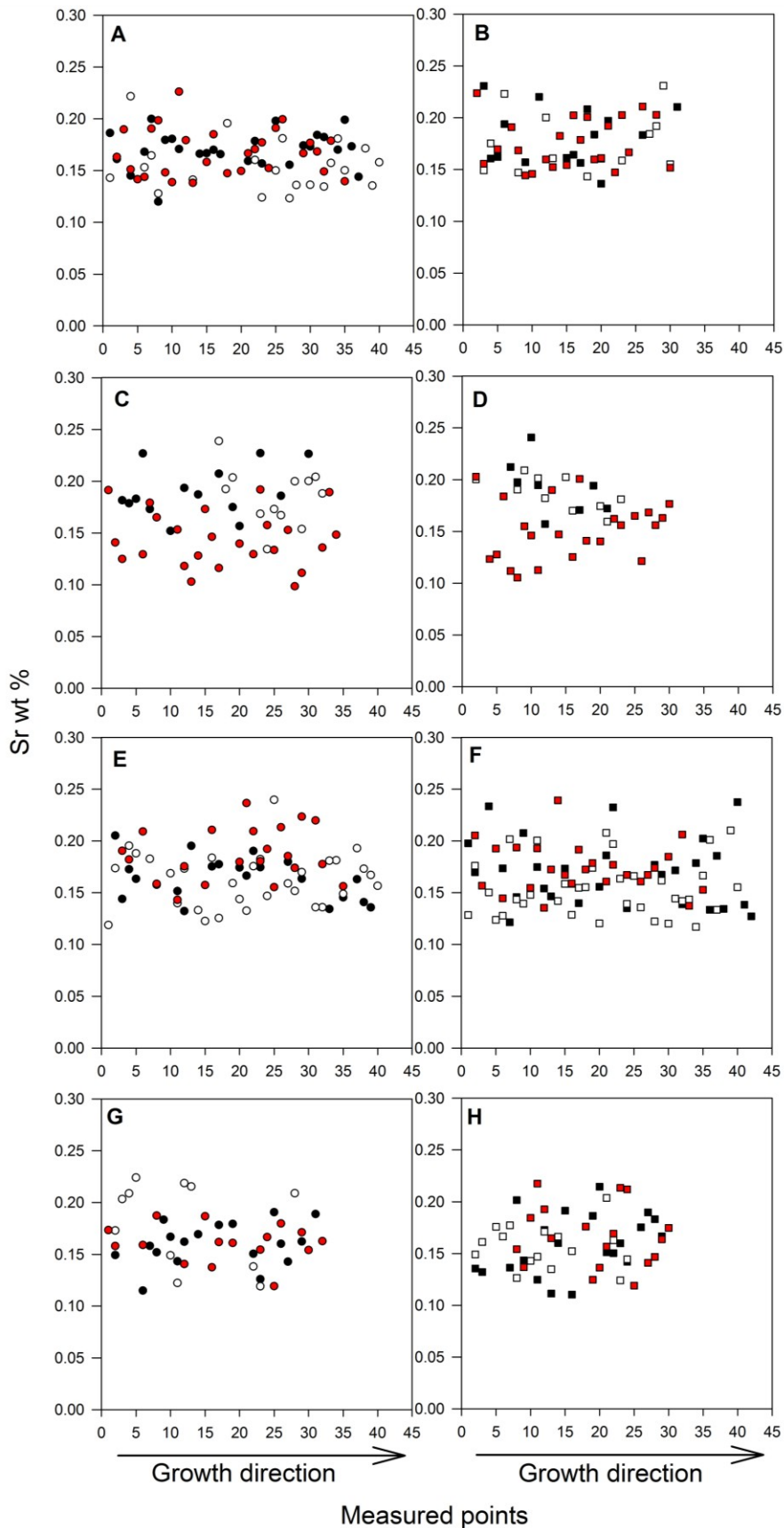
**Appendix Figure A7 – *L. uva* - Ca concentration from the spot point method of wild growth (circle symbols) and experimental growth (square symbols) in the temperature control (A, B), pH control (C, D), pH 7.75 treatment (E, F) and pH 7.54 treatment (G, H). Different coloured symbols refer to different individuals within each treatment. Growth direction is indicated.**



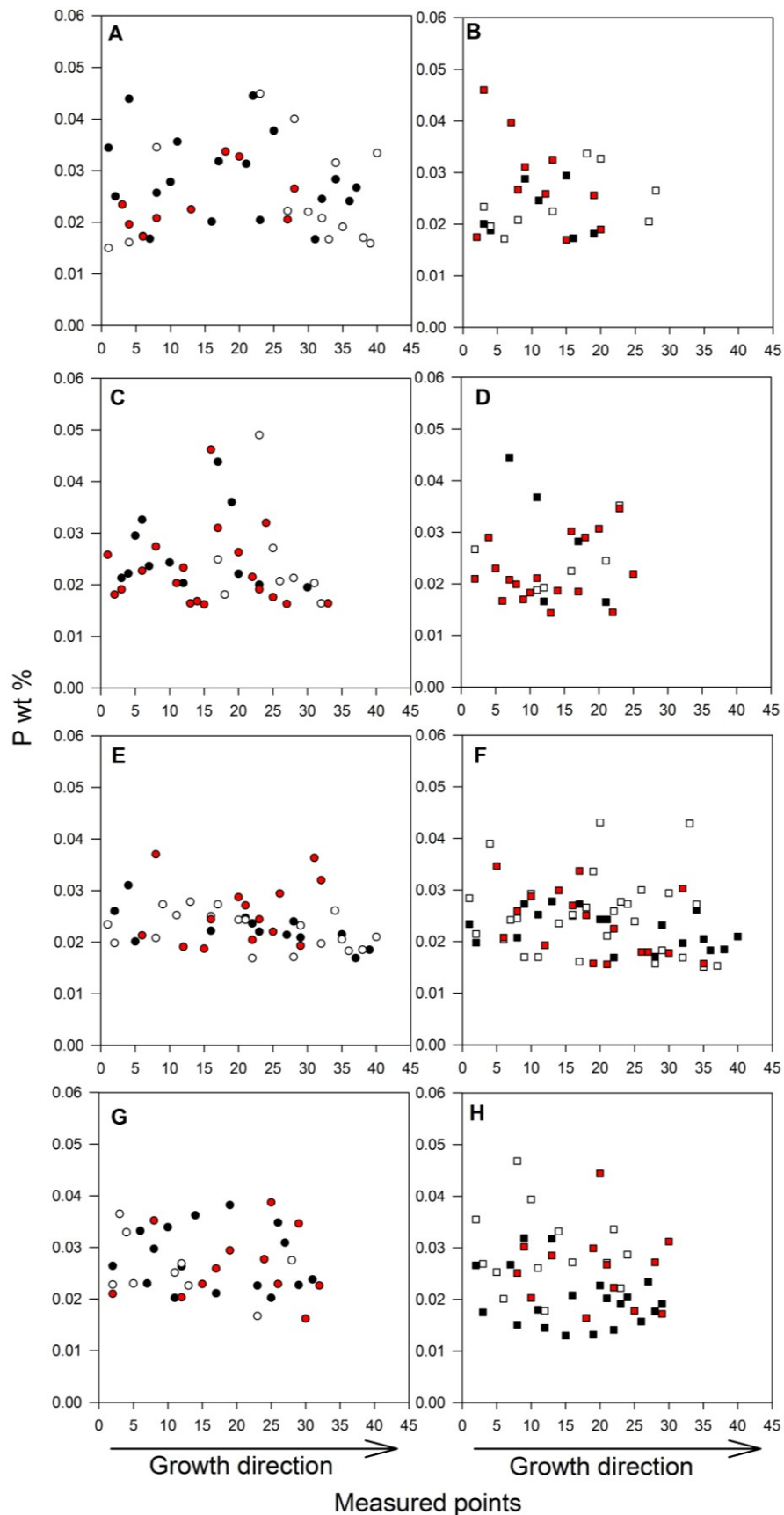
**Appendix Figure A8 – *L. uva* - Mg concentration from the spot point method of wild growth (circle symbols) and experimental growth (square symbols) in the temperature control (A, B), pH control (C, D), pH 7.75 treatment (E, F) and pH 7.54 treatment (G, H). Different coloured symbols refer to different individuals within each treatment. Growth direction is indicated.**



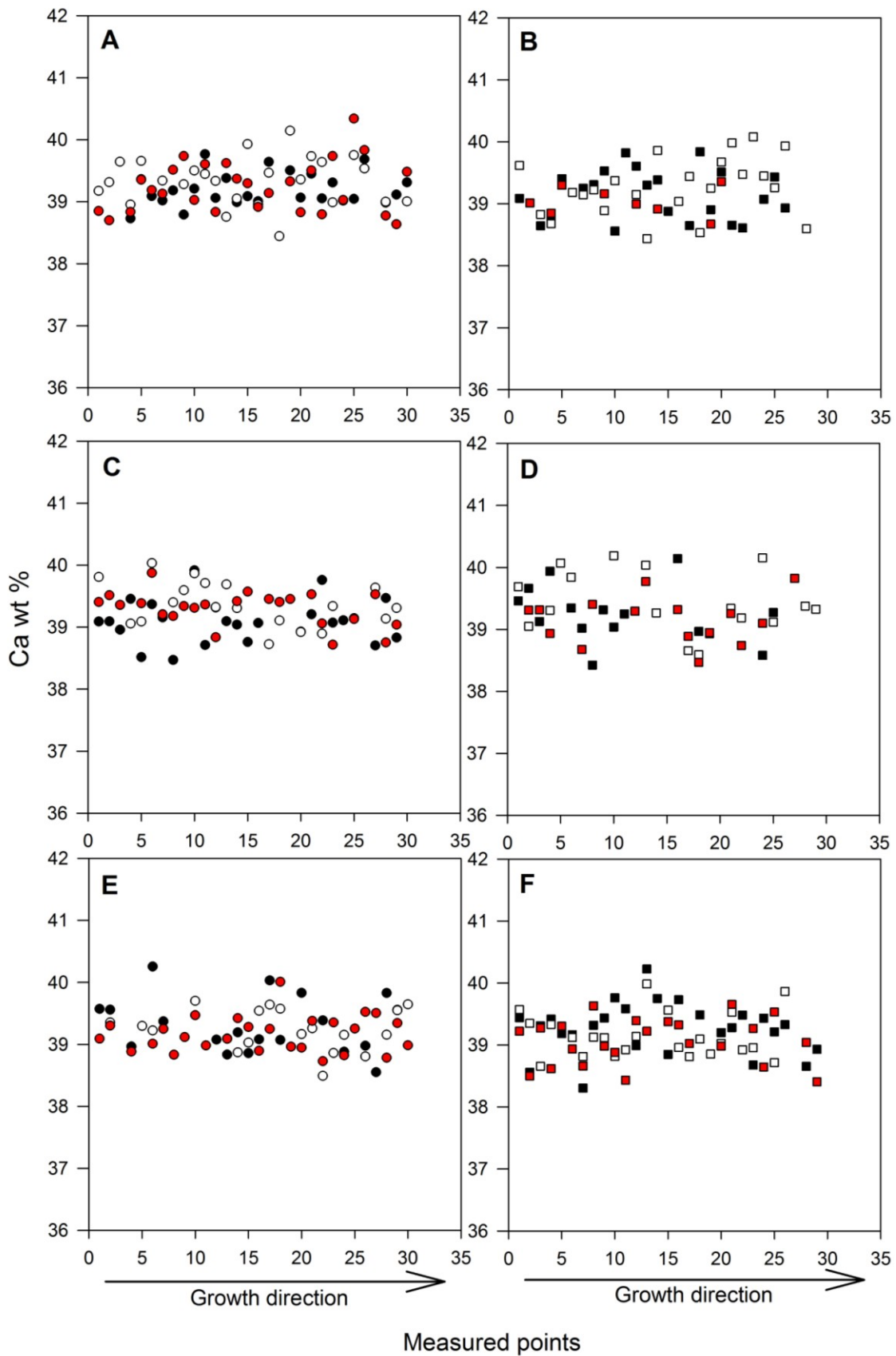
**Appendix Figure A9 – *L. uva* - Na concentration from the spot point method of wild growth (circle symbols) and experimental growth (square symbols) in the temperature control (A, B), pH control (C, D), pH 7.75 treatment (E, F) and pH 7.54 treatment (G, H). Different coloured symbols refer to different individuals within each treatment. Growth direction is indicated.**



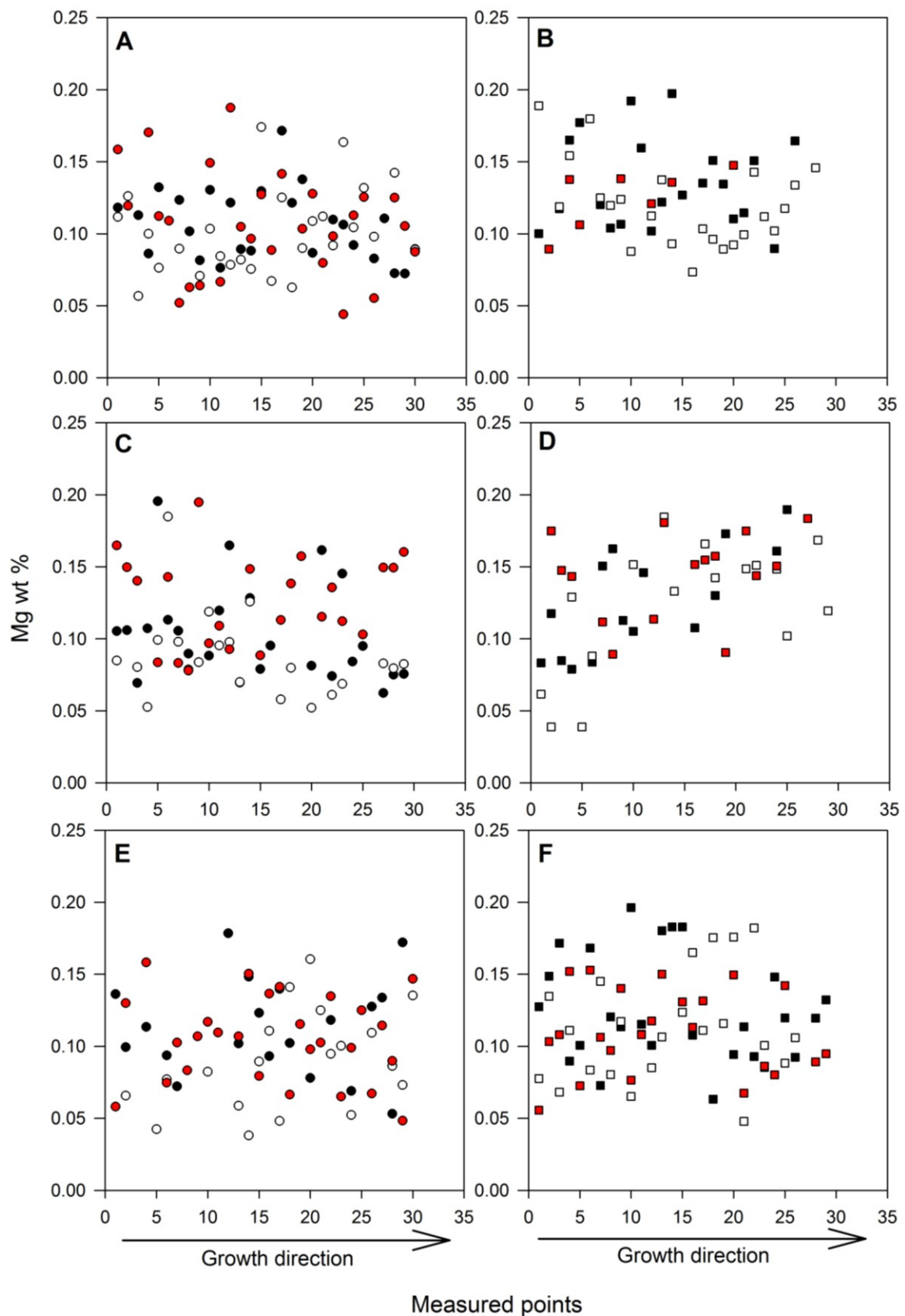
**Appendix Figure A10 – *L. uva* - Sr concentration from the spot point method of wild growth (circle symbols) and experimental growth (square symbols) in the temperature control (A, B), pH control (C, D), pH 7.75 treatment (E, F) and pH 7.54 treatment (G, H). Different coloured symbols refer to different individuals within each treatment. Growth direction is indicated.**



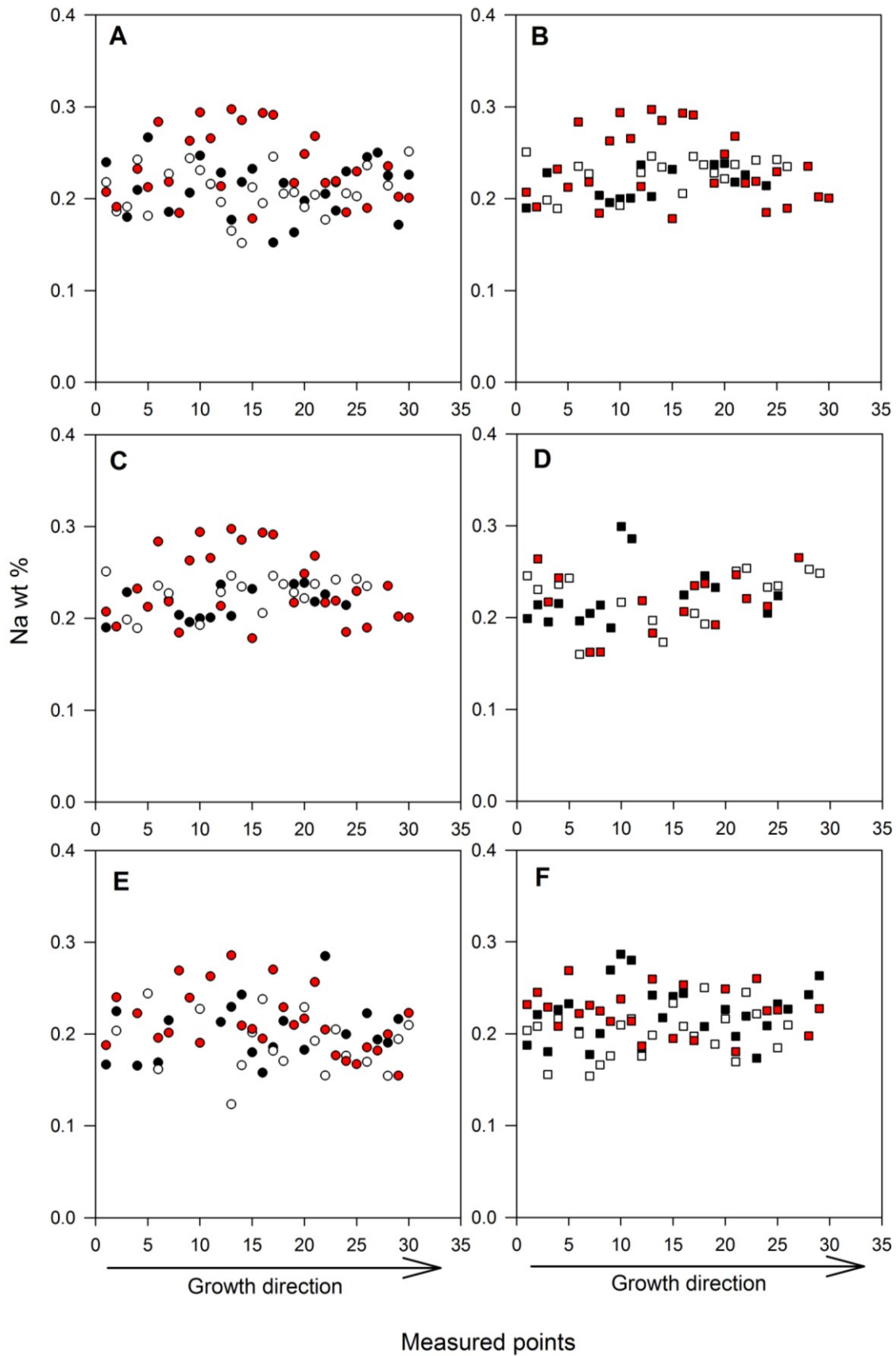
**Appendix Figure A11 – *L. uva* – P concentration from the spot point method of wild growth (circle symbols) and experimental growth (square symbols) in the temperature control (A, B), pH control (C, D), pH 7.75 treatment (E, F) and pH 7.54 treatment (G, H). Different coloured symbols refer to different individuals within each treatment. Growth direction is indicated.**



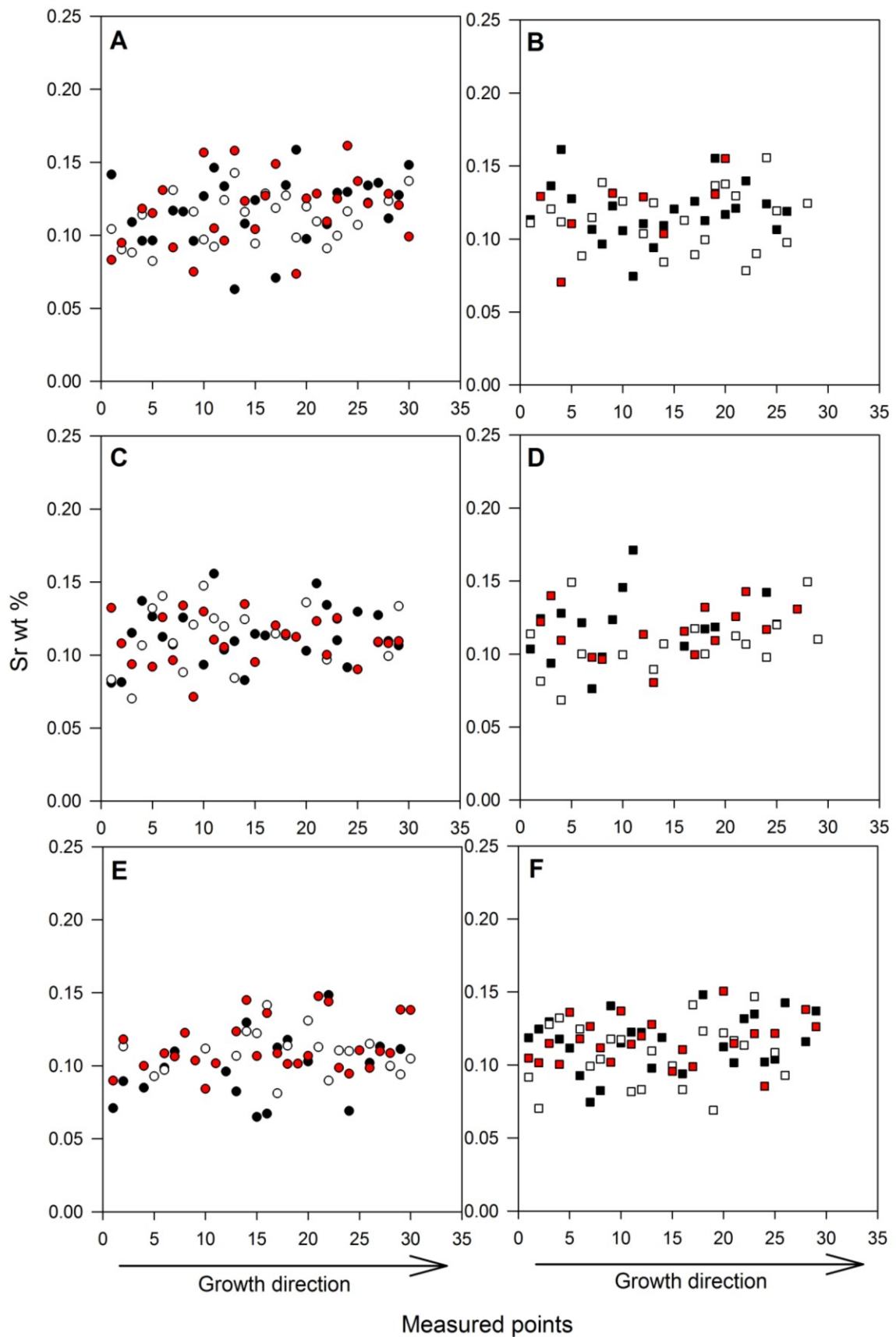
**Appendix Figure A12 – *C. inconspicua* - Ca concentration from the spot point method of wild growth (circle symbols) and experimental growth (square symbols) in the pH control (A, B), pH 7.8 (C, D) and pH 7.6 treatment (E, F). Different coloured symbols refer to different individuals within each treatment. Growth direction is indicated.**



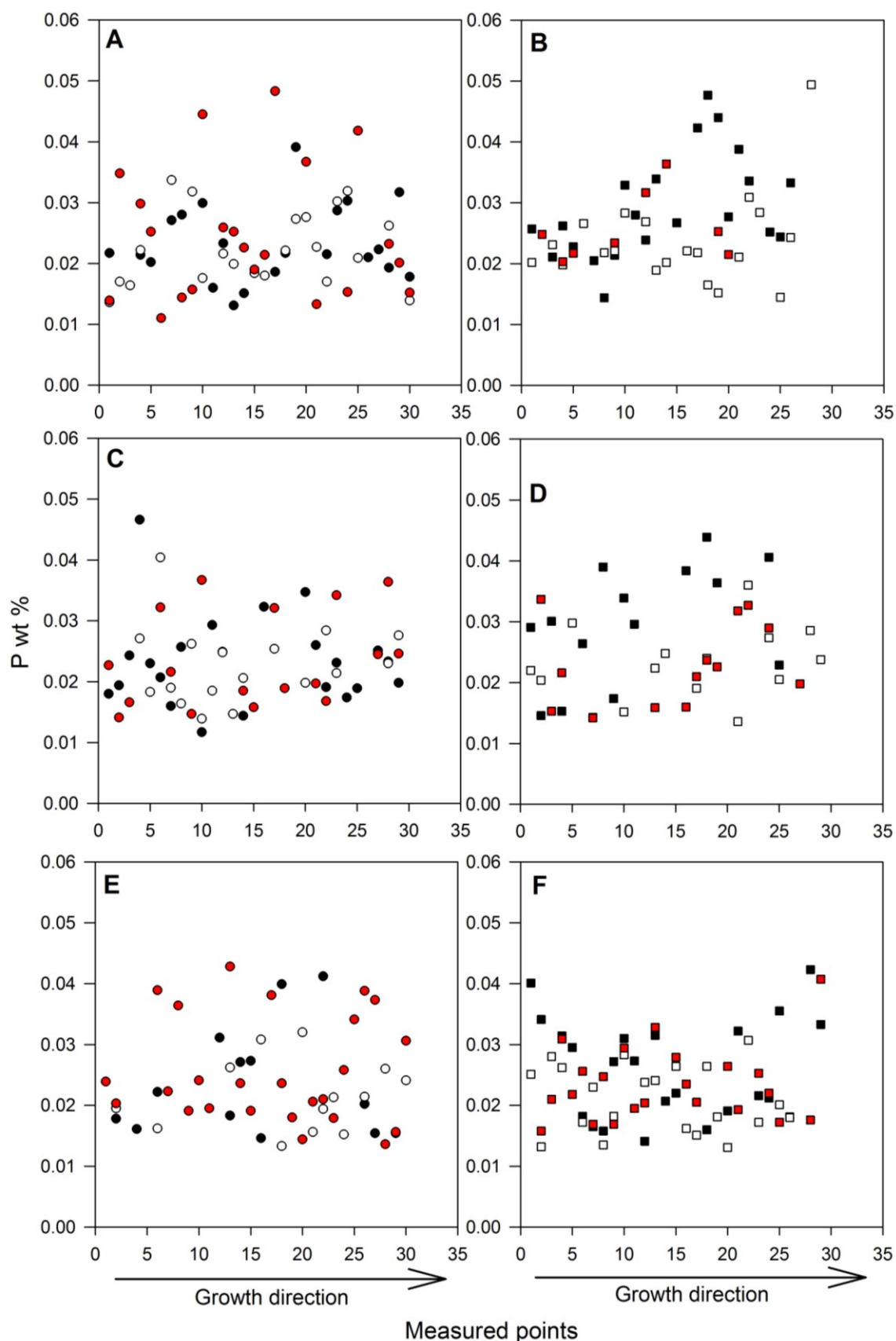
**Appendix Figure A13 – *C. inconspicua* - Mg concentration from the spot point method of wild growth (circle symbols) and experimental growth (square symbols) in the pH control (A, B), pH 7.8 (C, D) and pH 7.6 treatment (E, F). Different coloured symbols refer to different individuals within each treatment. Growth direction is indicated.**



**Appendix Figure A14 – *C. inconspicua* - Na concentration from the spot point method of wild growth (circle symbols) and experimental growth (square symbols) in the pH control (A, B), pH 7.8 (C, D) and pH 7.6 treatment (E, F). Different coloured symbols refer to different individuals within each treatment. Growth direction is indicated.**



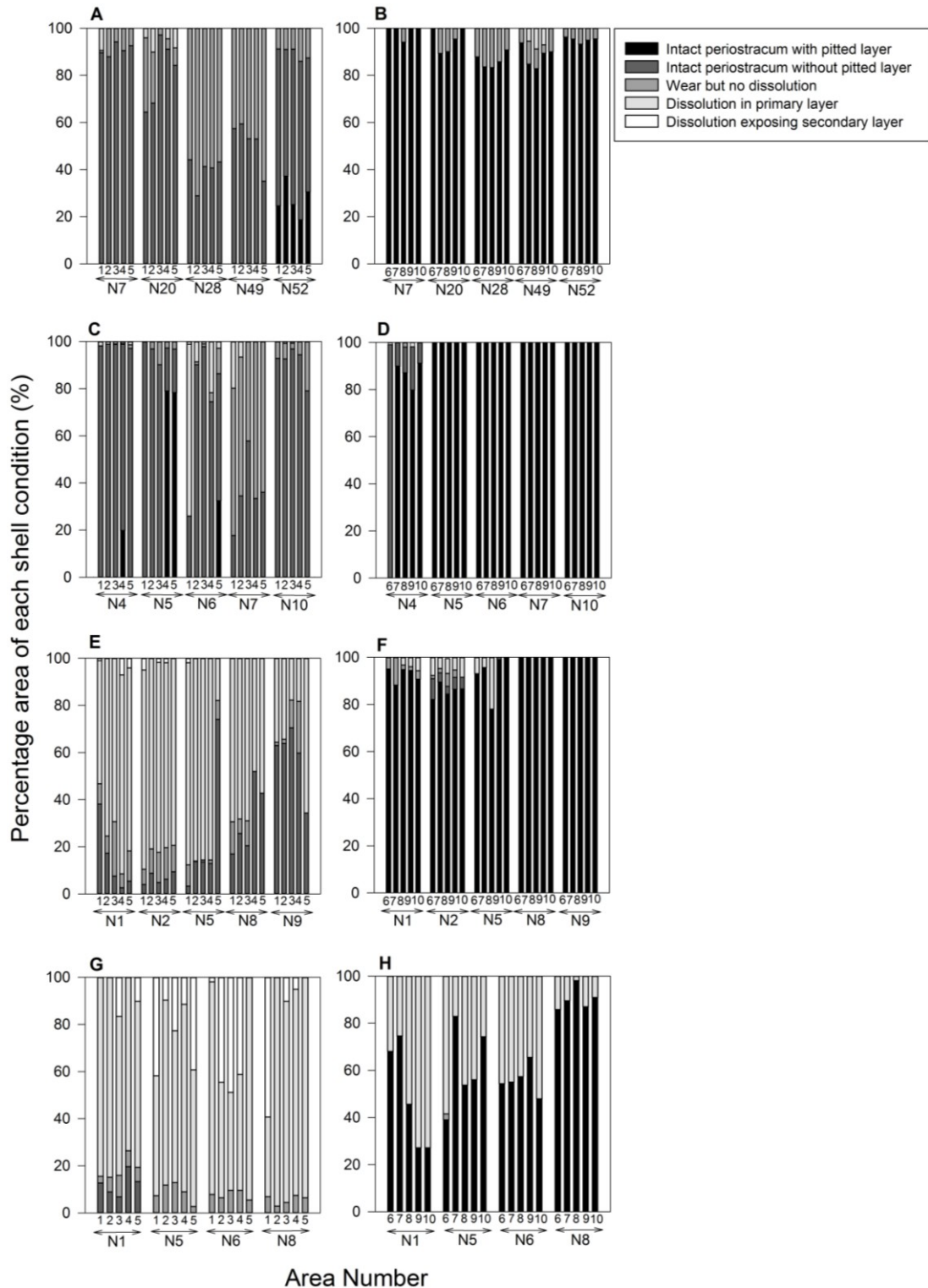
**Appendix Figure A15 – *C. inconspicua* - Sr concentration from the spot point method of wild growth (circle symbols) and experimental growth (square symbols) in the pH control (A, B), pH 7.8 (C, D) and pH 7.6 treatment (E, F). Different coloured symbols refer to different individuals within each treatment. Growth direction is indicated.**



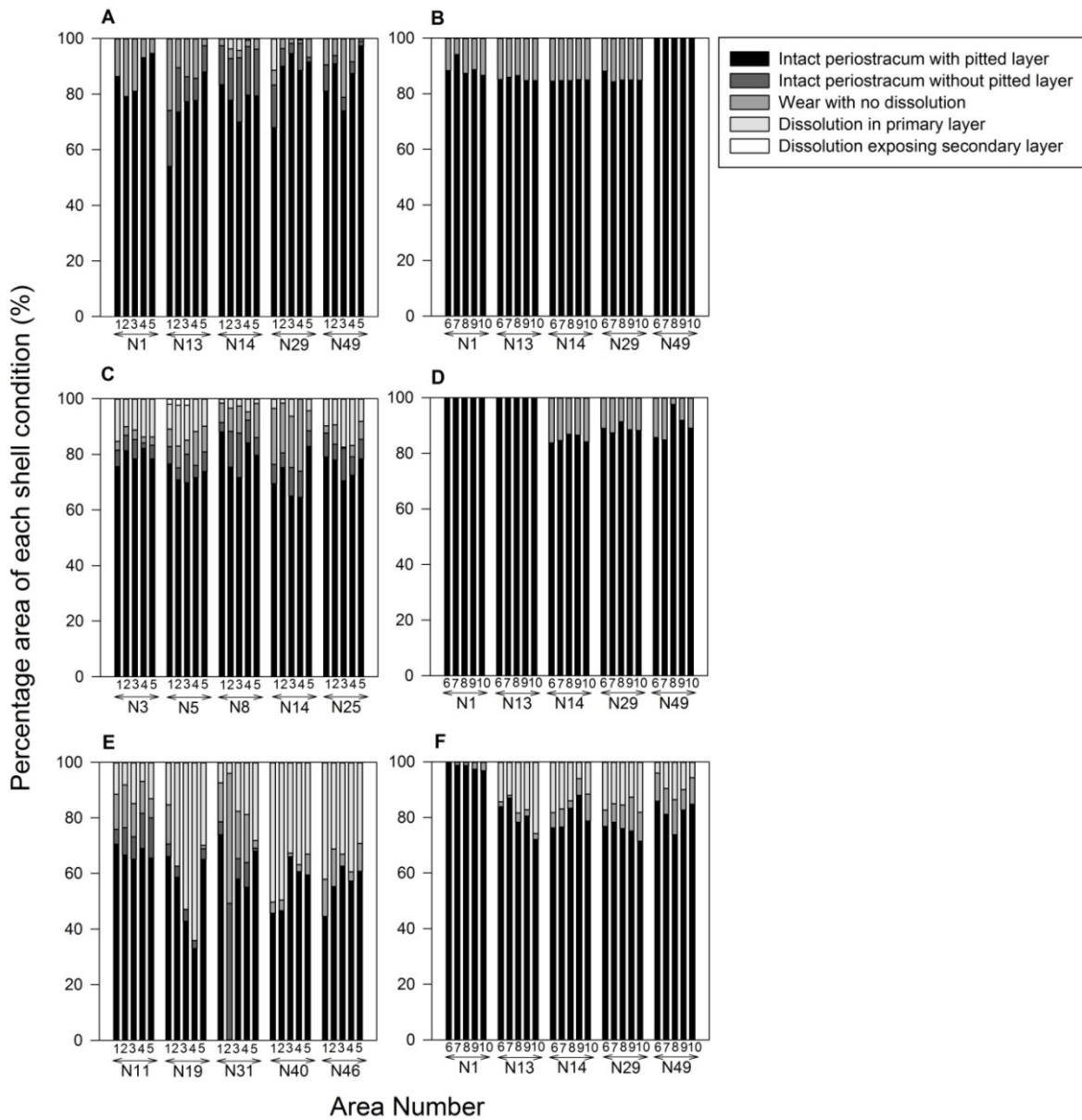
**Appendix Figure A16 – *C. inconspicua* - P concentration from the spot point method of wild growth (circle symbols) and experimental growth (square symbols) in the pH control (A, B), pH 7.8 (C, D) and pH 7.6 treatment (E, F). Different coloured symbols refer to different individuals within each treatment. Growth direction is indicated.**

## Appendix B

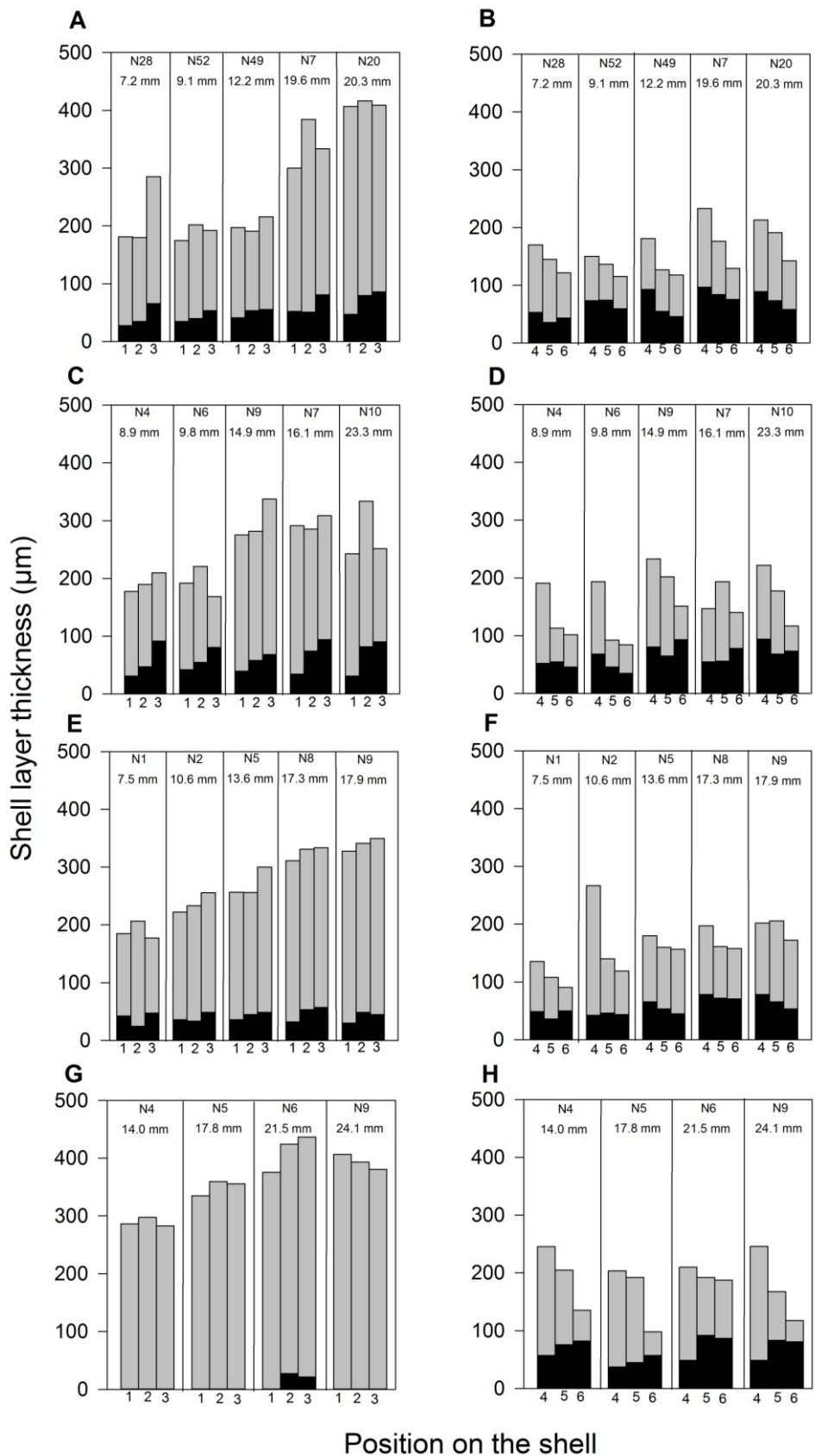
Supporting material for Chapter 4 (Do polar and temperate brachiopods maintain their shell integrity under predicted end-century acidified conditions?)



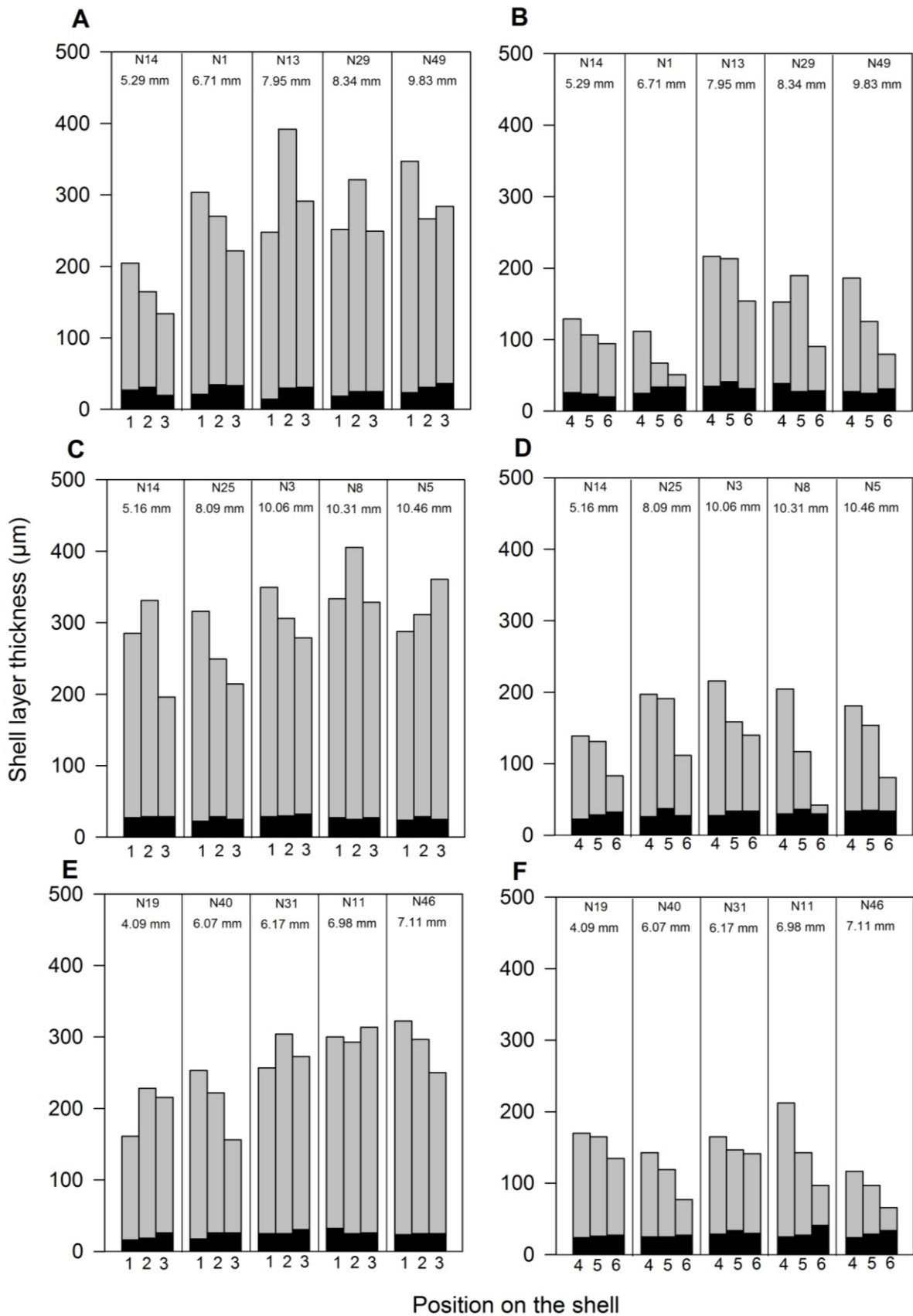
**Appendix Figure B1 – *L. uva* – Percentage areas of each type of shell condition of individuals in wild growth (area numbers 1-5) and experimental growth (area numbers 6-10) in temperature control (A, B), pH control (C, D), pH 7.75 (E, F) and pH 7.54 (G, H). Lighter grey tones indicate an increase in wear and/or shell dissolution (see legend). N details the individual number.**



Appendix Figure B2 – *C. inconspicua* – Percentage areas of each type of shell condition of individuals in wild growth (area numbers 1-5) and experimental growth (area numbers 6-10) in pH control (A, B), pH 7.8 (C, D) and pH 7.6 (E, F). Lighter grey tones indicate an increase in wear and/or shell dissolution (see legend). N details the individual number.



**Appendix Figure B3 – *L. uva* – Primary layer (black bars), secondary layer (grey bars) and total thickness (whole bars) of individuals from wild growth (A, C, E, G) and experimental growth (B, D, F, H) in temperature control (A, B), pH control (C, D), pH 7.75 (E, F) and pH 7.54 (G, H). Initial size of each individual is indicated.**



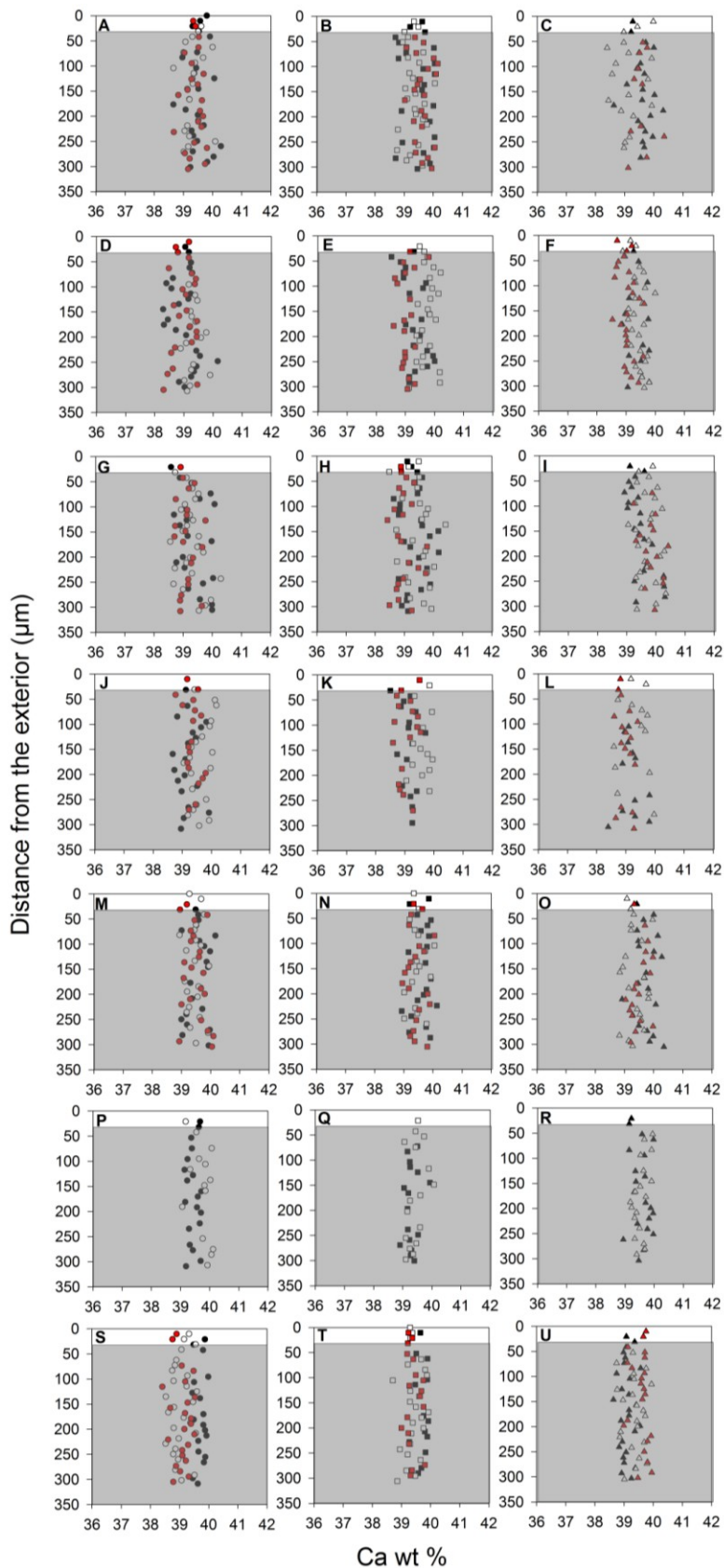
Appendix Figure B4 – *C. inconspicua* – Primary layer (black bars), secondary layer (grey bars) and total thickness (whole bars) of individuals from wild growth (A, C, E) and experimental growth (B, D, F) in pH control (A, B), pH 7.8 (C, D), pH 7.6 (E, F). Initial size of each individual is indicated.

## Appendix C

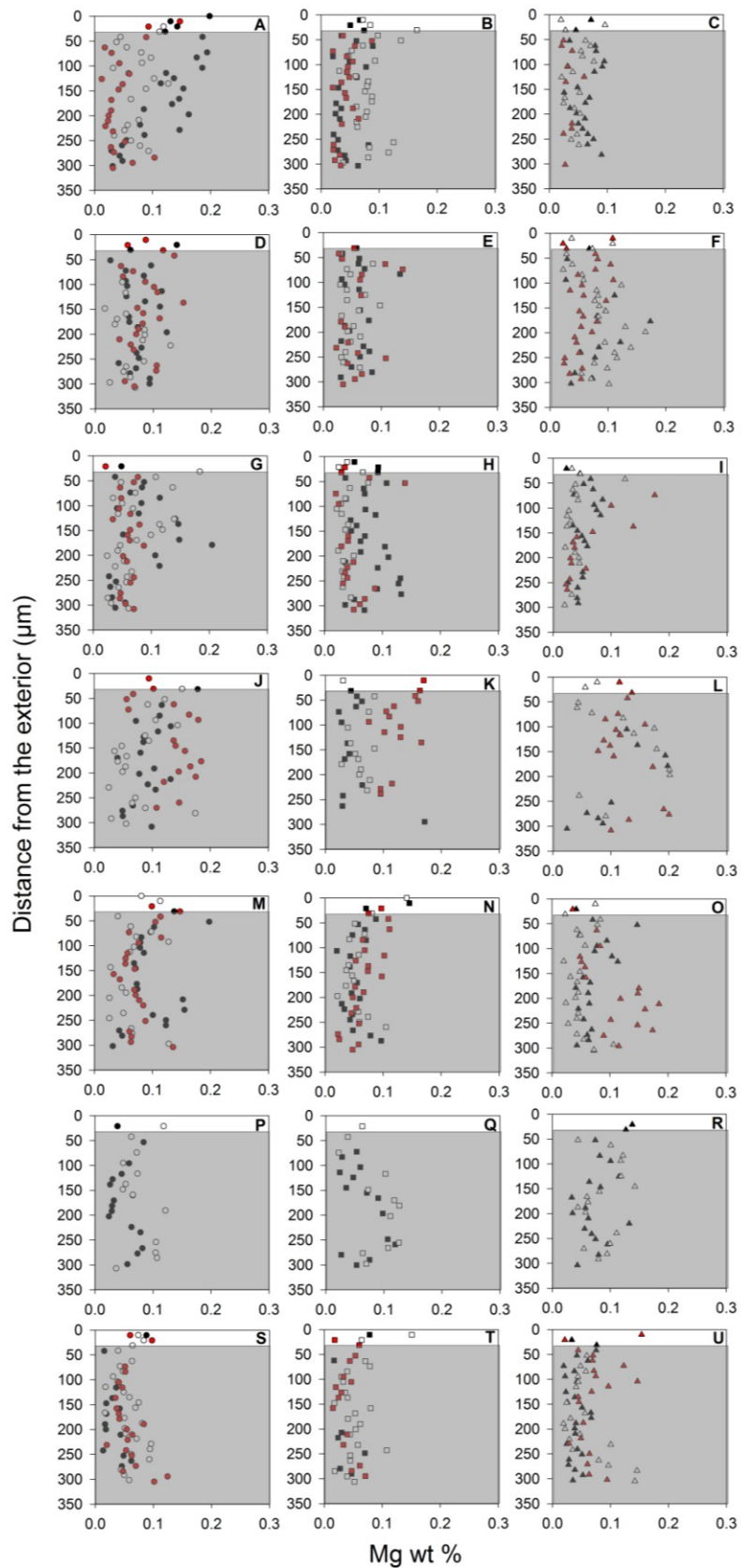
Supporting material for Chapter 5 (Acclimation of *Calloria inconspicua* to environmental change over the last 110 years).

**Appendix Table C1 – Specific details about the collection and storage sites of the museum specimens.**

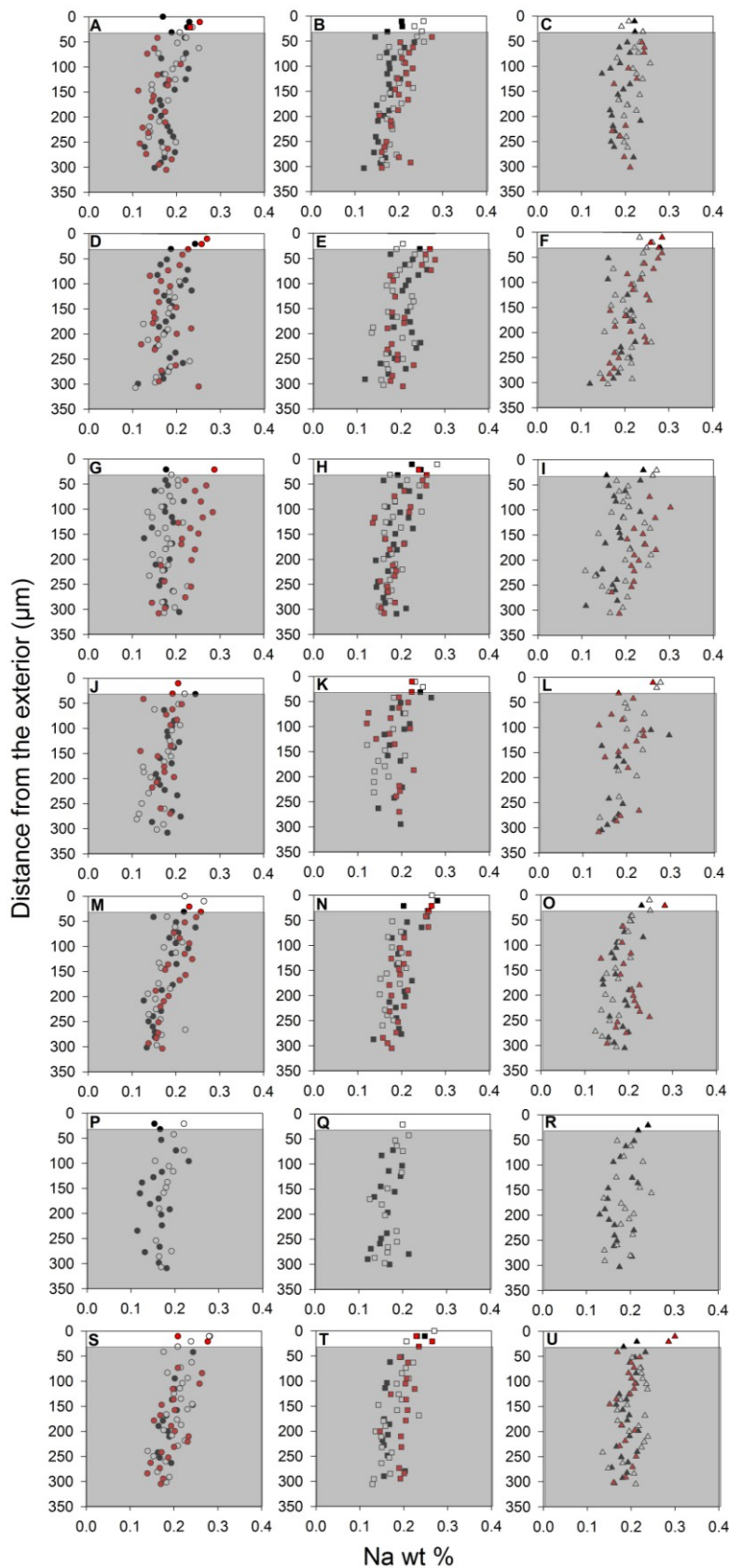
Year	Sample ID	Institute sample obtained from	Specific location collected	Depth collected (metres)
1900	BR000088	Te Papa Museum	Stewart Island	Not given
1914	BR001686		Oyster beds 3.2 km east of Halfmoon Bay, Stewart Island	42 m
1926	BR001062		Golden Bay, Stewart Island (46° 54'S, 168° 7'E)	Not given
1934	2006.12.140	Canterbury Museum	Horseshoe Bay, Butterfly Beach, Stewart Island	Not given
1935	MA79003	Auckland Museum	Stewart Island (46° 40'S, 168° 8'E)	Not given
1942	MA79298		Stewart Island (46° 54'S, 168° 8'E)	Not given
1942	2005.188.39	Canterbury Museum	Oyster beds in Foveaux Strait	Not given
1947	AU20001	University of Auckland	Foveaux Strait	60 m
1955	BR001331	Te Papa Museum	Halfmoon Bay, Stewart Island (46° 54'S, 168° 7'E)	Not given
1960	NIWA 62858 B243	National Institute of Water and Atmospheric Research	Near Abrahams Bay, further in Paterson Inlet than Ulva Island, Stewart Island (46° 94'S, 168° 05'E)	21 m
1967	NIWA 62892 E833		In between Ulva Island and Big Glory Bay, Paterson Inlet, Stewart Island (46° 95'S, 168° 15'E)	53 m
1977	NIWA 62891 K989		East Ulva Island, Stewart Island (46° 94'S, 168° 16'E)	22 m
1980	NIWA 62890 S265		Deep Bay, north of Ulva Island, Paterson Inlet, Stewart Island (46° 91'S, 168° 12'E)	10 m
	NIWA 62919 S263		East Ulva Island, Paterson Inlet, Stewart Island (46° 94'S, 168° 16'E)	27 m
2010	Cruise OS15	Geology Department, University of Otago	Just outside of Paterson Inlet (46° 59'S, 168° 16'E)	42 m
2014	2014	Collected by Dr Miles Lamare	Inside Paterson Inlet (46° 57'S, 168° 09'E)	20 m



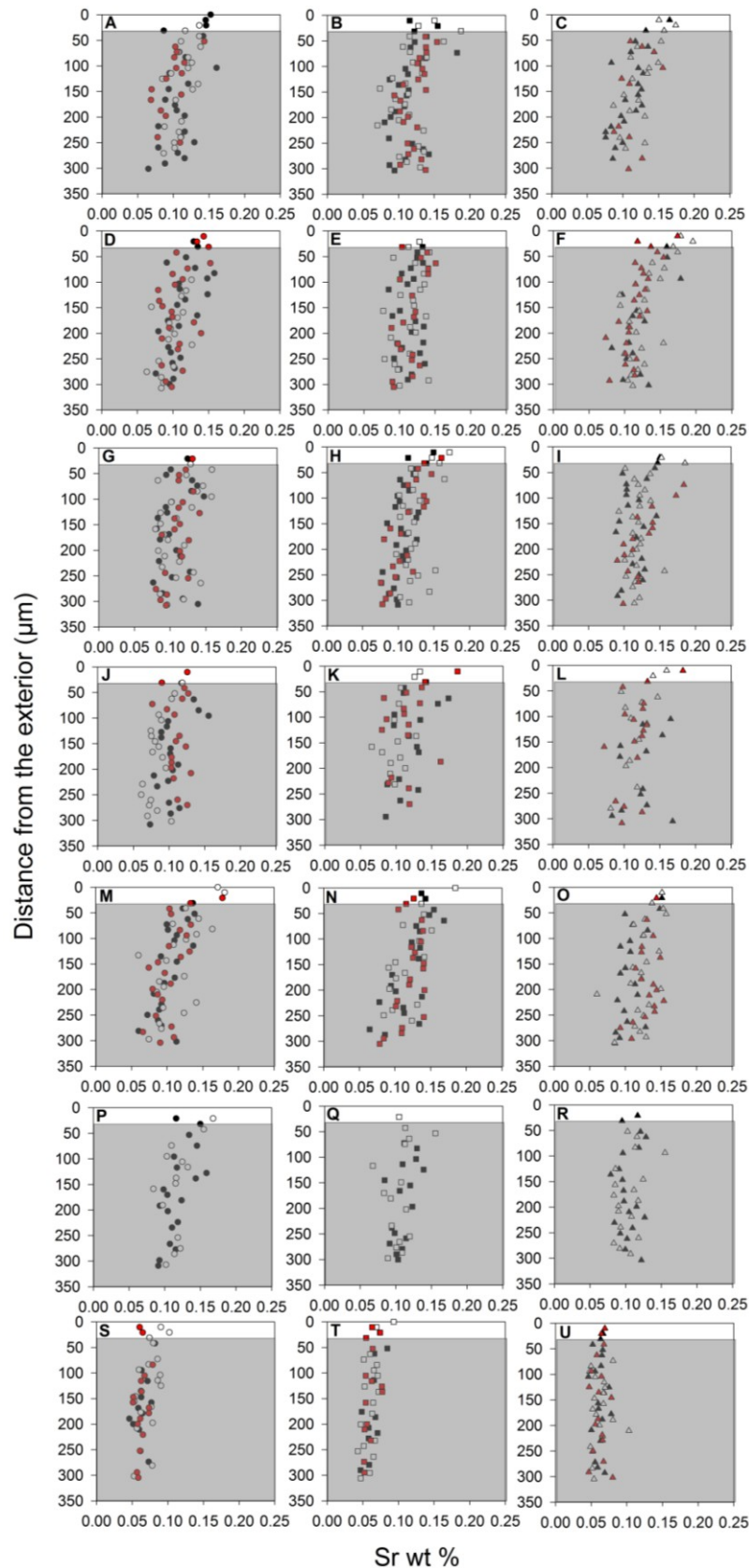
**Appendix Figure C1 – Ca concentration from near the umbo region (circle symbols), in the middle of the shell (square symbols) and near the shell margin (triangle symbols) in 1900 (A, B, C), 1926 (D, E, F), 1942 (G, H, I), 1960 (J, K, L), 1980 (M, N, O), 2010 (P, Q, R) and 2014 (S, T, U). Different coloured symbols refer to different individuals within each layer. White area is the primary layer and grey area is the secondary layer.**



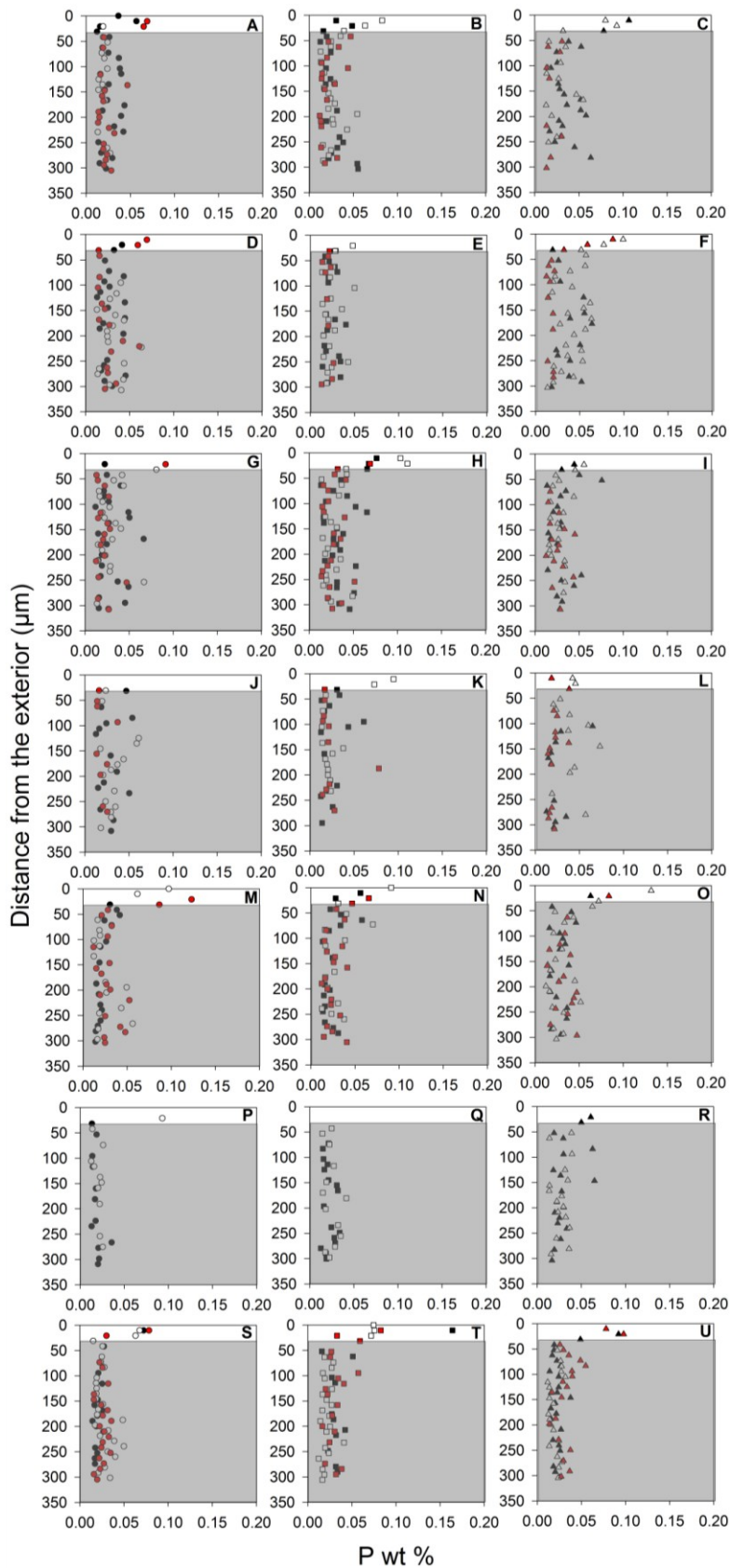
**Appendix Figure C2 – Mg concentration from near the umbo region (circle symbols), in the middle of the shell (square symbols) and near the shell margin (triangle symbols) in 1900 (A, B, C), 1926 (D, E, F), 1942 (G, H, I), 1960 (J, K, L), 1980 (M, N, O), 2010 (P, Q, R) and 2014 (S, T, U). Different coloured symbols refer to different individuals within each treatment. White area is the primary layer and grey area is the secondary layer.**



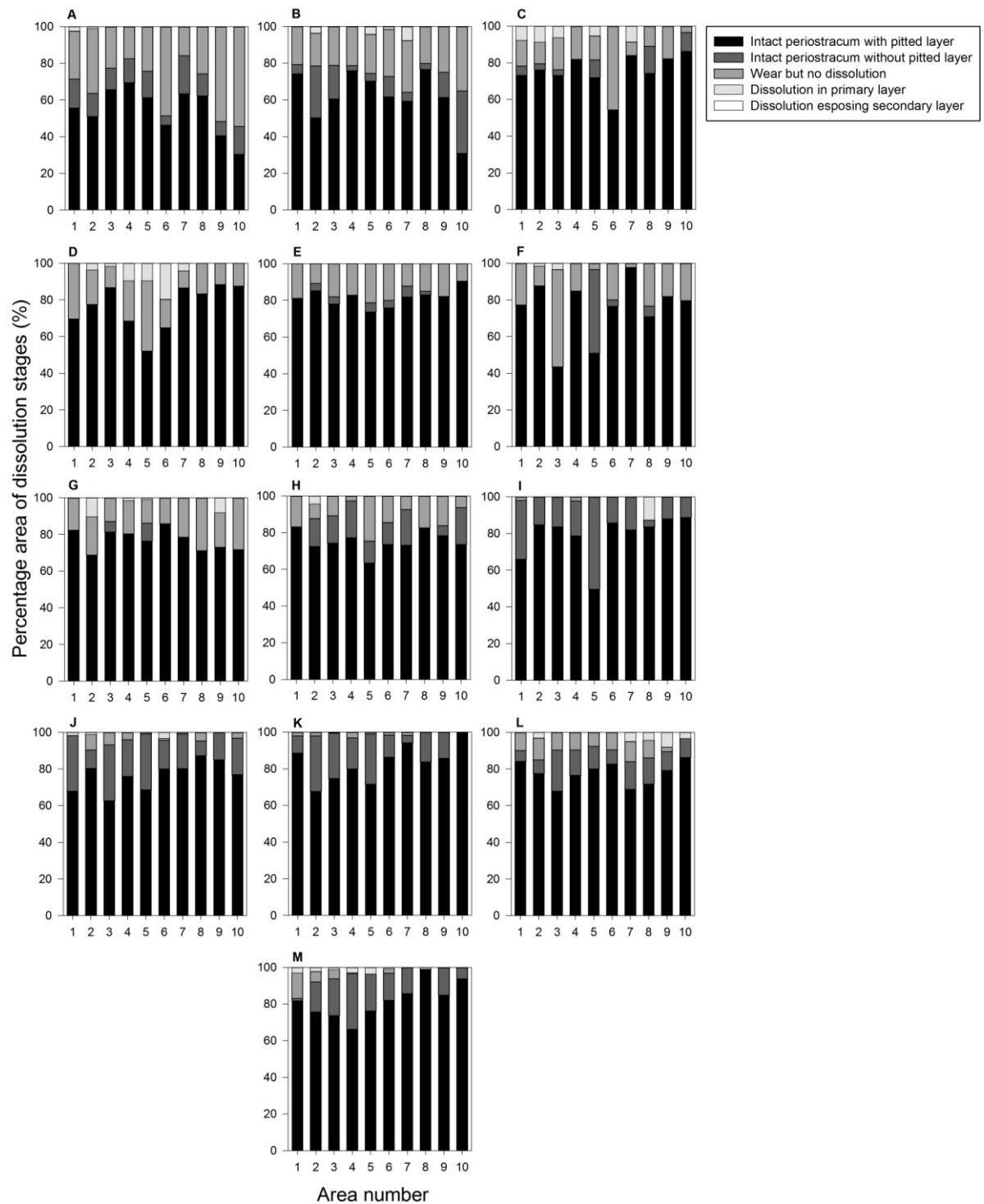
**Appendix Figure C3 – Na concentration from near the umbo region (circle symbols), in the middle of the shell (square symbols) and near the shell margin (triangle symbols) in 1900 (A, B, C), 1926 (D, E, F), 1942 (G, H, I), 1960 (J, K, L), 1980 (M, N, O), 2010 (P, Q, R) and 2014 (S, T, U). Different coloured symbols refer to different individuals within each treatment. White area is the primary layer and grey area is the secondary layer.**



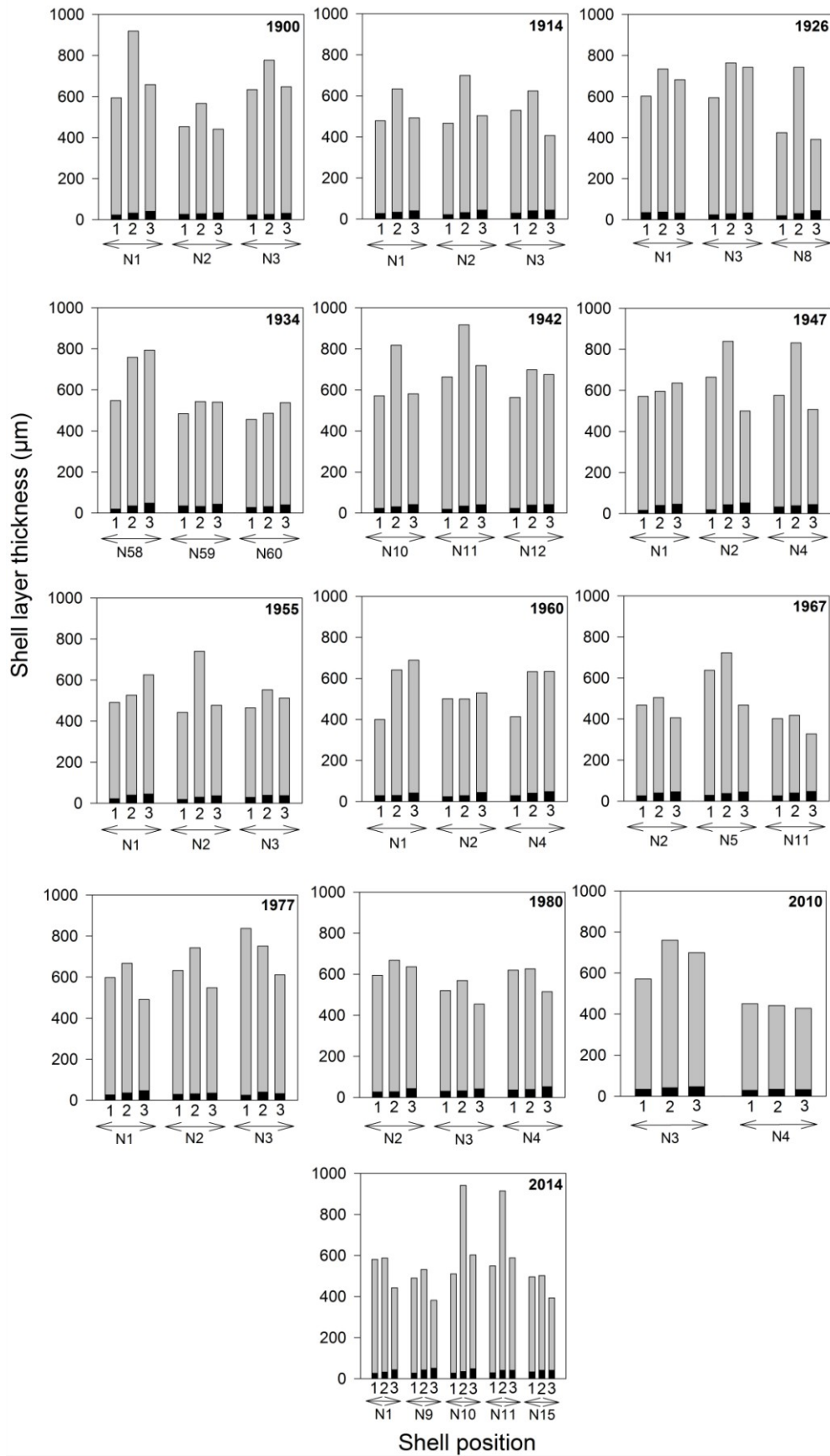
**Appendix Figure C4 – Sr concentration from near the umbo region (circle symbols), in the middle of the shell (square symbols) and near the shell margin (triangle symbols) in 1900 (A, B, C), 1926 (D, E, F), 1942 (G, H, I), 1960 (J, K, L), 1980 (M, N, O), 2010 (P, Q, R) and 2014 (S, T, U). Different coloured symbols refer to different individuals within each treatment. White area is the primary layer and grey area is the secondary layer.**



**Appendix Figure C5 – P concentration from near the umbo region (circle symbols), in the middle of the shell (square symbols) and near the shell margin (triangle symbols) in 1900 (A, B, C), 1926 (D, E, F), 1942 (G, H, I), 1960 (J, K, L), 1980 (M, N, O), 2010 (P, Q, R) and 2014 (S, T, U). Different coloured symbols refer to different individuals within each treatment. White area is the primary layer and grey area is the secondary layer.**



**Appendix Figure C6 – Average percentage area of the different types of shell conditions in 1900 (A), 1914 (B), 1926 (C), 1934 (D), 1942 (E), 1947 (F), 1955 (G), 1960 (H), 1967 (I), 1977 (J), 1980 (K), 2010 (L) and 2014 (M). Lighter grey tones indicate an increase in wear and/or shell dissolution (see legend).**



**Appendix Figure C7 – Primary layer (black bars), secondary layer (grey bars) and total thickness (whole bar) of individuals from near the umbo region (1), in the middle of the shell (2) and near the shell margin (3) from each decade. N denotes the individual number.**